



10112/
15112

CHEMKIN Tutorials Manual

CHEMKIN[®] Software

CK-TUT-10112-1112-UG-1
December 2011

Licensing:

For licensing information, please contact Reaction Design at (858) 550-1920 (USA) or licensing@ReactionDesign.com.

Technical Support:

Reaction Design provides an allotment of technical support to its Licensees free of charge. To request technical support, please include your license number along with input or output files, and any error messages pertaining to your question or problem. Requests may be directed in the following manner: E-mail: support@ReactionDesign.com, Fax: (858) 550-1925, Phone: (858) 550-1920.

Additional technical support hours may also be purchased. Please contact Reaction Design for the hourly rates.

Copyright:

Copyright© 2011 Reaction Design. All rights reserved. No part of this book may be reproduced in any form or by any means without express written permission from Reaction Design.

Trademark:

CHEMKIN® and REACTION DESIGN® are registered trademarks of Reaction Design in the United States and other countries. AURORA, CONP, CHEMKIN-CFD, CHEMKIN, CRESLAF, ENERGICO, EQUIL, EQUILIB, FORTÉ, KINETICS, MODEL FUELS CONSORTIUM, OPPDIF, OVEND, PARAMETER STUDY FACILITY, PARTICLE TRACKING FEATURE, PASR, PLUG, PREMIX, REACTION WORKBENCH, SENKIN, SHOCK, SPIN, SURFACE CHEMKIN, SURFTHERM, TRANSPORT, TWAFAER, TWOPNT are all trademarks of Reaction Design or Sandia National Laboratories. All other trademarks are the property of their respective holders.

Limitation of Warranty:

The software is provided "as is" by Reaction Design, without warranty of any kind including, without limitation, any warranty against infringement of third party property rights, fitness or merchantability, or fitness for a particular purpose, even if Reaction Design has been informed of such purpose. Furthermore, Reaction Design does not warrant, guarantee, or make any representations regarding the use or the results of the use, of the software or documentation in terms of correctness, accuracy, reliability or otherwise. No agent of Reaction Design is authorized to alter or exceed the warranty obligations of Reaction Design as set forth herein. Any liability of Reaction Design, its officers, agents or employees with respect to the software or the performance thereof under any warranty, contract, negligence, strict liability, vicarious liability or other theory will be limited exclusively to product replacement or, if replacement is inadequate as a remedy or in Reaction Design's opinion impractical, to a credit of amounts paid to Reaction Design for the license of the software.

Literature Citation for CHEMKIN and CHEMKIN-PRO:

CHEMKIN 10112 should be cited as:
CHEMKIN 10112, Reaction Design: San Diego, 2011.

CHEMKIN-PRO 15112 should be cited as:
CHEMKIN-PRO 15112, Reaction Design: San Diego, 2011.

Table of Contents

1	Introduction.....	19
2	Combustion in Gas-phase Processes	23
2.1	Equilibrium	23
2.1.1	Adiabatic Flame Temperature	23
2.2	Using Equivalence Ratio	24
2.2.1	Example: Propane in Air.....	25
2.2.2	Example: Stoichiometric Products.....	27
2.3	Ignition, Flames and Flammability.....	28
2.3.1	Steady-state Gas-phase Combustion.....	28
2.3.2	Autoignition for H ₂ /Air.....	30
2.3.3	Ignition-delay Times for Propane Autoignition.....	33
2.3.4	Burner-stabilized Flame.....	38
2.3.5	NO Emission from High-pressure Flames with Gas Radiation [CHEMKIN-PRO Only]	41
2.3.6	Soot Formation in Radiating Opposed-flow Diffusion Flame [CHEMKIN-PRO Only]	47
2.3.7	Flame Speed of Stoichiometric Methane/Air Premixed Flame with Reaction Path Analyzer [CHEMKIN-PRO Only].....	55
2.3.8	Parameter Study: Propane/Air Flame Speed as a Function of Equivalence Ratio and Unburned Gas Temperature.....	71
2.3.9	Hydrogen/Air Opposed-flow Flame	81
2.3.10	Flame Extinction Analysis [CHEMKIN-PRO Only].....	85
2.3.11	Stagnation Flame Analysis [CHEMKIN-PRO Only].....	94
2.4	Internal Combustion Engine.....	97
2.4.1	Homogeneous Charge Compression Ignition (HCCI) Engine	97
2.4.2	Multi-zone HCCI Engine Simulation [CHEMKIN-PRO Only]	103
2.5	Simulating a Shock-tube Experiment.....	110
2.5.1	Shock-heated Air (Shock).....	110
2.6	Combustion in Complex Flows.....	111
2.6.1	Gas Turbine Network.....	111
2.6.2	Jet Flame Network.....	114
2.6.3	Using Tear Streams to Estimate Initial Gas Composition in an HCCI Engine with Exhaust Gas Recirculation (EGR) [CHEMKIN-PRO Only].....	119
2.6.4	Partially Stirred Reactor for Methane/Air	127
2.6.5	Side Inlet on a Plug Flow Reactor	132
2.6.6	Co-flowing Non-premixed CH ₄ /Air Flame.....	135

2.7	Particle Tracking Feature [CHEMKIN-PRO Only]	141
2.7.1	Soot Formation and Growth in a JSR/PFR Reactor [CHEMKIN-PRO Only]	141
2.7.2	Soot Particles in Flame Simulators [CHEMKIN-PRO Only]	147
2.7.3	Sectional Method for Particle-Size Distribution with Pre-mixed Laminar Burner-Stabilized Stagnation Flame [CHEMKIN-PRO Only]	153
2.7.4	Simulating Particle-Size Distributions in a Burner-Stabilized Stagnation Flame	159
2.7.5	Detailed Particle Aggregation in a Batch Reactor [CHEMKIN-PRO Only]	162
2.8	Uncertainty Analysis [CHEMKIN-PRO Only]	170
2.8.1	Uncertainty Analysis of NO _x Emissions [CHEMKIN-PRO Only]	170
2.9	Chemistry Sets	173
2.9.1	Hydrogen/Air	173
2.9.2	Methane/Air	174
2.9.3	NO _x and CH ₄ , C ₂ H ₄ , C ₂ H ₆ , C ₃ H ₆ , and C ₃ H ₈	175
2.9.4	Propane/Air	175
2.9.5	Ethylene/Air Combustion and Soot Formation and Growth	175
2.9.6	C2_NO _x Mechanism	178
3	Catalytic Processes	181
3.1	Catalytic Combustors, Converters and Aftertreatment	181
3.1.1	Two-Stage Catalytic Combustor	181
3.1.2	Engine Exhaust Aftertreatment with a Transient Inlet Flow	191
3.2	Parameter Studies	200
3.2.1	Parameter Study Facility for Surface Chemistry Analysis	200
3.3	Chemistry Sets	204
3.3.1	Methane Oxidation on Pt	204
3.3.2	Pt/Rh Three-way Catalyst	205
4	Materials Problems	207
4.1	Chemical Vapor Deposition	207
4.1.1	Equilibrium Analysis of Chlorosilane CVD	208
4.1.2	PSR Analysis of Steady-state Thermal CVD	210
4.1.3	Approximations for a Cylindrical Channel Flow	214
4.1.4	Deposition in a Rotating Disk Reactor	219
4.1.5	Trichlorosilane CVD in Planar Channel Flow Reactor	223
4.2	Atomic Layer Deposition (ALD)	226
4.2.1	Time-dependent Simulations of ALD Process	227
4.3	Plasma Etching	233
4.3.1	Steady-state Chlorine Plasma	233
4.3.2	Spatial Chlorine Plasma PFR with Power Profile	237
4.3.3	Fluorocarbon Plasma Etching of Silicon Dioxide	241
4.4	Chemistry Sets	246
4.4.1	Silicon Nitride CVD from Silicon Tetrafluoride and Ammonia	246
4.4.2	Silicon Deposition from Silane	247
4.4.3	Silicon Deposition from Trichlorosilane	247
4.4.4	Alumina ALD	248
4.4.5	Chlorine Plasma	250
4.4.6	Fluorocarbon Plasma with SiO ₂ Etch Products	251
5	Chemical Mechanism Analysis	253
5.1	Mechanism Analyzer	253
5.1.1	Background Information	254
5.1.2	Reaction Mechanism for Diamond CVD	256

Index	269
-------------	-----

List of Tables

1-1	Reactor Models Used in Sample Problems.....	20
2-1	Reactant Mole Fractions Sum to 1.0.....	25
2-2	Relative Moles Normalized So Mole Fractions Sum to 1.0.....	25
2-3	N ₂ as Added Diluent	26
2-4	N ₂ as Component of Oxidizer	26
2-5	Determining Stoichiometric Products	27
2-6	Initial Temperatures and Ignition Times	36
2-7	Inlet velocities for pressures studied by Thomsen et al.	45
2-8	Test Engine Specifications	98
2-9	Composition of Initial Gas Mixture.....	99
2-10	Engine parameters of the validation case.	103
2-11	Natural gas composition used in the validation case.	103
2-12	Zone configuration used by the multi-zone model analysis for the validation case.	104
2-13	Components in Fuel and Oxidizer Streams.....	133
2-14	Properties of the Co-flowing Jets	136
3-1	Excerpt of Data Representing Engine-out Test Measurements.....	193

List of Figures

2-1	Adiabatic Flame Temperatures—Hydrogen/Air Mixture.....	24
2-2	Steady-state Gas-phase Combustion—Hydrogen/Air Temperatures	29
2-3	Steady-state Gas-phase Combustion—Molar Conversions	30
2-4	Autoignition for Hydrogen/Air—Temperature Profile	32
2-5	Autoignition for Hydrogen/Air—Species Composition Profiles	32
2-6	Autoignition for Hydrogen/Air—Sensitivity Coefficients	33
2-7	Temperature and OH Mole Fraction Profiles as a Function of Time.....	36
2-8	Ignition Based on Varying Criteria.....	37
2-9	Ignition Times vs. Inverse of Temperature (Semi-log)	37
2-10	Burner-stabilized Flame—Experimental Gas Temperature Profile	40
2-11	Burner-stabilized Flame—Mole Fractions	41
2-12	Axial gas temperature profiles predicted with and without gas radiation heat loss as compared against experimental temperature profile for the $\phi=0.6$ CH ₄ /O ₂ /N ₂ flame at 14.6 atm.	46
2-13	Comparisons of measured and predicted NO mole fraction profiles as a function of axial distance from the burner surface for the $\phi=0.6$ CH ₄ /O ₂ /N ₂ flame at 14.6 atm.	46
2-14	Measured and predicted NO concentrations behind the $\phi=0.6$ CH ₄ /O ₂ /N ₂ flame versus pressure.....	47
2-15	Predicted axial velocity profile of Flame 1 studied by Atreya et al. ¹³ (p. 48). The location of (velocity) stagnation plane is indicated by the blue dash-dotted line.	51
2-16	Predicted gas temperature profile is compared against the experimental profile for Flame 1 studied by Atreya et al. ¹³ (p. 48)	52
2-17	Comparisons of predicted and measured fuel (CH ₄) and oxidizer (O ₂) profiles for Flame 1 studied by Atreya et al. ¹³ (p. 48)	52
2-18	Comparisons of predicted and measured profiles of H ₂ and CO for Flame 1 studied by Atreya et	

al. ¹³ (p. 48)	53
2-19 Predicted and measured C ₂ H ₂ and OH profiles of Flame 1 studied by Atreya et al. ¹³ (p. 48). The OH peak indicates the flame front and the C ₂ H ₂ peak marks the major soot growth region.	53
2-20 Predicted pyrene (A4) profile showing soot inception mainly occurs in the region between the stagnation plane and the diffusion flame in Flame 1 studied by Atreya et al. ¹³ (p. 48)	54
2-21 Predicted soot volume fraction profile is compared against the experimental profile as a function of distance from the fuel nozzle for Flame 1 studied by Atreya et al. ¹³ (p. 48)	54
2-22 Flame Speed—Temperature Profile Panel	56
2-23 C1_ Flame Speed—Reactor Physical Properties	56
2-24 Flame Speed—Axial Velocity vs. Distance	58
2-25 Flame Speed—Temperature vs. Distance	59
2-26 Flame Speed—Output Calculation pane with Sensitivity Option.	60
2-27 Flame Speed—Analyze Results panel with Reaction Path Analyzer option	61
2-28 Flame Speed—Altering the solution chosen, and y variable shown in the solution plot.	62
2-29 Flame Speed—Switching to a hierarchical layout option.	63
2-30 Flame Speed—Increased complexity in the diagram due to changing the solution point, and increasing the number of allowed species.	64
2-31 Flame Speed—Altering the zoom setting to see the contents of the diagram.	65
2-32 Flame Speed—Decomposition pathways starting with methane.	66
2-33 Flame Speed—The Rate of Production and Sensitivity charts of methane.	67
2-34 Flame Speed—Splitting a composite reaction pathway into one per reaction.	68
2-35 Flame Speed—Tree layout method of the decomposition of methane.	69
2-36 Flame Speed—Setting the hydroxide radical and oxygen radical as side species. The source was switched from methane to oxygen, and the element filter was changed to O element.	70
2-37 Flame Speed—Colored reactions based on influence of side species.	71
2-38 Panel for Setup of Parameter Studies.....	73
2-39 Automatic Estimation of Starting Temperature Profile	74
2-40 Auto-Populate Option	76
2-41 Varying Each Parameter Independently	77
2-42 Parameter Study After Setup Is Complete	77

2-43	Post-Processor Options After Running Parameter Studies	79
2-44	Cluster Endpoint vs. Parameter	80
2-45	Flame-Speed Calculated Values as a Function of Equivalence Ratio	81
2-46	Hydrogen/Air Flame—Temperature vs. Axial Distance.....	83
2-47	Hydrogen/Air Flame—Mole Fractions	83
2-48	Hydrogen/Air Flame—Temperature Sensitivity to Reaction Rates	84
2-49	Hydrogen/Air Flame—Temperature Sensitivity to Heats of Formation	84
2-50	Icon for Extinction of Premixed or Opposed Flow Flame reactor	85
2-51	Extinction— Basic reactor properties	87
2-52	Dynamic plotting of Temperature vs. extinction response, showing a turn at $\sim 550 \text{ s}^{-1}$	89
2-53	Output file opposed-flow_flame__extinction_ExtinctionResponse.csv	90
2-54	Output file ExtinctionProfilesOut.	91
2-55	Flame response curve showing extinction (turning) for premixed stoichiometric methane-air flame. The inlet temperature is 296 K and ambient pressure is 1 atm. The calculated extinction strain rate is 550 /s.	92
2-56	Axial velocity and temperature profile for premixed stoichiometric methane-air flame at extinction point. The global strain rate at extinction is 289 s^{-1}	93
2-57	Axial velocity and velocity gradient magnitude for premixed stoichiometric methane-air flame at extinction point. Also shown are the points corresponding to the definitions of various extinction strain rates	93
2-58	Icon for Premixed Laminar Burner-Stabilized Stagnation Flame model.	94
2-59	Parameter Study set-up	95
2-60	Temperature and velocity profiles for two inlet velocities	96
2-61	Major species mole fraction profiles for each of two simulation runs.	97
2-62	IC Engine Icon.....	98
2-63	C1_ IC Engine—Reactor Physical Property for HCCI Woschni Heat Loss model.....	100
2-64	HCCI Engine—EGR Temperature Comparison.....	101
2-65	HCCI Engine—EGR Pressure Comparison	102
2-66	HCCI Engine—EGR Heat Loss Comparison	102
2-67	Reactor model palette showing the multi-zone model icon in the CHEMKIN User Interface.....	104

2-68	Diagram view of a multi-zone simulation project.....	104
2-69	Dialog for specifying the number of zones in the multi-zone simulation.	105
2-70	Engine parameters in Reactor Physical Properties tab for multi-zone model.	106
2-71	Zone Properties table.	106
2-72	Individual Zone Properties tab of the multi-zone model graphic user interface using a temperature profile called "zone5"	107
2-73	Temperature profiles predicted by the single-zone and the multi-zone models. The transition angle is set to 3 degrees BTDC.....	108
2-74	Comparison of number density distributions obtained with and without aggregation model.....	109
2-75	Zone volume profiles predicted by the multi-zone models.	109
2-76	Nitrogen Atom Reaction in CHEMKIN Format	110
2-77	Shock Tube Experiment—NO Mole Fraction	111
2-78	Gas Turbine Network—Schematic	113
2-79	Gas Turbine Network—Diagram View	113
2-80	Gas Turbine Network—Temperature Comparisons	114
2-81	Gas Turbine Network—CO and NO Comparisons	114
2-82	Jet Flame Network—Diagram View	115
2-83	Jet Flame Network—Temperature Distribution	117
2-84	Jet Flame Network—CO Distribution	117
2-85	Jet Flame Network—NO Distribution	118
2-86	Jet Flame Network—Mole Fractions	119
2-87	Diagram view of the EGR_network project.	120
2-88	Reactor Properties panel of the EGR_Merge reactor.	121
2-89	Stream Properties panel of the fresh fuel-air mixture entering the EGR_Merge reactor	121
2-90	Engine Properties panel of the HCCI engine model.....	122
2-91	Properties of the Heat_Loss reactor.....	123
2-92	Initialization panel of the inlet stream to the Heat_Loss reactor.....	123
2-93	Properties of the inlet stream to the Heat_Loss reactor.....	123
2-94	Split Factor panel for the Gas Splitter.	124

2-95	Tear Stream Controls panel.	124
2-96	Popup reminder for the "initialize Tear Streams" panel.	124
2-97	Panel for entering guess properties of the Tear Stream.	125
2-98	Detail view of the calculations in which clusters of the same Tear Stream are grouped together and highlighted.	125
2-99	Project Results	125
2-100	Solution selection panel.	126
2-101	Comparison of EGR effect on in-cylinder pressure. Solid line: no EGR; Dash-dotted line: 30% EGR by mass.	126
2-102	Comparison of EGR effect on gas temperature. Solid line: no EGR; Dash-dotted line: 30% EGR by mass.	126
2-103	Comparison of EGR effect on CO ₂ emission. Solid line: no EGR; Dash-dotted line: 30% EGR by mass.	127
2-104	Comparison of EGR effect on NO emission. Solid line: no EGR; Dash-dotted line: 30% EGR by mass.	127
2-105	PaSR Methane/Air—Temperature Comparison.....	130
2-106	PaSR Methane/Air—Temperature Variance Comparison.....	131
2-107	PaSR Methane/Air—CO Comparison.....	131
2-108	PaSR Methane/Air—Select the Import File Format.....	132
2-109	PaSR Methane/Air—PDF(T) Comparison.....	132
2-110	Illustration of the System to be Modeled.	133
2-111	Total Flow Growing Directly as a Result of Side Inlet Flow.	134
2-112	Peaking of NO Concentration Dependent on Temperature in a PFR with an Approximated Mixing Region.	135
2-113	Confined Co-flowing Annular Jet Configuration.	136
2-114	Preferences Panel Showing the Display User Routine Options Is Enabled.....	137
2-115	Get Initial Solution Profile from User Routine Check box.....	138
2-116	Visualization of Full Computational Domain Can Be Acquired by Selecting Proper Reflect Contour Data Option in the CHEMKIN Post-Processor Panel.....	139
2-117	Contour Plot Window Showing the Pull-down List Selections of the Insert Menu.....	140
2-118	Colorbar Property Panel.....	140

2-119	Final 3-D Temperature Contours of the Entire Physical Domain with Vertical Contour Legend (Colorbar)	141
2-120	A schematic of the JSR/PFR reactor configuration used by Marr ²⁷	142
2-121	Diagram View of the CHEMKIN Project Used to Simulate the JSR/PFR Experiment	143
2-122	Specifying Particle Tracking Feature Parameters and Initial Conditions of Particle Size Moments in the Reactor	143
2-123	Tolerances for Particle Size Moments Can Be Given Explicitly in the Solver Window	144
2-124	Comparisons of Mole Fraction Profiles of Selected Gas Phase Species Inside the PFR for the 1630K and F = 2.2 Case of the C ₂ H ₄ /O ₂ /N ₂ JSR/PFR Experiment by Marr ²⁷ . Symbols: data; Solid lines: predictions with HACA and PAH condensation growth mechanisms.....	145
2-125	Comparisons of Soot Mass Concentration Profiles Inside the PFR for the 1630K and F = 2.2 Case of the C ₂ H ₄ /O ₂ /N ₂ JSR/PFR Experiment by Marr ²⁷ . Symbols: data; Solid line: prediction with both HACA and PAH condensation growth mechanisms; Dash-dot line: prediction with HACA growth mechanism only	146
2-126	The Particle Diameter Evolution Inside the PFR Predicted by the Present Soot Module for the 1630K and F = 2.2 Case of the C ₂ H ₄ /O ₂ /N ₂ JSR/PFR Experiment by Marr ²⁷ (see p. 141)	146
2-127	Distance vs temperature and particle volume fraction	151
2-128	Distance vs species mole fraction and particle number density	151
2-129	Distance vs Temperature and Particle volume fraction	152
2-130	Distance vs species mole fraction and particle number density	153
2-131	Selecting the Sectional Method on the Reactor Physical Properties tab.	155
2-132	Appearance of the Dispersed Phase tab when the Sectional Method is selected.	155
2-133	Sectional Method plot of temperature and mole fraction of pyrene (A4).	157
2-134	Particle-size distribution as a function of distance.	158
2-135	PDF as a function of distance	159
2-136	Particle-size distribution at the stagnation plane for three conditions imposed by the parameter study. 161	161
2-137	Imposed temperature profile with the mole fraction of the precursor TiCl ₄	165
2-138	Imposed temperature profile with the nucleation rate of the precursor TiCl ₄	165
2-139	Complete Aggregation - Aggregate number density as a function of the volume equivalent section diameter.	166
2-140	Evolution of the primary particle diameter.	167
2-141	Number density distributions obtained without aggregation.	168

2-142	Collision diameter as a function of (volume equivalent) section diameter.	169
2-143	Comparison of the total particle number and surface area densities as a function of time with and without aggregation model	170
2-144	Setting Up an Uncertainty Analysis for Heat Loss.....	172
2-145	Setting Up the Uncertainty Distribution for Heat Loss.....	172
2-146	Probability Density Function of NO	173
3-1	Turbine Flow Capacity.....	182
3-2	Two-Stage Catalytic Combustor—Diagram View	185
3-3	Catalytic Pre-combustor (C1_)—Honeycomb Monolith, Catalyst sub-tab	185
3-4	Catalytic Pre-combustor (C1_)—Honeycomb Monolith, Honeycomb sub-tab	186
3-5	Homogeneous Stage Combustor (C3_)—Reactor Physical Property	186
3-6	Two Stage Catalytic Combustor—Excess_Air_Dilution (Cluster 4) Output Results	187
3-7	Two Stage Catalytic Combustor—Temperature Comparison	189
3-8	Two Stage Catalytic Combustor—Pressure Comparison	189
3-9	Two Stage Catalytic Combustor—CH ₄ Comparison.....	190
3-10	Two Stage Catalytic Combustor—CO Comparison	190
3-11	Two Stage Catalytic Combustor—NO Comparison	191
3-12	Sample USRINLET Subroutine for User-Defined Transient Inlet Conditions.....	196
3-13	Engine Exhaust Aftertreatment—Molar Conversion Rates	199
3-14	Engine Exhaust Aftertreatment—Mole Fractions	199
3-15	Engine Exhaust Aftertreatment—Gas Temperatures.....	200
3-16	Setting Up a Parameter Study for Sticking Coefficients vs. Predicted Temperature Profiles	202
3-17	Varying Rate Constants of Reactions 1 and 6.	203
4-1	Chlorosilane CVD—Equilibrium Calculations.....	209
4-2	Chlorosilane CVD—Mole Fractions.....	210
4-3	Steady-state Thermal CVD—Deposition Rate vs. SiF ₄ Mole Fraction.....	212
4-4	Steady-state Thermal CVD—ROP Comparison.....	213
4-5	Steady-state Thermal CVD—Growth Rates.....	213
4-6	Steady-state Thermal CVD—Site Fractions.....	214

4-7	Cylindrical Channel Flow—Shear-flow Simulation of SiF ₄ Mole Fractions	216
4-8	Cylindrical Channel Flow—SiF ₄ Mole Fractions Comparison	217
4-9	Cylindrical Channel Flow—Deposition Rates Comparison	218
4-10	Cylindrical Channel Flow—Axial Gas Velocities Comparison	218
4-11	Deposition in a Rotating Disk—Gas Velocity Components	220
4-12	Deposition in a Rotating Disk—Mole Fractions	221
4-13	Deposition in a Rotating Disk—Si Atom Concentrations	222
4-14	Deposition in a Rotating Disk—Experimental Data	222
4-15	Trichlorosilane CVD—Gas Temperatures vs. Axial and Radial Distance	224
4-16	Trichlorosilane CVD—Trichlorosilane Mole Fraction	225
4-17	Trichlorosilane CVD—Silicon Deposition Rate	225
4-18	Trichlorosilane CVD—Mole Fractions	226
4-19	Time-dependent ALD Simulations—PSR, Total Flow Rates vs. Time	230
4-20	Time-dependent ALD Simulations—TMA Contour Plot	230
4-21	Time-dependent ALD Simulations—O Mole Fraction	231
4-22	Time-dependent ALD Simulations—Stagnation-flow Site Fractions	231
4-23	Time-dependent ALD Simulations—O Mole Fractions Comparison	232
4-24	Time-dependent ALD Simulations—Deposition Thickness Comparison	232
4-25	Steady-state Chlorine Plasma—Electron Temperatures vs. Power	235
4-26	Steady-state Chlorine Plasma—Mole Fractions	235
4-27	Steady-state Chlorine Plasma—Cl and Cl ₂ Mole Fractions	236
4-28	Steady-state Chlorine Plasma—ROP Analysis	237
4-29	Spatial Chlorine Plasma—Plasma Power vs. Distance	239
4-30	Spatial Chlorine Plasma—Electron Mole Fraction	239
4-31	Spatial Chlorine Plasma—Cl Mole Fraction	240
4-32	Spatial Chlorine Plasma—Cl ⁺ and Cl ₂ ⁺ Mole Fractions	240
4-33	Spatial Chlorine Plasma—Electron Temperature	241
4-34	Fluorocarbon Plasma Etching of Silicon Dioxide—SiO ₂ Etch Rates Variations	243

4-35	Fluorocarbon Plasma Etching of Silicon Dioxide—10 Highest Mole Fractions	244
4-36	Fluorocarbon Plasma Etching of Silicon Dioxide—Positive Ion Mole Fractions.....	244
4-37	Fluorocarbon Plasma Etching of Silicon Dioxide—Surface Site Fractions	245
4-38	Fluorocarbon Plasma Etching of Silicon Dioxide—Highest ROP	245

1 Introduction



The information provided in this manual describes both CHEMKIN and CHEMKIN-PRO. Feature descriptions that apply only to CHEMKIN-PRO are highlighted with a “CHEMKIN-PRO Only” tag in the heading and a  icon in the margin.

The CHEMKIN® software is designed for modeling many chemically reacting flow configurations. This manual consists of tutorials that illustrate how to use the CHEMKIN Reactor Models to address a variety of problems. The tutorials generally represent realistic situations that might be encountered by practicing scientists or engineers. They have been chosen to demonstrate the wide range of software capabilities, and the different ways CHEMKIN can be used.

In this manual, we address three major categories of chemically-reacting flow problems: Combustion problems are covered in [Chapter 2](#), Catalysis in [Chapter 3](#), and Materials Processing in [Chapter 4](#). Methods for analyzing chemical reaction mechanisms are covered in [Chapter 5](#). For use of the Reaction Path Analyzer, please see the [CHEMKIN Visualization Manual](#). In many cases, the same reactor models are used for simulations in different categories of problems. [Table 1-1](#) lists the tutorials in this manual along with a cross-reference to the Reactor Models employed in that tutorial.



Hint: Before working with the tutorials in this manual, we recommend that users first review [Getting Started with CHEMKIN Manual](#) to become familiar with the operation of the CHEMKIN Interface and the available Reactor Models.

The files for the sample problems have been copied to a location specified by the user during the CHEMKIN installation. On a Windows machine, the default location is `%userprofile%\chemkin\samples2010`. On a UNIX machine, the default location is `$HOME/chemkin/samples2010`. The sample-problem files have a uniform naming convention based on the relevant Reactor Model name combined with a descriptor for that specific system. For example, a project file called `plasma_psr_chlorine.ckprj` uses the Plasma PSR Reactor Model, and involves chlorine chemistry. The data files used for a given sample are located in subdirectories of the `samples2010` directory. For the example project mentioned above, the corresponding chemistry and profile files (if used) would be located in the `samples2010\plasma_psr\chlorine` directory. Sample problems involving multiple models or networks of reactors are treated as separate groups.

In the interest of keeping computational times reasonable, the sample problems generally do not include any of the larger chemical reaction mechanisms that are often used in combustion and plasma research. Some of the mechanisms are included only for the purposes of illustration, and should not be used for scientific research or engineering projects without consulting the current scientific literature.

Table 1-1 Reactor Models Used in Sample Problems

<i>Tutorial</i>	<i>Reactor Models Used</i>
2.1.1 Adiabatic Flame Temperature	Equilibrium Calculation
2.3.1 Steady-state Gas-phase Combustion	Perfectly Stirred Reactor
2.3.2 Autoignition for H ₂ /Air	Close Homogeneous Batch Reactor
2.3.3 Ignition-delay Times for Propane Autoignition	Closed Homogeneous Batch Reactor
2.3.4 Burner-stabilized Flame	Premixed Burner-stabilized Flame
2.3.5 NO Emission from High-pressure Flames with Gas Radiation [CHEMKIN-PRO Only]	Premixed Burner-stabilized Flame Radiation Model
2.3.6 Soot Formation in Radiating Opposed-flow Diffusion Flame [CHEMKIN-PRO Only]	Opposed Flow Flame Radiation Model
2.3.7 Flame Speed of Stoichiometric Methane/Air Premixed Flame with Reaction Path Analyzer [CHEMKIN-PRO Only]	Premixed Flame-speed Calculation Reaction Path Analyzer
2.3.8 Parameter Study: Propane/Air Flame Speed as a Function of Equivalence Ratio and Unburned Gas Temperature	Premixed Flame-speed Calculation
2.3.9 Hydrogen/Air Opposed-flow Flame	Opposed-flow Flame
2.3.10 Flame Extinction Analysis [CHEMKIN-PRO Only]	Extinction of Premixed or Opposed Flow Flame

Table 1-1 Reactor Models Used in Sample Problems (Continued)

<i>Tutorial</i>	<i>Reactor Models Used</i>
2.3.11 Stagnation Flame Analysis [CHEMKIN-PRO Only]	Pre-mixed Stagnation Flame
2.4.1 Homogeneous Charge Compression Ignition (HCCI) Engine	Internal Combustion Engine
2.4.2 Multi-zone HCCI Engine Simulation [CHEMKIN-PRO Only]	Multi-Zone Engine Simulator
2.5.1 Shock-heated Air (Shock)	Normal Incident Shock
2.6.1 Gas Turbine Network	Perfectly Stirred Reactor Plug Flow Reactor
2.6.2 Jet Flame Network	Perfectly Stirred Reactor
2.6.3 Using Tear Streams to Estimate Initial Gas Composition in an HCCI Engine with Exhaust Gas Recirculation (EGR) [CHEMKIN-PRO Only]	Internal Combustion Engine Perfectly Stirred Reactor
2.6.4 Partially Stirred Reactor for Methane/Air	Partially Stirred Reactor
2.6.5 Side Inlet on a Plug Flow Reactor	Plug Flow Reactor
2.6.6 Co-flowing Non-premixed CH ₄ /Air Flame	Cylindrical Shear Flow Reactor
2.7.1 Soot Formation and Growth in a JSR/PFR Reactor [CHEMKIN-PRO Only]	Jet-Stirred Reactor Plug Flow Reactor
2.7.2 Soot Particles in Flame Simulators [CHEMKIN-PRO Only]	Pre-mixed Flame-speed Calculation Opposed-flow Flame
2.7.3 Sectional Method for Particle-Size Distribution with Pre-mixed Laminar Burner-Stabilized Stagnation Flame [CHEMKIN-PRO Only]	Pre-mixed Laminar Burner-Stabilized Stagnation Flame
2.7.4 Simulating Particle-Size Distributions in a Burner-Stabilized Stagnation Flame	Pre-mixed Laminar Burner-Stabilized Stagnation Flame
2.7.5 Detailed Particle Aggregation in a Batch Reactor [CHEMKIN-PRO Only]	Constant Pressure and Given Temperature Batch Reactor
2.8.1 Uncertainty Analysis of NO _x Emissions [CHEMKIN-PRO Only]	Perfectly Stirred Reactor
3.1.1 Two-Stage Catalytic Combustor	Perfectly Stirred Reactor Plug Flow Reactor Honeycomb Reactor
3.1.2 Engine Exhaust Aftertreatment with a Transient Inlet Flow	Perfectly Stirred Reactor
3.2.1 Parameter Study Facility for Surface Chemistry Analysis	Honeycomb Catalytic Reactor
4.1.1 Equilibrium Analysis of Chlorosilane CVD	Equilibrium
4.1.2 PSR Analysis of Steady-state Thermal CVD	Perfectly Stirred Reactor

Table 1-1 Reactor Models Used in Sample Problems (Continued)

<i>Tutorial</i>	<i>Reactor Models Used</i>
4.1.3 Approximations for a Cylindrical Channel Flow	Perfectly Stirred Reactor Plug Flow Reactor Cylindrical Shear Flow
4.1.4 Deposition in a Rotating Disk Reactor	Rotating Disk CVD Reactor
4.1.5 Trichlorosilane CVD in Planar Channel Flow Reactor	Planar Shear Flow
4.2.1 Time-dependent Simulations of ALD Process	Perfectly Stirred Reactor Stagnation Flow CVD Reactor
4.3.1 Steady-state Chlorine Plasma	Plasma Perfectly Stirred Reactor
4.3.2 Spatial Chlorine Plasma PFR with Power Profile	Plasma Plug Flow Reactor
4.3.3 Fluorocarbon Plasma Etching of Silicon Dioxide	Plasma Perfectly Stirred Reactor
5.1.2 Reaction Mechanism for Diamond CVD	Mechanism Analyzer

2 Combustion in Gas-phase Processes

2.1 Equilibrium

2.1.1 Adiabatic Flame Temperature

2.1.1.1 Project Description

This user tutorial presents the use of a gas-phase equilibrium calculation to determine the adiabatic flame temperature for the hydrogen/air system. The adiabatic flame temperature is a measure of the maximum temperature that could be reached by combusting a particular gas mixture under a specific set of conditions. In a real system which includes heat losses, chemical kinetic and/or mass transport limitations, the flame temperature is likely to be lower than the adiabatic flame temperature.

2.1.1.2 Project Setup

The project file is called ***equilibrium__gas.ckprj***. The data files used for this sample are located in the ***samples2010\equilibrium\gas directory***. This reactor diagram consists of a single equilibrium reactor.

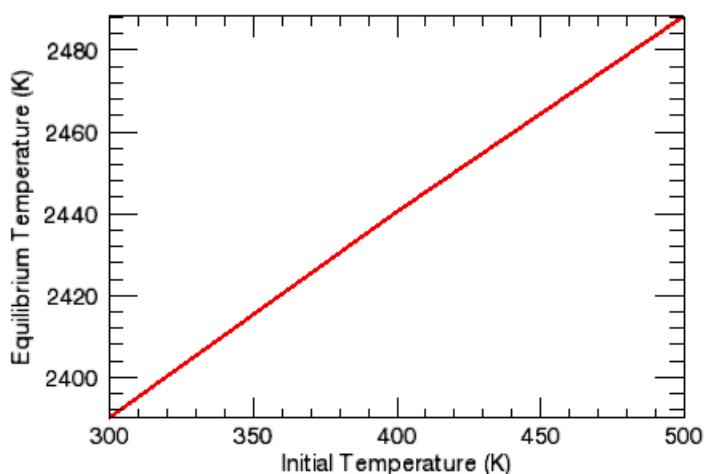
The equilibrium calculation only needs a list of species with their thermodynamic data. There is no need for a reaction list. For this sample problem, the chemistry input file includes only 3 elements: H, O and N; and 9 species: H₂, H, O₂, O, OH, HO₂, H₂O, N₂, and H₂O₂. It is important to include all likely radical species as well as stable species in the product list so as to obtain an accurate flame temperature prediction. For equilibrium calculations generally, it is better to include many unimportant species than to leave out species that may turn out to be important.

Setting up this problem first involves the C1_Equilibrium panel. The problem type (constant pressure and enthalpy), initial temperature (300 K) and pressure (1 atm) are entered on the Reactor Physical Properties tab. An estimated solution temperature of 2000 K is used to help ensure that the solution obtained is for an ignited gas rather than the unburned state. The presence of an estimated solution temperature is often unnecessary for equilibrium simulations but required when a trivial secondary solution may exist. The starting composition is entered on the Reactant sub-tab of the Reactant Species tab. The reactant mixture defines the initial state, which provides the initial moles of chemical species and the initial energy of the system. The Continuations panel is used to specify two additional simulations with increasing initial temperatures.

2.1.1.3 Project Results

Figure 2-1 shows the equilibrium temperatures from these simulations, which represent the adiabatic flame temperatures for a hydrogen/air mixture with a H/O ratio of 2.0. The temperatures are on the order of ~2400 K, and thus clearly correspond to the combusted gas. As expected, these adiabatic flame temperatures increase with increasing initial gas temperature.

Figure 2-1 Adiabatic Flame Temperatures—Hydrogen/Air Mixture



2.2 Using Equivalence Ratio

Many properties of combustion processes strongly depend on the stoichiometry of the combustion mixture. The parameter used most frequently to describe the stoichiometry of the mixture is the equivalence ratio, ϕ . CHEMKIN gives the user an option of describing the initial mixture composition by either of two methods:

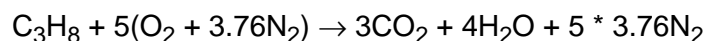
- Listing all of the reactant species and their respective mole or mass fractions.

- Alternately, by identifying fuel, oxidizer and complete-combustion (stoichiometric) product species, the mole fraction of any additional species (such as an inert like Ar or N₂) and the equivalence ratio.

Examples of the use of the equivalence ratio can be found in [Section 2.3.1](#), Steady-state Gas-phase Combustion, and [Section 2.3.8](#), Parameter Study: Propane/Air Flame Speed as a Function of Equivalence Ratio and Unburned Gas Temperature.

2.2.1 Example: Propane in Air

The stoichiometric equation for propane combustion in air is:



Here, the equivalence ratio, ϕ , is defined as the ratio of the actual fuel/oxidizer ratio to the fuel/oxidizer ratio in the stoichiometric equation, as follows:

$$\phi = \frac{X_{\text{C}_3\text{H}_8}/X_{\text{O}_2}}{(X_{\text{C}_3\text{H}_8}/X_{\text{O}_2})_{\text{stoich}}} = 5(X_{\text{C}_3\text{H}_8}/X_{\text{O}_2})$$

CHEMKIN is able to interpret all of the input formats as illustrated in [Tables 2-1 to 2-4](#). Tables [2-1](#) and [2-2](#) illustrate the use of mole fractions to specify mixture stoichiometry and tables [2-3](#) and [2-4](#) illustrate the use of equivalence ratio.

Table 2-1 Reactant Mole Fractions Sum to 1.0

	<i>Name</i>	<i>Mole Fraction</i>
Reactant	C ₃ H ₈	0.04
Reactant	O ₂	0.202
Reactant	N ₂	0.758

Table 2-2 Relative Moles Normalized So Mole Fractions Sum to 1.0

	<i>Name</i>	<i>Mole Fraction</i>
Reactant	C ₃ H ₈	0.2
Reactant	O ₂	1
Reactant	N ₂	3.76

Note that in [Table 2-2](#), the relative moles given will be normalized such that the total mole fractions sum to 1.0. However, it is often more convenient to enter relative moles, as described in [Tables 2-3](#) and [2-4](#), using the equivalence ratio option.

Table 2-3 N₂ as Added Diluent

<i>Equivalence ratio = 1</i>		
	<i>Name</i>	<i>Mole Fraction</i>
Fuel	C ₃ H ₈	1.0
Oxidizer	O ₂	1.0
Added Species	N ₂	0.758
Complete-combustion Product	H ₂ O	
Complete-combustion Product	CO ₂	

Table 2-4 N₂ as Component of Oxidizer

<i>Equivalence ratio = 1</i>		
	<i>Name</i>	<i>Mole Fraction</i>
Fuel	C ₃ H ₈	1.0
Oxidizer	O ₂	1.0
Oxidizer	N ₂	3.76
Complete-combustion Product	H ₂ O	
Complete-combustion Product	CO ₂	
Complete-combustion Product	N ₂	

Note that while using equivalence ratio ([Tables 2-3](#) and [2-4](#)), N₂ can be considered as either an added diluent ([Table 2-3](#)), or a component of the oxidizer, i.e., air ([Table 2-4](#)). If it is considered part of the oxidizer then it must be included in the complete-combustion products list. Also, the oxidizer composition can be given in relative moles or in mole fractions that sum to one (relative moles will subsequently be normalized to sum to 1.0). If using the equivalence ratio input format ([Tables 2-3](#) and [2-4](#)), the mole fraction of fuel is relative to the total number of moles of fuel and the mole fraction of oxidizer is relative to the total number of moles of oxidizer; they will equal to unity unless more than one species is given for each field of fuel and/or oxidizer. However, the “added species” mole fractions are relative to the total number of moles of the reactants, thus the total mole fraction of added species should not sum up to unity or higher.

In general, the equivalence ratio is a good parameter for quantification of mixture stoichiometry for combustion of hydrocarbon fuels (composed only of hydrogen and carbon atoms) in air or in oxygen. However, one has to be careful when applying ϕ to describe fuel stoichiometry for oxygenates (oxygen is chemically bound to the fuel molecule) as well as other non-traditional fuels and oxidizers. Because the definition of the equivalence ratio does not properly account for the oxygen that might be chemically bound in the fuel, it might not be a useful parameter for some fuels.¹

When trying to determine the Complete-combustion or Stoichiometric Products for such fuels, one must remember that a species can be a saturated Stoichiometric Product if and only if the valence orbitals of all of its constituent atoms are filled. That is, if the oxidation numbers of all of the atoms in a given product species sum up to zero.

2.2.2 Example: Stoichiometric Products

Table 2-5 Determining Stoichiometric Products

<i>Element</i>	<i>Oxidation number</i>
C	+4
H	+1
O	-2
N	0
Ar	0

The oxidation numbers of the atoms in CO_2 sum up to $(+4) + 2 * (-2) = 0$ and in H_2O they sum up to $(-2) + 2 * (+1) = 0$ as well, thus CO_2 and H_2O are Stoichiometric Products. However, oxidation numbers of the atoms in O_2 do not sum up to zero $(-2 + -2 = -4)$, thus O_2 can not be entered as a Stoichiometric Product.^{2,3}

1. C. J. Mueller, M. P. B. Musculus, L. M. Pickett, W. J. Pitz, C. K. Westbrook. "The Oxygen Ratio: A Fuel-Independent Measure of Mixture Stoichiometry", *30th International Symposium on Combustion* (2004).
2. D. W. Oxtoby, H. P. Gillis, and N. H. Nachtrieb, *Principles of Modern Chemistry*, Thompson Learning, Inc. (2002).
3. S. S. Zumdahl, *Chemistry*. D.C. Heath and Company, Lexington, Massachusetts (1989).

2.3 Ignition, Flames and Flammability

2.3.1 Steady-state Gas-phase Combustion

2.3.1.1 Project Description

This user tutorial presents the simulation of the steady-state combustion of a mixture of hydrogen, nitrogen, and oxygen in a perfectly-stirred reactor at atmospheric pressure. This project uses the chemistry set for hydrogen combustion, described in [Section 2.9.1](#). This project demonstrates the use of equivalence ratio for specifying the starting gas mixture, as well as the use of a continuation to alter the equivalence ratio.

2.3.1.2 Project Setup

The project file is called *psr_gas.ckprj*. The data files used for this sample are located in the *samples2010\psr\gas directory*. This reactor diagram contains one gas inlet, one perfectly stirred reactor model, and an outlet.

Many of the important parameters for this simulation are input on the C1_PSR panel. On the Reactor Physical Properties tab, the Problem Type is first set to Solve Gas Energy Equation, and the Steady State Solver is chosen. The residence time of the gas in the PSR (0.03 milliseconds), the estimated gas temperature (1700 K), system pressure (1 atm) and volume (67.4 cm³) are also set on this panel. No value is input for the Heat Loss, so the system will be treated as adiabatic. The Species-specific Properties tab provides an input field for an estimate of the gas composition to help the solver converge on a solution. In the current case, no solution estimates are supplied for the species fractions, so an equilibrium calculation will be performed at 1700 K with the reactant mixture to determine the initial estimates for them. These initial estimates are used as the starting point for the iterations that converge to the steady-state conditions.

Parameters pertaining to the incoming gas are input on the C1_Inlet1 panel. In this case, the Stream Property Data tab only has the value of 298 K for the inlet temperature. The gas residence time and reactor volume are input on the Reactor Physical Properties tab of the C1_PSR panel, such that including a flow rate here would over-specify the problem. The Equivalence Ratio box is checked at the top of the Species-specific Properties tab of the C1_Inlet1 panel, and a value for the fuel/air equivalence ratio of 1.0 is supplied. As defined on the Fuel Mixture sub-tab, the fuel is composed of 80% H₂ and 20% N₂. Likewise, on the Oxidizer Mixture sub-tab, the oxidizer is defined as 79% N₂ and 21% O₂ (air). Use of the equivalence-ratio form of input requires that the user specify the products of complete combustion for the Fuel

and Oxidizer specified. This is defined on the Complete-Combustion Products sub-tab. In this case, the product species are H_2O and N_2 , where N_2 is included because it is part of the fuel and oxidizer mixtures. Note that all of the elements contained in the fuel and oxidizer species must also appear in the product species.

For this example, all inputs except Relative Tolerance are left at default on the Basic tab of the Solver panel. We use the default settings, in which the application first solves a fixed-temperature problem and then uses the results of this solution as the initial guess to solve the full problem including the energy equation. On the Advanced tab of the Solver panel, the minimum bounds of species fractions have been specified as smaller than the default, to aid in convergence to a physical solution.

On the Continuations panel, 8 additional simulations are specified where the equivalence ratio is gradually changed. There are no inputs on the Output Control panels for this problem, since default output options will be used.

2.3.1.3

Project Results

[Figure 2-2](#) shows the steady-state temperatures for the combusting hydrogen/air/nitrogen mixture. In this case, the temperature peaks at a fuel/air equivalence ratio of about 1.20. As shown by the molar conversions in [Figure 2-3](#), neither the fuel nor the oxidizer is completely consumed in this combustor, as a result of the PSR residence time.



To get the plot in [Figure 2-3](#), be sure to select the “molar_conversion” in the Select Results panel when the Post-Processor is first launched.

Figure 2-2

Steady-state Gas-phase Combustion—Hydrogen/Air Temperatures

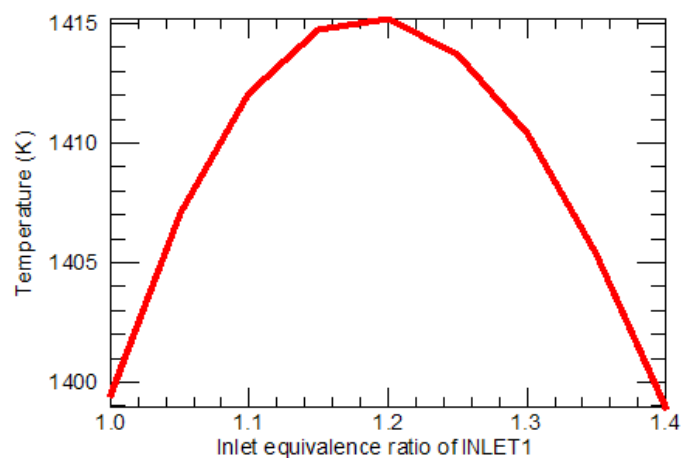
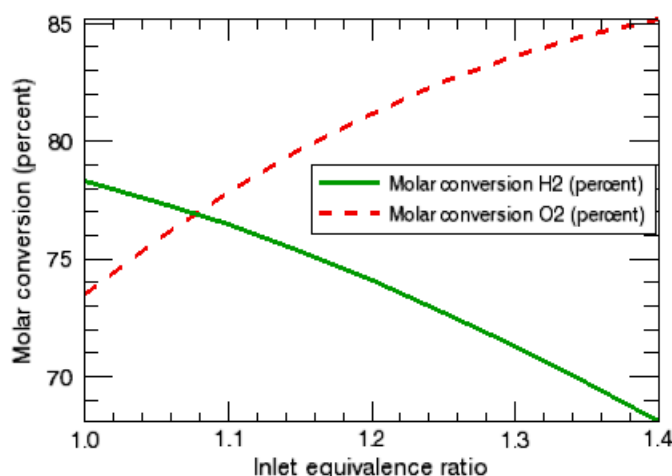


Figure 2-3 Steady-state Gas-phase Combustion—Molar Conversions



2.3.2 Autoignition for H₂/Air

2.3.2.1 Project Description

This user tutorial presents a transient simulation of the spontaneous ignition of a stoichiometric hydrogen/air mixture at constant pressure. This project uses the chemistry set for hydrogen combustion described in [Section 2.9.1](#). Here we are interested in determining the ignition time under a specified set of initial pressure and temperature conditions, assuming no heat loss to the environment (adiabatic conditions). In addition, we would like to determine which reactions contribute most to the CHEMKIN results, using sensitivity analysis. The system is a closed or batch process, so there is no flow of mass into or out of the reactor.

2.3.2.2 Project Setup

The project file is called ***closed_homogeneous_transient.ckprj***. The data files used for this sample are located in the ***samples2010\closed_homogeneous_transient*** directory. This reactor diagram contains only one closed homogeneous reactor.

The Closed_Homogeneous (C1) group of panels become active after running the Pre-Processing step. On the Reactor Physical Properties tab of the C1_Closed Homogeneous panel, first the problem type is selected as Constrain Pressure And Solve Energy Equation (the default). The end time of the simulation is set to 0.0002 sec. The initial temperature (1000 K) is then input, along with the pressure (1 atm). A volume is not specified as it is not important for the results of this simulation, so the default value of 1 cm³ will be used for the initial volume. Since this is a closed homogeneous system, the results in terms of species fraction and temperature will be the same, regardless of the volume value. If surface chemistry were included, the

volume-to-surface ratio would be important, but in this case it is gas only. On the Reactant Species sub-tab, the starting gas mixture is given in relative moles as 2.0 H₂, 1.0 O₂, and 3.76 N₂. Writing it this way makes it easy to see that the O₂/N₂ ratio matches the composition of air, and that the fuel/air ratio is stoichiometric (two H₂ per one O₂). The **Normalize** button will set the mole fractions so that they sum to one, although this is optional, since the normalization will also occur automatically within the program.

The text output file lists a value for the ignition time near the end of the file. The criterion for Ignition Delay is specified using a Temperature Delta of 400 K in the Ignition Delay sub-panel of the Output Control panel. This means that ignition will be registered when the temperature reaches a value of 400 K above the initial temperature. This panel shows other possible definitions of ignition time.

On the Output Control panel, the checkbox for All A-factor Sensitivity has been marked. This results in sensitivities being calculated for all species and all reactions, saved in the XML Solution File, and printed in the output file. This option should be used with care, as the computation time and solution-file sizes increase as a higher power of the size of the reaction mechanism. Except in the case of a very small reaction mechanism, such as the one being used in the sample problem, it is better to use the Species Sensitivity and ROP panel to request that these quantities be output only for a few species of highest interest. Including a value for the Threshold for Species Sensitivity that is higher than the default value of 0.001 will also help keep the amount of information to a manageable level.

There are no Continuations used for this problem.

2.3.2.3 Project Results

Figure 2-4 shows the temperature profile as a function of time for this problem. At the end of this simulation, the temperature is still rising; if it is run much longer, the temperature increases another ~300 K, nearing the adiabatic flame temperature. Although not shown, the volume in this constant-pressure system shows a corresponding increase at ignition. The text output file lists a value for the ignition time of 1.7263E-04 sec, where ignition is defined as the time at which the gas reaches a temperature of 1400 K. *Figure 2-5* shows a close-up of species mole fractions as a function of time. Note that zooming in on the x-axis shows the expected increase in radical species and the products at ignition, along with a decrease in hydrogen and oxygen reactants.

Figure 2-4 Autoignition for Hydrogen/Air—Temperature Profile

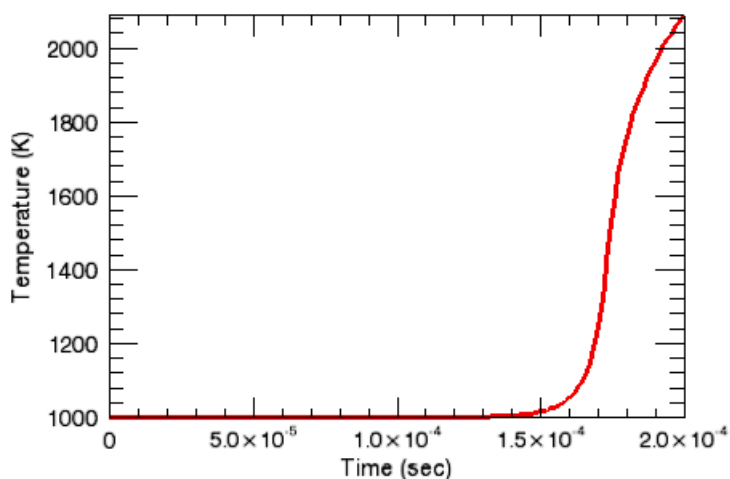


Figure 2-5 Autoignition for Hydrogen/Air—Species Composition Profiles

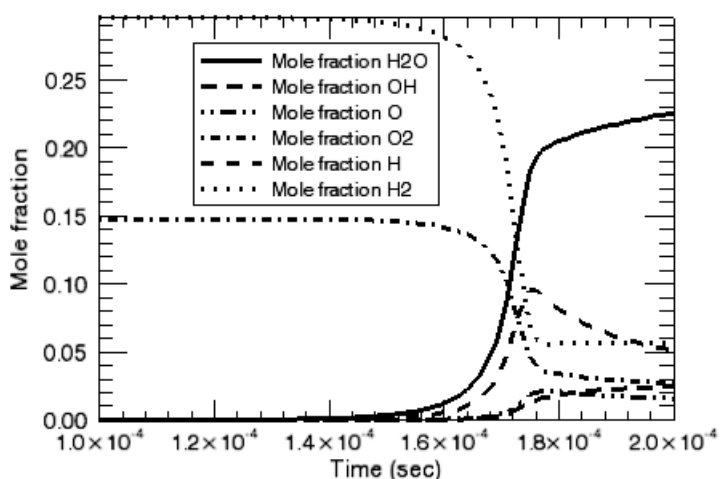
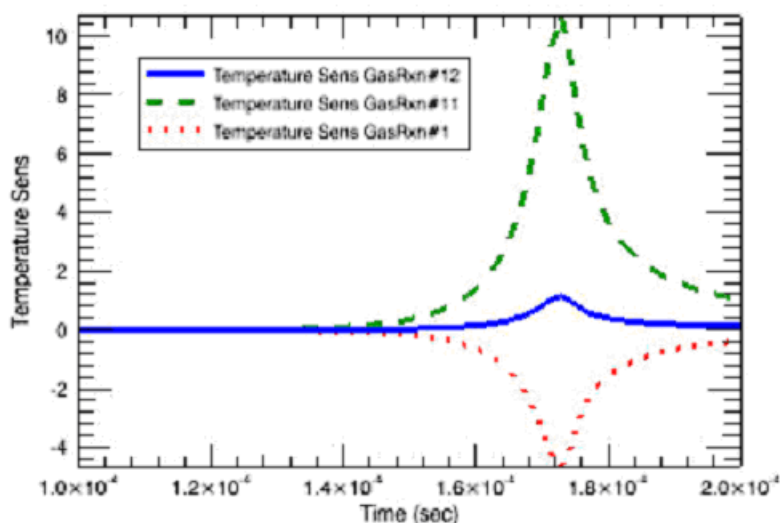


Figure 2-6 shows normalized sensitivity coefficients as a function of time for the four reactions that have the largest effect on the gas temperature. As one might expect, the largest sensitivity occurs near the time of ignition, when the most rapid change in temperature is taking place. The results also show that the dominant reaction for determining the temperature during ignition is the exothermic radical-recombination reaction #11: $\text{O} + \text{OH} \leftrightarrow \text{O}_2 + \text{H}$. The sensitivity coefficient for this reaction is positive, indicating that increasing the rate of this reaction will lead to a higher temperature (more heat production). In contrast, the sensitivity coefficient for reaction #1 is large and negative, indicating that increasing the rate of this reaction will lead to a lower temperature (less heat production).

Figure 2-6 Autoignition for Hydrogen/Air—Sensitivity Coefficients



2.3.3 Ignition-delay Times for Propane Autoignition

2.3.3.1 Project Description

This user tutorial presents an ignition-delay time calculation for the homogeneous, isobaric, adiabatic combustion of propane in air. The ignition times are computed using two distinct definitions. Discrepancies between results are presented.

Premixed combustion technology is well established in the gas turbine industry. One of the major concerns of such technology, however, is avoiding the autoignition phenomenon to protect combustor components as well as to limit levels of pollutant emissions. Numerical predictions of the ignition time can be very useful in understanding the autoignition parameters, which can be important for the automotive and turbine industries. Chemical kineticists can also benefit from predicting ignition times. Work in validation and testing of detailed mechanisms as well as reduction of detailed mechanisms often requires analyzing ignition times. One of the better-known validation techniques for detailed chemical kinetic mechanisms consists of comparing computational predictions of the ignition-delay times to shock-tube experiments.^{4, 5, 6} Such comparisons can provide a good understanding of the underlying chemistry, since the 0-D computations are free from transport effects.

4. Reaction and Ignition Delay Times in Oxidation of Propane, B.F. Mayers and E.R. Bartle, AIAA Journal, V.7, No10, p.1862
5. Validation of Detailed Reaction Mechanisms for Detonation Simulation, E. Schultz and J. Sheperd, Explosion Dynamics Laboratory Report FM99-5, California Institute of Technology, Pasadena, CA, February 8, 2000
6. A Small Detailed Chemical-Kinetic Mechanism for Hydrocarbon Combustion, M.V. Petrova and F.A. Williams, Combustion and Flame, Volume 144, Issue 3, February 2006, p. 526

There are various ways of defining the ignition time, experimentally as well as computationally, for combustion applications. For example, it is often defined as the time at which either the maximum or onset of certain species concentrations is reached, the time at which a specified rate of increase of temperature occurs, the time at which luminous radiant output from the system is first observed, etc. The reported experimental data can vary greatly, depending on which definition was used in the experiments^{5, 7}. Thus, it is often useful to select which ignition-delay time definition should be used in numerical computations. CHEMKIN allows the user such flexibility. For example, in CHEMKIN's closed homogeneous batch reactor, the ignition time can be defined to be the time during which the maximum amount of heat is released during a combustion process (as indicated by the inflection point in the temperature profile), as well as the time corresponding to the maximum of a certain species concentration chosen by the user. CHEMKIN further allows users to input a specific definition of the ignition time via the Ignition Criterion User Routine.

2.3.3.2 Project Setup

The project file is called ***closed_homogeneous_ignition_delay.ckprj***. The data files used for this sample are located in the ***samples2010\closed_homogeneous\ttransient\ignition_delay*** directory. This sample uses the mechanism and thermodynamic data from the University of California, San Diego^{6, 8}. This reactor diagram contains only one closed homogeneous reactor.

Open the project file. After running the Pre-Processor step, on the Reactor Physical Properties tab of the C1_Closed Homogeneous panel, the problem type is selected as Constrain Pressure And Solve Energy Equation (the default). The initial temperature (1200 K) is then input, along with the pressure (1 atm). A volume is not specified as it is not important for the results of this simulation, so the default value of 1 cm³ will be used for the initial volume. Since this is an isobaric closed homogeneous system, the results in terms of species fraction and temperature will be the same, regardless of the volume value. If surface chemistry were included, the volume-to-surface ratio would be important, but in this case only gas-phase chemistry is present. On the Reactant Species sub-tab, the starting gas mixture is given as 0.02 C₃H₈, 0.05 O₂, and 0.93 Ar. These rather dilute conditions are representative of shock-tube experimental conditions.

7. *Combustion Theory*, Second Edition, F.A. Williams, Addison-Wesley Publishing Company, The Advanced Book Program, Redwood City, CA, 1985.

8. <http://www-mae.ucsd.edu/~combustion/cermech/>

The end time is specified on the Reactor Physical Properties panel. It is important to check the resulting output file after the run is complete to make sure that the End Time is large enough to allow for ignition to occur. If no ignition time is provided at the end of the output file, ignition has not yet occurred and the End Time of the simulation should be adjusted.

On the Output Control tab, on the Ignition Delay sub-tab, the Temperature Inflection Point box is checked as well as Species Maximum Fraction, for the computational ignition time criteria. Species Maximum Fraction is set to the OH species. This means the ignition time will be computed based on the maximum of the OH concentration. The user can choose any species from the pull-down menu. The ignition time will also be computed at the point where the rate of change of temperature with respect to time is the largest (Temperature Inflection Point criteria). The user can choose any or all of the definitions of ignition times provided by CHEMKIN.

It is of interest to run the same problem, but vary the initial temperature in order to demonstrate ignition time dependence on temperature as well as its dependence on the chosen ignition time criteria. For this purpose CHEMKIN's Parameter Study Facility is used. The initial Temperature is changed over a range of 1200 - 2600 K. Please refer to the [CHEMKIN Advanced Analyses Manual](#) for guidance in setting up a Parameter Study.

Once the project is run, the ignition times (based on peak OH concentration and temperature inflection point) for the three runs are printed in the text output files and also stored in the solution files, stored in the ***closed_homogeneous_ignition_delay_<date>_<time>*** folder, contained in your working directory. You can look at the output files by clicking on **Click to View Results** under **Run Calculations**, using the Display Detail option.

2.3.3.3 Project Results

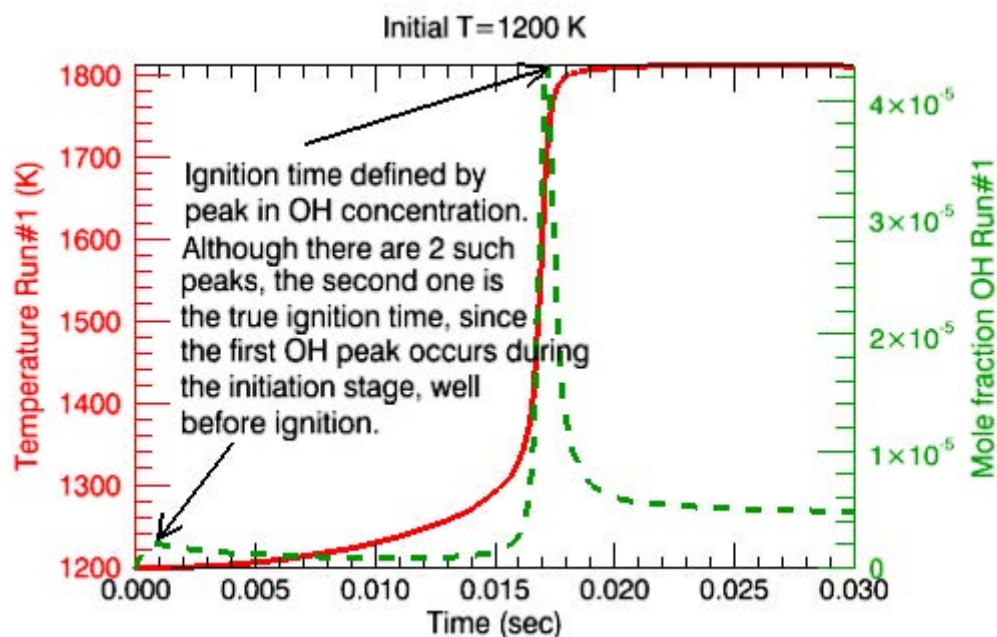
On the Run Calculations panel, click on Display Detail and then on Click to View Results to view the output files corresponding to each temperature. [Table 2-6](#) lists the initial temperatures as well as ignition times based on temperature inflection and OH concentration maximum for some of the runs obtained from the bottom of the output files. The ignition times based on the two criteria differ more and more with increasing initial temperature. Looking at temperature and OH mole fraction profiles will give the user better insight as to how the ignition times are obtained.

Table 2-6 Initial Temperatures and Ignition Times

<i>T</i> [K]	<i>Ignition time</i> [sec]	
	<i>T inflection</i>	<i>OH max</i>
1200	1.69E-02	1.71E-02
1600	1.85E-04	2.11E-04
2600	1.95E-06	9.03E-06

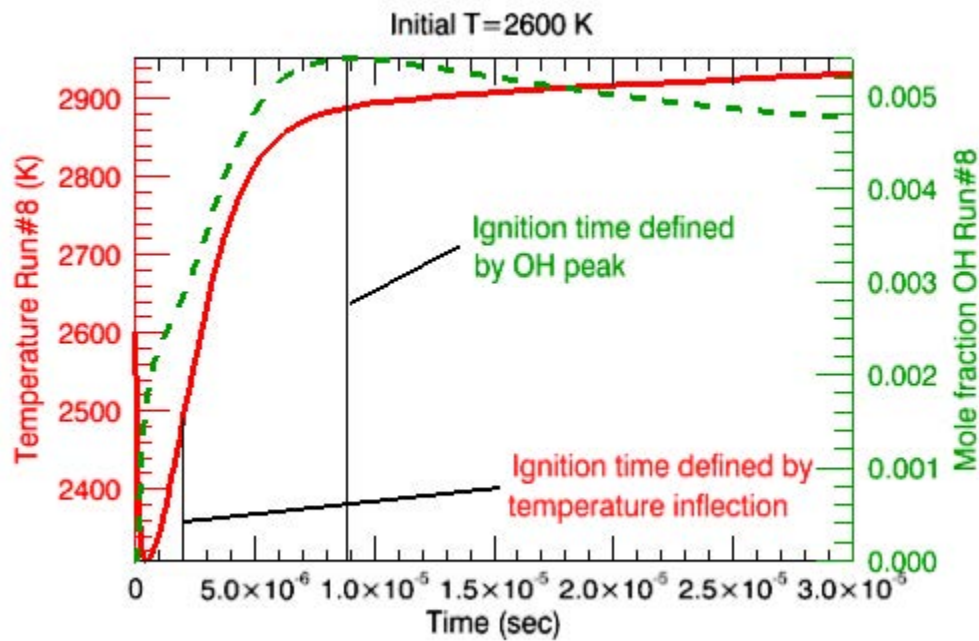
Figure 2-7 shows OH mole fraction and temperature profiles as a function of time, for the 1200-K case, obtained with CHEMKIN's Graphical Post-Processor. The solid line is the temperature profile and the dashed line is the OH mole fraction. There is an obvious spike in OH mole fraction at the time of ignition, which in this lower-temperature case corresponds very nicely to the maximum rate of change of the temperature (the inflection point). This is also a good example of how one should be careful when interpreting numerical results for ignition times. In this example, CHEMKIN produces two numbers for ignition times for the OH mole fraction peak. Only one of these numbers represents the ignition time.

Figure 2-7 Temperature and OH Mole Fraction Profiles as a Function of Time



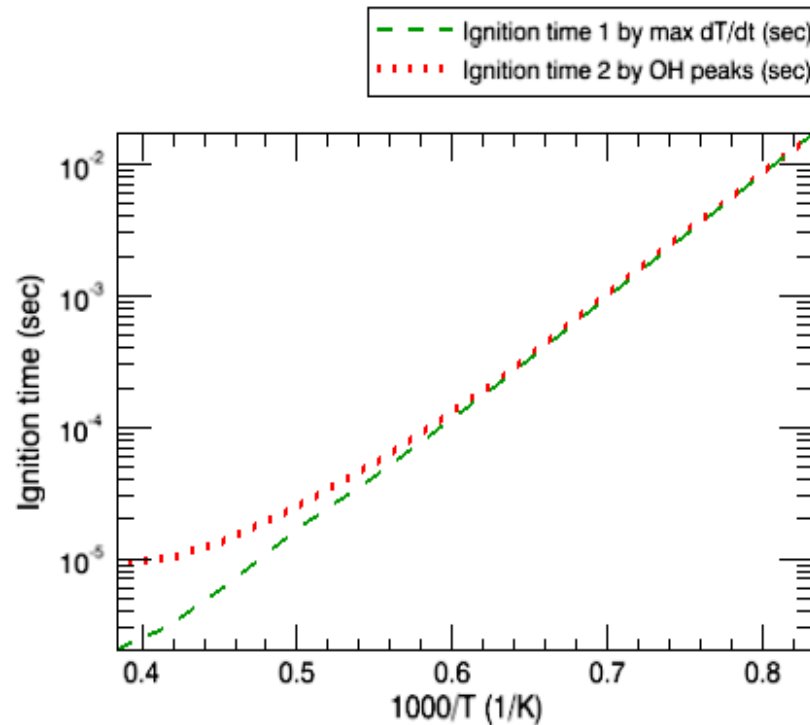
In *Figure 2-8*, there is an obvious difference (about a factor of four) between the ignition time values as defined by the two chosen criteria. This plot demonstrates why one should be mindful of ignition time definitions used in computations. The solid line is the temperature profile and the dashed line is the OH mole fraction.

Figure 2-8 Ignition Based on Varying Criteria



Finally the ignition times vs. the inverse of temperature, are shown in [Figure 2-9](#) on a semi-log plot. Here the difference between the two ignition time definitions is obvious.

Figure 2-9 Ignition Times vs. Inverse of Temperature (Semi-log)



2.3.4 Burner-stabilized Flame

2.3.4.1 Project Description

This user tutorial presents a simulation of a burner-stabilized laminar premixed flame of hydrogen and oxygen at low pressure. This project uses the chemistry set for hydrogen combustion described in [Section 2.9.1](#). Burner-stabilized laminar premixed flames are often used to study chemical kinetics in a combustion environment. Such flames are effectively one-dimensional and can be made very steady, facilitating detailed experimental measurements of temperature and species profiles. Also, laminar flame speed is often used to characterize the combustion of various fuel-oxidizer combinations. Therefore, the ability to model chemical kinetics and transport processes in these flames is critical to interpreting flame experiments and to understanding the combustion process itself. Examples of the use of flame modeling to interpret experimental observations and to verify combustion chemistry and pollution formation can be found in Miller, et al.⁹

2.3.4.2 Project Setup

The project file is called ***pre-mixed_burner__burner_stabilized.ckprj***. The data files used for this sample are located in the ***samples2010\pre-mixed_burner\burner_stabilized*** directory. This reactor model is simple and contains a gas inlet, a premixed-burner reactor, and an outlet.

On the Reactor Physical Properties tab of the C1_ Pre-Mixed Burner panel, the problem type is selected as Fix Gas Temperature because a measured temperature profile is used rather than computing the gas temperatures from the energy equation. For these laminar flames, the gas temperatures are often obtained from experiment rather than by solving an energy conservation equation. This is because there can be significant heat losses to the external environment, which are unknown or difficult to model. For cases where the heat losses are known or negligible, the user can solve a burner-stabilized flame problem in which the temperatures are determined from the energy conservation equation. Even if the energy equation is to be solved for the temperatures, the iteration converges more reliably if the species profiles are first computed using a fixed temperature profile. In any case, the user needs to input an estimate of the temperature profile. For this example, a temperature profile called ***pre-mixed_burner__burner_stabilized_TPRO.ckprf*** is input on the Reactor Physical

9. J. A. Miller, R. E. Mitchell, M. D. Smooke, and R. J. Kee, in *Proceedings of the Nineteenth Symposium (International) on Combustion*, The Combustion Institute, Pittsburgh, Pennsylvania, 1982, p. 181. J. A. Miller, M. D. Smooke, R. M. Green, and R. J. Kee, *Combustion Science and Technology* **34**:149 (1983). J. A. Miller, M. C. Branch, W. J. McLean, D. W. Chandler, M. D. Smooke, and R. J. Kee, in *Proceedings of the Twentieth Symposium (International) on Combustion*, The Combustion Institute, Pittsburgh, Pennsylvania, 1985, p. 673.

Properties tab and only the species transport equations are solved using the temperature as a constraint. The system pressure (25 Torr) is also input on this panel, along with the choice of Mixture-averaged Transport and the use of the Correction Velocity Formalism.

The Ending Axial Position (10 cm) for the simulation is input on the Grid Properties tab of the C1_ Pre-Mixed Burner panel, along with a number of parameters concerning the gridding of the problem. A few of the grid parameters have been changed from the default values. The pre-mixed burner reactor model has adaptive gridding. The initial simulations are therefore done on a very coarse mesh that may have as few as five or six points. After obtaining a solution on the coarse mesh, new mesh points are added in regions where the solution or its gradients change rapidly. The initial guess for the solution on the finer mesh is obtained by interpolating the coarse mesh solution. This procedure continues until no new mesh points are needed to resolve the solution to the degree specified by the user.

The simulation also needs a starting estimate from which to begin its iteration. This estimate is given in terms of a reaction zone in which the reactants change from their unreacted values (the unburned composition) to the products. Intermediate species are assumed to have a Gaussian profile that peaks in the center of the reaction zone with the width such that the profile is at 1/10 of its peak value at the edges of the reaction zone. The user provides estimates for the location and thickness of this reaction zone on the Initial Grid Properties tab of the C1_ Pre-Mixed Burner panel.

Starting estimates for the gas composition in various parts of the flame are input on the Species-specific Properties tab of the C1_ Pre-Mixed Burner panel. The species on the Intermediate Fraction tab are generally short-lived radical species, or species that are expected to be present throughout the flame. The species on the Product Fraction sub-tab are those expected to be present in the fully burned state. If no product species estimates are given, an equilibrium composition will be used for the product estimate. Within the reaction zone the model uses straight lines between the initial and final values for both the reactants and products. On the hot side, the product species are flat at the estimated product values. Note that any given species can be both a reactant and a product species. For example, the nitrogen in an air flame will be both a reactant and a product, while the excess fuel in a rich flame will also be both a reactant and a product.

Parameters pertaining to the incoming gas are input on the C1_Inlet1 panel. The input mass flow rate ($4.6 \text{ mg cm}^{-2}\text{sec}^{-1}$), which corresponds to an experimental value, is the only input on the Stream Properties Data tab. The composition of the fuel-rich input gas (28% H_2 , 9% O_2 and 63% Ar) is input on the Species-specific Data tab of the C1_Inlet1 panel. The Solver panel has some inputs where the default settings are being replaced. There are no additional inputs on the Output Control panel and no Continuations are used for this project.

2.3.4.3 Project Results

[Figure 2-10](#) shows the experimental gas temperature profile as a function of distance imposed on the simulation. The gas composition in [Figure 2-11](#) exhibits the expected behavior of the primary combustion species as a function of distance above the burner, with most of the oxygen reacting away within the first 2 cm. At the larger distances, some of the H atoms recombine to form molecular hydrogen. This would not have been significant in a fuel-poor flame, but does occur in this fuel-rich situation. An inspection of the text file shows that the simulation now has 33 grid points, a significant increase from the initial six. The grid is more dense at the lower distances, as needed to resolve the more rapid changes in chemical composition and temperature occurring in that region.

Figure 2-10 Burner-stabilized Flame—Experimental Gas Temperature Profile

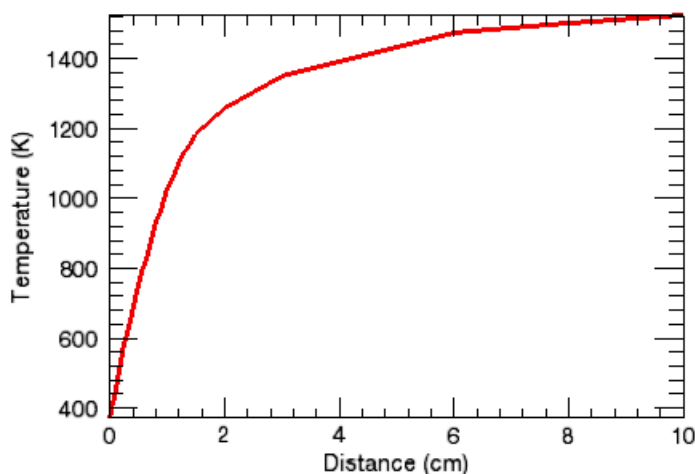
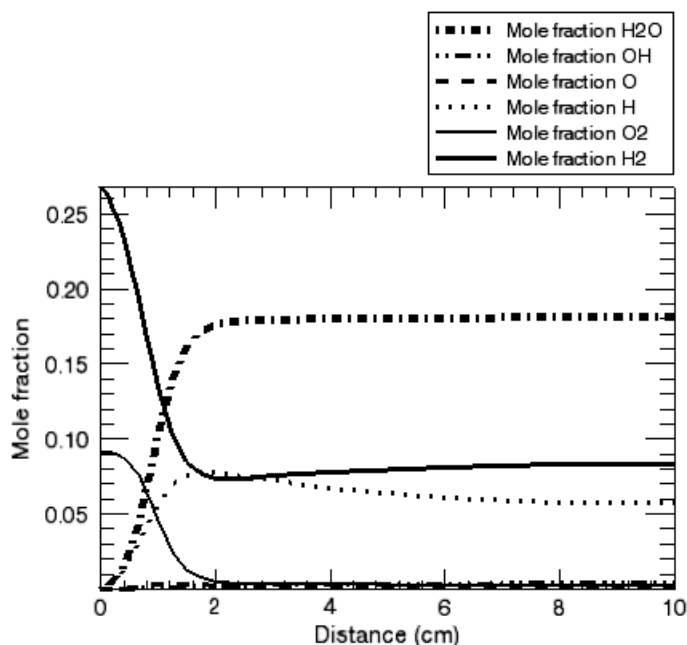


Figure 2-11 Burner-stabilized Flame—Mole Fractions



2.3.5 NO Emission from High-pressure Flames with Gas Radiation [CHEMKIN-PRO Only]

2.3.5.1 Project Description

This tutorial presents a simulation of a burner-stabilized, lean premixed methane/oxygen/nitrogen flame at high pressure. This project uses the chemistry set for the C2_NOx mechanism described in [Section 2.9.6. C2_NOx Mechanism](#). The flame configuration represented in this sample is frequently featured in studies of premixed flame structure and chemistry, because of its simple geometry. Simulations are typically carried out with a fixed temperature profile obtained from the experiments, which minimizes the impact of temperature uncertainties on reaction rates. When a reliable temperature profile is not available experimentally, however, we have to resort to solving the energy equation, either by neglecting heat loss or by estimating the heat loss from the flame to the surroundings. The radiation-model option is a good way to include the first-order effect of heat loss, without having to make extra measurements. This project uses the radiation heat-transfer model option to estimate the radiation heat loss to the environment from gas products in the flame and post-flame region. The optically-thin limit assumed by the radiation model for both gas and dispersed phases is described in the [CHEMKIN Theory Manual](#). This project assumes that CO₂, H₂O, CO, and CH₄ are the only gas species emitting thermal

radiation. Emissivity of individual gas species is expressed as a temperature polynomial and is provided as an optional input of the thermodynamic data. . For this project, the emissivity information is already included in the C2_NOx chemistry set installed with CHEMKIN.

The premixed radiating flames modeled in this project are from the CH₄/O₂/N₂ flames studied by Thomsen et al.¹⁰. The equivalence ratio of the unburned mixture is 0.6, with an N₂-O₂ ratio of 2.2 (this is more oxygen-rich relative to air, where the molar N₂-O₂ ratio of air is 3.76). The pressure of the experiments is 14.6 atm. The goal of this project is to demonstrate the impact of gas radiation on temperature prediction at high pressure and, consequently, on the NO emission predictions.

2.3.5.2 Project Setup

The project file is called *pre-mixed_burner_GasRadiation.ckprj*. The data files used for this sample are located in the *samples2010\pre-mixed_burner\GasRadiation* directory. This sample project consists of a gas inlet, a premixed-burner reactor, and an outlet. Since this is a burner-stabilized flame, the project setup follows similar steps as the burner-stabilized flame project described in [Section 2.3.4](#); please refer to this sample for more information about general set-up instructions. For this tutorial, only the key inputs that are different for this project, i.e., for specifying gas radiation, are discussed.

On the Reactor Physical Properties tab of the C1_Pre-Mixed Burner panel, the problem type is selected as **Solve Gas Energy Equation** because the gas temperature will be computed from the energy equation with radiation heat loss from the gas mixture. This project utilizes the feature for automatic estimation of the temperature profile, such that user input of an estimated temperature profile is not necessary. The unburned gas temperature, however, is a required input and it is set to 360 K for all flames simulated here. Pre-processing of the chemistry set determines whether thermal absorption coefficients are available for any of the gas-phase species in the mechanism. When such coefficients are found during pre-processing, the **Include Gas Radiation** option will appear on the panel and will be activated by default. The **Ambient Temperature** needed by the radiation heat loss calculation is estimated to be **1500 K**. For this experiment, the flame is enclosed in a pressure chamber and there is no active cooling of the wall. For this reason, the temperature to which the flame radiates should be much higher than typical ambient temperatures of open flames. That estimation was made by matching the experimental temperature gradient of an atmospheric flame. If no ambient temperature is given, the default

10. D. D. Thomsen, F. F. Kuligowski, and N. M. Laurendeau, *Combustion and Flame* **119**:307-318 (1999).

value is **298 K**. The gas radiation calculation can be turned off entirely by clearing the check mark in the **Include Gas Radiation** box. It is also possible to exclude certain gas species from the thermal radiation calculation. All gas species for which absorption coefficient data are available in the thermodynamic data file are listed under the Radiating Gas-Phase Species tab on the Species-specific Properties panel. By deselecting a species on the list, its contribution to radiation heat loss will be omitted.

The Pre-mixed Burner-Stabilized Flame model enforces a zero-gradient condition for all variables at the hot boundary by default. While the zero-gradient boundary condition is appropriate for adiabatic flames and for prediction species participating only in the combustion process (i.e., not in emissions formation), it can lead to uncertainties for simulations involving heat loss and slow-forming pollutant species, such as NO. Fortunately, the post-flame region of a burner-stabilized premixed flame behaves almost like a plug flow. In this way, any inaccuracy at the downstream hot boundary is unlikely to propagate very far upstream. Since measurement is usually taken in the vicinity of the flame, the impact of inaccurate boundary treatment can be minimized by increasing the size of the computational domain, moving the boundary constraint away from the flame region. In the experimental facility modeled, the are located within 1 cm from the burner surface. A series of test simulations with various end points indicates that a computational domain greater than 3 cm is sufficient to eliminate impact of the boundary constraint on solution profiles within 1 cm from the burner surface. An ending axial position of 10 cm is used in the simulations and this information is entered on the Basic tab under the Grid Properties panel.

2.3.5.3 Project Results

The experimental NO concentration is reported in the units of ppm @ 15% O₂ wet, which is not a readily available quantity in the CHEMKIN Post-processor. To convert the raw PPM value to these units, the solution must be exported from the Post-processor to a text file so that an external application, such as Excel, could be used to convert NO mole fraction to the correct unit.

The NO concentration corrected to 15% O₂ wet-basis, $X_{NO,15\%O_2wet}$, can be computed from NO mole fraction, using the formulation given by Eq. (15.8) in Turns' combustion textbook¹¹:

$$X_{NO,15\%O_2wet} = X_{NO} \cdot \frac{N_{mix}}{N_{mix,15\%O_2wet}}$$

X_{NO} is the predicted NO mole fraction. N_{mix} and $N_{mix, 15\%O_2 wet}$, respectively, are the total number of moles in “original” and “corrected” mixtures and are defined by Eq. (15.9 a) as¹¹ (p. 44)

$$N_{mix} = 1 + 3.2 \times \left[\frac{2 + X_{O_2}}{1 - 3.2 X_{O_2}} \right]$$

and

$$N_{mix, 15\% O_2 wet} = 1 + 3.2 \times \left[\frac{2 + 0.15}{1 - 3.2 \times 0.15} \right] = 14.23$$

with $x = 1$ and $y = 4$ for CH_4 . Note that the constant 4.76 in Turns' formulation is changed to 3.2 in the above equations because the N_2 - O_2 ratio in this case is 2.2 instead of 3.76 for air.

[Figure 2-12](#) compares gas temperature predictions with and without radiation heat loss to experimental data near the burner surface. The two temperature profiles obtained by the models stay very close to each other and only start to deviate at the flame zone where major radiating species such as CO_2 and H_2O are formed by combustion. The temperature predicted by the adiabatic model, although showing good agreement with the data, remains almost constant behind the flame. In contrast, both experiment and radiation model indicate that the gas temperature decreases gradually in the post-flame region. The axial temperature profile obtained by the radiation model also agrees well with the measurement, but slightly over-predict the heat loss rate, such that the predicted temperature drops faster than observed with the experimental data.

Measured and predicted profiles of NO concentration corrected to 15% O_2 wet are presented in [Figure 2-13](#). The adiabatic model (neglecting radiation) significantly over-predicts NO formation rate and NO level in the post-flame region. Without any temperature decrease in the post-flame region, the adiabatic model finds the NO level increasing constantly and fails to capture the eventual slowdown of NO formation indicated by the experimental profile. The radiation model, predicting a cooler temperature behind the flame, yields an NO profile that is in excellent agreement with the measurement.

11. S. R. Turns, *An Introduction to Combustion: Concepts and Applications*, 2nd Ed., McGraw-Hill, New York, p. 556, 2000.

The substantial difference in NO solution profiles between the adiabatic and the radiation models suggests that thermal radiation in the post-flame region is critical for predicting accurate NO emission from high pressure premixed flames. A follow-up rate-of-production or sensitivity analysis can reveal the NO formation pathways that are affected by the cooler post-flame temperature due to gas radiation.

This project can be easily expanded to study the pressure effect on NO emission from this CH₄/O₂/N₂ premixed flame by setting up a parameter study with respect to pressure (Reactor Properties panel) and inlet velocity (Inlet Stream Properties Panel). [Table 2-7](#) lists inlet velocities for all pressures investigated by Thomsen et al.¹⁰ (p. 42) in the phi=0.6 flame experiments.

Table 2-7 Inlet velocities for pressures studied by Thomsen et al.

<i>Pressure (atm)</i>	<i>Volumetric Flow Rate (slpm)</i>	<i>Inlet Velocity (cm/sec)</i>
1.00	3.50	13.0517
3.05	6.20	7.5804
6.10	9.10	5.5630
9.15	10.95	4.4626
11.90	12.75	3.9954
14.60	14.50	3.7035

NO emission from the phi=0.6 CH₄/O₂/N₂ flame at different pressures are presented in [Figure 2-14](#). Here, the model with radiation continues to show very good agreement with data, over the range of pressures. NO emission values from measurements and predictions are taken at 0.3 cm from the burner surface except for the atmospheric pressure ones, which are at 0.7 cm from the burner surface. The predicted NO emissions shown in [Figure 2-14](#) are obtained by interpolation from the NO solution profiles.



Alternatively, there are two ways to obtain the computed NO value at the exact location where measurement is taken: you can provide an initial grid containing the measurement location (0.3 cm) rather than using the automatic grid option; or you can utilize the continuation option by setting the end point at the measurement location (0.3 cm) in the first run, and then extend the end point to its final location (10 cm) in the continuation run.

Figure 2-12 Axial gas temperature profiles predicted with and without gas radiation heat loss as compared against experimental temperature profile for the $\phi=0.6$ CH₄/O₂/N₂ flame at 14.6 atm.

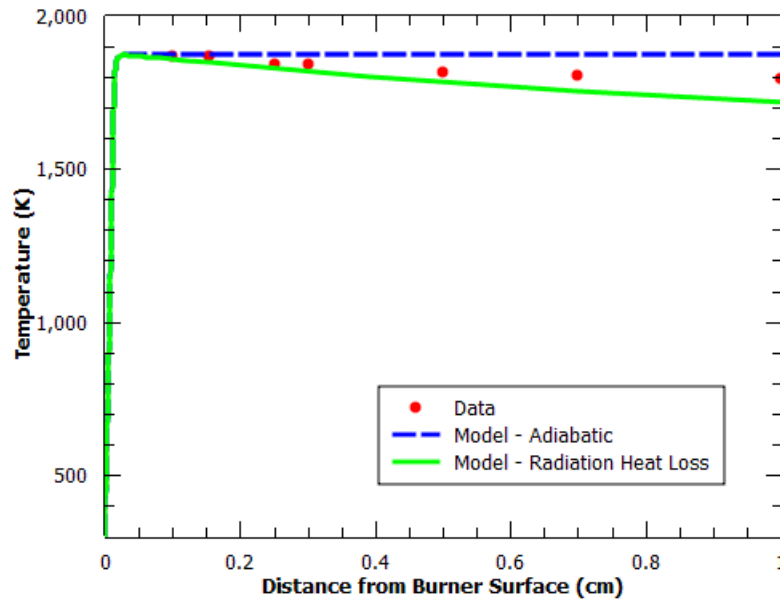


Figure 2-13 Comparisons of measured and predicted NO mole fraction profiles as a function of axial distance from the burner surface for the $\phi=0.6$ CH₄/O₂/N₂ flame at 14.6 atm.

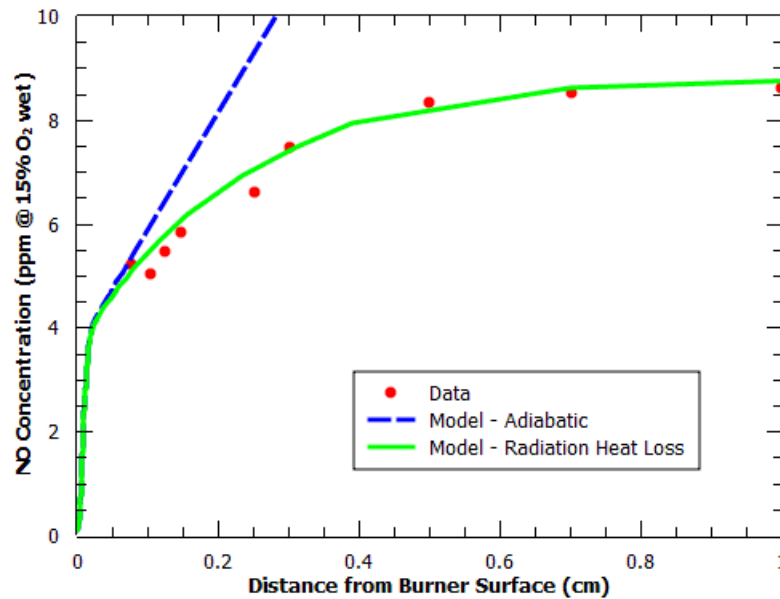
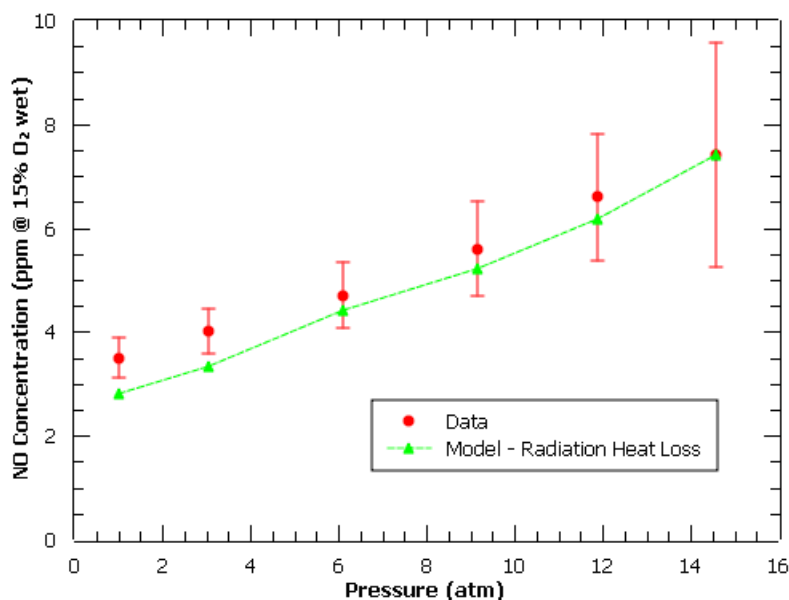


Figure 2-14 Measured and predicted NO concentrations behind the $\phi=0.6$ CH₄/O₂/N₂ flame versus pressure.

2.3.6 Soot Formation in Radiating Opposed-flow Diffusion Flame [CHEMKIN-PRO Only]

This tutorial presents a simulation of a sooting opposed-flow diffusion flame at atmospheric pressure, including the effects of heat loss from radiating soot particles. This project uses the chemistry set for Ethylene/Air Combustion and Soot Formation and Growth as described in [Section 2.9.5](#). Since the fuel stream is diluted with helium, the gas-phase mechanism is modified by replacing all instances of argon with helium. Although this is an approximation, the uncertainties introduced are likely small for the purposes of this project. Opposed-flow flames have been gathering popularity recently as targets for studying soot formation and oxidation, because they offer simple flow fields with no wall interference and can facilitate both non-premixed (diffusion) and premixed flames. Two classes of sooting diffusion flames can be established in the opposed-flow configuration¹². When the flame is located on the oxidizer side of the stagnation plane, soot particles formed on the fuel side of the flame will be carried away from the flame and oxidizer, and a soot formation (SF) flame is created, i.e., soot oxidation is absent. If the flame is instead located on the fuel side of the stagnation plane, soot particles will be pushed towards the flame and oxidizer and a soot formation/oxidation (SFO) flame is produced.

12. J. Y. Hwang and S. H. Chung, *Combustion and Flame* **125**:752-762 (2001).

This project simulates an SF flame (flame 1) investigated by Atreya et al.¹³ The simulation starts from scratch, with no estimated profiles necessary for either gas phase or dispersed phase (soot particle). It is also possible to initiate the calculation from a converged gas-phase-only solution of the same conditions. By adding a surface reaction input file containing soot inception, growth and oxidation, a gas-only simulation could be expanded to predict sooting characteristics of the system. The restart arrangement provides a convenient and efficient method for soot mechanism development because it can be easily adopted into parametric studies of soot formation/growth rate coefficients.

For this project, the radiation heat transfer model is employed to compute the radiation heat loss to the environment from both gas and dispersed phases. The optically-thin limit assumed by the radiation model for both gas and dispersed phases is described in the *CHEMKIN Theory Manual*.

2.3.6.1

Project Setup

The project file is called ***opposed-flow_flame__gas_soot_radiation.ckprj***. The data files used for this sample are located in the ***samples2010\opposed-flow_flame\gas_soot_radiation*** directory. The diagram for this sample project consists of two gas inlets, an opposed-flow flame reactor, and an outlet. Please refer to the *Hydrogen/Air Opposed-flow Flame* tutorial in *Section 2.3.9* for general instructions on setting up an opposed-flow flame simulation. Similarly, procedures regarding soot-particle simulations and the gas radiation model option are available in tutorials for *Soot Particles in Flame Simulators [CHEMKIN-PRO Only]* (*Section 2.7.2*) and *NO Emission from High-pressure Flames with Gas Radiation [CHEMKIN-PRO Only]* (*Section 2.3.5*), respectively. This project focuses on the additional inputs required and results obtained for modeling radiation heat transfer from soot particles within a sooting flame.

The restart file must be specified in the IniSource2 panel of Initialization Data Sets. Use the browse button to select the **Solution File** as ***XMLrestart_opposed-flow_flame__gas_only.zip*** in the working directory. This solution file was obtained by running this project without including the surface reaction mechanism in the chemistry set. The gas-only solution contains 99 gas species and 196 grid points. It is possible to redistribute the grid points in the solution during the restart; however, this option is not used here.

13. A. Atreya, C. Zhang, H. K. Kim, T. Shamim, and J. Suh, *Proceedings of the Combustion Institute* **26**:2181-2189 (1996).

On the Reactor Physical Properties tab of the C1_Opposed-flow Flame panel, the **Problem Type** is selected as **Solve Gas Energy Equation**, because the gas temperature will be computed from the energy equation with radiation heat loss from both the gas and the soot particles. Because absorption coefficient data for CO₂, H₂O, CO, and CH₄ are given in the thermodynamic data file in the chemistry set used in this project, the gas radiation model is activated automatically. The default value of **298 K** is used for the **Ambient Temperature**.

On the Dispersed Phase::CARBON tab, the **Scaling Factor for Moments** under the Basic tab is set to **106**. This factor controls the magnitude of the moment terms in the equations being solved, which helps to improve convergence behavior when considering particle populations that may be very larger or very small. Reduce this scaling factor if more soot is expected in the system, and increase it if less soot is expected. The **Aggregation Model** is turned off in this project to allow focus on the radiation effects. The **Particle Radiation Model** is defined under the tab bearing the same name. Unlike the gas radiation model, the particle radiation model is off by default. Check the box next to **Include Particle Radiation** to activate particle radiation in the simulation. The total particle radiation input parameter is **700 (K⁻¹-m⁻¹)**. This is a semi-empirical parameter that is described in the [CHEMKIN Input Manual](#).

The simulation uses a segregated solver in which gas-phase conservation equations and those of the dispersed phase are solved separately from the particle equations, with iteration to resolve the equation coupling. When the dispersed phase, i.e., soot, is solved, the gas phase properties such as species mass fractions and gas temperature are kept constant, and vice versa. On the Basic tab of the Solver panel, a **Relaxation Factor** of **0.7** is used to speed up the convergence rate of the segregated solver. During the first few iterations between the gas phase and the dispersed phase, the dispersed phase calculation tend to over-estimate surface consumption rates of some PAH species, which could cause mass fractions of these PAH species to become slightly negative in ensuing gas-phase calculation. Therefore, to keep the gas phase calculation from failing, especially for heavily sooting flames, the lower-bounds value for gas species mass fractions must be increased (relaxing the solver constraint) from the default. The **Minimum Bounds on Species Fractions** can be found under the Advanced tab and is set to **-0.01** in this project. The negative mass fraction issue will be corrected in the following iterations as the dispersed-phase solution settles down. Since the gas-species lower-bounds value is very relaxed, it is important to make sure there is no large negative gas species mass fraction in the final solution. It is also necessary to increase the number of pseudo time steps allowed by the steady-state solver. When the dispersed phase is solved for the first time, the steady-state solver might need to take many small time steps to grow the

particle size moments toward values that are more easily tracked by the steady-state solver. Consequently, the **Maximum Number of Pseudo Time Stepping Operation Allowed** is increased from **100** to **3000** to prevent the solver from failing due to this limitation.

2.3.6.2 Project Results

Atreya et al.¹³ (p. 48) reported that the stagnation plane, where axial velocity is zero, and the diffusion flame of Flame 1 in their study are located at 1.23 cm and at 1.93 cm from the fuel side, respectively. Soot particles are observed experimentally between the stagnation plane and the flame. According to the definition of Hwang and Chung¹² (p. 47), this Flame 1 is a typical SF flame. Once the soot particles are created, they will be pushed away from the flame and towards the stagnation plane and from the diffusion flame in this case. Once the soot particles are created, they will be pushed away from the flame by convection, such that no soot oxidation will occur.

The axial velocity profile shown in [Figure 2-15](#) indicates the stagnation plane predicted by the model is at 1.236 cm from the fuel side. This good agreement is a result of adjusting the fuel inlet velocity gradient in the model. Matching the stagnation plane is important, because it ensures that the strain rate in the model is comparable to the one in the experiment, and inlet-velocity gradients are often very difficult to know accurately. From the computed velocity profile, the strain rate is 8.7 sec^{-1} ($1/2$ velocity gradient at the stagnation plane) while the actual value is 5.6 sec^{-1} . While this is ~40% difference, that is considered relatively good agreement (i.e., same order of magnitude), since the strain rate is a particularly difficult and sensitive measurement.

The predicted and measured gas temperature profiles are presented in [Figure 2-16](#). The temperature on the oxidizer side of the flame agrees well with the experimental profile, but the model over-predicts the temperature on the fuel side of the flame. Since all soot particles settle between the flame and the stagnation plane, it is plausible that the particle emissivity used by the radiation model is too low. The predicted peak temperature location is also slightly off towards the fuel side at 1.89 cm.

[Figure 2-17](#) to [2-20](#) compare computed and measured profiles of some major and radical species. In general, the model does well in predicting major species in the system. The OH peak in [Figure 2-19](#) reveals the location and the thickness of the diffusion flame. The Acetylene (C_2H_2) profile in [Figure 2-19](#) and the pyrene (A4) profile in [Figure 2-20](#) show the regions where soot inception and mass growth take place, respectively.

Figure 2-21 compares the predicted soot volume fraction (cm^3/cm^3) against the experimental data as a function of distance from the fuel nozzle. The peak soot volume fraction predicted by the model is about the same as the measurement and the location and the width of the sooting zone agree well with the data. The model also captures salient features of the soot volume fraction profile: a sharp drop in soot volume at the fuel side of the sooting zone, marking the particle stagnation plane, and a gradual decay in soot volume on the opposite side. The soot volume peak coincides with the particle stagnation plane and is on the fuel side of the peak soot inception location, represented by the pyrene peak in *Figure 2-20*. The O_2 and the OH profiles in *Figure 2-17* and *Figure 2-19* suggest that there is no significant O_2 or OH penetration into the sooting zone and that soot oxidation is negligible in this flame.

Figure 2-15 Predicted axial velocity profile of Flame 1 studied by Atreya et al.¹³ (p. 48). The location of (velocity) stagnation plane is indicated by the blue dash-dotted line.

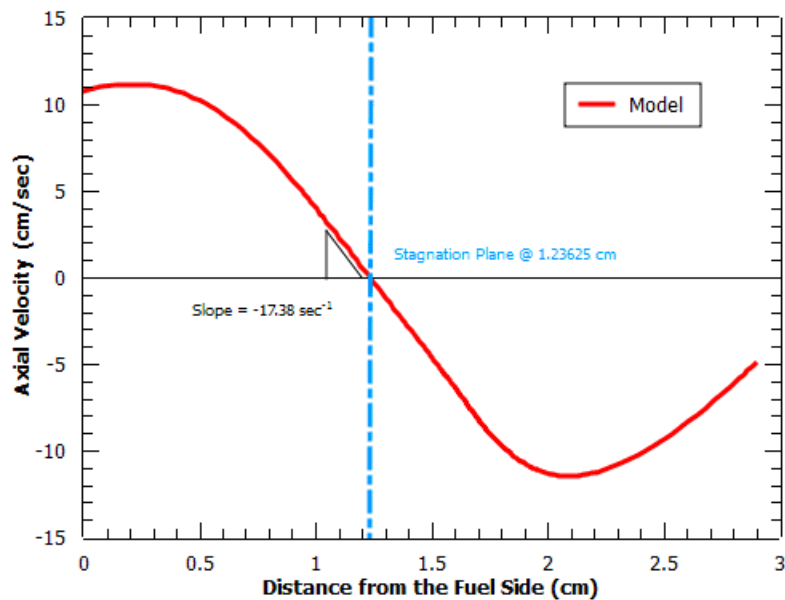


Figure 2-16 Predicted gas temperature profile is compared against the experimental profile for Flame 1 studied by Atreya et al. ¹³ (p. 48).

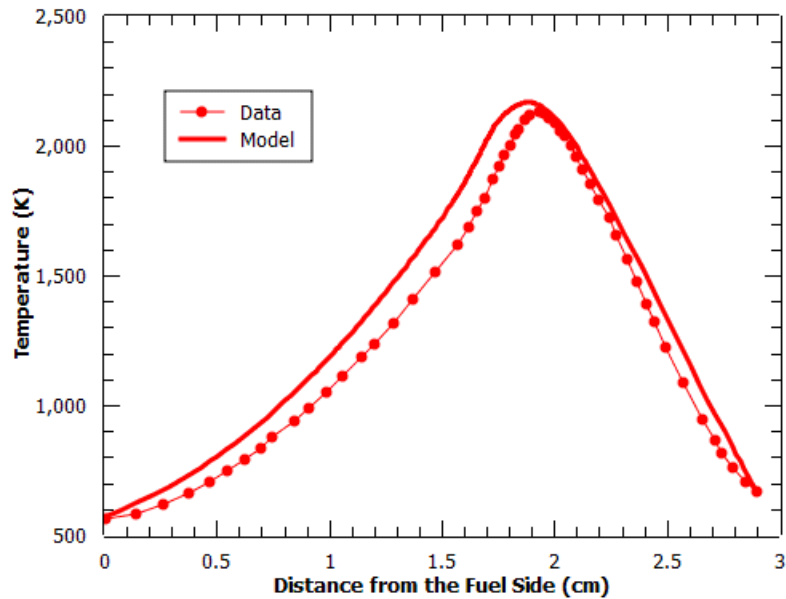


Figure 2-17 Comparisons of predicted and measured fuel (CH_4) and oxidizer (O_2) profiles for Flame 1 studied by Atreya et al. ¹³ (p. 48).

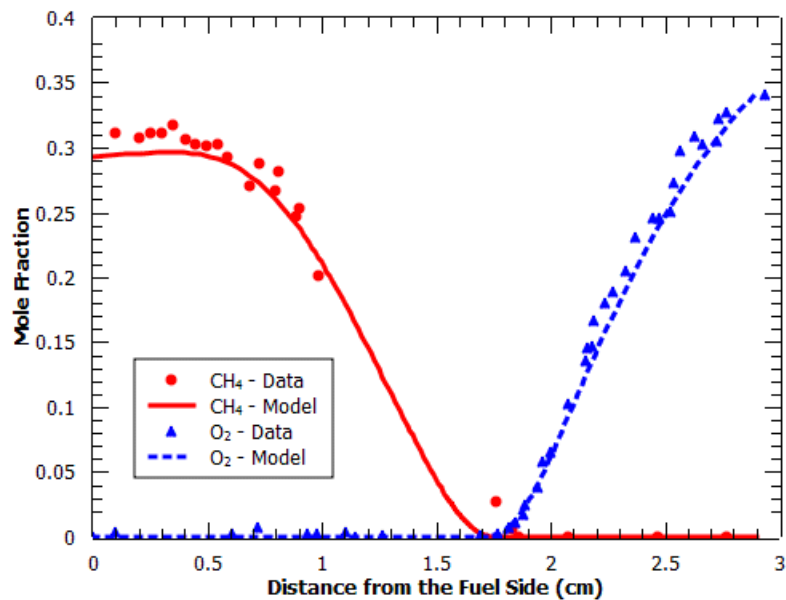


Figure 2-18 Comparisons of predicted and measured profiles of H₂ and CO for Flame 1 studied by Atreya et al. ¹³ (p. 48).

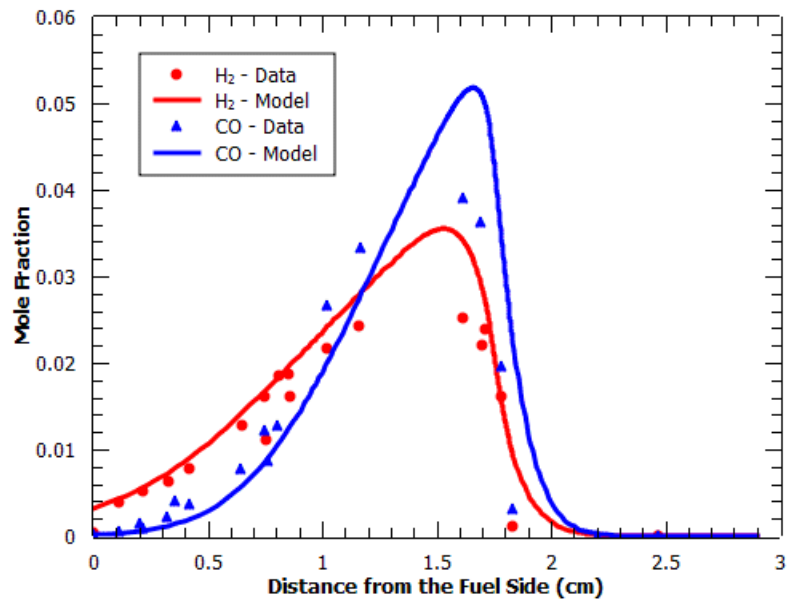


Figure 2-19 Predicted and measured C₂H₂ and OH profiles of Flame 1 studied by Atreya et al. ¹³ (p. 48). The OH peak indicates the flame front and the C₂H₂ peak marks the major soot growth region.

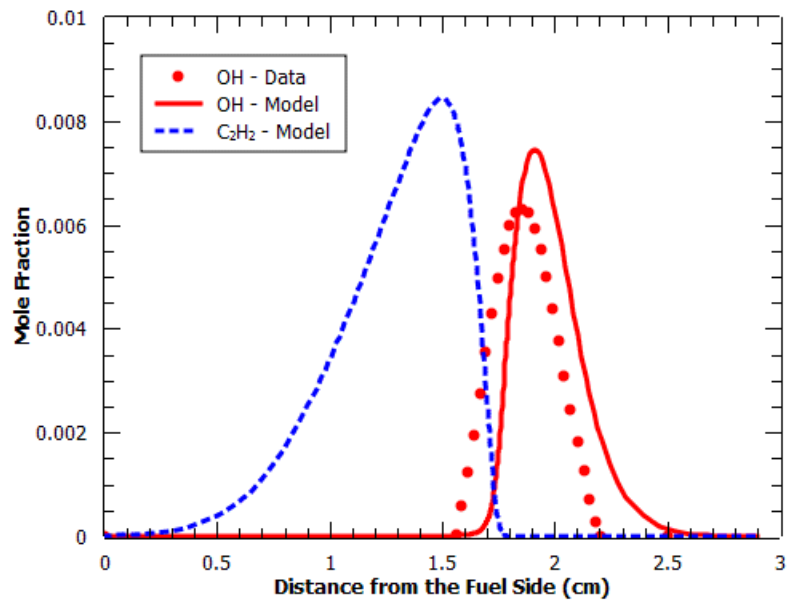


Figure 2-20 Predicted pyrene (A4) profile showing soot inception mainly occurs in the region between the stagnation plane and the diffusion flame in Flame 1 studied by Atreya et al. ¹³ (p. 48).

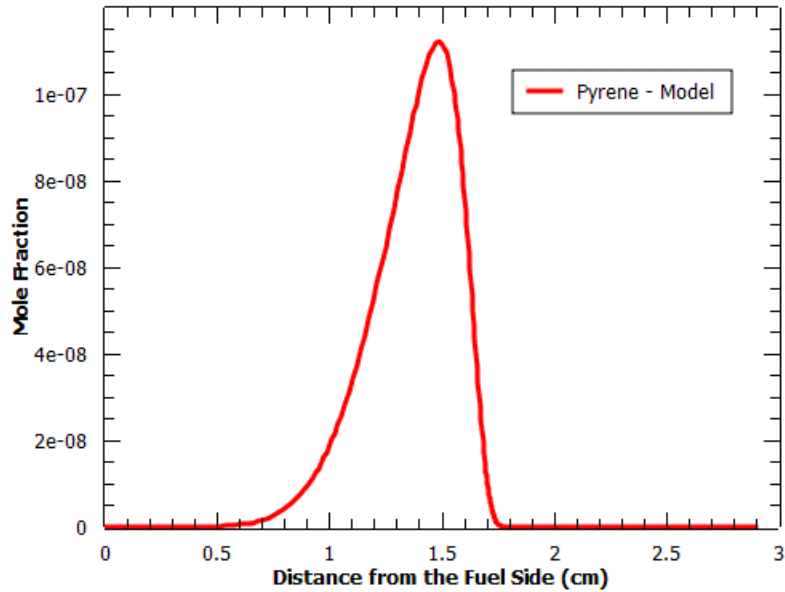
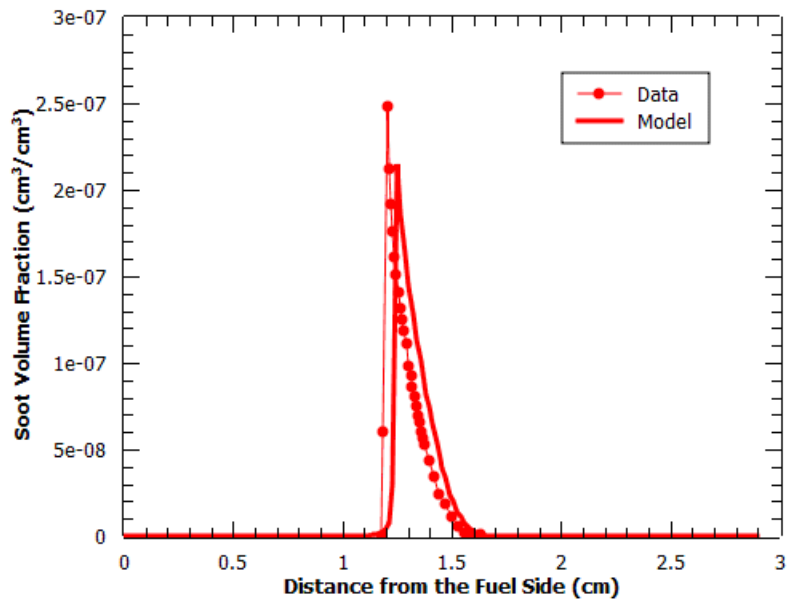


Figure 2-21 Predicted soot volume fraction profile is compared against the experimental profile as a function of distance from the fuel nozzle for Flame 1 studied by Atreya et al. ¹³ (p. 48).





2.3.7 Flame Speed of Stoichiometric Methane/Air Premixed Flame with Reaction Path Analyzer [CHEMKIN-PRO Only]

2.3.7.1 Problem Description

In this tutorial we seek to determine the laminar flame speed and structure of an adiabatic, atmospheric-pressure, freely propagating, stoichiometric methane-air gas mixture, and also use the Reaction Path Analyzer to acquire a visual representation of the connecting reactions that form or deplete chemical species.

To assist in the solution of the freely propagating flame problem, we follow one popular strategy for assuring quick convergence to an accurate solution. This method uses continuations to successively refine the domain and grid of the solution until a desired accuracy and grid-independence is achieved.

2.3.7.2 Problem Setup

The project file for this tutorial is called *flame_speed_freely_propagating.ckprj* and is located in the *samples2010* directory. Since we are not interested in NO_x formation here, we use a skeletal methane-air combustion mechanism to speed up the calculation. As long as it contains all essential steps for methane oxidation under the desired conditions, the skeletal mechanism should yield adequate results while still providing the essential high-temperature chemistry of methane-air oxidation.

The Flame-speed Calculator simulates a freely propagating flame, in which the point of reference is a fixed position on the flame. In this coordinate system, the flame-speed is defined as the inlet velocity (velocity of unburned gas moving towards the flame) that allows the flame to stay in a fixed location, which is an eigenvalue of the solution method (see the [CHEMKIN Theory Manual](#) for details). To set up the flame-speed calculation, we need to specify the properties of the fresh gas mixture. Composition of the unburned methane-air mixture is input on the Species-specific Properties tab of the C1_Inlet1 panel and the initial guess of the mass flow rate on the Stream Properties Data tab. The unburned gas temperature is specified in the Reactor Physical Properties tab of the C1_Flame Speed panel. The pressure and an initial, coarse temperature profile are also input on the Reactor Physical Properties tab of the C1_Flame Speed panel (see [Figure 2-22](#) and [Figure 2-23](#)).

Figure 2-22 Flame Speed—Temperature Profile Panel

Profile: C:\Documents and Settings\kpuduppakkam\chemkin\samples45\flame_speed\freely_propagating\flame_sp...

Distance: **cm**

Start Value: End Value: Number of Values: **Populate**

User-specified Estimated Temperature: **K**

Start Value: End Value: Number of Values: **Populate**

Add Profile Data: Distance User-specified Estimated Temperature **Add**

Distance	User-specified Estimated Temperature
0.0	298.0
0.03	300.0
0.05	400.0
0.06	766.0
0.07	1512.0
0.08	1892.0
0.09	2000.0
0.1	2030.0

Delete Row **Clear**

Import **Export** **Save** **Save As** **Done**

Figure 2-23 C1_Flame Speed—Reactor Physical Properties

C1_Flame Speed (flame_speed_freely_propagating:Flame_Speed (C1))

Reactor Physical Properties | Grid Properties | Species-specific Properties

Skip Intermediate Fixed-Temperature Solution

Use Thermal Diffusion (Soret Effect)

Use Mixture-averaged Transport

Use Multicomponent Transport

Use Correction Velocity Formalism

Use Trace Species Approximation

Unburnt Gas Temperature: **K**

Automatic Estimated Temperature Profile

User-specified Estimated Temperature: **flame_speed_...**

Pressure: **atm**

Optional User-defined Temperature Constraint: **K**

Minimum for Product Estimates: **mole fraction**

Minimum for Estimated Intermediate Fraction: **mole fraction**

Gas Reaction Rate Multiplier:

Use New Scheme For Convective Flux

Use Extrapolation For Species Boundary

First, we establish a fixed-flame coordinate system by explicitly constraining the gas temperature to stay at the initial fixed value at one grid point in the computational domain. The fixed temperature grid-point should be unique and must lie between the unburned temperature and the expected adiabatic flame temperature for the gas mixture. The temperature value to be fixed is specified on the Reactor Physical Properties tab, as the optional user-defined Temperature Constraint. If no value is given for this input, a default value of the average of the unburned temperature and the adiabatic flame temperature is used. An initial guess is required for the temperature profile and for the inlet velocity of the unburned gas (i.e., initial guess of the flame speed that will be calculated). The temperature values used in the profile, except the first point, are estimates, and so only a very rough estimate of the temperature profile is required.

The convergence rate normally is not very sensitive to the initial guess of mass flow rate but a good mass flow rate guess can be very helpful when the equivalence-ratio is close to the flammability limit. Note that the mixing zone width is larger than the initial domain. This is fine as these parameters have relatively little physical meaning, but we find that more spread-out guesses are often more likely to lead to convergence than narrow ones.

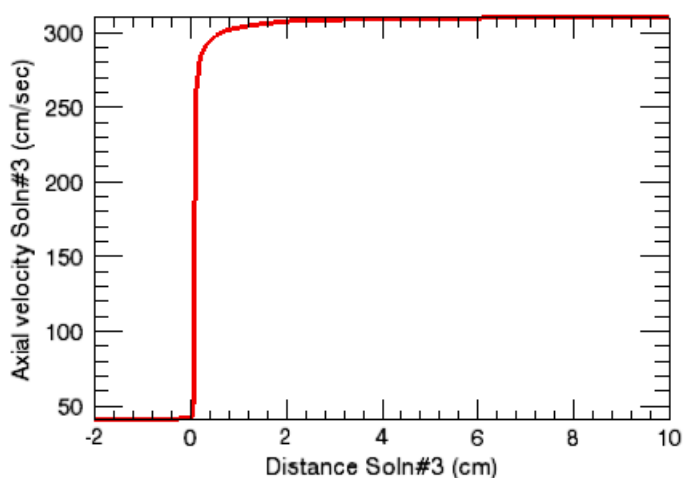
To compute an accurate flame speed, it is important to have the boundaries sufficiently far from the flame itself so that there is negligible diffusion of heat and mass through the boundary. In other words we need to have the domain sufficiently large that the flame is 'freely' propagating, unconstrained by the boundaries of the domain. However, in the solution strategy described here, we start with an initial run on a very coarse grid that contains only a few grid points and a computational domain just wide enough to encompass the flame, and then use continuations to gradually expand the domain until we have a domain-independent solution.

Once we obtain an initial solution on this coarse grid, we expand the domain while reducing/tightening the parameters that control the degree to which the solution gradient and curvature is resolved. We repeat this process a couple of times until the temperature and species slopes at the boundaries are close to zero and both gradient and curvature controls are at least 0.5 or less. The parameters varied during continuations runs are defined in the Continuations panel of the CHEMKIN Interface. The continuation runs start from the solution of the previous run and so rapidly converge to the refined solution.

2.3.7.3 Project Results

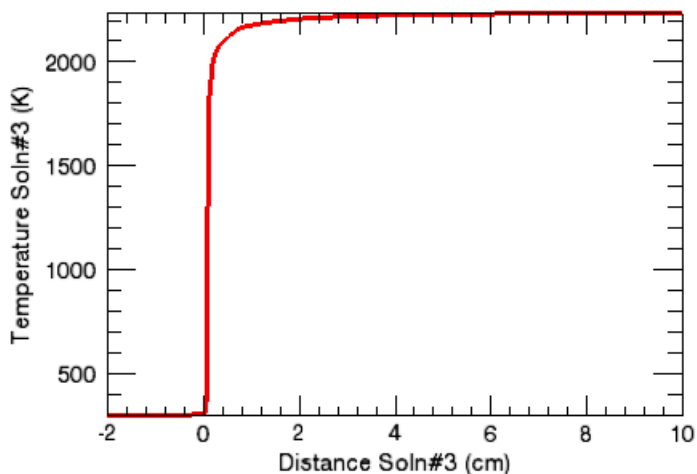
Solutions from the last continuation (solution number 3) are shown in [Figure 2-24](#) and [Figure 2-25](#). The fact that the burned gas temperature of 2234 K ([Figure 2-25](#)) is within 3 K of the published adiabatic flame temperature for these conditions is indicative of the accuracy of the chemistry mechanism used in this simulation. The laminar flame speed by definition is the relative speed between the unburned gas mixture and the flame front. Since the coordinate system is fixed to the flame, all velocity solutions are actually relative velocities with respect to the flame front. Accordingly, the flame speed should be the velocity solution at the point where temperature and composition are the same as the unburned gas mixture. It is important to check the gradients of gas temperature and major species to make sure those values are nearly zero at both boundaries. If there is a non-zero gradient at one of the boundaries, we would need to extend the domain farther to ensure that the assumed adiabatic and zero-diffusive-flux conditions are met. As [Figure 2-24](#) and [Figure 2-25](#) show, however, the species and temperature gradients at both boundaries are sufficiently small that there is no appreciable loss of mass or energy through the boundaries. The predicted flame speed is therefore 41.01 cm/sec, which corresponds to the minimum temperature in [Figure 2-24](#). This value is also reported in the text output file and is available as a result for post-processing of a flame-speed-based parameter study. The laminar flame speed measured by Egolfopolous *et al.*¹⁴ for the stoichiometric methane-air flame at one atmosphere is 36.53 cm/sec. The discrepancy may be due to the simplified kinetics used in the simulation or to potential non-adiabatic conditions in the experimental measurement.

Figure 2-24 Flame Speed—Axial Velocity vs. Distance



14. F.N. Egolfopolous *et al.*, *Proceedings of Combustion Institute* vol. 23 p. 471 (1988).

Figure 2-25 Flame Speed—Temperature vs. Distance

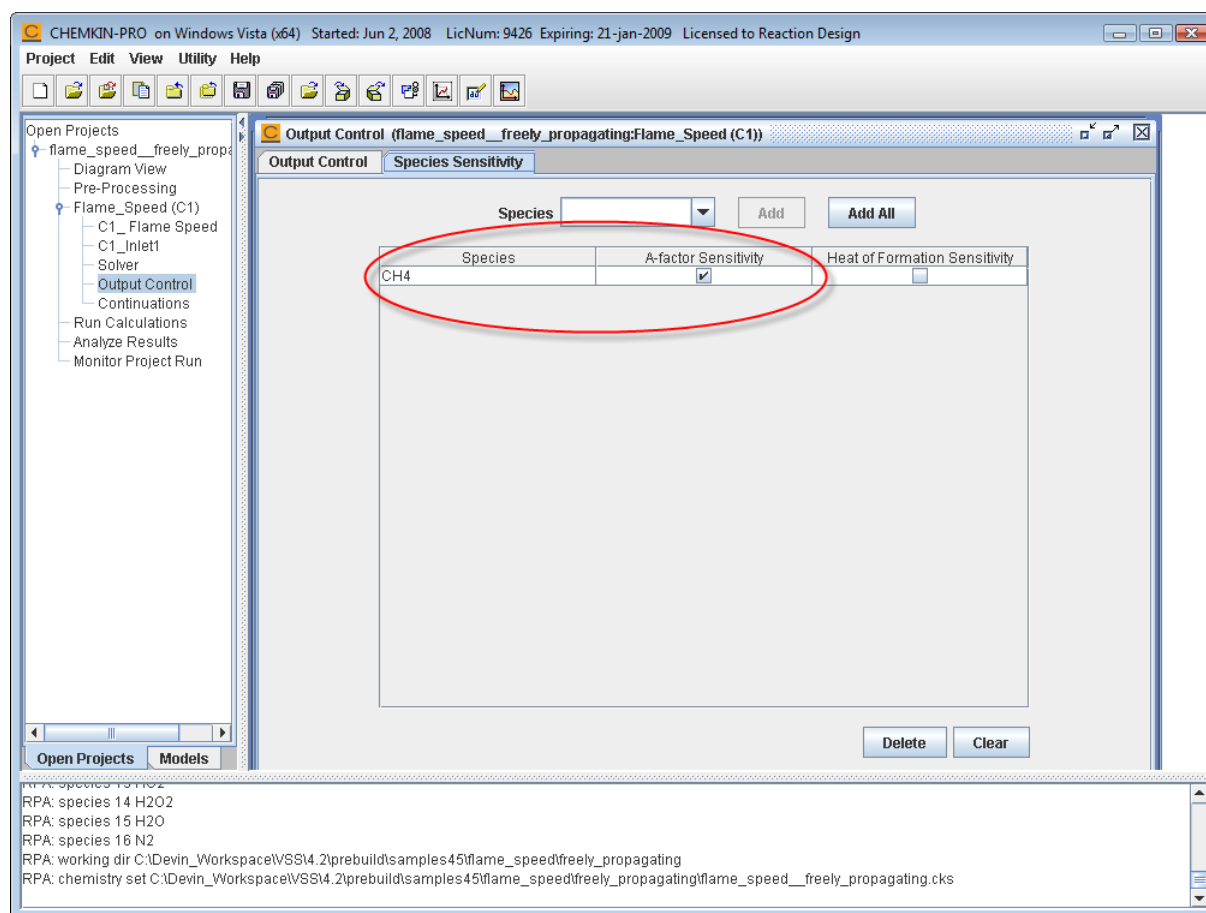


2.3.7.4 Reaction Path Analysis

Applying the CHEMKIN Reaction Path Analyzer (RPA) described in the [CHEMKIN Visualization Manual](#) to the results provides a visual representation of the connecting reactions that form or deplete chemical species. Employing the RPA, the decomposition pathways at different sections of the methane/air flame-speed calculation become evident.

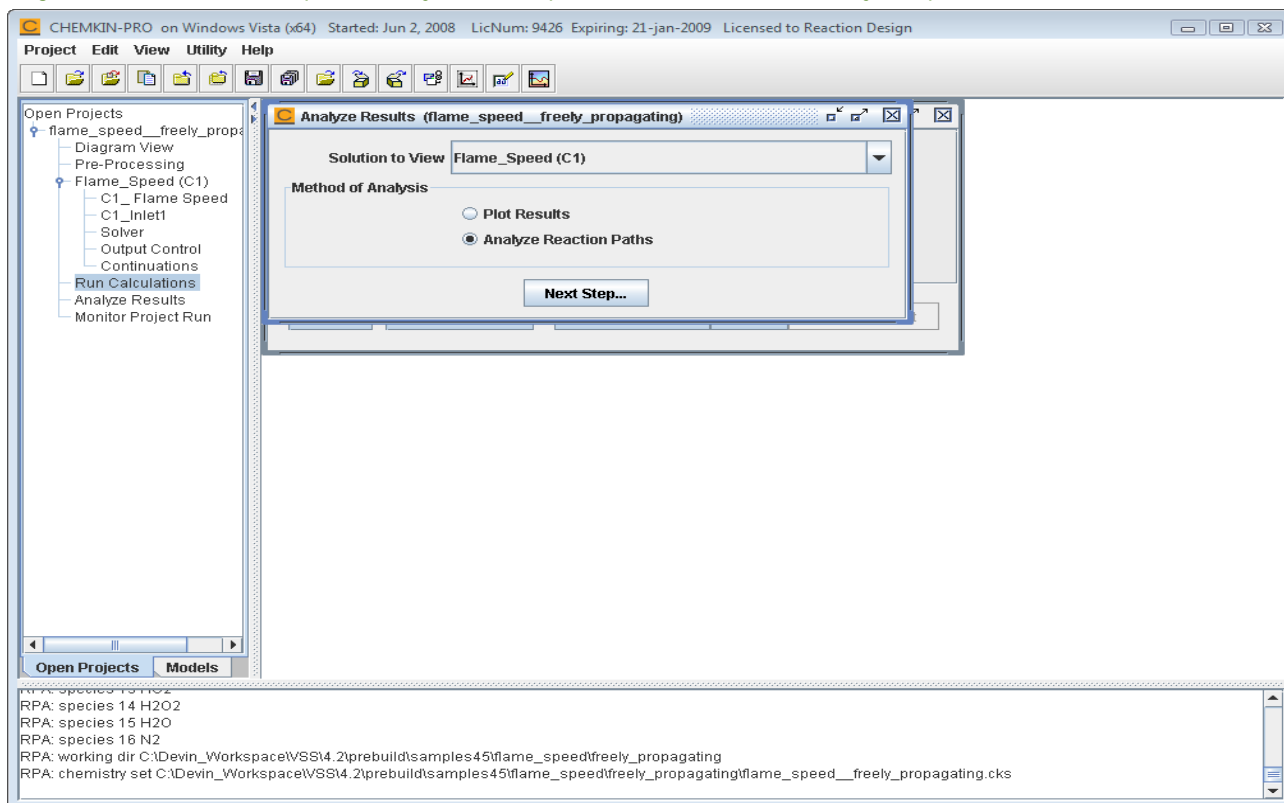
To see the sensitivities on methane, the appropriate output calculation must be added to this sample calculation, as shown in [Figure 2-26](#).

Figure 2-26 Flame Speed—Output Calculation pane with Sensitivity Option.



Begin by selecting **Analyze Reaction Paths** from the Analyze Results panel, as shown in [Figure 2-27](#). In this case, methane was explicitly added in the sensitivities calculations on the Species Sensitivity tab of the Output Control panel. After adding the sensitivity, **Run Calculations** must be double-clicked in the project tree to open the Analyze Results panel with the Analyze Reaction Paths option and **Begin Analysis** button.

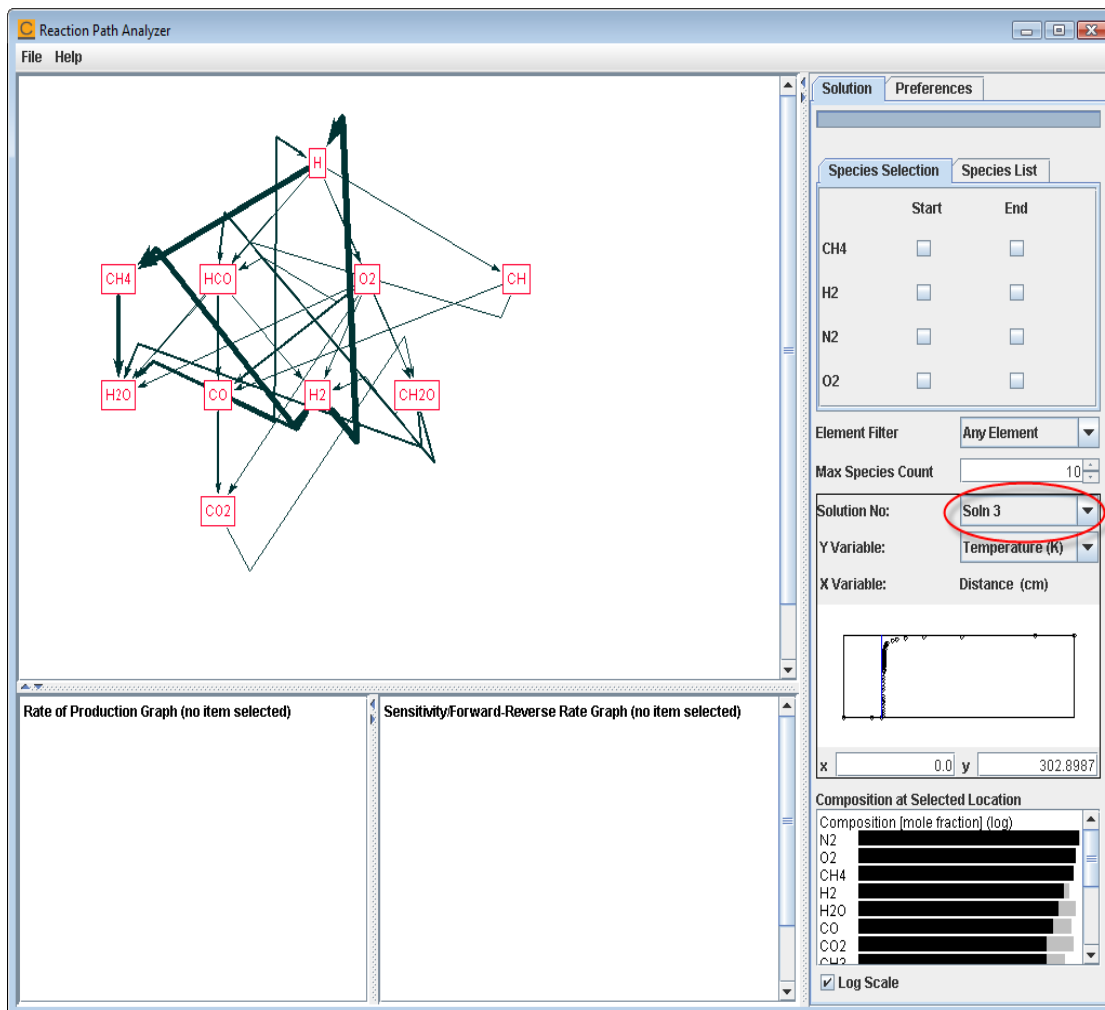
Figure 2-27 Flame Speed—Analyze Results panel with Reaction Path Analyzer option.



Hint: Calculate sensitivities only for the species that most interest you: this decreases the size of the solution and consequently speeds up the RPA.

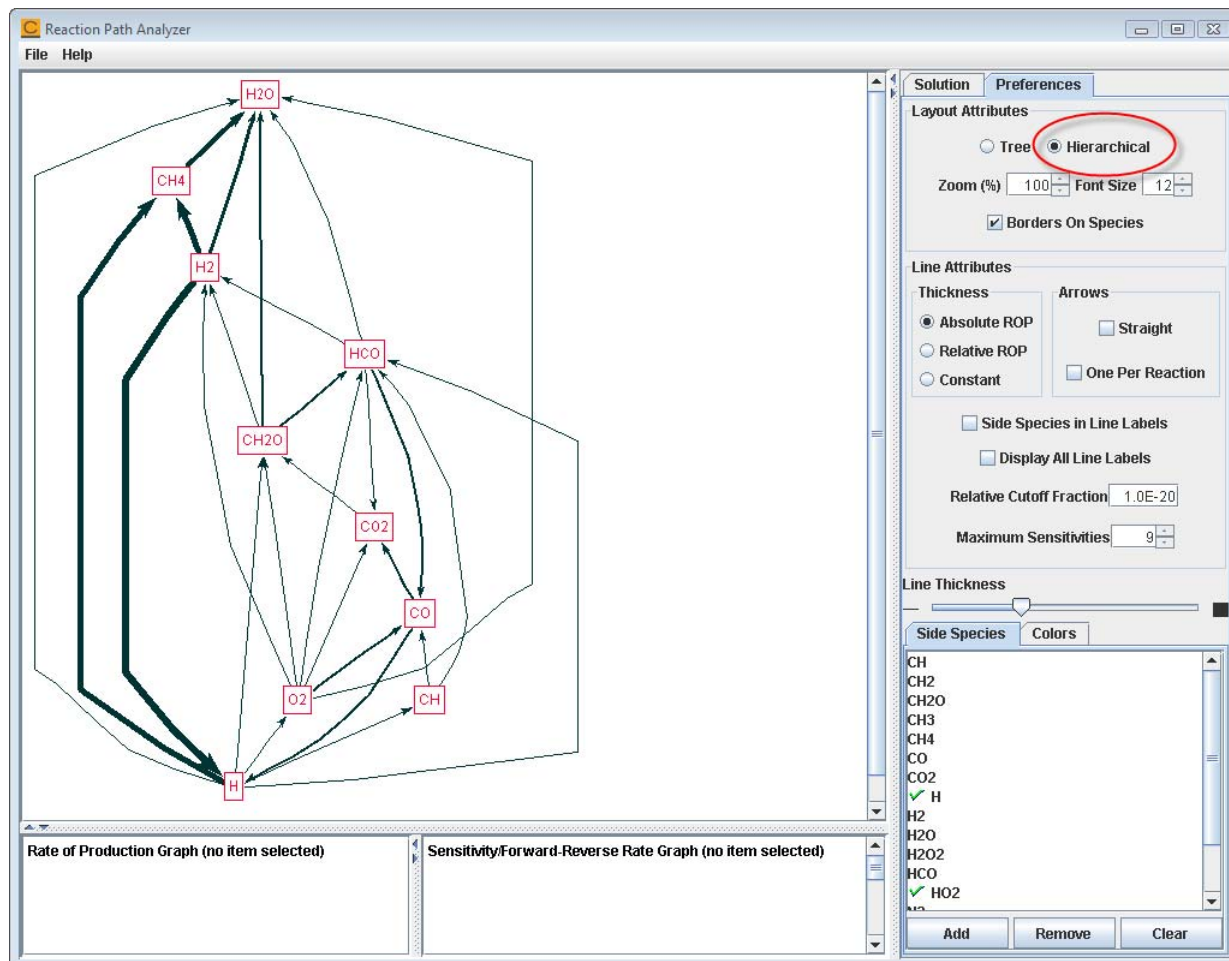
The RPA will then generate the diagram for the initial point in the premixed solution. Clicking in the variable solution plot selects another point in the solution file. Since this project has two continuations with ever-increasing grid resolution, the third solution is chosen to display, as seen in [Figure 2-28](#). The Y variable is also chosen to be temperature, so we can determine where the flame region begins.

Figure 2-28 Flame Speed—Altering the solution chosen, and y variable shown in the solution plot.



On Windows architecture, if the Graphviz option has been selected in the installer, then a Hierarchical layout option is available in the Preferences tab. Selecting the Hierarchical option will change the way that the species are laid out in the diagram.

Figure 2-29 Flame Speed—Switching to a hierarchical layout option.



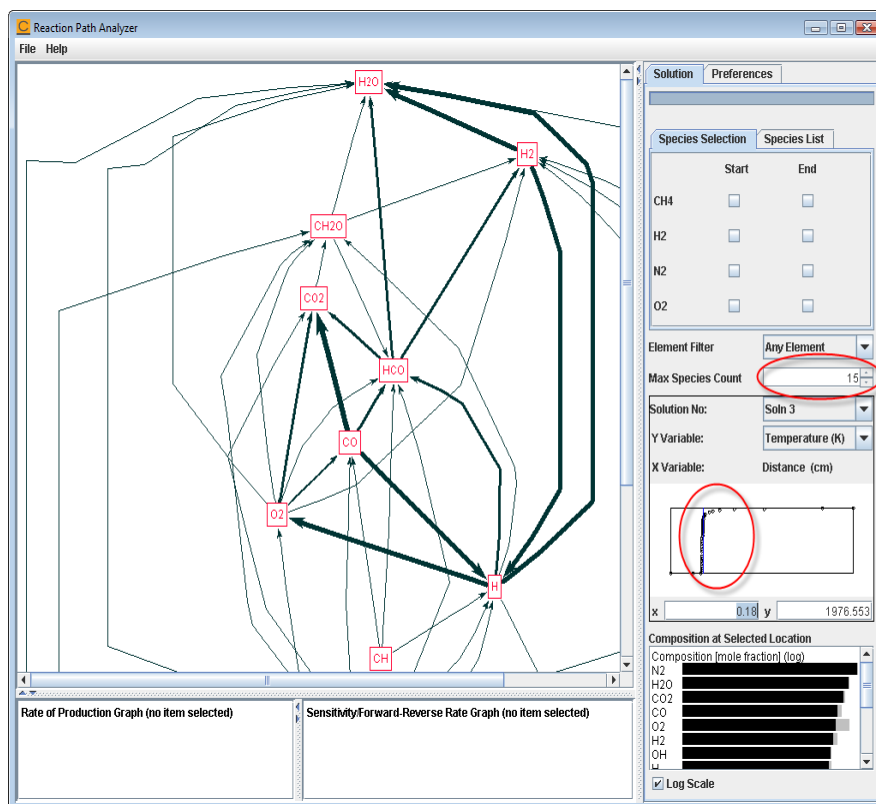
The solution point is altered by entering the value 0.18 into the Distance text field, and the number of species is increased to 15. The complexity of the diagram increases due to the high temperature activation of various reaction channels, as well as an increased number of species allowed in the diagram. Consequently, only a small section of the diagram is currently visible, as seen in [Figure 2-30](#).



Tip: Clicking left and right within the solution plot will decrement and increment the position within the solution. Changing the point will require a reread of the solution file.

Figure 2-30

Flame Speed—Increased complexity in the diagram due to changing the solution point, and increasing the number of allowed species.



A simple method to see the entire diagram is to decrement the zoom setting found under the second tab, labeled Preferences, as shown in [Figure 2-31](#).

Figure 2-31 Flame Speed—Altering the zoom setting to see the contents of the diagram.

The screenshot displays the Reaction Path Analyzer software interface. The main window shows a complex reaction network diagram with nodes and arrows. The Preferences panel on the right is open, and the 'Zoom (%)' setting is highlighted with a red circle, showing a value of 60. Other settings in the Preferences panel include 'Layout Attributes' (Tree and Hierarchical), 'Line Attributes' (Thickness, Arrows, Side Species in Line Labels, Display All Line Labels, Relative Cutoff Fraction, Maximum Sensitivities), and 'Line Thickness'. The 'Side Species' list at the bottom right includes CH, CH2, CH2O, CH3, CH4, CO, CO2, H, H2, H2O, H2O2, HCO, and HO2, with H and HO2 checked.

Reaction Path Analyzer

File Help

Solution Preferences

Layout Attributes

Tree Hierarchical

Zoom (%) 60 Font Size 12

Borders On Species

Line Attributes

Thickness

Absolute ROP Straight

Relative ROP One Per Reaction

Constant

Side Species in Line Labels

Display All Line Labels

Relative Cutoff Fraction 1.0E-20

Maximum Sensitivities 9

Line Thickness

Side Species Colors

CH
CH2
CH2O
CH3
CH4
CO
CO2
✓ H
H2
H2O
H2O2
HCO
✓ HO2

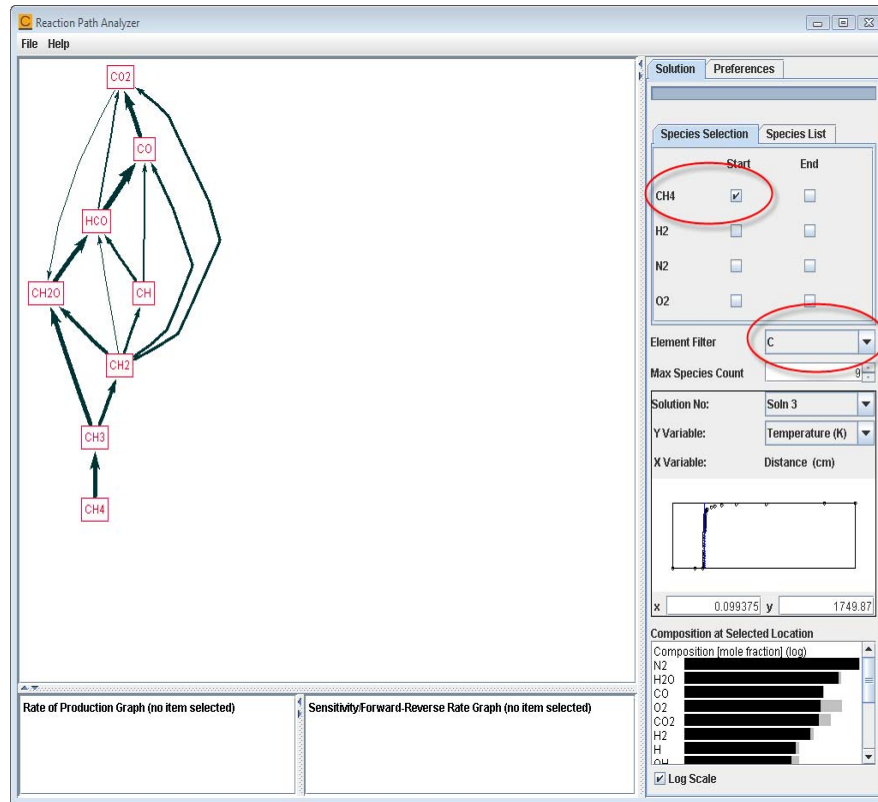
Add Remove Clear

Rate of Production Graph (no item selected)

Sensitivity/Forward-Reverse Rate Graph (no item selected)

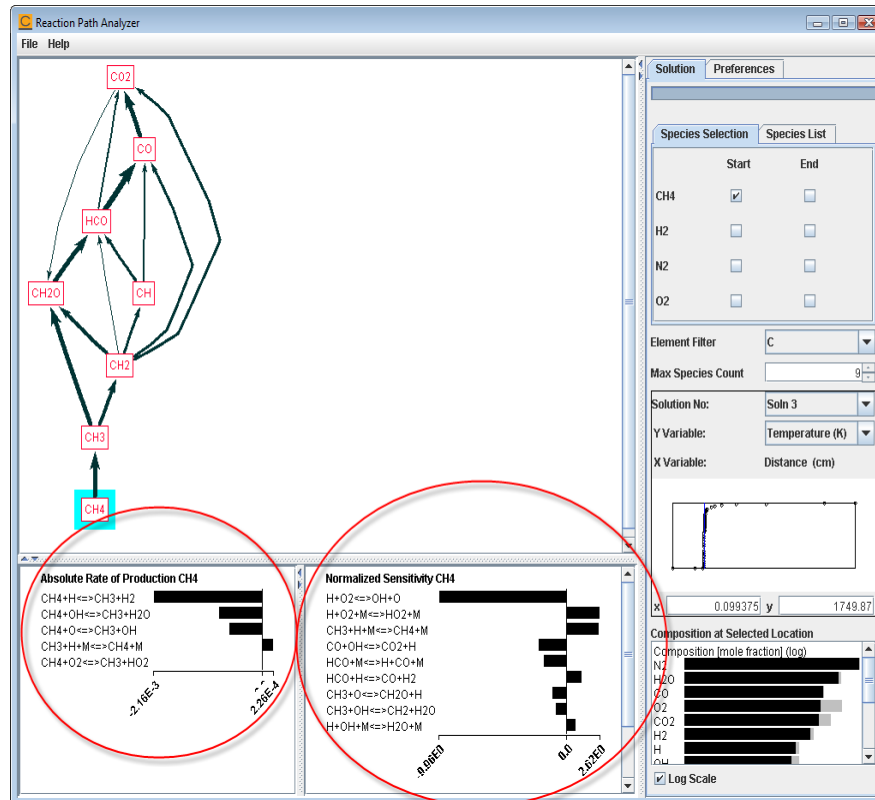
Back near the colder side of the flame, the diagram is altered to focus on the decomposition pathway of methane, and the number of species is reduced back to ten. This results in a simpler diagram that follows the major pathways flowing out from methane, as shown in [Figure 2-32](#). Additionally, a C element filter is applied, restricting the kind of species displayed in the diagram to those containing Carbon.

Figure 2-32 Flame Speed—Decomposition pathways starting with methane.



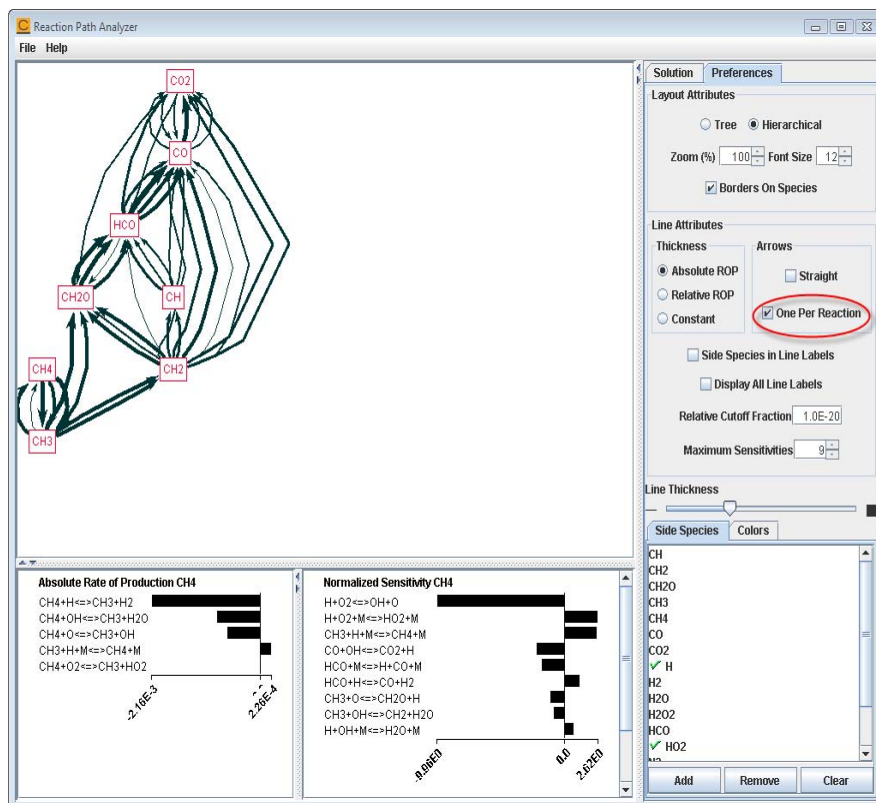
Clicking on the methane species in this diagram creates two plots, as shown in [Figure 2-33](#). The first plot describes the Rates of Production of all reactions that influence the composition of methane at this solution point. The second plot shows the Sensitivity of the selected species, in relation to the rates of the reactions within the mechanism.

Figure 2-33 Flame Speed—The Rate of Production and Sensitivity charts of methane.



Each connection can be split into constituent reactions. This way each reaction is represented on the screen, explicitly illustrating the contributions, as shown in [Figure 2-34](#).

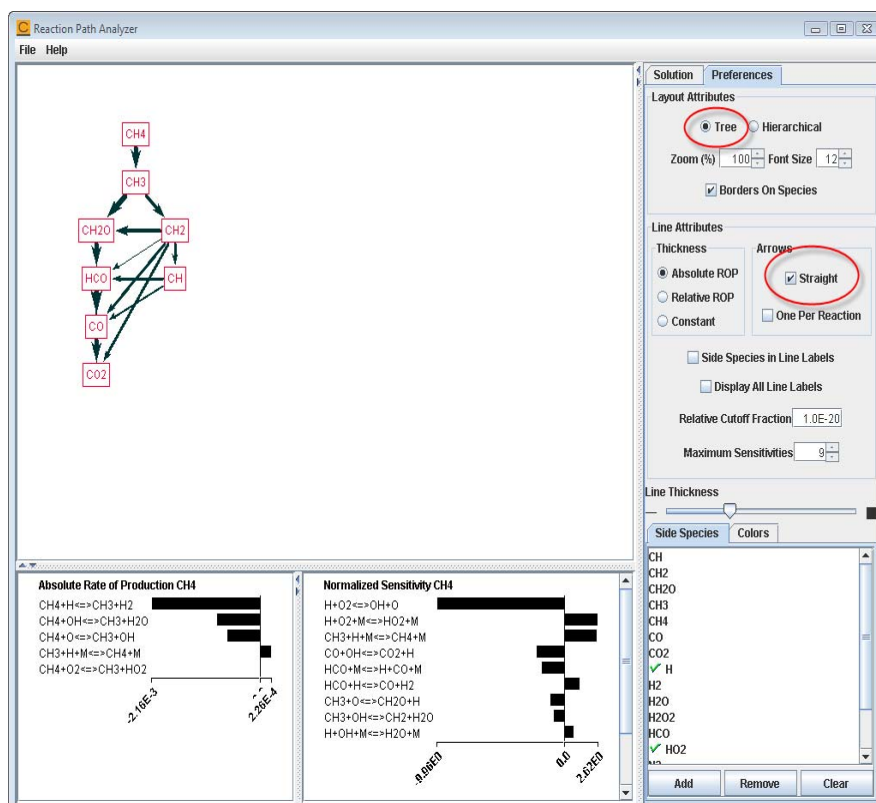
Figure 2-34 Flame Speed—Splitting a composite reaction pathway into one per reaction.



A relative rate analysis can be accomplished while each reaction is split. This kind of analysis will scale the width of exiting arrows relative to the total of all reactions depleting a species. This scaling helps to determine which reaction has the largest influence on the removal of a species locally. The absolute rate analysis will scale every reaction pathway relative to a single global value.

The default layout method, the tree format, is available, which graphically illustrates decomposition as the downward flow of a species. A selected start species is chosen and the other species are laid out in generations from the selected root, as shown in [Figure 2-35](#).

Figure 2-35 Flame Speed—Tree layout method of the decomposition of methane.



Tip: On the Preferences panel, using the **Straight** line option compresses the diagram and makes it easier to manage.

A second way to decrease the complexity of a diagram is to, for example, remove one branch of a bimolecular reaction product. This can be done by specifying one of the reaction products as a side species. A side species is one that may be important to a reaction, but for some reason should not be drawn explicitly in the diagram. For

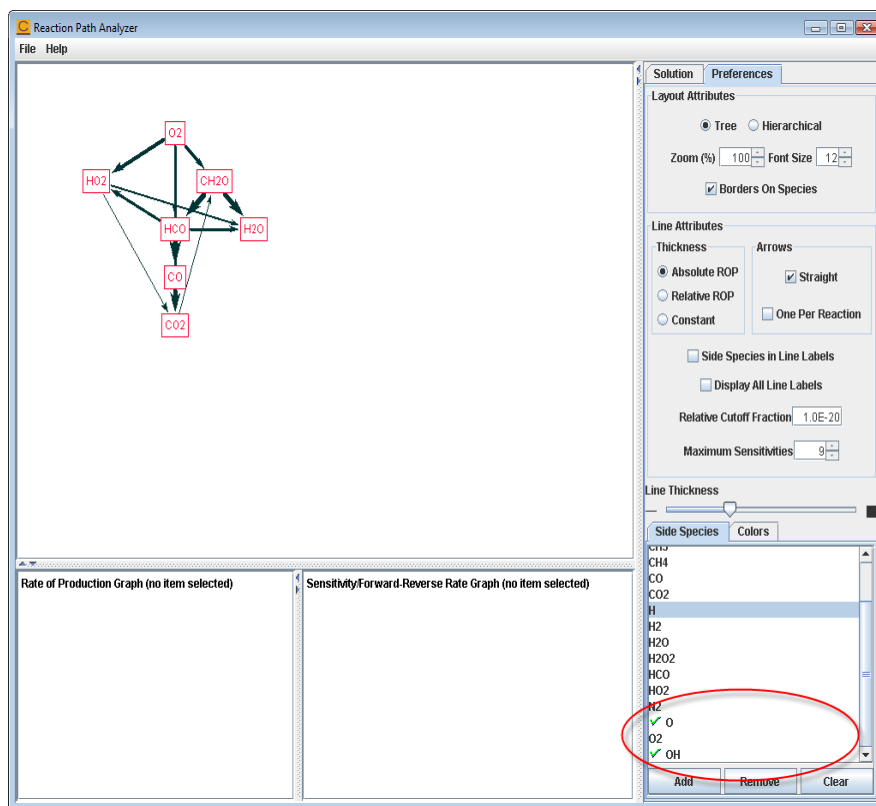
example, in [Figure 2-36](#) the hydroxide radical and oxygen radical are chosen as side species. Consequently, the hydroxide radical will not be drawn in the diagram. The other two default side species (H and HO₂) were removed from the side species list for this example.



Tip: If a species appears isolated from the others on the diagram, try decreasing the Relative Cutoff Fraction.

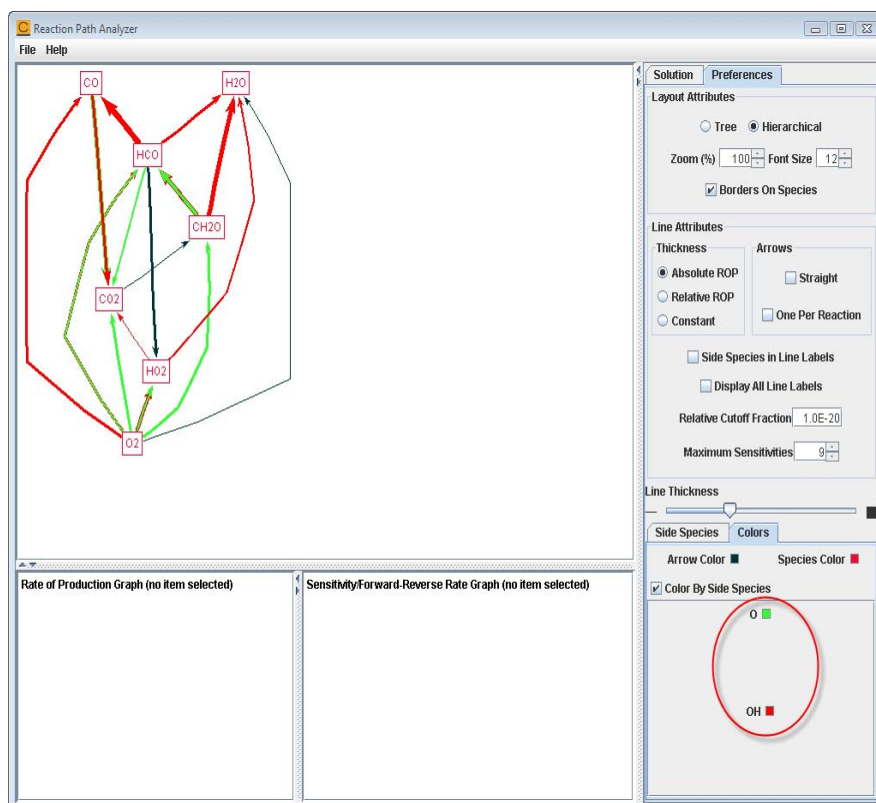
Figure 2-36

Flame Speed—Setting the hydroxide radical and oxygen radical as side species. The source was switched from methane to oxygen, and the element filter was changed to O element.



Colors can help distinguish the effect of a side species on the reactions in a diagram. For example, in [Figure 2-37](#), after setting the color preferences, any reaction with the hydroxide radical is colored red, and any reaction with the oxygen radical is colored green.

Figure 2-37 Flame Speed—Colored reactions based on influence of side species.



The coloring provides an easy way to distinguish the effects that one species may have on the formation or depletion of another.

These diagrams graphically show the decomposition pathways of the fuel, and the primary formation pathways of the products in the flame speed calculation.

2.3.8 Parameter Study: Propane/Air Flame Speed as a Function of Equivalence Ratio and Unburned Gas Temperature

2.3.8.1 Project Description

This tutorial illustrates using the Parameter Study Facility to calculate laminar flame speeds of propane-air mixtures over a wide range of equivalence ratios and unburned gas temperatures at atmospheric pressure. The tutorial also illustrates some features in the CHEMKIN flame speed calculator model for easy setup.

The behavior of flames in fuel-lean and fuel-rich systems at a range of unburned gas temperatures are of interest in several applications, such as engine combustion. In this tutorial, the flame speeds of propane-air mixtures are calculated for the following conditions:

1. Equivalence ratios of 0.6 –1.4.
2. Initial temperatures of 300 K and 700 K.
3. Pressure of 1 atm

Equivalence ratio and unburned gas temperature are set as parameter studies. A total of 18 parameter-study cases are run to cover the range of operating conditions.

Parameter studies can be used for several purposes:

- ✓ To study the impact of varying inputs of operating conditions such as pressure or stream properties such as concentrations.
- ✓ To analyze the sensitivity of output to reaction rate parameters and transport properties, and to analyze the impact of uncertain parameters.

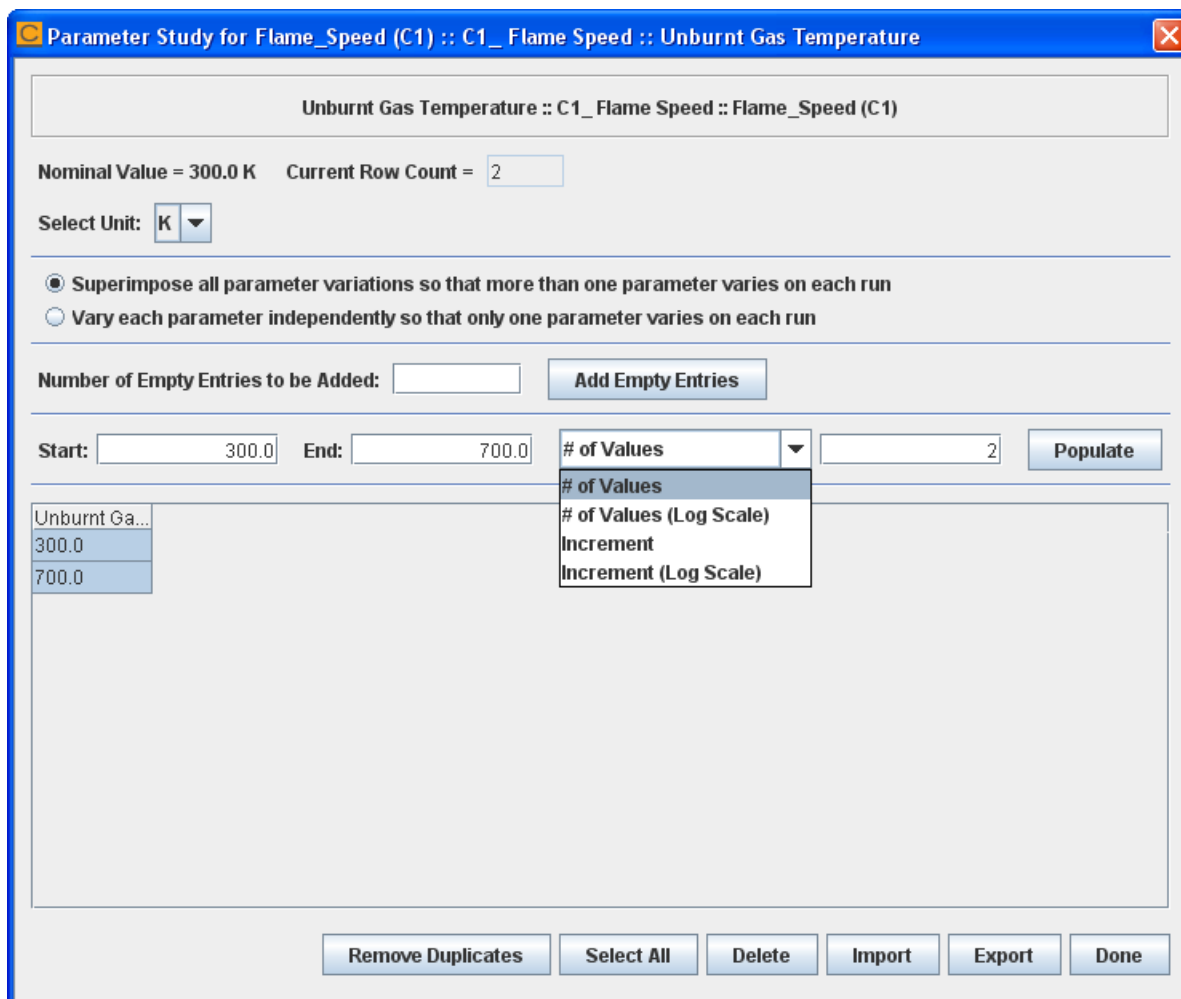
The problem uses the chemistry set described in [Section 2.9](#). The project file is named *flame_speed_parameter_study.ckprj*. The data files for this project are located in the *samples2010\flame_speed\parametric_study* directory.

2.3.8.2 Project Setup

Most of the inputs are conceptually similar to the tutorial on flame speed calculation of methane/air flame in [Section 2.3.7](#). CHEMKIN provides useful defaults for several inputs, including the automated generation of a guess temperature profile at which to start the calculations. We will use this option, along with an initial grid based on this automated temperature profile. We will also use the default values for all the solver parameters and the inlet velocity guess value.

On the Reactor Physical Properties panel, the pressure is specified as 1 atm. A parameter study is set up for the Unburned Gas Temperature. The nominal value of the Unburned Gas Temperature is specified as 300 K, and a parameter study is set up with 2 values of the unburned gas temperature, 300 K and 700 K, as shown in [Figure 2-38](#). To set up the parameter study based on unburned temperature, the adjacent  icon (see [Figure 2-39](#)) is selected, and the window shown in [Figure 2-38](#) appears. The parameter study can be populated by entering the **Start** and **End** value for the equivalence ratio, and selecting one of 4 options from the dropdown list for the appropriate distribution of values between the beginning and end value specified, as shown in [Figure 2-38](#).

Figure 2-38 Panel for Setup of Parameter Studies



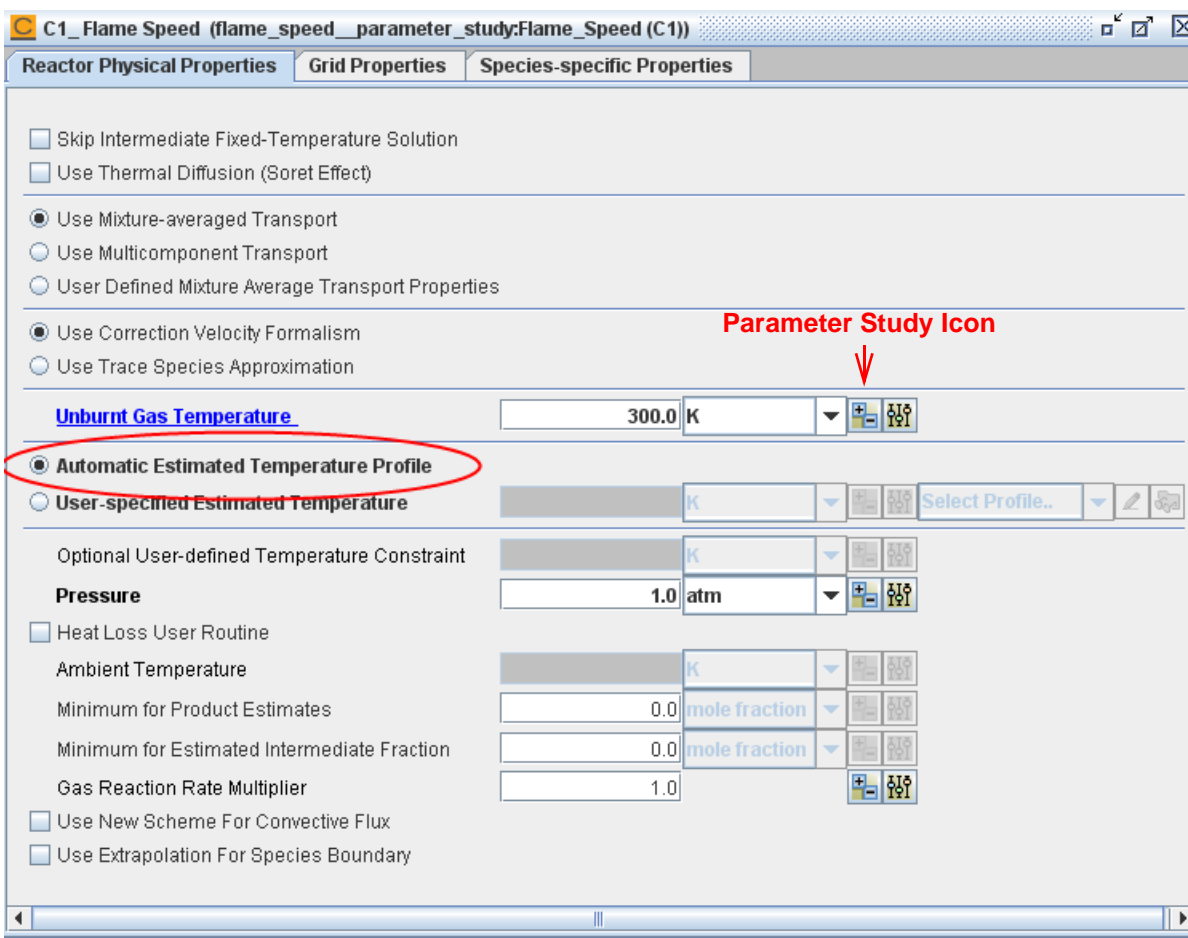
- To modify one of the values, double-click it.
- To delete a value, select it and press the **Delete** button.
- To add a value, press the **Populate** button.

Once the setup is filled out, click the **Done** button to complete the setup. After the specification of the inputs for the parameter study are complete, the parameter will appear in blue and be underlined, as shown in [Figure 2-39](#). This indicates that the setup of the parameter study is complete for that parameter.

In the Reactor Physical Properties panel, we have used the automatic estimation of the starting temperature profile, as shown below. This guess temperature profile can sometimes have a large influence on convergence. The automatic estimation of the temperature profile feature has been added for easier model setup, and this

estimated temperature profile provides a good starting guess and aids convergence. If the automated estimation of the starting temperature profile option is chosen, the optional user-defined temperature constraint input is grayed out, and CHEMKIN calculates this value.

Figure 2-39 Automatic Estimation of Starting Temperature Profile



Mixture-averaged transport properties are used in this tutorial, with correction velocity formulation.

Under the Grid Properties panel, the domain-size-related inputs and the grid-resolution inputs are specified. As with the freely propagating tutorial in [Section 2.3.7](#), we will start the problem on a small domain and a coarse grid, and subsequently use Continuations to expand the domain and refine the grid, which improves convergence. A starting small domain of 0.3 cm is specified in the Grid Properties panel. Subsequently, in the Continuations panel, the domain is expanded to 12 cms.

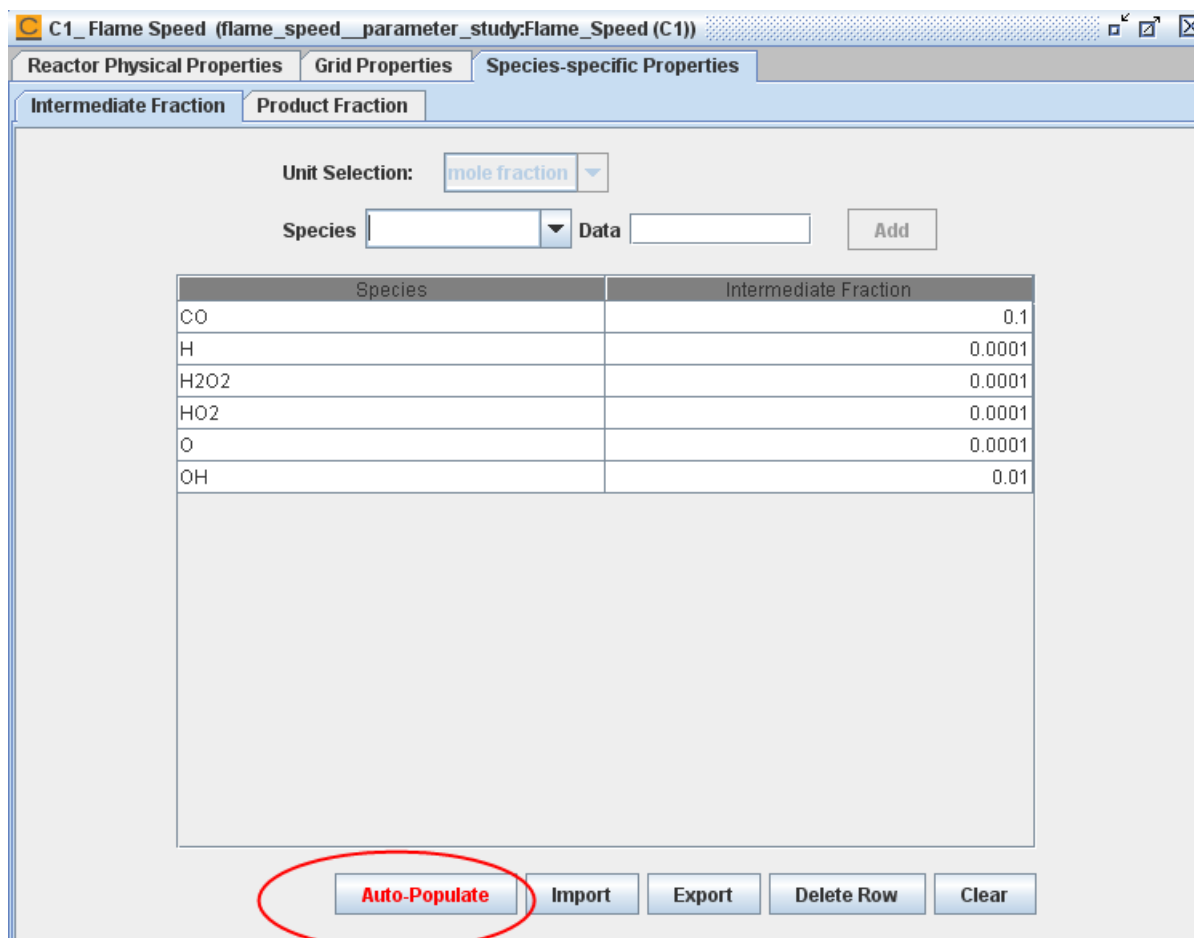
(starting axial position is expanded to -2 cm, and ending axial position to 10 cms). This ensures that the gradients of gas temperature and major species are nearly zero at both boundaries, so that the requirement of adiabatic and zero-diffusive-flux conditions at the boundaries are met.

The model uses a non-uniform grid that is successively and automatically adapted based on solution gradients and curvatures determined on an initially coarse grid. Relative gradient and curvature parameters that determine the extent to which the solution will be refined are model inputs. The relative gradient and curvature parameters for the grid refinement are both set in the Grid Properties panel to 0.9. Subsequently, in the Continuations panel, these values are both lowered to 0.1, to obtain a finer grid. To allow sufficient grid points for a well refined grid, we set the maximum number of grid points to 300.

In the Grid Properties panel, the estimated center position and zone width are left to program defaults. These inputs are grayed out when the automated estimation of the temperature profile option is chosen.

In the Species-specific properties panel, Intermediate fractions and Product fractions of species can be specified to provide a starting guess of species profiles. These are optional inputs, but typically help in convergence. The CHEMKIN model incorporates features that make these specifications easier. For the Intermediate fractions, there is an **Auto-Populate** button that can be used, as shown below. Based on the mechanism used in the problem, the Auto-Populate gives a reasonable guess for the intermediate fractions. If no product species guess values are specified, equilibrium values are calculated by CHEMKIN and used for the product fraction initial guesses.

Figure 2-40 Auto-Populate Option



On the Inlet panel, the inlet velocity guess value is left to default. In this tutorial, the reactant concentrations are specified in terms of equivalence ratio. The equivalence ratio is a measure of the fuel/oxidizer ratio, as compared with the stoichiometric value (explained further in [Section 2.2](#)). In this tutorial, the fuel consists of pure propane, while the oxidizer consists of air. For specifying the oxidizer as air, the **Auto-Populate Air** button under the Oxidizer Mixture panel can be used. The stoichiometric products from combustion must be specified; once the Fuel Mixture and the Oxidizer Mixture have been specified, the **Auto-Populate** button can be used for specifying the Complete-Combustion Products, and in this way CHEMKIN automatically determines the complete-combustion products. The nominal value of the equivalence ratio has been set to 1.0. Now, a parameter study varying the equivalence ratio can be set up. Nine values have been used to provide a range of equivalence ratios of 0.6 – 1.4. We would like to create a parameter study to set up equivalence ratios of 0.6 – 1.4 for each of the unburned gas temperature values of 300 K and 700 K. To achieve this, we click on the  next to the equivalence ratio, and then select the **Vary each parameter independently so that only one parameter varies on each run** option, as shown in [Figure 2-41](#).

Figure 2-41 Varying Each Parameter Independently

Parameter Study for Flame_Speed (C1) :: C1_Inlet1 :: Equivalence Ratio

Equivalence Ratio :: C1_Inlet1 :: Flame_Speed (C1)

Nominal Value = 1.0 Current Row Count = 2

Superimpose all parameter variations so that more than one parameter varies on each run
 Vary each parameter independently so that only one parameter varies on each run

Number of Empty Entries to be Added: Add Empty Entries

Start: End: Increment Populate

Once this parameter study is set up, there will be 18 parameter study runs, varying the equivalence ratio and unburned temperature, as shown below.

Figure 2-42 Parameter Study After Setup Is Complete

Parameter Study for Flame_Speed (C1) :: C1_Inlet1 :: Equivalence Ratio

Equivalence Ratio :: C1_Inlet1 :: Flame_Speed (C1)

Nominal Value = 1.0 Current Row Count = 18

Superimpose all parameter variations so that more than one parameter varies on each run
 Vary each parameter independently so that only one parameter varies on each run

Number of Empty Entries to be Added: Add Empty Entries

Start: End: Increment Populate

Equivalenc...	Unburnt Ga...
0.6	300.0
0.6	700.0
0.7	300.0
0.7	700.0
0.8	300.0
0.8	700.0
0.9	300.0
0.9	700.0
1.0	300.0
1.0	700.0
1.1	300.0
1.1	700.0
1.2	300.0
1.2	700.0
1.3	300.0
1.3	700.0
1.4	300.0
1.4	700.0

Remove Duplicates Select All Delete Import Export Done

All Solver panel inputs are left at defaults. There are several solver input options that CHEMKIN provides for the advanced user that can be used when convergence is more difficult.

Continuations have been set to expand the initial domain and refine the grid, as explained above.

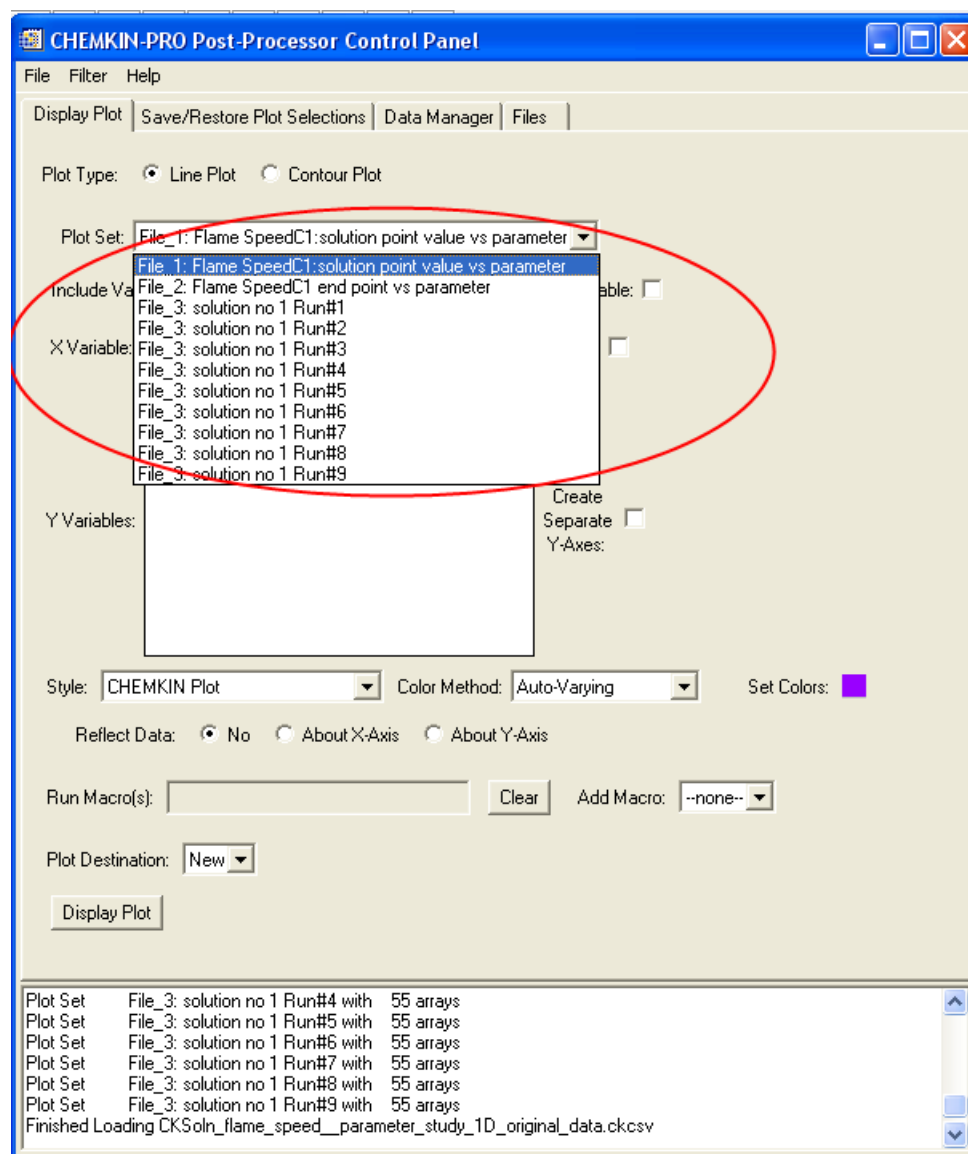
No other inputs need to be explicitly provided. For several model inputs, the default values provided in the CHEMKIN Interface have been used.

Once the setup is done, to run the parameter study, select the Run Calculations panel from the project tree, and click on **Begin**. While the model is running, the Progress Monitor and the message area show the status of the runs. Results can be post-processed after the runs are finished (using the Analyze Results node of the project tree).

2.3.8.3 Project Results

After running the parameter studies, several additional post-processing options are available. By selecting the Line plot from **Plot Type** in the Post-Processor, options appear for accessing the calculated results as shown in [Figure 2-43](#). The first and second options are exclusive to parameter studies.

Figure 2-43 Post-Processor Options After Running Parameter Studies



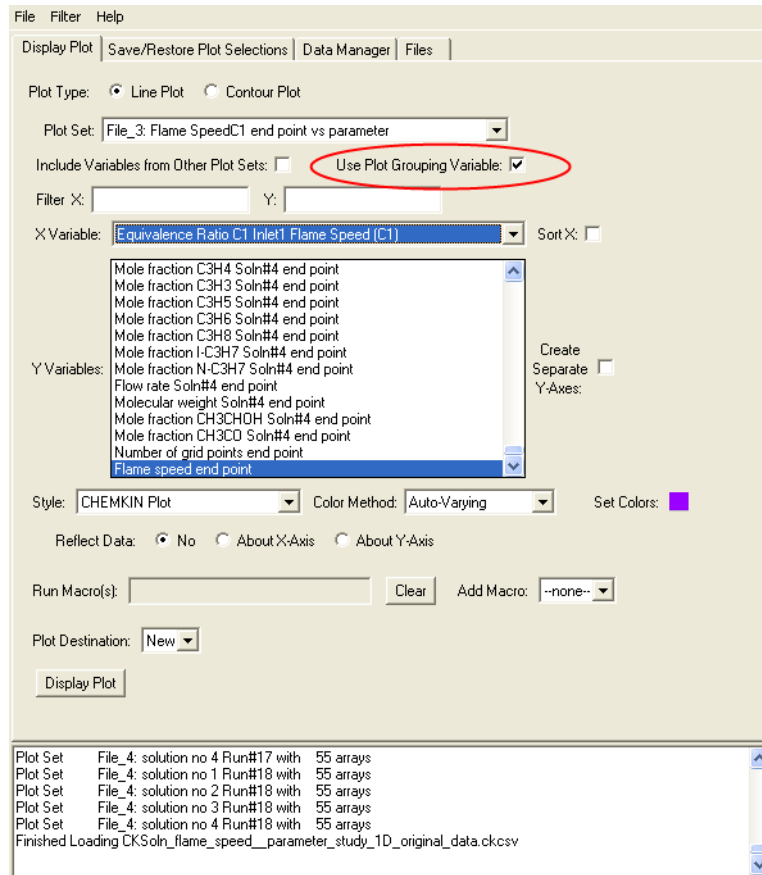
2.3.8.3.1

Cluster endpoint vs parameter

In this tutorial, we have used parameter studies to cover a range of operating conditions, and continuations to refine and expand the grid for each parameter study. Since we have used continuations for each parameter study, there are multiple solutions available for each parameter study run. Consequently, there would be multiple flame speed values for each parameter study run. Since we have used continuations only for refining the grid, we are interested in only the flame speed value of the final continuation. To access this value in the post-processor, we can use the The second option in the **Plot Set** (under **Plot Type** as **Line plot**), i.e., Cluster1C1 end point vs parameter, and one of the values here is the **Flame Speed end point**.

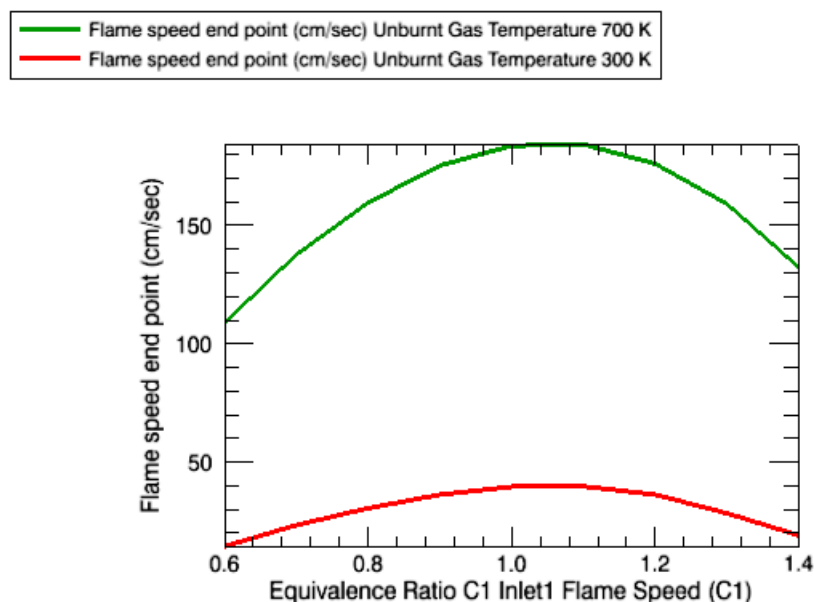
We can now plot the flame speed values as a function of equivalence ratio. Since there are two unburned gas temperatures, it would be good to separate the flame speed vs. equivalence ratio plots into two series. This is done through the **Use Plot Grouping Variable** option as shown in *Figure 2-44*, and choosing the unburned gas temperature.

Figure 2-44 Cluster Endpoint vs. Parameter



The flame speeds can now be plotted as shown below.

Figure 2-45 Flame-Speed Calculated Values as a Function of Equivalence Ratio



2.3.9 Hydrogen/Air Opposed-flow Flame

2.3.9.1 Project Description

This user tutorial presents a simulation of opposed flow diffusion flame of hydrogen and air at low pressure. This project uses the chemistry set for hydrogen combustion described in [Section 2.9.1](#). The opposed-flow geometry makes an attractive experimental configuration, because the flames are flat, allowing for detailed study of the flame chemistry and structure. The two or three-dimensional flow is reduced mathematically to one dimension. This problem uses cylindrical coordinates where one stream contains fuel and the other oxidizer. It also demonstrates the use of sensitivity analysis for reaction rates and species heats of formation. The latter analysis is useful for evaluating the effects of thermochemical parameters that may have been estimated, or have high uncertainties.

2.3.9.2 Project Setup

The project file is called ***opposed-flow_flame_h2_air.ckprj***. The data files used for this sample are located in the ***samples2010\opposed-flow_flameh2_air*** directory. This reactor diagram contains two gas inlets, one Opposed-flow Flame Reactor, and an outlet.

On the Reactor Physical Properties tab of the C1_ Opposed-flow Flame panel, the problem type of Solve Gas Energy Equation is selected. Here, the use of Mixture-averaged Transport properties is also selected, as is the choice of a plateau-shaped, rather than a linear, profile for the starting guess used in the simulation. An optional value for the maximum temperature to be used in the initial profile is provided to help convergence.

On the Grid Properties tab of the C1_ Opposed-flow Flame panel, the use of cylindrical geometry is selected for this problem, and the axial length of the simulation (2 cm) is input. In this reactor model, the fuel always enters the system at the origin, and the oxidizer inlet is located at the Ending Axial Position. The opposed-flow reactor model uses adaptive gridding, and in this case, the spacing of the 14 initial grid points have been specified by use of a profile file, ***opposed-flow_flame_h2_air.ckprf***. There are 4 optional parameters on this panel that provide input for the adaptive gridding, two of which have values that we have input to override the defaults. The simulation also needs a starting estimate of the solution from which to begin its iteration, and the Estimated Center Position and Estimated (reaction) Zone Width help specify that. The gas composition giving the expected combustion products that are input on the Product Fraction sub-tab of the Species-specific Properties tab on the C1_ Opposed-flow Flame panel are also part of the initial guess.

The gas inlet panels are named to reflect their function. The inlet gas velocities (100 cm sec^{-1}) are input on the Stream-specific Data tabs of the Fuel and Oxidizer panels, along with inlet gas temperatures (300 K). The inlet gas compositions, pure hydrogen and pure air, are input on the Reactant Fraction sub-tab of the Species-specific Properties tab of the Fuel and Oxidizer panels, respectively.

On the Solver panel, there are a number of inputs on the Basic and Advanced tabs to override the default values and assist convergence. On the Output Control tab of the Output Control panel, boxes are checked to request that sensitivity calculations be done for all variables with respect to both reaction-rate A factors and species heats of formation. On the Species Specific Data tab, three species are listed as being Output Species. There are no inputs on the Cluster Properties or Continuations panels for this project.

2.3.9.3

Project Results

Figure 2-46 shows the gas temperature from the simulation as a function of axial distance. The flame is located on the fuel side of the stagnation plane, which is a result of using hydrogen as the fuel. Most fuels require more air than fuel by mass, so the diffusion flame usually sits on the oxidizer side of the stagnation plane. In a stoichiometric mixture, the fuel usually diffuses through the stagnation plane to

establish the flame. For H_2 however, more fuel is required than air. The mole fractions in [Figure 2-47](#) for the major species show that the flame sits on the fuel side of the stagnation plane in this case. An inspection of the text file shows that the simulation now has 45 grid points, a significant increase from the initial 14 grid points.

Figure 2-46 Hydrogen/Air Flame—Temperature vs. Axial Distance

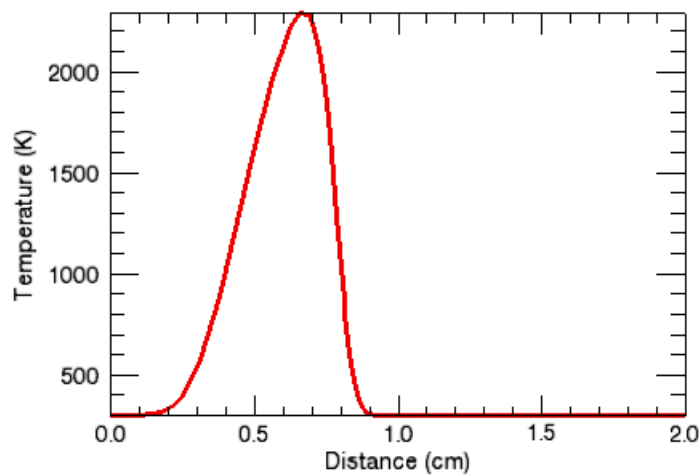
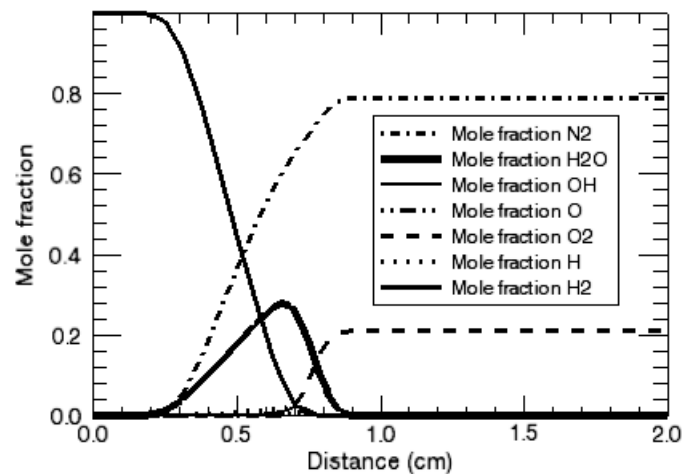


Figure 2-47 Hydrogen/Air Flame—Mole Fractions



[Figure 2-48](#) shows the normalized sensitivity coefficients as a function of distance for the five reactions with the largest temperature sensitivities. Reaction #1, $H + O_2 + M = HO_2 + M$, has both the most positive and most negative values. Increasing the rate of this reaction would increase the temperature on the fuel side,

and decrease it at the oxidizer side of the flame. *Figure 2-49* shows the sensitivity coefficients as a function of distance for the five species with the largest temperature sensitivities for heats of formation. The temperature is most sensitive to the heat of formation of H_2O , which makes sense as this is the primary product species.

Figure 2-48 Hydrogen/Air Flame—Temperature Sensitivity to Reaction Rates

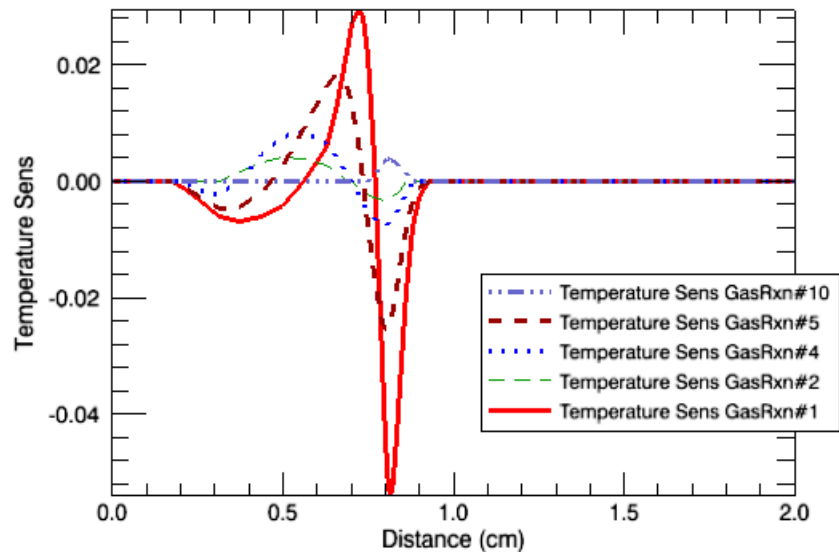
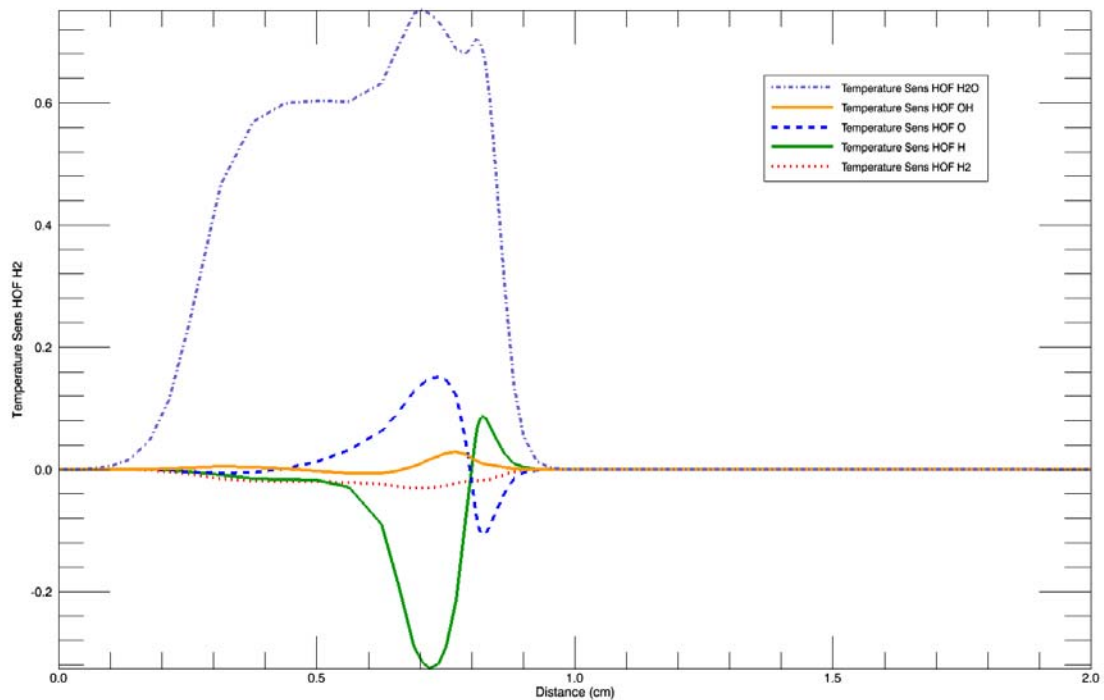


Figure 2-49 Hydrogen/Air Flame—Temperature Sensitivity to Heats of Formation





2.3.10 Flame Extinction Analysis [CHEMKIN-PRO Only]

2.3.10.1 Project Description

This tutorial describes how to use the reactor model named Extinction of Premixed or Opposed Flow Flame, which is available under the Flame Simulators (see [Figure 2-50](#)). Flame extinction studies are fundamental to flame characterization and response analysis. Moreover, such studies also provide data for validation of reaction mechanisms. In a typical flame extinction experiment, premixed fuel-air mixture is supplied from one nozzle and an inert gas for the other. The sample presented here simulates one such case for a premixed methane-air mixture.

This extinction simulator can read an existing Opposed-Flow Flame model solution file and start the extinction analysis or can originate an opposed-flow flame problem and carry it out to extinction analysis.

Figure 2-50 Icon for Extinction of Premixed or Opposed Flow Flame reactor



As discussed in the [CHEMKIN Theory Manual](#), extinction analysis is conducted using successive flame-controlling continuations. The “flame-control” is achieved by using internal boundary conditions on temperature. (See [Section 13.6](#) in the [CHEMKIN Theory Manual](#).) In this tutorial, the one-point temperature control method is used. The one-point control method is more appropriate when a premixed mixture is supplied from one nozzle and an inert gas from the other; as in this tutorial example. On the other hand, when fuel and oxidizer are supplied from each nozzle separately (i.e., a “diffusion” flame), two-point control can be considered more “flame-controlling”. Mathematically, however, the problem is well-posed with either technique although numerical difficulties can appear when one-point control is used for the “diffusion” flame.

When setting up an extinction analysis, it is important to remember the following one-point and two-point temperature control conventions. With one-point temperature control, the internal boundary condition on temperature is set for $0 < x < x_{flame}$, where x is the spatial coordinate and x_{flame} is the flame (maximum temperature) location. For two-point control, the simulator chooses a temperature control point on either side of the flame. By default, inlet 1 is located at $x = 0$. If you name the inlets as “Fuel” and “Oxidizer”, the Fuel inlet is treated as inlet 1 and is located at $x = 0$. For all inlet pairs, inlet 1 is at $x = 0$, as in the default case. As described in [Section 2.3.10.4](#), the simulator reports the extinction strain rate assuming that the Fuel (or premixed fuel-air) inlet is located at $x = 0$.

2.3.10.2 Project Set-up

The project file is named ***opposed-flow_flame__extinction.ckprj*** and is located in the ***samples2010*** directory. Extinction analysis is conducted for a premixed stoichiometric methane-air flame at 1 atm pressure.

A reduced (17 species) methane-air mechanism is used in this tutorial; the chemistry set is described in [Section 2.9.2.2](#). After successfully preprocessing the mechanism, the extinction problem can be set up. Note that, unlike an Opposed-flow Flame reactor model, a fixed-temperature problem is meaningless for extinction and thus the energy equation is always solved. In addition to the three tabs that appear for the Opposed-flow Flame reactor, the Reactor Properties tab has one extra sub-tab named Basic. In the following discussion, the set-up of the options pertaining to the nominal Opposed-flow Flame model is described first, followed by the details of controls on the Basic sub-tab.

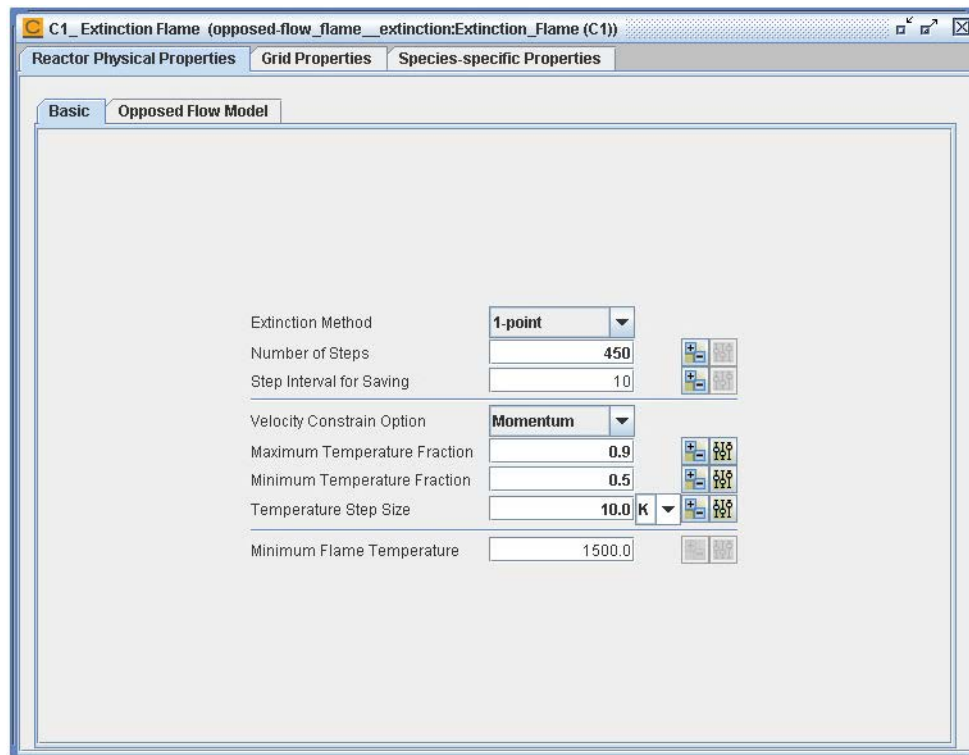
The controls for the nominal opposed-flow flame model are on the Opposed Flow Model sub-tab of the Physical Properties tab. In this tutorial, pressure is set to 1 atm while all other controls are left at their default values. Ending Axial Position is set to 1.4 cm in the Grid Properties tab. The adaptive mesh control options, for both the solution gradient and curvature, are set to 0.1 while the maximum number of grid points allowed is set to 1000.

The stoichiometric methane-air mixture is assigned to inlet 1 (named *MethaneAir*) while pure nitrogen (N₂) is assigned to inlet 2 (named *Nitrogen*). The inlet gas temperature for both inlets is set to 296 K. The inlet velocities for both nozzles are set to 80 cm/s. Note that the first opposed-flow flame solution is thus calculated for these parameters.

[Figure 2-51](#) illustrates the controls set on the Basic tab. As mentioned earlier, the one-point option is chosen for the extinction method because a premixed mixture is used. The number of extinction steps is effectively the number of successive opposed-flow flame simulations to be conducted in search of the extinction turning point. Although its default value is 100, in this tutorial lesson the number of steps is set to 450. Typically, the number of steps can be of the order of 500 and this value depends not only on the temperature step size used but also on all the other controls on the Basic tab. The step interval for saving option dictates solution saving frequency. This control can be useful for restarting a new extinction analysis from a failed run or continuing from a previous simulation, if the extinction (turning) point is not reached within the initial value of the number of steps. Also since extinction analysis is computationally intensive, a new run (for example, for different stoichiometry) can be restarted from an intermediate solution from a previous run.

The nozzle velocities can be constrained for the one-point control method (see [Section 13.6](#) in the *CHEMKIN Theory Manual*). In this case, we choose momentum constraint, which gives the stagnation plane roughly at the middle of the computation domain. For two-point control, such constraint on the nozzle inlet velocities cannot be enforced and, if specified, is ignored by the simulator. The maximum and minimum temperature fractions are set to 0.9 and 0.5 whereas temperature steps of 10 K are used. At any point during the calculations, if the maximum temperature obtained is less than that specified by the minimum flame temperature, the calculations stop declaring that the flame existence criterion is violated. The default value of this control is 1500 K. This control is useful to avoid taking too many steps beyond the extinction point.

Figure 2-51 Extinction— Basic reactor properties



The input parameters maximum temperature fraction, minimum temperature fraction, and temperature step size control the location and magnitude of internal boundary condition on temperature. Because this tutorial simulation is not a restart from an old solution, the simulator first computes a nominal flame for the given input parameters. (For a restart, it uses the solution supplied.) Then it finds the location at which the following statement is satisfied:

$$T = \text{maximum temperature fraction} * (\text{Current maximum temperature} - \text{Inlet temperature})$$

The temperature at this location is then successively decreased by the user-specified temperature-step-size until it reaches $T = \text{minimum temperature fraction} * (\text{Current maximum temperature} - \text{Inlet temperature})$. A new location is then selected using the maximum temperature fraction. This process is repeated until the desired number of steps is reached or until the flame is effectively extinguished as dictated by the minimum flame temperature control.

As an example, suppose that the initial flame solution has a maximum temperature of 2100 K for the inlet temperature of 300 K and the maximum and minimum temperature fractions specified are 0.8 and 0.5, respectively. The simulator would then find the first location between $x = 0.0$ and x (at T_{max}) such that $x(T) \geq 300 + 0.8*(2100-300) \geq 1740$ K. (For two-point control, such a location is found on either side of the flame.) We will label this location $xc1$. The internal boundary condition ($T = 1740$ K) is imposed at this point. After a flame solution for this new problem is calculated, the new boundary condition at this location will be $T = 1740$ K - temperature step size, and a new flame solution is computed. This process is repeated until the temperature at the control location is reduced to $T = 300 + 0.5*(2100-300) = 1200$ K. After a flame solution corresponding to this temperature is obtained, a new location ($xc2$) is computed using the maximum temperature fraction and the flame temperature calculated for the problem in which $T = 1200$ K is imposed at $xc1$. The process is then repeated for $xc2$.

2.3.10.3

Project Results

The text output file generated by an extinction project contains the output from each opposed-flow flame simulation conducted along the path to the extinction point. Typically, size of the output text-file is large since all the solutions are written to it. The solution file contains corresponding solutions saved according to the specified saving frequency. The output file corresponding to extinction analysis is ***opposed-flow_flame_extinction_ExtinctionResponse.csv***. As the path to extinction is calculated, it is dynamically displayed in a plot that is monitoring the content of this text output file, as shown in [Figure 2-52](#). The display of this plot is optional, and can be turned off in User Preferences by clicking on Show Plot Monitor. This file can be opened with a simple text editor. While a more detailed overview of the general contents of this file is given in the next section, the following observations can be made from the contents of this file generated by the tutorial problem. For the initial solution at nozzle velocities of 80 cm/s, the maximum temperature is about 2066 K. The simulator then searches for the location of the control temperature computed as $296 + 0.9*(2066-296) = 1889$ K. Since there is no grid-point at which the temperature exactly matches this value, the first grid point with $x > 0$ at which temperature exceeds this value is chosen. The temperature at this grid point is approximately 1908 K. The

continuation process then decreases the temperature at the control point in steps of 10 K until the control temperature is equal to or less than $296 + 0.5 \cdot (2066 - 296) = 1181$ K. This happens at the 74th step; at this point the flame temperature is about 2027 K.

Figure 2-52 Dynamic plotting of Temperature vs. extinction response, showing a turn at $\sim 550 \text{ s}^{-1}$



As described earlier, the simulator then finds a new control location such that the temperature there is $296 + 0.9 \cdot (2027 - 296) = 1854$ K. The fuel and oxidizer nozzle velocities continuously increase to the value in the neighborhood of 200 cm s^{-1} . The “turning point” is reached when the MethaneAir nozzle velocity reaches about 203 cm s^{-1} (after 425 steps). The global strain rate at the turning point is $(203 + 201)/1.4 = 289 \text{ s}^{-1}$. The extinction strain rate (see the definition in [Section 2.3.10.4](#)) is 550 s^{-1} .

2.3.10.4 Post-processing

The user input parameter “step interval for saving” controls the number of solutions saved. In this tutorial, it is set to 10. Thus, there are $450/10 = 45$ total solutions that are saved in the solution file. Just as in the case of the nominal opposed-flow flame solution file, the data for all variables and corresponding derived quantities such as heat release, rate of production, etc., is available for all these solutions. However, from a design point of view, only the data at or near the extinction point are important.

The extinction simulator creates two raw-data output files named **opposed-flow_flame_extinction_ExtinctionResponse.csv** and **opposed-flow_flame_extinction_ExtinctionProfiles.out**. Figure 2-53 and Figure 2-54 show snapshots of these files. The former contains the data such as control temperature, pressure eigenvalue, global strain rate, “extinction” strain rate, and maximum temperature at each solution point. (The definitions of the strain rates are given later in this section). As mentioned in the previous section, a plot of the extinction curve is dynamically displayed using the data from this csv file. By default it shows T_{max} vs KExt (see the definitions below). However, data in any two columns can be plotted against each other using the drop-down boxes at the bottom of the plot. The velocity and temperature profiles at each solution point are stored in the **opposed-flow_flame_extinction_ExtinctionProfiles.out** with the global strain rate identifying each solution.

Figure 2-53 Output file **opposed-flow_flame_extinction_ExtinctionResponse.csv**

SolNum	TFix1 [K]	H [g/cm3-s2]	VFuel [cm/s]	Voxid [cm/s]	Fjj[g/cm2-s]	KGlobal [/s]	KExt [/s]	KFuel [/s]	KOxid [/s]	Tmax[K]
1	1.908005E+03	-2.902521E+01	7.976197E+01	-7.921887E+01	-4.568301E-02	1.135577E+02	1.917435E+02	4.937039E+03	5.802298E+02	2.066463E+03
2	1.898005E+03	-2.942481E+01	8.072301E+01	-8.017337E+01	-4.623344E-02	1.149260E+02	1.955269E+02	4.912252E+03	5.690986E+02	2.064451E+03
3	1.888005E+03	-3.001195E+01	8.190268E+01	-8.134500E+01	-4.690908E-02	1.166055E+02	2.009097E+02	4.908100E+03	5.606898E+02	2.062760E+03
4	1.878005E+03	-3.060675E+01	8.305922E+01	-8.249367E+01	-4.757148E-02	1.182521E+02	2.052717E+02	4.906469E+03	5.527762E+02	2.060945E+03
5	1.868005E+03	-3.114204E+01	8.409679E+01	-8.352418E+01	-4.816574E-02	1.197293E+02	2.091027E+02	4.897182E+03	5.450848E+02	2.058753E+03
6	1.858005E+03	-3.136004E+01	8.470219E+01	-8.412546E+01	-4.851248E-02	1.205912E+02	2.115694E+02	4.858106E+03	5.388656E+02	2.055475E+03
7	1.848005E+03	-3.180566E+01	8.558515E+01	-8.500240E+01	-4.901819E-02	1.218483E+02	2.146119E+02	4.846291E+03	5.295366E+02	2.053278E+03
8	1.838005E+03	-3.218387E+01	8.636433E+01	-8.577627E+01	-4.946445E-02	1.229576E+02	2.172403E+02	4.829779E+03	5.256255E+02	2.051315E+03
9	1.828005E+03	-3.275342E+01	8.739304E+01	-8.679798E+01	-5.005364E-02	1.244222E+02	2.205782E+02	4.839692E+03	5.209903E+02	2.050206E+03
10	1.818005E+03	-3.315392E+01	8.816363E+01	-8.756333E+01	-5.049499E-02	1.255193E+02	2.231357E+02	4.828443E+03	5.174890E+02	2.050084E+03
1	1.808005E+03	-3.340344E+01	8.870517E+01	-8.810118E+01	-5.080515E-02	1.262903E+02	2.250287E+02	4.801720E+03	5.133039E+02	2.047631E+03
2	1.798005E+03	-3.381904E+01	8.946091E+01	-8.885177E+01	-5.123799E-02	1.273662E+02	2.275287E+02	4.798108E+03	5.096189E+02	2.046181E+03
3	1.788005E+03	-3.424181E+01	9.022503E+01	-8.961069E+01	-5.167564E-02	1.284541E+02	2.299666E+02	4.805197E+03	5.062733E+02	2.047178E+03
4	1.778005E+03	-3.450740E+01	9.073768E+01	-9.011984E+01	-5.196925E-02	1.291839E+02	2.317069E+02	4.793431E+03	5.024285E+02	2.045610E+03
5	1.768005E+03	-3.487400E+01	9.136408E+01	-9.074199E+01	-5.232802E-02	1.300758E+02	2.336848E+02	4.797422E+03	4.982015E+02	2.044891E+03
6	1.758005E+03	-3.484224E+01	9.144648E+01	-9.082382E+01	-5.237521E-02	1.301931E+02	2.340075E+02	4.764852E+03	4.964955E+02	2.043148E+03
7	1.748005E+03	-3.508045E+01	9.186792E+01	-9.124239E+01	-5.261659E-02	1.307931E+02	2.353301E+02	4.763265E+03	4.932157E+02	2.042719E+03
8	1.738005E+03	-3.534232E+01	9.230614E+01	-9.167763E+01	-5.286758E-02	1.314170E+02	2.366917E+02	4.763222E+03	4.918060E+02	2.042329E+03
9	1.728005E+03	-3.556087E+01	9.267634E+01	-9.204531E+01	-5.307961E-02	1.319440E+02	2.378398E+02	4.769216E+03	4.903522E+02	2.041816E+03
10	1.718005E+03	-3.563894E+01	9.286295E+01	-9.223065E+01	-5.318648E-02	1.322097E+02	2.384025E+02	4.761716E+03	4.889238E+02	2.041077E+03
1	1.708005E+03	-3.583272E+01	9.318589E+01	-9.255139E+01	-5.337145E-02	1.326695E+02	2.394105E+02	4.764930E+03	4.878287E+02	2.040746E+03
2	1.698005E+03	-3.600213E+01	9.346879E+01	-9.283236E+01	-5.353478E-02	1.330722E+02	2.402835E+02	4.766518E+03	4.867216E+02	2.040440E+03
3	1.688005E+03	-3.603602E+01	9.357028E+01	-9.293316E+01	-5.359160E-02	1.332167E+02	2.406314E+02	4.754880E+03	4.864493E+02	2.039516E+03
4	1.678005E+03	-3.619294E+01	9.382888E+01	-9.319000E+01	-5.373971E-02	1.335849E+02	2.414295E+02	4.757490E+03	4.857566E+02	2.039297E+03
5	1.668005E+03	-3.634169E+01	9.407369E+01	-9.343315E+01	-5.387993E-02	1.339335E+02	2.421882E+02	4.760031E+03	4.850715E+02	2.039062E+03
6	1.658005E+03	-3.647179E+01	9.429084E+01	-9.364882E+01	-5.400430E-02	1.342426E+02	2.428641E+02	4.761108E+03	4.843790E+02	2.038812E+03
7	1.648005E+03	-3.661016E+01	9.451622E+01	-9.387266E+01	-5.413338E-02	1.345635E+02	2.435614E+02	4.763428E+03	4.836865E+02	2.038645E+03
8	1.638005E+03	-3.674440E+01	9.473437E+01	-9.408933E+01	-5.425833E-02	1.348741E+02	2.442273E+02	4.766235E+03	4.830048E+02	2.038485E+03
9	1.628005E+03	-3.687576E+01	9.494643E+01	-9.429994E+01	-5.437978E-02	1.351760E+02	2.448910E+02	4.768789E+03	4.823257E+02	2.038319E+03
10	1.618005E+03	-3.700271E+01	9.515137E+01	-9.450348E+01	-5.449716E-02	1.354677E+02	2.455095E+02	4.771599E+03	4.816500E+02	2.038153E+03
1	1.608005E+03	-3.719350E+01	9.491311E+01	-9.426685E+01	-5.436070E-02	1.351285E+02	2.448714E+02	4.737217E+03	4.805062E+02	2.036430E+03
2	1.598005E+03	-3.690439E+01	9.509444E+01	-9.444694E+01	-5.446455E-02	1.353867E+02	2.454409E+02	4.738677E+03	4.796618E+02	2.036264E+03
3	1.588005E+03	-3.701198E+01	9.527061E+01	-9.462192E+01	-5.456545E-02	1.356375E+02	2.459760E+02	4.739778E+03	4.789070E+02	2.036070E+03
4	1.578005E+03	-3.700972E+01	9.530293E+01	-9.465401E+01	-5.458396E-02	1.356835E+02	2.461013E+02	4.730439E+03	4.782175E+02	2.035561E+03
5	1.568005E+03	-3.711135E+01	9.546906E+01	-9.481901E+01	-5.467911E-02	1.359200E+02	2.466222E+02	4.731623E+03	4.774695E+02	2.035201E+03
6	1.558005E+03	-3.721112E+01	9.563184E+01	-9.498069E+01	-5.477234E-02	1.361518E+02	2.471177E+02	4.732809E+03	4.767242E+02	2.035047E+03
7	1.548005E+03	-3.729172E+01	9.576942E+01	-9.511733E+01	-5.485114E-02	1.363477E+02	2.475483E+02	4.732421E+03	4.761587E+02	2.034774E+03
8	1.538005E+03	-3.738947E+01	9.592803E+01	-9.527486E+01	-5.494198E-02	1.365735E+02	2.480450E+02	4.733826E+03	4.756126E+02	2.034631E+03
9	1.528005E+03	-3.748581E+01	9.608410E+01	-9.542986E+01	-5.503137E-02	1.367957E+02	2.485204E+02	4.735183E+03	4.750942E+02	2.034493E+03
10	1.518005E+03	-3.756272E+01	9.621486E+01	-9.555974E+01	-5.510626E-02	1.369919E+02	2.489260E+02	4.734116E+03	4.746018E+02	2.034234E+03
1	1.508005E+03	-3.765777E+01	9.636805E+01	-9.571188E+01	-5.519400E-02	1.371999E+02	2.494074E+02	4.736126E+03	4.74130E+02	2.034105E+03
2	1.498005E+03	-3.775193E+01	9.651951E+01	-9.586231E+01	-5.528075E-02	1.374156E+02	2.498711E+02	4.737559E+03	4.736980E+02	2.033980E+03
3	1.488005E+03	-3.784528E+01	9.666938E+01	-9.601116E+01	-5.536659E-02	1.376290E+02	2.503248E+02	4.738997E+03	4.732858E+02	2.033858E+03
4	1.478005E+03	-3.792329E+01	9.679946E+01	-9.614036E+01	-5.544109E-02	1.378142E+02	2.507399E+02	4.739046E+03	4.729047E+02	2.033735E+03
5	1.468005E+03	-3.801641E+01	9.694813E+01	-9.628801E+01	-5.552633E-02	1.380358E+02	2.511987E+02	4.740628E+03	4.72529E+02	2.033522E+03
6	1.458005E+03	-3.810897E+01	9.709563E+01	-9.643451E+01	-5.561072E-02	1.382358E+02	2.516432E+02	4.742003E+03	4.72169E+02	2.033412E+03
7	1.448005E+03	-3.805456E+01	9.705477E+01	-9.639393E+01	-5.558732E-02	1.381776E+02	2.515469E+02	4.728818E+03	4.71852E+02	2.033260E+03
8	1.438005E+03	-3.809202E+01	9.713142E+01	-9.647005E+01	-5.563121E-02	1.382868E+02	2.518006E+02	4.724982E+03	4.715582E+02	2.033200E+03

Figure 2-54 Output file ExtinctionProfilesOut.

```

Global StrainRate= 113.56
1 0.000000E+00 7.976197E+01 2.960000E+02
2 3.500000E-02 7.937422E+01 2.960000E+02
3 7.000000E-02 7.821647E+01 2.960000E+02
4 1.050000E-01 7.629953E+01 2.960000E+02
5 1.400000E-01 7.363393E+01 2.960000E+02
6 1.750000E-01 7.022907E+01 2.960000E+02
7 1.925000E-01 6.824842E+01 2.960000E+02
8 2.100000E-01 6.607924E+01 2.960000E+02
9 2.275000E-01 6.372238E+01 2.960000E+02
10 2.450000E-01 6.117873E+01 2.960000E+02
11 2.625000E-01 5.844900E+01 2.960001E+02
12 2.712500E-01 5.701407E+01 2.960003E+02
13 2.800000E-01 5.553202E+01 2.960008E+02
14 2.887500E-01 5.400350E+01 2.960026E+02
15 2.975000E-01 5.242963E+01 2.960081E+02
16 3.062500E-01 5.081272E+01 2.960252E+02
17 3.150000E-01 4.915791E+01 2.960771E+02
18 3.237500E-01 4.747757E+01 2.962305E+02
19 3.325000E-01 4.580239E+01 2.966726E+02
20 3.368750E-01 4.499606E+01 2.971927E+02
21 3.412500E-01 4.424869E+01 2.981703E+02
22 3.456250E-01 4.361396E+01 2.999834E+02
23 3.478125E-01 4.337390E+01 3.014536E+02
24 3.500000E-01 4.321591E+01 3.035204E+02
25 3.521875E-01 4.316996E+01 3.064059E+02
26 3.543750E-01 4.327491E+01 3.104019E+02
27 3.565625E-01 4.358003E+01 3.158836E+02
28 3.587500E-01 4.414596E+01 3.233194E+02
29 3.609375E-01 4.504465E+01 3.332732E+02
30 3.631250E-01 4.635765E+01 3.463937E+02
31 3.653125E-01 4.817217E+01 3.633865E+02
32 3.664062E-01 4.990600E+01 3.736441E+02
33 3.675000E-01 5.061083E+01 3.852377E+02
34 3.685937E-01 5.209781E+01 3.982611E+02
35 3.696875E-01 5.377695E+01 4.127998E+02
36 3.707812E-01 5.565682E+01 4.289287E+02
37 3.718750E-01 5.774443E+01 4.467103E+02
38 3.729687E-01 6.004511E+01 4.661942E+02
39 3.740625E-01 6.256248E+01 4.874159E+02
40 3.751562E-01 6.529845E+01 5.103976E+02
41 3.762500E-01 6.825330E+01 5.351477E+02
42 3.773437E-01 7.142569E+01 5.616613E+02
43 3.784375E-01 7.481275E+01 5.899206E+02
44 3.795312E-01 7.841011E+01 6.198952E+02
45 3.806250E-01 8.221196E+01 6.515427E+02
46 3.817187E-01 8.621116E+01 6.848091E+02
47 3.828125E-01 9.039937E+01 7.196300E+02

```

The file *opposed-flow_flame_extinction_ExtinctionResponse.csv* prints four strain rates. These are:

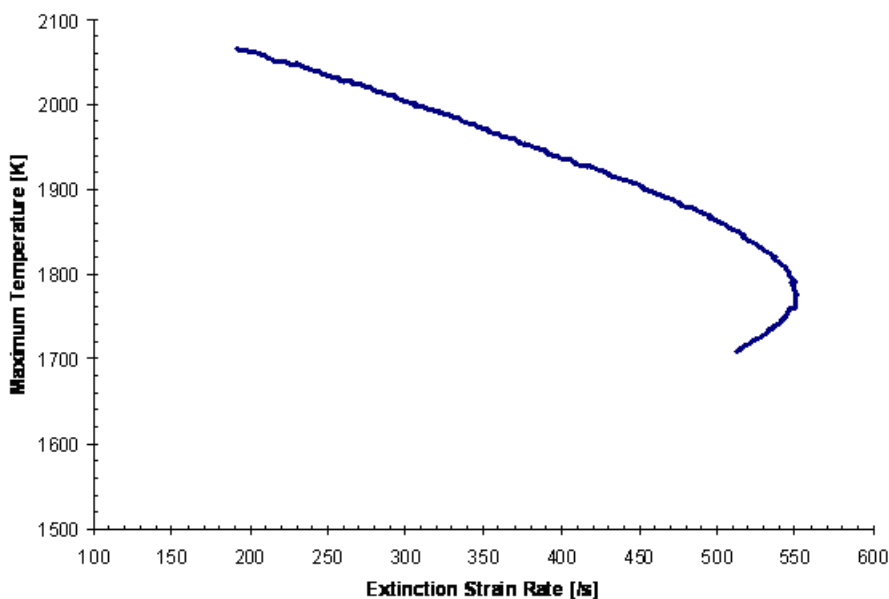
1. KGlobal = Global strain rate = (Fuel velocity – Oxidizer velocity) / Separation distance.
2. KExt = Extinction strain rate = Maximum axial velocity gradient on the fuel side just before the flame.
3. KFuel = Maximum strain rate on fuel side.
4. KOxid = Maximum strain rate on the oxidizer side.

In these definitions, the fuel side refers to $x = 0$, i.e., left of the stagnation plane and the oxidizer side refers to $x = x_{\max}$, i.e., right side of the stagnation plane.

The dynamic plot monitor does not close after the simulation ends and so continues to provide the information about the simulation. In addition, the Analyze Results panel provides an **Analyze Extinction Results** radio button that is selected by default. Clicking the **Next Step** button after selecting this radio button will allow you to access contents of the csv file through the Post-Processor. Alternatively, the file *opposed-flow_flame_extinction_ExtinctionResponse.csv* can be imported to a plotting utility

such as Microsoft Excel™, employing the fixed-width format. [Figure 2-55](#) shows the plot of flame temperature vs. extinction strain rate. It can be seen that the computed value of the extinction strain rate is about 550 s^{-1} . The global strain rate at this point is about 289 s^{-1} .

Figure 2-55 Flame response curve showing extinction (turning) for premixed stoichiometric methane-air flame. The inlet temperature is 296 K and ambient pressure is 1 atm. The calculated extinction strain rate is 550 /s .



Solution point number 425 corresponds to the turning point. Since the solution saving frequency is 10, solution numbers 42 and 43 are the closest saved solutions.

However, the file `opposed-flow_flame__extinction_ExinctionProfiles.out` can be used to get the velocity and temperature profiles at the turning point. For this purpose, for the current case you can search for the character string "Global StrainRate [s] = 289" and retrieve the appropriate block. Each block contains grid point number, x location (cm), axial velocity (cm/s), and temperature (K). Plotted in [Figure 2-56](#) are the velocity and temperature profiles at extinction point obtained by using the data block for global strain rate of 289.42 s^{-1} (use fixed-width format in Excel when loading this data block) while [Figure 2-57](#) shows the velocity profile along with local strain rates obtained using first-order finite difference. The locations corresponding to various strain rates are also shown in [Figure 2-57](#).

Figure 2-56 Axial velocity and temperature profile for premixed stoichiometric methane-air flame at extinction point. The global strain rate at extinction is 289 s^{-1}

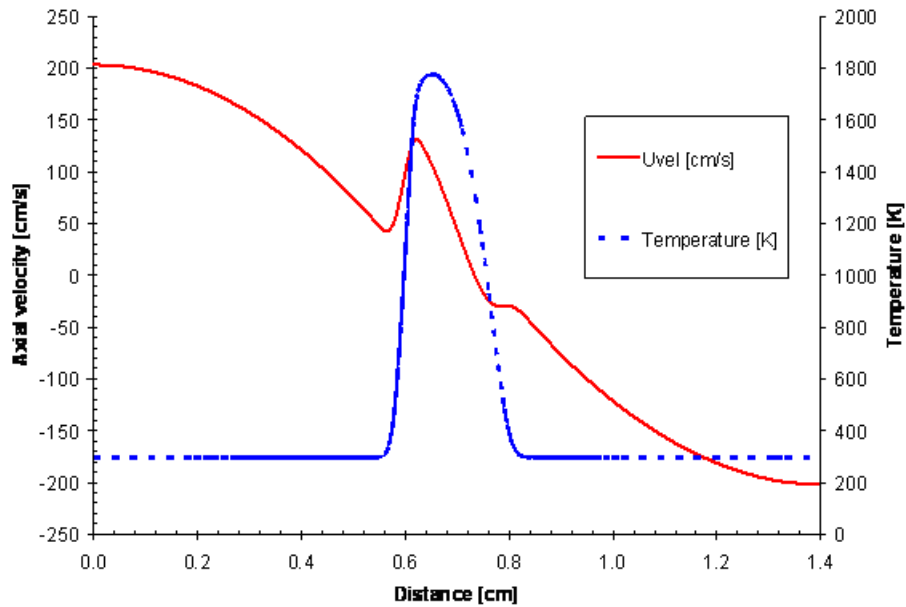
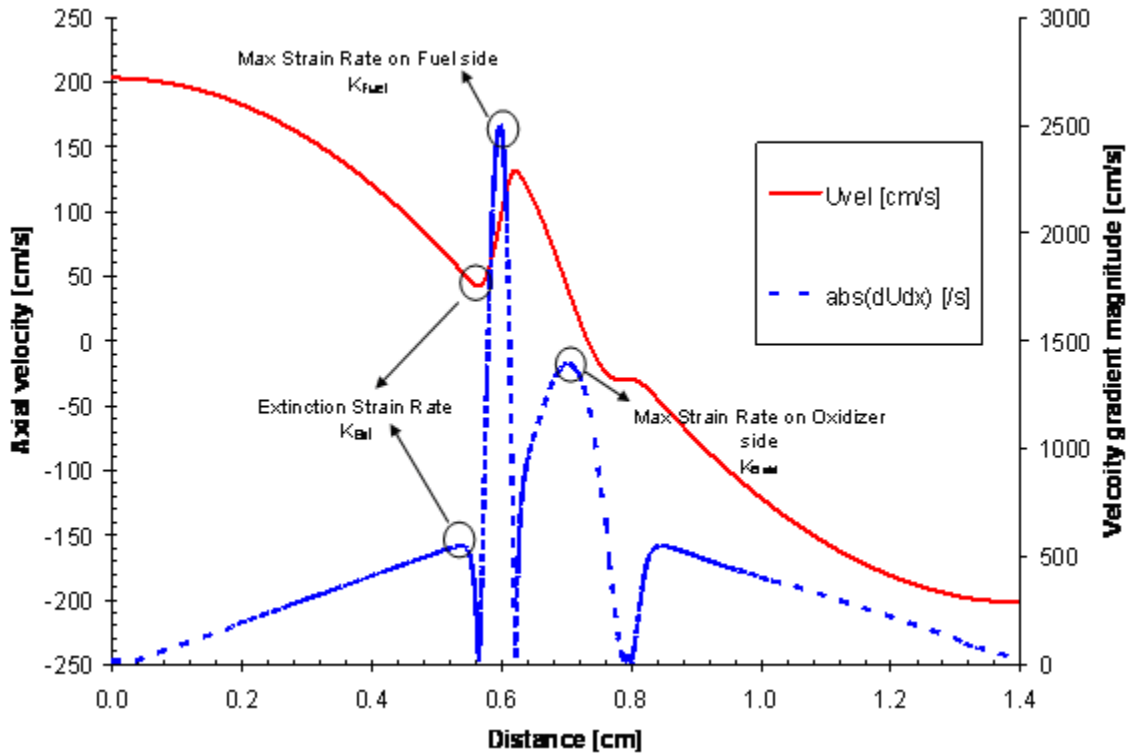


Figure 2-57 Axial velocity and velocity gradient magnitude for premixed stoichiometric methane-air flame at extinction point. Also shown are the points corresponding to the definitions of various extinction strain rates





2.3.11 Stagnation Flame Analysis [CHEMKIN-PRO Only]

2.3.11.1 Project Description

This tutorial describes how to use the Pre-mixed Stagnation Flame Model, which is available under the Flame Simulators in the model palette (see [Figure 2-58](#)). Stagnation flames are used in a variety of practical applications such as flame-based chemical vapor deposition, polymer film processing, etc. In such processes, the flame-generated radicals are utilized to alter the properties of the surface.

Figure 2-58 Icon for Premixed Laminar Burner-Stabilized Stagnation Flame model.



2.3.11.2 Project Set-up

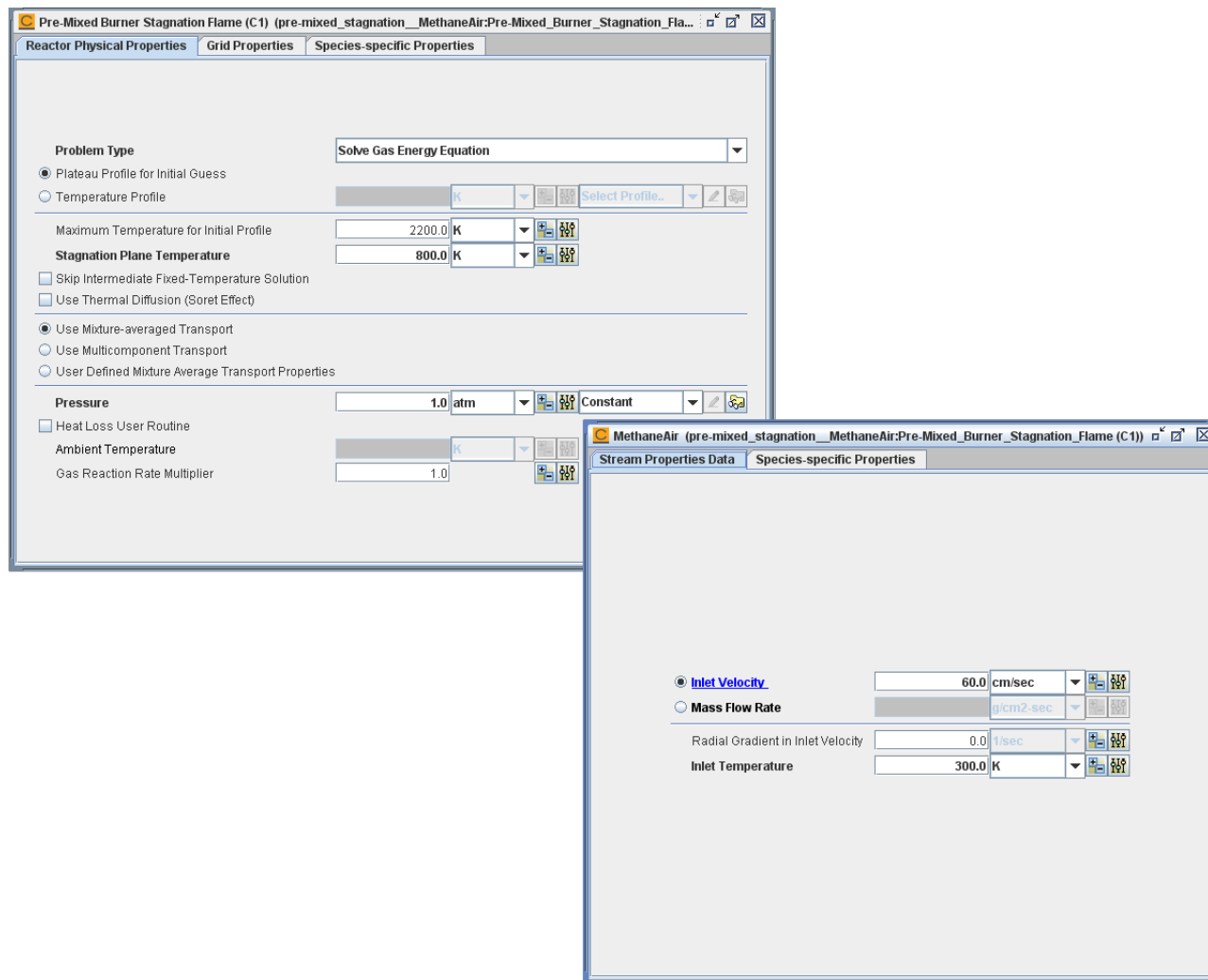
The project file for the burner-stabilized stagnation flame simulation is named ***pre-mixed_stagnation__MethaneAir.ckprj*** and is located in the ***samples2010*** directory. Because this is a new sample, it is possible that your "local" samples directory does not have this sample project. If this is the case, please copy the project file named ***pre-mixed_stagnation__MethaneAir.ckprj*** and the corresponding directory named ***pre-mixed_stagnation*** from your installation location to the local samples directory. (On Windows operating systems, the local samples directory is usually ***C:\Documents and Settings\user\chemkin\samples2010***. The installation directory would be ***C:\Program Files\Reaction\15101_win64\samples2010 for Win64*** and ***C:\Program Files (x86)\Reaction\15101_pc\samples2010 for Win32***.)

The simulation is conducted for a premix stoichiometric methane-air flame at 1 atm pressure impinging on a wall at 800 K. The separation distance between the burner and the wall is 1 cm. A cylindrical coordinate system is used.

A reduced (17 species) methane-air mechanism is used in this tutorial; the chemistry set is described in (in [Section 2.9.2.2](#)). The computational domain is set to span 0.0 - 1.0 cm. The stoichiometric methane-air mixture is assigned to inlet 1 (named MethaneAir). The inlet gas temperature is set to 300 K and the ambient pressure is 1 atm. The wall temperature is set to 800 K. For the initial temperature profile, the guess value for maximum temperature is set to 2200 K. A mixture-averaged formulation is used for the transport model.

A parameter study is set up for the inlet velocity from the burner. Inlet velocity values of 30 cm/s and 60 cm/s are chosen. *Figure 2-59* shows relevant panels from setting up the Interface.

Figure 2-59 Parameter Study set-up.

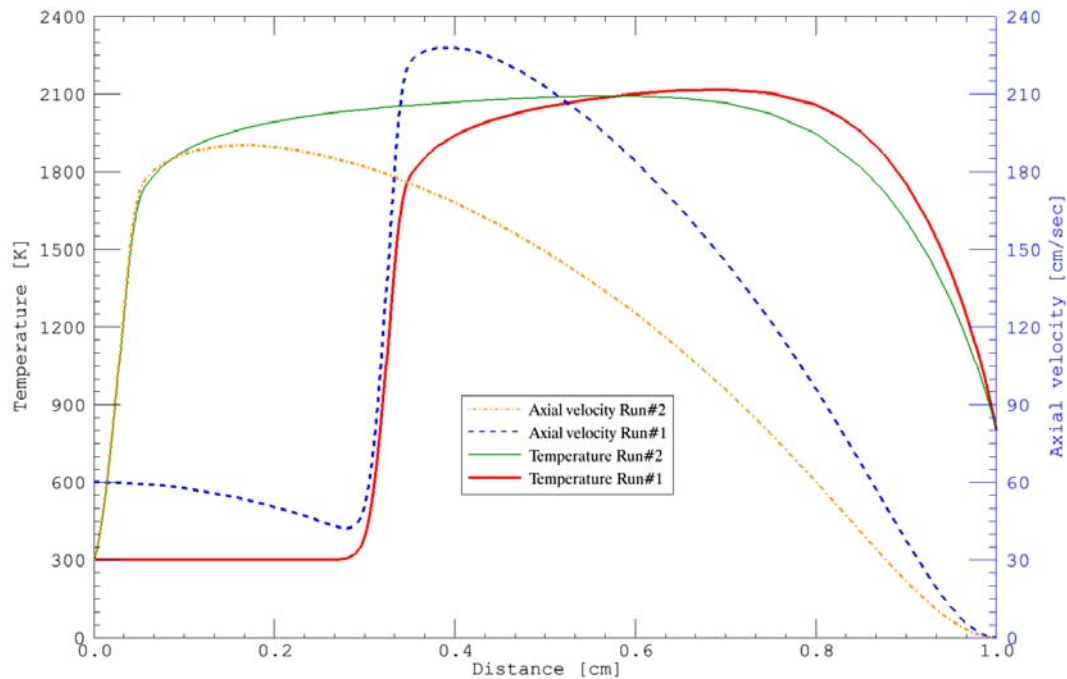


2.3.11.3 Project Results

The laminar flame speed of a stoichiometric methane-air flame at 1 atm pressure and 300 K unburned gas temperature is approximately 38 cm/s. Note that the two inlet velocities chosen in the parameter study lie on either side of this flame speed.

Figure 2-60 shows temperature and velocity profiles obtained for the two inlet velocities. Run 1 corresponds to an inlet velocity of 60 cm/s while run 2 corresponds to 30 cm/s. The flame blows off the burner for the first case and crawls upstream for the second.

Figure 2-60 Temperature and velocity profiles for two inlet velocities

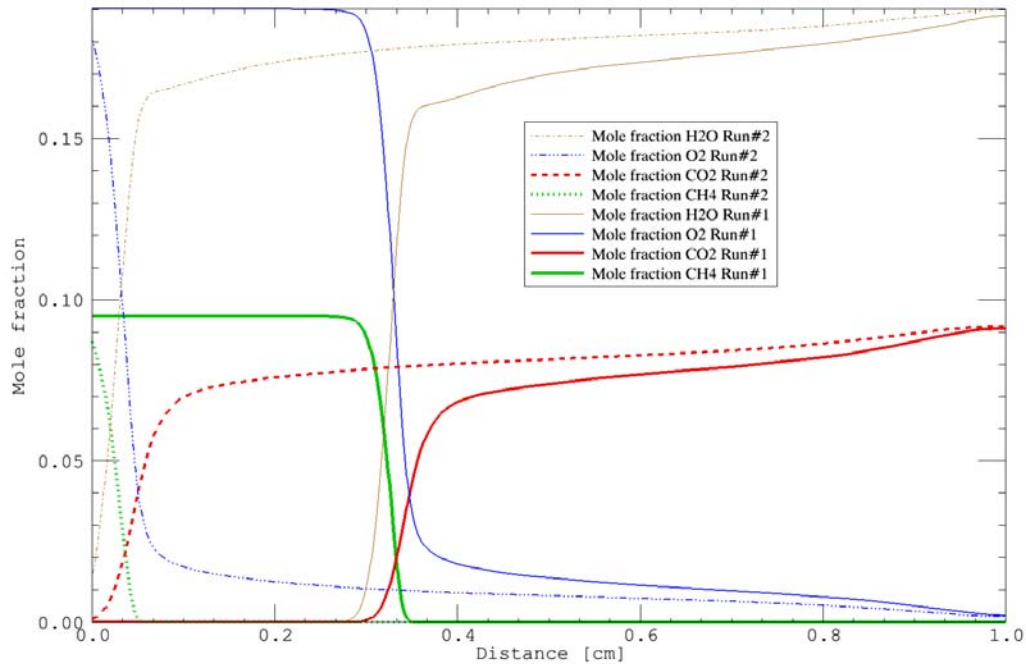


This behavior is expected, since the laminar flame speed is lower than the inlet velocity of run 1, and higher than that of run 2. The presence of a wall creates a boundary layer next to it and thus provides a mechanism for the flame in run 1 to stabilize. At the wall, the bulk velocity has to vanish. The flow thus slows down (and spreads). It can be seen that the minimum velocity just upstream of the flame for run 1 is almost equal to the laminar flame speed of 38 cm/s. As the temperature increases, the density decreases and therefore velocity increases. Since the wall is cooler than the flame, the gas temperature then drops down to the wall temperature. Further increase in the inlet velocity will push the flame towards the wall. At some critical velocity (strain rate), it will be impossible to establish a flame.

For run 2, the flame propagates upstream, because the laminar flame speed is higher than the inlet velocity. However, in doing so there is also heat loss to the burner as its temperature is fixed. The net result is a sharp temperature rise exactly at the lip of the burner.

Shown in [Figure 2-61](#) are the major species mole fraction profiles for the two simulation runs. It can be seen that the flame structure itself is quite similar, with a shift in the axial location. The mole fraction gradients vanish at the wall since thermal diffusion is not included

Figure 2-61 Major species mole fraction profiles for each of two simulation runs.



2.4 Internal Combustion Engine

2.4.1 Homogeneous Charge Compression Ignition (HCCI) Engine

2.4.1.1 Problem Description

Homogeneous Charge Compression Ignition, or HCCI, is an advanced combustion technology for internal combustion engines. The main appeal of the HCCI engine is the great potential for lowering emissions and improving fuel economy.

For this problem, we have some data from a single-cylinder HCCI test engine and would like to use the single-zone IC engine model to simulate the same HCCI process. We would also like to find out how sensitive the solutions are to the assumed heat loss at the cylinder wall.

The HCCI engine for this example runs on natural gas, a mixture of CH_4 , C_2H_6 and C_3H_8 , with exhaust gas recirculation (EGR). The use of EGR helps in more reliable ignition under a wider range of conditions. Additionally, CO_2 from the exhaust gas can keep combustion temperatures low due to its relatively large heat capacity. Specifications of the test engine that are related to our model setup are given in [Table 2-8](#).

Table 2-8 Test Engine Specifications

<i>Parameter</i>	<i>Setting</i>
Compression ratio	16.5
Cylinder clearance volume	103.3 cm ³
Engine speed	1000 rpm
Connecting rod to crank radius ratio	3.714286
Cylinder bore diameter	12.065 cm

2.4.1.2 Problem Setup

CHEMKIN has a pre-defined model for HCCI engine simulations. The model is called the Closed Internal Combustion Engine Simulator and we can select it either by drag-and-dropping to the Diagram View or by double-clicking on the reactor icon in the Models Palette (see [Figure 2-62](#)).

Figure 2-62 IC Engine Icon



The next step is to define the chemistry set, or combustion mechanism, for our HCCI simulation. Since methane is the main component of natural gas, the mechanism we have selected is the GRI Mech 3.0 to describe the combustion process and used methane as the “surrogate” fuel. After pre-processing the mechanism data, we specify the engine parameters in the Reactor Properties panel.

The IC Engine model is appropriate for a closed system, representing the time between intake-valve closure and exhaust-valve opening in the engine cycle. The start time (or start crank angle) therefore represents the time of intake-valve closure. As a convention, engine events are expressed in crank rotation angle relative to the top dead center (TDC). The intake valve close (IVC) time of our test engine is 142 degrees (crank angle) before TDC (BTDC). Since the GUI requires input as the crank angle after TDC, we should set our simulation starting crank angle to -142

degrees (ATDC). We let the simulation run for 257 crank angle degrees to 115 degrees (ATDC). The gas mixture pressure and temperature at IVC are 107911 Pa (or 1.065 atm) and 447 K, respectively. The composition of the initial gas mixture is a combination of natural gas, air, and EGR gas and is given in [Table 2-9](#).

Table 2-9 Composition of Initial Gas Mixture

<i>Species</i>	<i>Mole Fraction</i>
CH4	0.0350
C2H6	0.0018
C3H8	0.0012
O2	0.1824
CO2	0.0326
H2O	0.0609
N2	0.6861

There are two different approaches to defining the heat loss through the cylinder wall. One approach assumes the cylinder is adiabatic and the other considers heat loss through the cylinder wall.

The project file for this HCCI engine simulation problem is called ***ic_engine__hcci_heat_loss_methane.ckprj*** and is located in the ***samples2010*** directory. This project file actually contains two “sub-projects”: the *ic_engine__hcci_adiabatic* project assumes the cylinder is adiabatic and the other project, *ic_engine__hcci_heat_loss_woschni*, considers heat loss through the cylinder wall. By default CHEMKIN will append the new project to an existing project file if the name of the new project is different from the ones already saved in the file. Therefore, we can group similar projects into the same project file by saving those projects one by one to the same project file name.

Parameters that describe heat transfer between the gas mixture inside the cylinder and the cylinder wall are specified on the Reactor Physical Properties panel. For non-adiabatic conditions, we have several ways to describe the heat loss to the wall: a constant heat transfer rate (where a positive value corresponds to for heat loss from the gas to environment), a piecewise-linear heat-transfer rate-profile, a user-defined subroutine, or a heat-transfer correlation specifically designed for engine cylinders. Here we choose the heat-transfer correlation for our HCCI problem. We also apply the Woschni correction¹⁵ to get better estimates of gas velocity inside the cylinder. The parameters used in the heat-transfer correlation are shown in [Figure 2-63](#).

Figure 2-63 C1_ IC Engine—Reactor Physical Property for HCCI Woschni Heat Loss model

Property	Value	Units
End Time	0.043	sec
Engine Crank Revolutions		
Engine Crank Angle		degrees
Engine Compression Ratio	16.5	
Engine Cylinder Clearance Volume	103.3	cm3
Engine Cylinder Displacement Volume		cm3
Engine Connecting Rod to Crank Radius Ratio	3.714286	
Engine Speed	1000.0	rpm
Starting Crank Angle (ATDC)	-142.0	degrees
Temperature	447.0	K
Pressure	1.065	atm
Volume Profile		cm3
Heat Loss		cal/sec
Heat Transfer Correlation		
Coefficient a	0.035	
Coefficient b	0.71	
Coefficient c	0.0	
Chamber Bore Diameter	12.065	cm
Wall Temperature	400.0	K
Heat Loss User Routine		
Prandtl Number	0.7	
Woschni Correlation of Average Cylinder Gas Velocity		
Coefficient C11	2.20	
Coefficient C12	0.308	
Coefficient C2	3.24	cm/sec-K
Ratio of Swirl Velocity to Mean Piston Speed	0.0	
Reference Viscosity		g/cm-sec
Reference Temperature for Viscosity		K
Exponent for Viscosity		
Reference Thermal Conductivity		erg/cm-K-sec
Reference Temperature for Thermal Conductivity		K
Exponent for Thermal Conductivity		
Use Initial Conditions as Reference		
Wall Heat Transfer Coefficient		cal/cm2-K-sec
Wall Thermal Mass		cal/K
Gas Reaction Rate Multiplier	1.0	

2.4.1.3

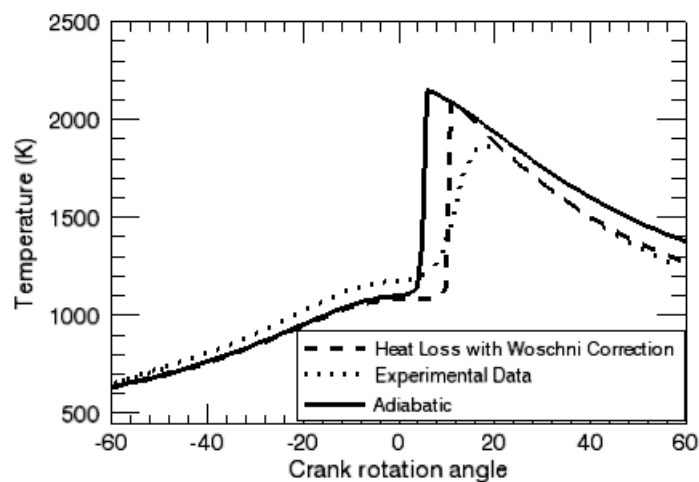
Project Results

After successfully running both adiabatic and heat-transfer-correlation IC Engine projects, we can launch the CHEMKIN Post-Processor from the Analyze Results panel of one the projects. We can load the solutions from the other project by using the **File > Open Solution File** option of the Post-Processor Control Panel.

15. J. B. Heywood, *Internal Combustion Engines Fundamentals*, McGraw-Hill Science/Engineering/Math, New York, 1988.

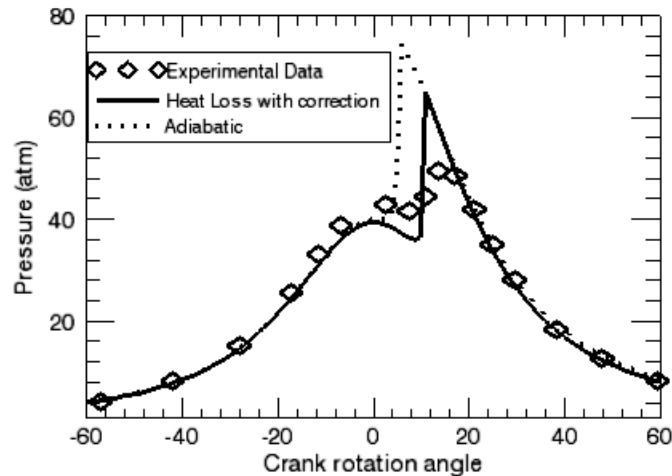
The temperature solutions are shown in [Figure 2-64](#). Again, a crank-rotation angle of 0 degrees corresponds to TDC. We notice that the measured gas temperature before ignition is higher than the one predicted by the adiabatic model. If the measurement was done correctly, this could mean that a small portion of fuel starts burning before TDC and our model fails to capture this phenomenon. The ignition time predicted by the adiabatic model is about 5 degrees earlier than those obtained by experiment and by the non-adiabatic model. The temperature solution from the non-adiabatic model generally agrees with the measurement. Both models predict stronger ignition in the cylinder as indicated by the sharp increases in the temperature profiles. The weaker ignition shown by the experimental data is likely due to temperature variation inside the real cylinder. Although gas composition is homogeneous throughout the cylinder, gas temperature in the core region can be different from that in the boundary layer. The temperature difference can be large if heat loss at the cylinder wall is large. If the gas mixture of the hot core region ignites first, the mean temperature inside the cylinder will not jump as sharply as predicted by the models.

Figure 2-64 HCCI Engine—EGR Temperature Comparison



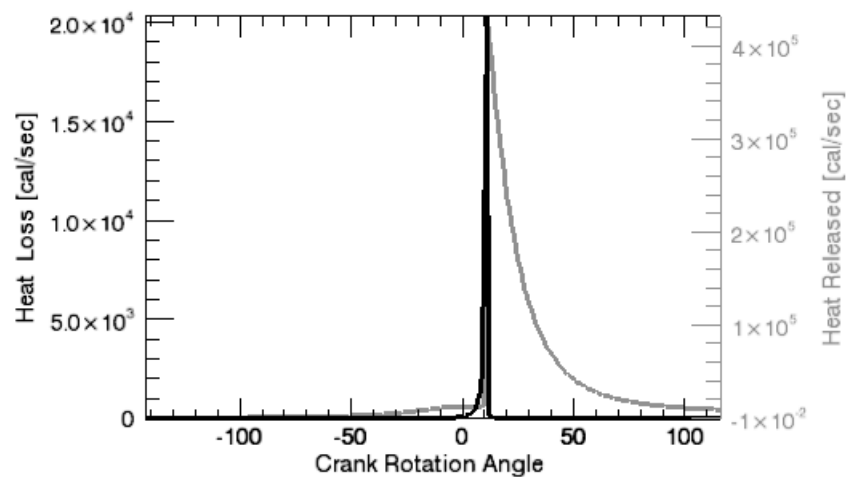
[Figure 2-65](#) gives the comparisons of the measurement and the predictions. In general, the profiles show similar trends as observed in the temperature profiles except that the pressure results are less sensitive to heat loss.

Figure 2-65 HCCI Engine—EGR Pressure Comparison



We can examine the heat-release rate profile for the timing and the magnitude of heat generated by combustion. Since the temperature profile predicted by the non-adiabatic model is in good agreement with the measurement, we can determine how much thermal energy is dissipated to the environment, i.e., the heat loss rate, during the combustion/expansion period. The heat-release rate and the heat loss rate profiles predicted by the non-adiabatic model are shown in [Figure 2-66](#). Note that the heat-release profile usually contains narrow spikes. If we want to calculate the total heat-release from the heat release rate profile, we must make sure the profile has enough time resolution to reduce numerical error.

Figure 2-66 HCCI Engine—EGR Heat Loss Comparison





2.4.2

Multi-zone HCCI Engine Simulation [CHEMKIN-PRO Only]

2.4.2.1

Project Description

This multi-zone model example is based on the 2-bar boost HCCI combustion analysis described in the 2000 SAE paper by Aceves et al.¹⁶ The supercharged HCCI engine is running on natural gas at very low equivalence ratio ($= 0.26$). Engine parameters needed to set up the multi-zone simulation are given in [Table 2-10](#). Composition of the natural gas is provided by Aceves et al.¹⁶ and is listed in [Table 2-11](#).

Table 2-10 Engine parameters of the validation case.

Displacement volume	1600 cm ³
Bore	12.065 cm
Stroke	14 cm
Connecting rod length	26 cm
Engine speed	1000 rpm
Compression ratio	21

Table 2-11 Natural gas composition used in the validation case.

component	CH ₄	C ₂ H ₆	C ₃ H ₈	N ₂	CO
Vol %	91.1	4.7	3.1	0.6	0.5

A 10-zone model is employed in the validation. Configuration and properties of the zones are summarized in [Table 2-12](#). The zone mass distribution recommended by Aceves et al.¹⁷ rather than the one used by the original HCT-multi-zone simulation is used. The distribution of zone surface-area fraction is somewhat arbitrary but, in general, it follows the zone mass distribution. Zone temperature profiles are provided by Aceves et al. and will be used to test the numerical stability of CHEMKIN multi-zone model when the energy equation is switched on at the transition angle (see [Section 8.4.2](#) of the [CHEMKIN Theory Manual](#)). The transition angle in the present multi-zone simulation is set at 3 degrees crank angle BTDC, the same as in the original simulation by Aceves et al.

16. Aceves, S. M., D. L. Flowers, et al. (2000). A multi-zone model for prediction of HCCI combustion and emissions. *SAE Technical Paper* 2000-01-0327.

17. Aceves, M. S., J. Martinez-Frias, et al. (2001). A Decoupled Model of Detailed Fluid Mechanics Followed by Detailed Chemical Kinetics for Prediction of Iso-Octane HCCI Combustion. *SAE Technical Paper* 2001-01-3612.

Table 2-12 Zone configuration used by the multi-zone model analysis for the validation case.

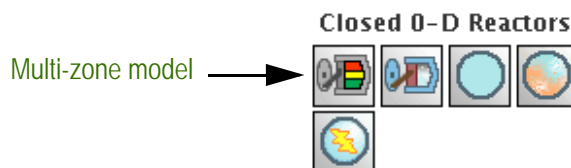
Zone #	1	2	3	4	5	6	7	8	9	10
Region	Crevice					Boundary Layer		Core		
Mass %	2	1	1	1	2	5	10	18	25	35
Area %	5	5	5	10	10	15	15	15	10	10

2.4.2.2 Project Setup

The project file is called *ic_engine_multizone.ckprj* and data files specifying zone temperature profiles are located in the *samples2010\ic_engine_multizone* directory. For convenience, the GRI 3.0 mechanism is used to model the oxidization of natural gas.

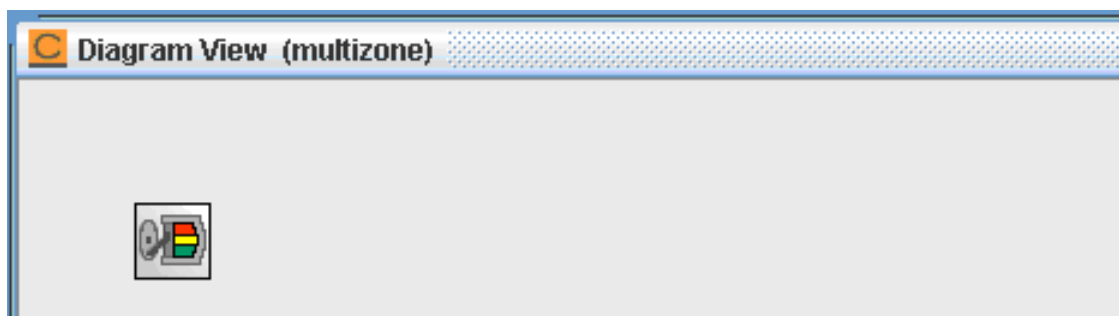
The icon for the multi-zone model can be found in the Models palette under Closed 0-D Reactors (see [Figure 2-67](#)).

Figure 2-67 Reactor model palette showing the multi-zone model icon in the CHEMKIN User Interface.



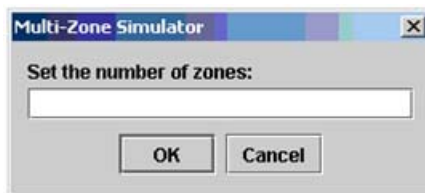
[Figure 2-68](#) shows the diagram view of a multi-zone simulation project. Since the multi-zone model is a closed reactor, the project does not require any inlet or flow connection.

Figure 2-68 Diagram view of a multi-zone simulation project.



When a new multi-zone project is created, a dialog prompts for the number of zones to be used in the simulation, as shown in [Figure 2-69](#). This information is needed once and cannot be changed after the project is created. To use a different number of zones for the same engine simulation, a new multi-zone project must be created.

Figure 2-69 Dialog for specifying the number of zones in the multi-zone simulation.



The User Interface of the CHEMKIN multi-zone model is very similar to its single-zone counterpart. Engine parameters such as compression ratio and parameters for the Woschni wall heat transfer correlation are specified in the Reactor Physical Properties panel, [Figure 2-70](#). The multi-zone model has additional tabs in the Reactor Physical Properties panel for configuring individual zones. Individual zone properties such as zone mass fraction and initial zone temperature can be provided either in the “Zone Properties Table”, [Figure 2-71](#), or in the individual “Zone” tabs, [Figure 2-72](#). If the hybrid solution approach is employed, the transition time or crank angle can be assigned by the **Energy Calculation Switch** in the Reactor Physical Properties panel. [Figure 2-70](#) shows that the energy equation will be switched on at 357 degrees crank angle (i.e., 3 degrees BTDC).



To create a smaller solution file for the multi-zone model, go to the Output Control panel and select the **Store zone-average values only** option before running.

Figure 2-70 Engine parameters in Reactor Physical Properties tab for multi-zone model.

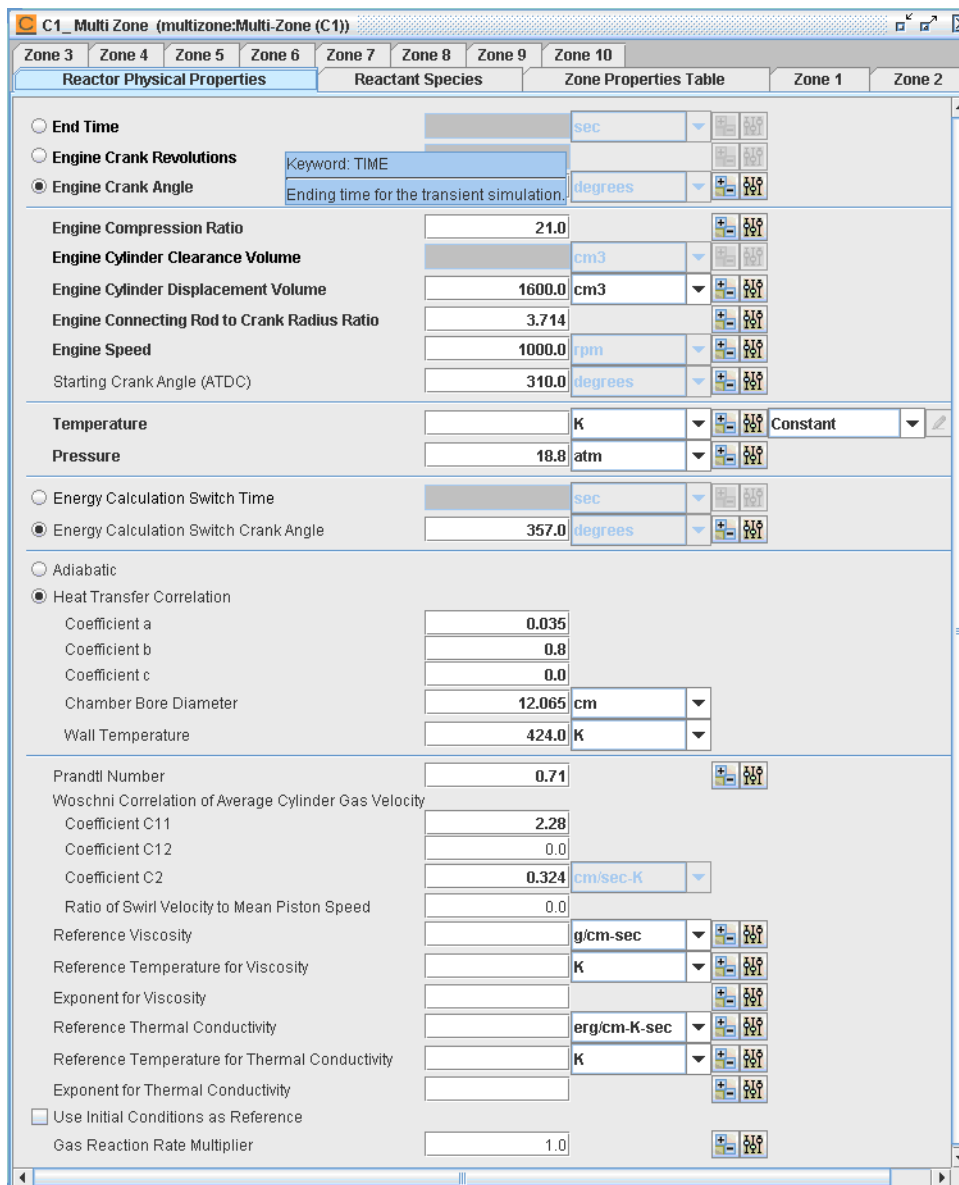
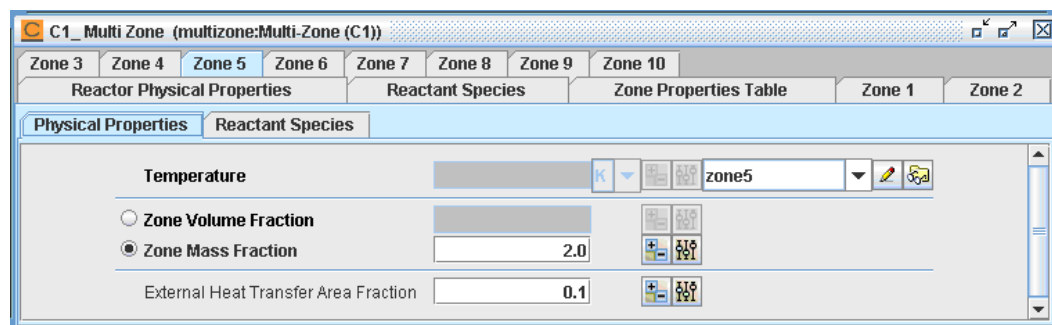


Figure 2-71 Zone Properties table.

C1_Multi Zone (multizone:Multi-Zone (C1))														
		Zone 3	Zone 4	Zone 5	Zone 6	Zone 7	Zone 8	Zone 9	Zone 10					
		Reactor Physical Properties			Reactant Species		Zone Properties Table			Zone 1	Zone 2			
		Properties of zone 6												
Zone Property	Units	Fill R...	Clear ...	Zone 1	Zone 2	Zone 3	Zone 4	Zone 5	Zone 6	Zone 7	Zone 8	Zone 9	Zone 10	
Temperature	K	Fill	Clear											
Zone Volume Fra...	none	Fill	Clear											
Zone Mass Fracti...	none	Fill	Clear	2.0	1.0	1.0	1.0	2.0	5.0	10.0	18.0	25.0	35.0	
External Heat Tra...	none	Fill	Clear	0.05	0.05	0.05	0.1	0.1	0.15	0.15	0.15	0.1	0.1	

Figure 2-72 Individual Zone Properties tab of the multi-zone model graphic user interface using a temperature profile called "zone5"



2.4.2.3 Project Results

Temperature profiles of individual zones predicted by the CHEMKIN multi-zone simulation are shown in [Figure 2-73](#) together with the average temperature and temperature prediction by the single-zone model. The transition angle is set to 3 degrees BTDC as given by Aceves, et al.¹⁶ (see p. 103) The model obtains zone temperatures for corresponding zone temperature profiles before the transition angle is reached. The option to use the temperature profile as a constraint allows the CHEMKIN multi-zone model to take advantage of the zone temperature history that is computed by CFD when heat release from chemical kinetics is not significant. At the transition angle, the model will stop utilizing the temperature profiles and begin to solve zone temperature based on the energy balance of the zone. The Woschni wall heat transfer correlation will be used once the energy equation is turned on. The smooth profiles indicate the temperature governing the equation switch does not give rise to any numerical problem. However, the transition angle seems to be somewhat late in this case, as zone temperatures deviate rapidly after the switch. In a later publication, Aceves et al.¹⁸ suggested that a better transition angle would be about 15.5 degrees before the TDC.

[Figure 2-74](#) compares measured and predicted cylinder pressure profiles. (Experimental data used in the graph for comparison are for illustration only and are not provided in the samples directory.) The CHEMKIN multi-zone model prediction overall shows good agreement with the experimental data. The single-zone prediction, also shown in [Figure 2-73](#), can match the experimental pressure curve very well up to the ignition point by properly adjusting wall heat transfer parameters.

18. Aceves, S. M., D. L. Flowers, et al. (2005). Analysis of Premixed Charge Compression Ignition Combustion with a Sequential Fluid Mechanics-Multizone Chemical Kinetics Model. *SAE Technical Paper* 2005-01-0115.

The multi-zone model is able to yield good predictions of maximum cylinder pressure and the timing of the pressure peak, while the single-zone model significantly over-predicts the maximum pressure and the predicted peak timing is a bit too early compared to the data.

Figure 2-73 Temperature profiles predicted by the single-zone and the multi-zone models. The transition angle is set to 3 degrees BTDC.

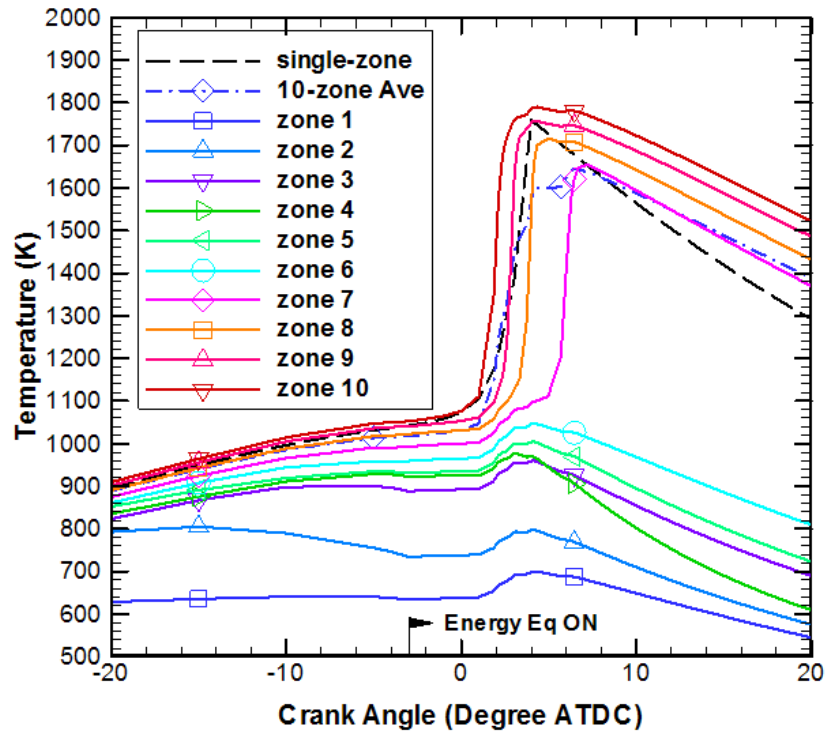


Figure 2-74 Comparison of number density distributions obtained with and without aggregation model.

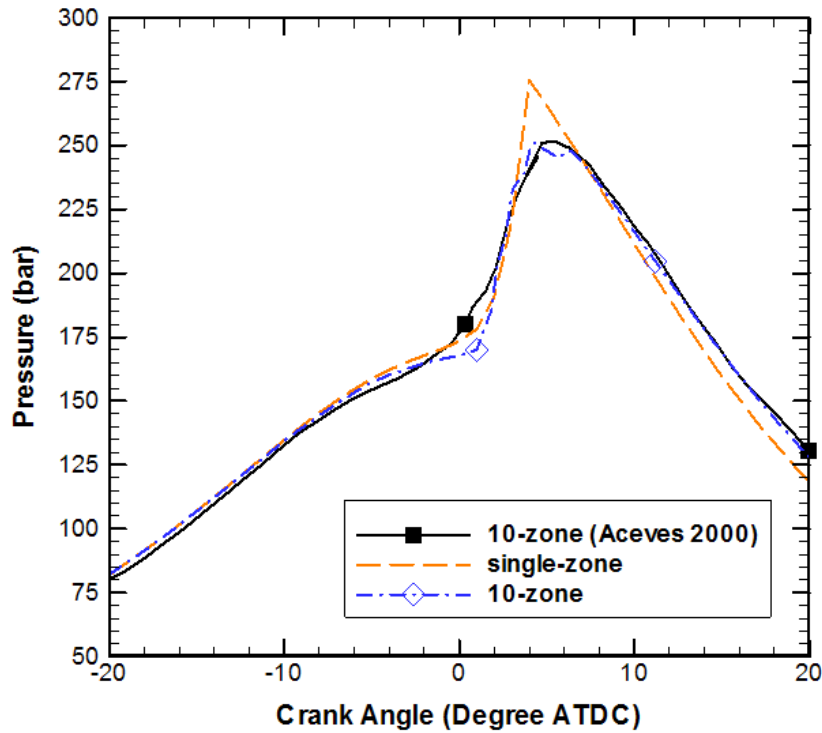
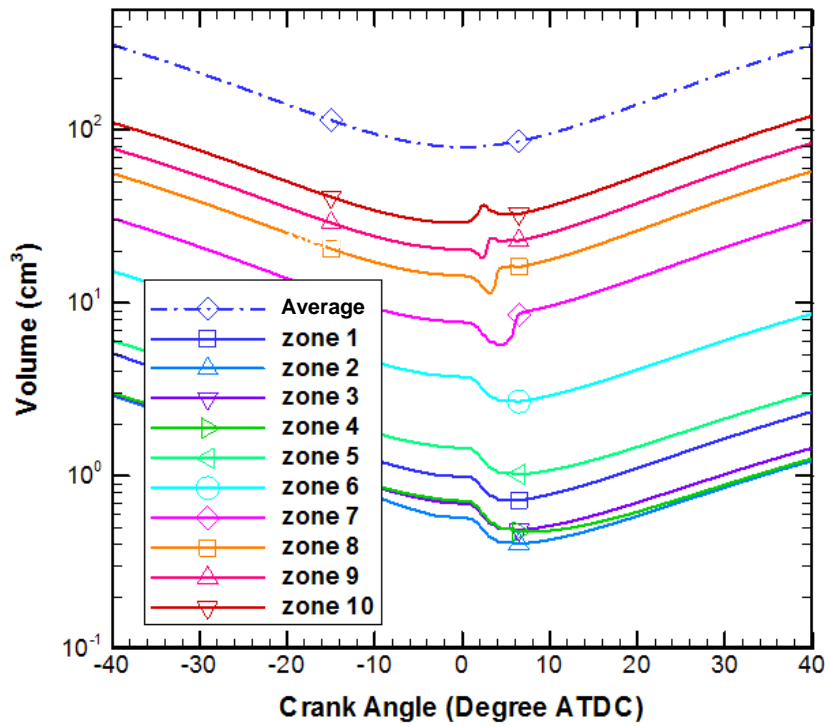


Figure 2-75 Zone volume profiles predicted by the multi-zone models.



2.5 Simulating a Shock-tube Experiment

Mechanism development often involves analyzing experimental data to understand the chemical reactions and extract rate parameters. Shock tube experiments are often used to obtain chemical kinetic data at high temperatures, which is especially relevant to combustion modeling.

2.5.1 Shock-heated Air (Shock)

2.5.1.1 Problem Description

Shock tube experiments are commonly used to study reaction paths and to measure reaction rates at elevated temperatures. We can apply the Normal Shock Reactor Model to validate the reaction mechanism or kinetic parameters derived from such experiments.

In this tutorial, we want to reproduce one of the shock tube experiments done by Camac and Feinberg.¹⁹ Camac and Feinberg measured the production rates of nitric oxide (NO) in shock-heated air over the temperature range of 2300 K to 6000 K. They also assembled a reaction mechanism with kinetic parameters derived from their experimental results. The reaction $N_2 + M = N + N + M$ in their mechanism has a different temperature dependency when the third body is a nitrogen atom (N). To properly incorporate different temperature dependencies for different third bodies, we exclude N from participating as a third body in the original reaction, i.e., the effective third body efficiency for N is set to zero. And we add a new reaction $N_2 + N = N + N + N$ to explicitly address the different temperature dependence of nitrogen atom as the third body. [Figure 2-76](#) shows these two reactions in CHEMKIN format.

Figure 2-76 Nitrogen Atom Reaction in CHEMKIN Format

```

N2+M=N+N+M      1.92E17  -0.5   224900.
N2/2.5/ N/0/
N2+N=N+N+N      4.1E22   -1.5   224900.

```

2.5.1.2 Problem Setup

Setting up a shock tube model requires information from the corresponding experiment. In addition to the conditions of the initial (unshocked) gas mixture, we will need to provide information on the diameter of the shock tube, the viscosity of the gas at 300 K, and the velocity of the incident shock. If we do not know the shock velocity

19. M. Camac and R.M. Feinberg, Proceedings of Combustion Institute, vol. 11, p. 137-145 (1967).

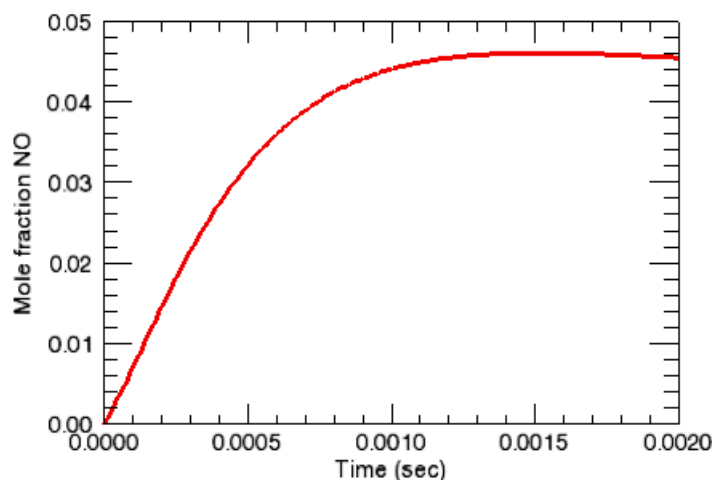
from the experiment, we can estimate it by using the Equilibrium Reactor Model with the Chapman-Jouguet detonation option. The shock tube diameter and the gas viscosity at 300 K are only required when the boundary-layer correction is used in the shock simulation.

The project file, *incident_shock_normal_air.ckprj*, is stored in the *samples2010* directory and the air dissociation mechanism by Camac and Feinberg is located in the associated working directory.

2.5.1.3 Project Results

The NO mole fraction behind the incident shock is shown in [Figure 2-77](#) as a function of time. The NO mole fraction profile rapidly rises to a peak value then gradually falls back to its equilibrium level. Reasons for the greater-than-equilibrium peak NO concentration can be found in the paper by Camac and Feinberg and references therein. The predicted peak NO mole fraction is 0.04609 and is in good agreement with the measured and the computed data by Camac and Feinberg.

Figure 2-77 Shock Tube Experiment—NO Mole Fraction



2.6 Combustion in Complex Flows

2.6.1 Gas Turbine Network

2.6.1.1 Problem description

This tutorial utilizes a PSR-PFR network to predict NO_x emission from a gas turbine combustor.

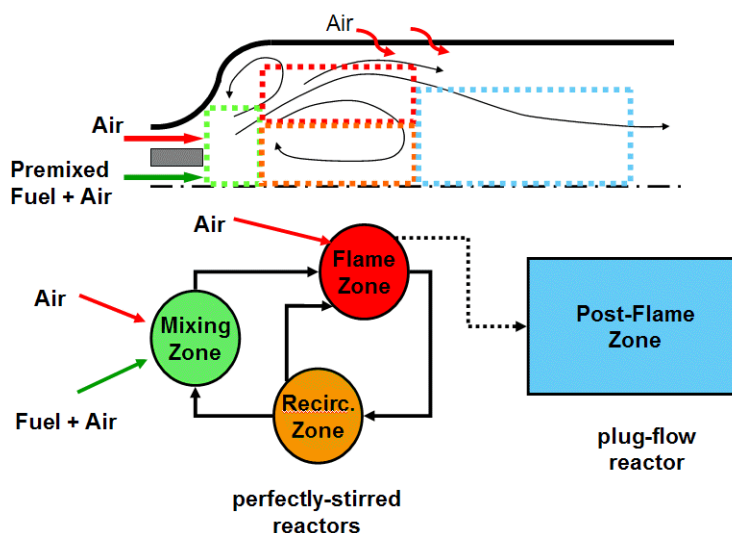
2.6.1.2 Problem setup

A PSR network or a hybrid PSR-PFR network is commonly used to simulate mixing and flow characteristics of a gas turbine combustor.^{20,21} This reactor network approach can greatly reduce the computational burden yet provide reasonable solutions for a complicated combustion process. However, constructing such a reactor network is rather empirical. Slight changes in combustor operating conditions often lead to a new reactor network configuration with a different number of reactors and connectivity. To speed up the time-consuming trial-and-error process, the CHEMKIN Interface provides a Diagram View that facilitates building and modification of a reactor network. A gas turbine reactor network is shown in [Figure 2-79](#). Typically, a gas turbine reactor network consists of a flame/ignition zone, a recirculation zone, and a post-flame zone. However, depending on how the fuel and oxidizer are delivered and the complexity of the flow field, additional reactors and inlets may be needed to properly represent the combustor. The reactor network shown in [Figure 2-79](#) has two reactor network clusters. The first cluster represents the region around the flame in the combustor and the second cluster uses a single PFR for the post-flame region between the flame and turbine inlet. We set the first PSR as the mixing zone because the fuel stream is partially premixed. A flame zone PSR is directly connected to the mixing zone and is followed by a recirculation zone for back mixing of hot combusted gas. The solutions of the through flow from the flame zone (the last reactor of cluster number 1) are automatically fed to the post-flame zone (the second cluster) as indicated by the gray line. [Figure 2-78](#) shows the reactor configuration that will be modelled.

20. A. Bhargava et al., *J of Engineering for Gas Turbines and Power* **122**:405-411 (2000).

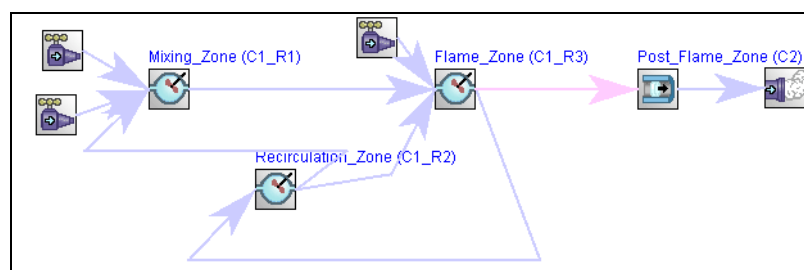
21. T. Rutar and P.C. Malte, *J of Engineering for Gas Turbines and Power* **124**:776-783 (2002).

Figure 2-78 Gas Turbine Network—Schematic



The project file, *reactor_network_gas_turbine.ckprj*, can be found in the **samples2010** directory. The reaction mechanism for methane-air combustion is the GRI Mech 3.0, as described in section [Section 2.9.2](#).

Figure 2-79 Gas Turbine Network—Diagram View



2.6.1.3 Project Results

The solutions from the reactor network are shown in [Figure 2-80](#) and [Figure 2-81](#). The temperature solutions in [Figure 2-80](#) indicate that the gas mixture ignites in the third reactor (flame zone) and the temperature continues to increase in the second reactor (recirculation zone) where part of the recycled CO is consumed. Gas temperature increases slightly in the post-flame region (the second cluster) as remaining CO is converted to CO₂ in the hot flue gas (see [Figure 2-81](#)).

The NO profiles are also given in [Figure 2-81](#). As we expected, NO level continues to rise in the post-flame region mainly due to the thermal NO formation.

Figure 2-80 Gas Turbine Network—Temperature Comparisons

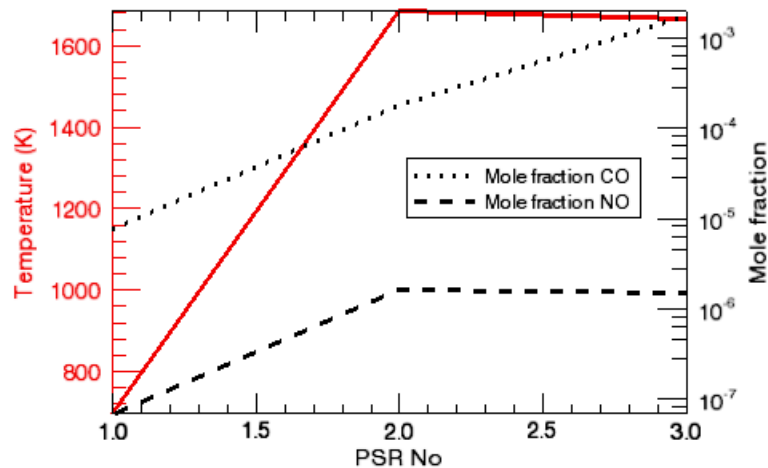
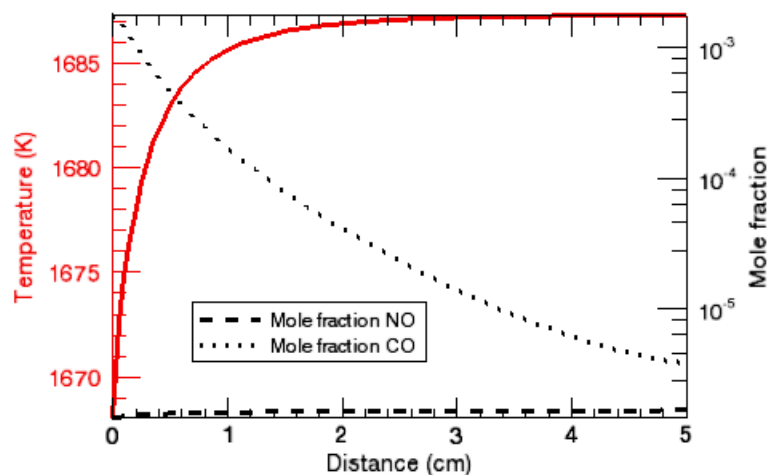


Figure 2-81 Gas Turbine Network—CO and NO Comparisons



2.6.2 Jet Flame Network

2.6.2.1 Problem Description

This user tutorial describes the mechanics of constructing a PSR (perfectly stirred reactor) cluster to represent a non-premixed jet flame.

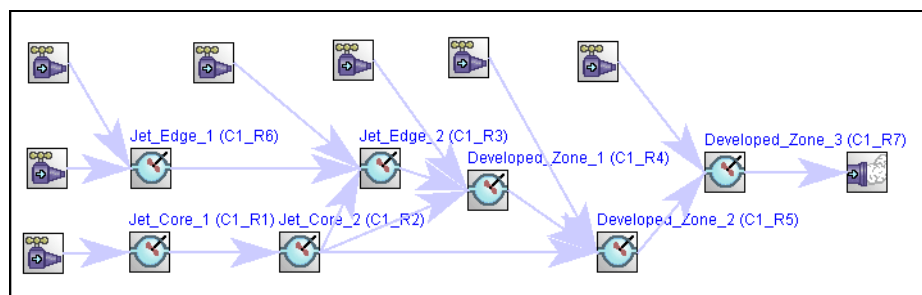
Often, chemical kinetics is either omitted entirely or greatly reduced to make CFD simulations possible for chemically reactive flow systems. When pollutant emissions are to be predicted, the assumption of local chemical equilibrium is not appropriate and the utilization of detailed reaction mechanism is needed. For example, the characteristic chemical time scale of NO is much larger than that of a typical flame species and is compatible to the characteristic time scale, or residence time, of the

flow system. Consequently, the local NO concentration level is far from its equilibrium value and depends on the chemical state, the age, and the history of the gas mixture. For simple flow fields, the exit concentration of the species of interest can be obtained by simply integrating its production rates along streaklines (or streaktubes). In this case, the detailed reaction mechanism is used to calculate production rates according to local chemical states and can be a component of the post-processing utility. However, this approach is not suitable for complex flow fields as strong mixing actions and re-circulations make tracking streaklines difficult. Building a reactor network from “cold” CFD solutions is a plausible approach under this situation as it can utilize the detailed reaction mechanism while preserving some key fluid dynamic features that are important to emission predictions such as the residence time. Discussions on how to identify the reactors and their connectivity are beyond the scope of this tutorial. General guidelines on deriving reactor networks from CFD solutions can be found in papers done by Bhargava *et al.*²⁰ (see p. 112) and Faravelli *et al.*²²

2.6.2.2 Problem Setup

For this problem, we assume that a seven-reactor network is derived from local gas composition and temperature solutions of a CH₄-air diffusion jet flame simulation. The residence times of these reactors and the connectivity and mass flow rates among them are also obtained from the velocity solutions of the CFD simulation. The PSR network representing the diffusion jet flame is given in *Figure 2-82*.

Figure 2-82 Jet Flame Network—Diagram View



We use GRI Mech 3.0, as described in section *Section 2.9.2*, for the gas phase reactions. Because we use PSR's in the network, no transport data is needed. The chemistry set file for this project, **reactor_network_jet_flame.cks**, is located in the working directory, **samples2010\reactor_network\jet_flame**. Since our reactor network model does not consider molecular transport processes, i.e., diffusion and thermal conduction, we cannot resolve the fine structure of the diffusion flame. The

22. Faravelli *et al.*, *Computers and Chemical Engineering* 25:613-618 (2001).

chemical state of each reactor in our model will be controlled by chemical kinetics, residence time, and compositions of gas mixtures entering the reactor, rather than by chemical kinetics and molecular diffusion of reactants as in a fully resolved diffusion flame.

The input parameters for properties of reactors and inlet streams can be found in the project file, *reactor_network_jet_flame.ckprj*, in the *samples2010* directory. Since reactor and stream inputs are straightforward and are already described in previous tutorials, we will focus only on the new Recycling panel here.

The Recycling panel allows us to direct a certain fraction of exit mass flow from one reactor to other reactors in the network. The recycling fraction must be a non-negative number and the sum of recycling fractions from a reactor must equal to one to conserve mass.

If all exit mass flow from reactor n is going to reactor $n + 1$, we do not need to provide a value for the through-flow stream, i.e., the default through-flow “recycling” fraction is 1. For instance, the recycling stream Jet_Edge_2 to Developed_Zone_1 on the Recycling panel is actually a through-flow stream from reactor C1_R3 to reactor C1_R4 (see [Figure 2-82](#)). We can leave the text box blank and CHEMKIN will use the default value of 1 for the “recycling” fraction. For other recycling streams, there is no default value and a recycling fraction (between zero and one) must be provided in the text box.

2.6.2.3 Project Results

The solution plots of a reactor network are difficult to interpret because the reactor number does not necessarily correspond to its actual location in the flow field. In our case, reactor C1_R6 actually represents the outer edge of the fuel jet and should be physically located right next to the fuel jet nozzle in an upstream region. On the other hand, reactors C1_R5 and C1_R7 are the flame zone and the post-flame region, respectively, and are both located downstream from reactor C1_R6. Therefore, when we look at the solution plots as a function of the reactor number, we should ignore the sudden changes corresponding to reactor C1_R6.

The predicted temperature distribution is shown in [Figure 2-83](#). The adiabatic flame temperature of the stoichiometric CH₄-air mixture is also given on the plot for reference. We can see that reactors C1_R3, C1_R4, C1_R5, and C1_R7 have temperatures close to the adiabatic flame temperature, which is a good indication for the flame zone and post-flame region. The reactor temperature dropping when coming from reactor C1_R5 to reactor C1_R7 is appropriate, since C1_R7 is in the

post-flame region. We can further confirm this speculation by checking the solutions of other variables. We also think the jet flame is slightly lifted from the fuel jet nozzle because the outer edge of the fuel jet (reactor C1_R6) stays at a relatively low temperature.

Figure 2-83 Jet Flame Network—Temperature Distribution

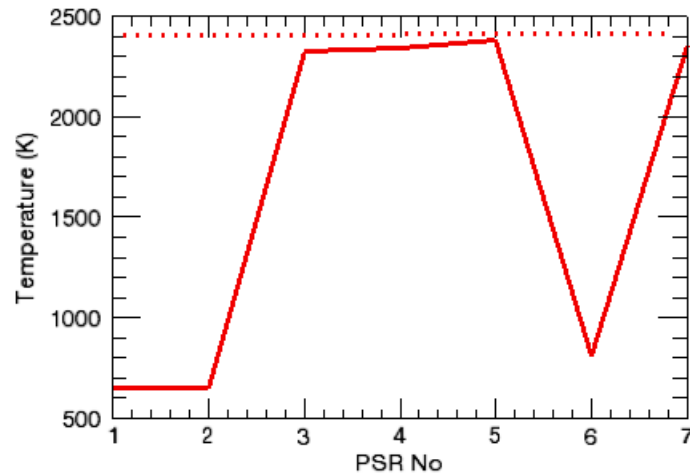
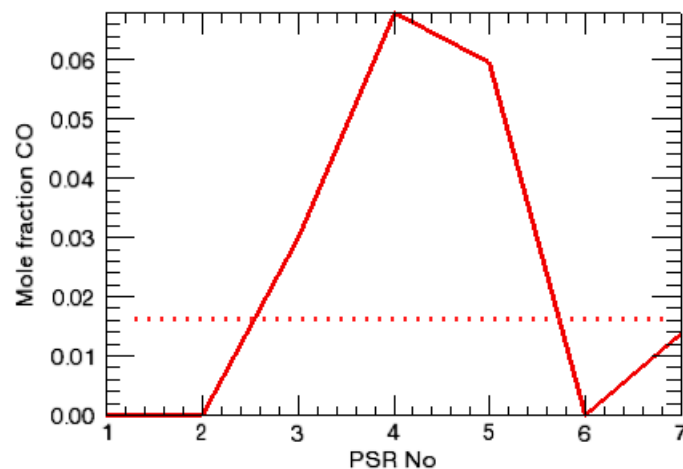


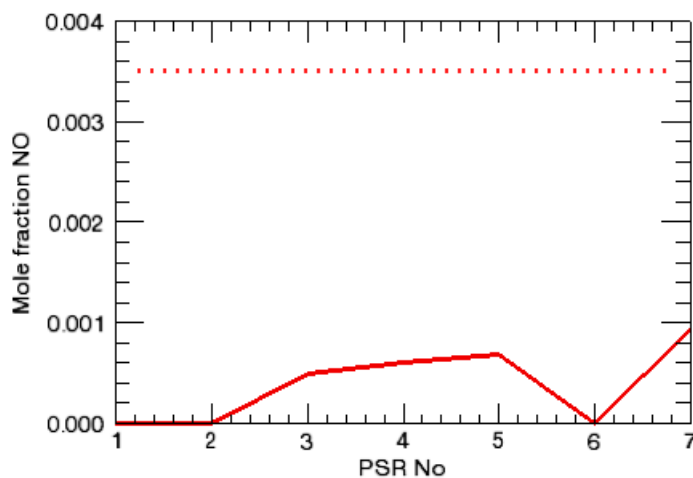
Figure 2-84 gives the CO mole fraction distribution among the reactors. Again, the CO mole fraction at the adiabatic flame condition is provided to show where the combustion zone ends. The CO profile shows a spike starting from reactor C1_R3 to reactor C1_R7. We ignore reactor #6 because it does not connect either to reactor C1_R5 or reactor C1_R7. This CO spike resembles the one we observe in a typical flame zone and makes us believe that the flame zone ends before reaching reactor C1_R7. The predicted CO mole fraction in reactor C1_R7 is also lower than its adiabatic flame value and is consistent with our observation for the post-flame region.

Figure 2-84 Jet Flame Network—CO Distribution



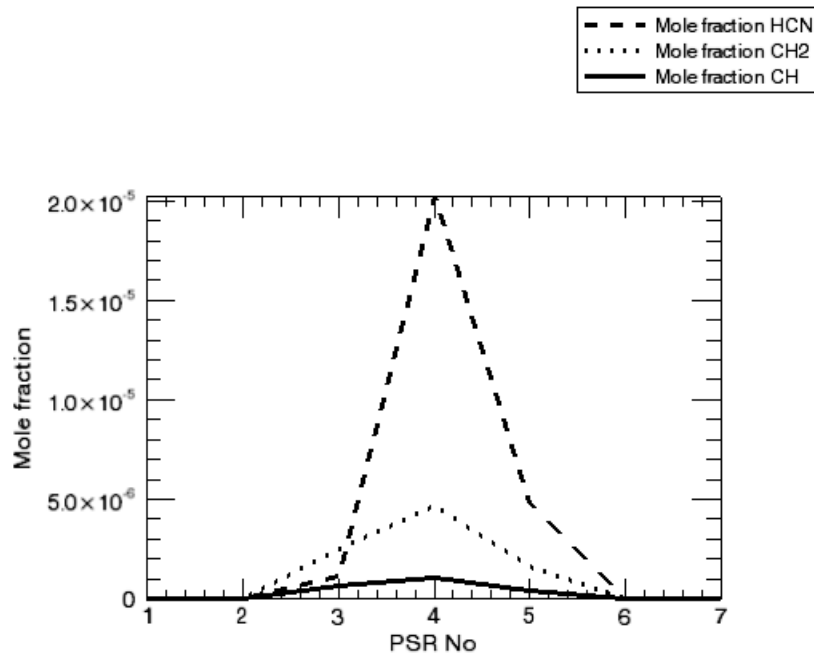
One of the advantages of using a reactor network is the ability to predict NO formation without running a full CFD calculation with detailed chemistry. The NO profile in [Figure 2-85](#) shows that NO starts to form in the flame zone (reactors C1_R3, C1_R4, and C1_R5) and continues to rise in the hot post-flame region (reactor C1_R7). We can find out which NO formation mechanism is responsible for the NO increase in the high temperature region. In the absence of fuel nitrogen, NO in our jet flame can be formed via prompt NO and thermal NO mechanisms.²³ Since the prompt NO mechanism is characterized by the existence of radicals such as CH and HCN, we can plot the profiles of these radicals to find out the region where thermal NO is the dominant NO formation mechanism. From the profiles in [Figure 2-86](#), we can see that all prompt-NO-related radicals disappear in the post-flame region (reactor C1_R7). so we can conclude that thermal NO is the main NO formation mechanism in the hot post-flame region. The reactor model also shows that, unlike gas temperature and CO mole fraction, the “exit” NO mole fraction is far below its equilibrium value. This is in accord with the fact that the characteristic chemical time scale of NO is greater than the fluid mechanical time scale of our jet-flame system.

Figure 2-85 Jet Flame Network—NO Distribution



23. Miller and Bowman, *Prog. Energy Combust. Sci.*, 15:287-338 (1989).

Figure 2-86 Jet Flame Network—Mole Fractions



2.6.3

Using Tear Streams to Estimate Initial Gas Composition in an HCCI Engine with Exhaust Gas Recirculation (EGR) [CHEMKIN-PRO Only]

2.6.3.1

Problem Description

This HCCI_EGR project simulates a homogeneous charged compression ignition (HCCI) engine with exhaust gas recirculation (EGR). One of the strategies to control ignition in an HCCI engine is to charge the cylinder with a mixture of exhaust gas and fresh fuel-air mixture. The introduction of exhaust gas impacts ignition in several ways. Thermodynamically, the added exhaust gas could increase the initial gas temperature and affect gas temperature during compression by modifying mixture-specific heat capacity. The presence of exhaust gas would also influence ignition kinetics by dilution and by alternative reaction pathways such as NO_x -mutual sensitization.

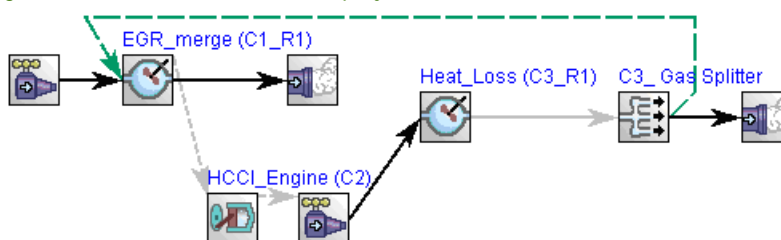
Since the composition and temperature of recycled exhaust gas mixture are part of the solution, they are not known prior to running the simulation. This project utilizes a tear-stream reactor network to estimate exhaust gas properties by running the simulation iteratively. Ideally, this iterative scheme would reach a “steady-state”, that is, initial gas properties inside the cylinder do not show significant cycle-over-cycle variations. Moreover, this kind of project could be employed to build correlations between inlet gas properties, engine operating conditions, EGR ratio, and initial gas

properties inside the cylinder and to map a “stable” HCCI engine operation regime in terms of EGR ratio, RPM, fuel equivalence ratio, and fuel type. The single-zone Internal-Combustion engine model in the EGR network can be replaced by the Multi-zone Engine Model if desired.

2.6.3.2 Problem Setup

The project is called *ic_engine_EGR_network.ckprj* and the combustion mechanism is GRI 3.0 methane oxidation mechanism. This *EGR_network* project contains three major components or clusters, as shown in [Figure 2-87](#). The HCCI Engine cluster (C1) represents the HCCI engine cylinder of which the initial condition at intake valve close (IVC) is not well known due to external EGR. The Heat_Loss (C3) cluster is a simplified model of the collection of pipes and valves that circulates exhaust gas back to the intake manifold. This project assumes 30% of exhaust gas mass gets recycled. Chemical reactions and heat transfer are allowed in the EGR pipe system. Cluster EGR_Merge (C1) simulates the mixing of the fresh fuel-air mixture and the recycled exhaust gas in the intake manifold. The green dash line in [Figure 2-87](#) represents the recycle, or “tear” stream of this *EGR_network*. The simulation is converged (or the *EGR_network* system is running at steady-state) when variations of properties of this “tear stream” satisfy a given criterion. The grey dashes lines indicate that the solution from the “source” reactor is used as the initial or inlet condition of the “target” reactor. The Gas_Splitter simply distributes the outgoing mass flow rate without considering any chemical or heat transfer effects.

Figure 2-87 Diagram view of the EGR_network project.



The EGR_Merge reactor facilitates the merge between the fresh fuel-air mixture and recycled exhaust gas. In this project, an open PSR model is used so that chemical reactions would take place as soon as the gases are mixed; otherwise, a Gas Mixer could be employed here. The Reactor Properties panel of the EGR_Merge reactor is shown in [Figure 2-88](#). Note that the reactor pressure should be the same as the in-cylinder pressure of the HCCI engine at IVC.

Figure 2-88 Reactor Properties panel of the EGR_Merge reactor.

Figure 2-89 shows the inlet properties panel of the fresh fuel-air stream. Temperature, composition, and flow rate of the fresh fuel-air mixture are specified here.

Figure 2-89 Stream Properties panel of the fresh fuel-air mixture entering the EGR_Merge reactor .

Parameters and operating conditions of the HCCI engine are entered in the corresponding Reactor Properties panel (Figure 2-90). Initial gas temperature, pressure, and composition are not needed here as they will be obtained directly from the solution of the EGR_Merge reactor.

Figure 2-90 Engine Properties panel of the HCCI engine model.

Initialization Panel	Reactor Physical Properties	Reactant Species
<input checked="" type="radio"/> End Time	0.045	sec
<input type="radio"/> Engine Crank Revolutions		
<input type="radio"/> Number of Engine Crank Angle		degrees
Engine Compression Ratio	16.5	
Engine Cylinder Clearance Volume	103.3	cm ³
Engine Cylinder Displacement Volume		cm ³
Engine Connecting Rod to Crank Radius Ratio	3.714	
Engine Speed	1000.0	rpm
Starting Crank Angle	180.0	degrees
Temperature		K
Pressure		atm
Volume Profile		cm ³
<input type="radio"/> Heat Loss		cal/sec
<input checked="" type="radio"/> Heat Transfer Correlation		
Coefficient a	0.035	
Coefficient b	0.71	
Coefficient c	0.0	
Chamber Bore Diameter	12.065	cm
Wall Temperature	400.0	K

The main purpose of the Heat Loss reactor is to provide a way to cool down the hot exhaust gas, so it is important to provide suitable values for residence time, heat transfer coefficient, internal surface area, and ambient temperature ([Figure 2-91](#)). The solution from the HCCI engine simulation will supply the temperature and composition of the inlet mixture. By default, values of the last time point in the solution file will be used. Since the HCCI engine is a closed model, i.e., it has no outlet mass flow rate, the mass flow rate of the inlet must be provided and the **Override Velocity with User Supplied Data** should be checked, as shown in [Figure 2-92](#). The value of mass flow rate must be chosen carefully so that the mass flow rate ratio of the recycled exhaust gas and the fresh fuel-air mixture gives the correct EGR ratio. In this case, the Heat_Loss reactor has a mass flow rate of 10 g/sec (see [Figure 2-93](#)) and the split ratio is 0.3 (see [Figure 2-94](#)), and therefore the mass flow rate of the recycled exhaust gas is 3 g/sec. Since the mass flow rate of fresh fuel-air mixture to the EGR_Merge reactor given in [Figure 2-89](#) is 7 g/sec, the mass ratio of the fresh fuel-air mixture and exhaust gas is 7:3 or 30% EGR by mass. Double-click on the Splitter node on the project tree to activate the Split Factor panel, and then enter the split factor ([Figure 2-94](#)).

Figure 2-91 Properties of the Heat_Loss reactor.

Reactor Physical Properties		Species-specific Properties	
Problem Type		Solve Gas Energy Equation	
<input checked="" type="radio"/> Steady State Solver <input type="radio"/> Transient Solver			
End Time			sec
Residence Time	0.02		sec
Temperature	900.0		K
Pressure	1.0		atm
<input checked="" type="radio"/> Volume <input type="radio"/> Volume User Routine		500.0	cm3
<input type="radio"/> Heat Loss <input checked="" type="radio"/> Heat Transfer Coefficient <input type="radio"/> Heat Loss User Routine		0.006	cal/cm2-K-sec
Ambient Temperature		350.0	K
<input checked="" type="radio"/> Surface Temperature Same as Gas Temperature <input type="radio"/> Surface Temperature <input type="radio"/> Wall Heat Transfer Coefficient			
Wall Thermal Mass			cal/K
Internal Surface Area		550.0	cm2

Figure 2-92 Initialization panel of the inlet stream to the Heat_Loss reactor.

Initialization Panel		Stream Properties Overrides		Species-specific Properties	
Solution for Initialization					0
Reactor Number for Initialization					1
Use Solution at Time					sec
Use Solution at Distance					cm
<input type="checkbox"/> Override Temperature Pressure with User-specified Data <input checked="" type="checkbox"/> Override Velocity with User-specified Data					

Figure 2-93 Properties of the inlet stream to the Heat_Loss reactor.

Initialization Panel		Stream Properties Overrides		Species-specific Properties	
<input checked="" type="radio"/> Mass Flow Rate <input type="radio"/> Volumetric Flow Rate in SCCM <input type="radio"/> Volumetric Flow Rate <input type="radio"/> Use Inlet User Routine		10.0	g/sec		
<input type="checkbox"/> Use SCCM for User Inlet Routine					
Inlet Temperature		1000.0	K		

Figure 2-94 Split Factor panel for the Gas Splitter.

Please specify all the fraction of flow listed and make sure they sum to 1.0.

Sum of fractions of flow from Heat_Loss of PSR (C3)	1.0
Fraction of flow from Heat_Loss of PSR (C3) to EGR_merge of PSR (C1)	0.3
Fraction of flow from Heat_Loss of PSR (C3) to C3_Product of Splitter3	0.7

Convergence of this iterative scheme is determined by properties of the tear stream. Convergence criteria can be supplied in the Tear Stream panel, which is activated by double-clicking on the Tear Stream Controls node on the Project tree. [Figure 2-95](#) shows the Tear Stream Controls panel along with the default values. It is possible to speed up the convergence process of the iterative scheme by providing “hot” initial guess values for the **Tear Stream**. The initial guesses are entered on the Initialize Tear Streams tab of the Tear Stream Controls panel.



Note that the “Initialize Tear Streams” functionality is optional. However, when it is applied, guess values of all stream properties must be provided. Every time the Initialize Tear Streams tab is clicked, a reminder will show up (see [Figure 2-96](#)). [Figure 2-97](#) shows the Tear Stream Properties panel where guess values could be given.

Figure 2-95 Tear Stream Controls panel.

Tear Acceleration Algorithm	Direct_Substitution
Absolute Tear Tolerance	1.0E-9
Relative Tear Tolerance	0.0001
Maximum Number of Tear Iteration	100
Tear Convergence Display	Default

Figure 2-96 Popup reminder for the “initialize Tear Streams” panel.

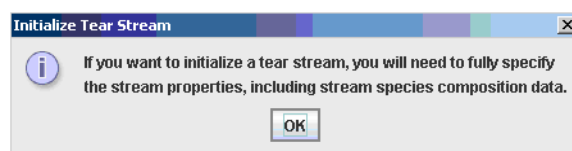
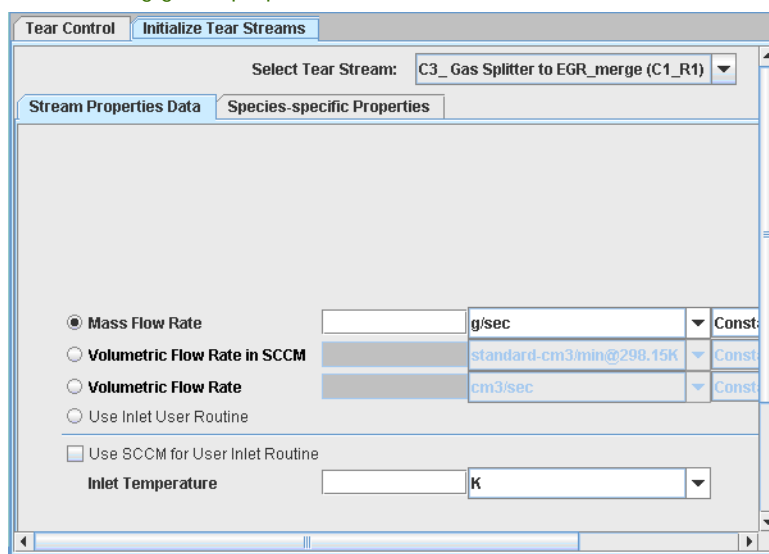


Figure 2-97 Panel for entering guess properties of the Tear Stream.



After the project is set up, it is run like other CHEMKIN projects. The only difference is that, in the “Detail View”, Clusters belonging to the same tear stream will be grouped together and highlighted, as shown in [Figure 2-98](#). When a project containing a tear stream is run, the Progress Monitor will provide text messages and two graphical bars indicating progress of the current iteration step and overall convergence.

Figure 2-98 Detail view of the calculations in which clusters of the same Tear Stream are grouped together and highlighted.

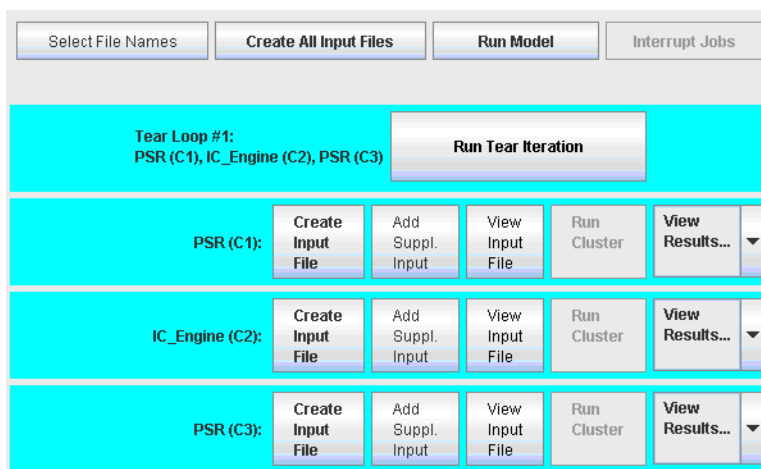
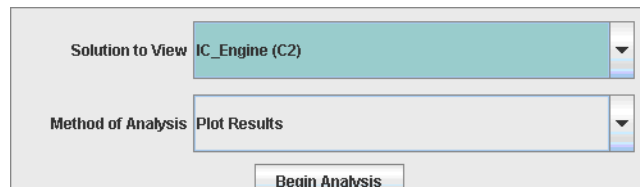


Figure 2-99 Project Results

The simulation results can be processed by clicking on the Analyze Results node on the project tree. Since the main interest of this project is the solution of the HCCI engine, select **IC_Engine (C2)** in the **Solution to View** box and click the **Begin Analysis** button as shown in [Figure 2-100](#). This will open the Graphical Post-Processor for plotting and/or exporting results from the HCCI engine simulation.

Figure 2-100 Solution selection panel.



Plots comparing “steady state” results of the current HCCI Engine simulation (30% EGR) and those without EGR are given in [Figure 2-101](#) to [Figure 2-104](#).

Figure 2-101 Comparison of EGR effect on in-cylinder pressure. Solid line: no EGR; Dash-dotted line: 30% EGR by mass.

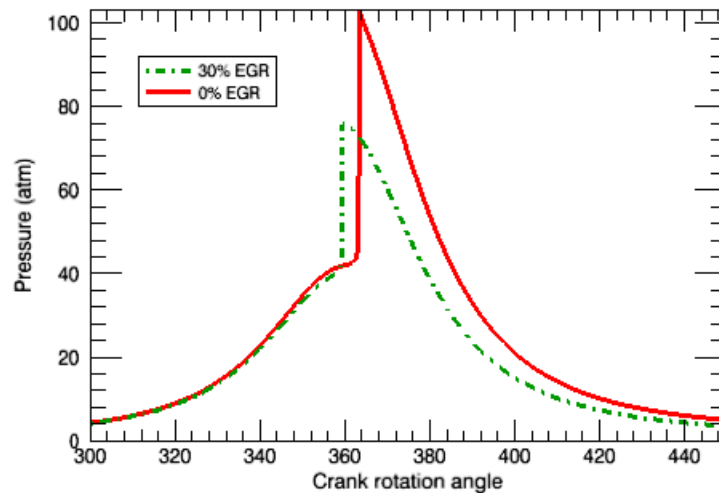


Figure 2-102 Comparison of EGR effect on gas temperature. Solid line: no EGR; Dash-dotted line: 30% EGR by mass.

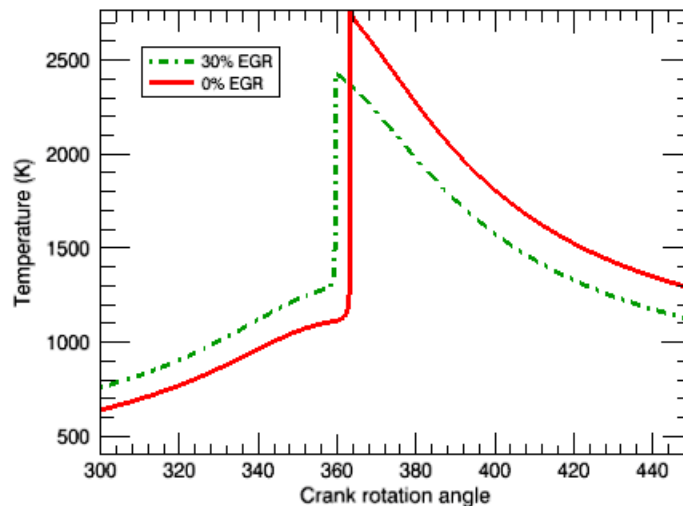


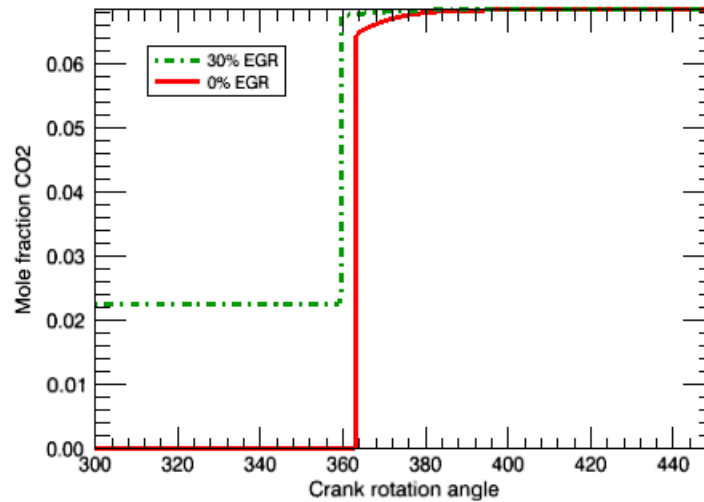
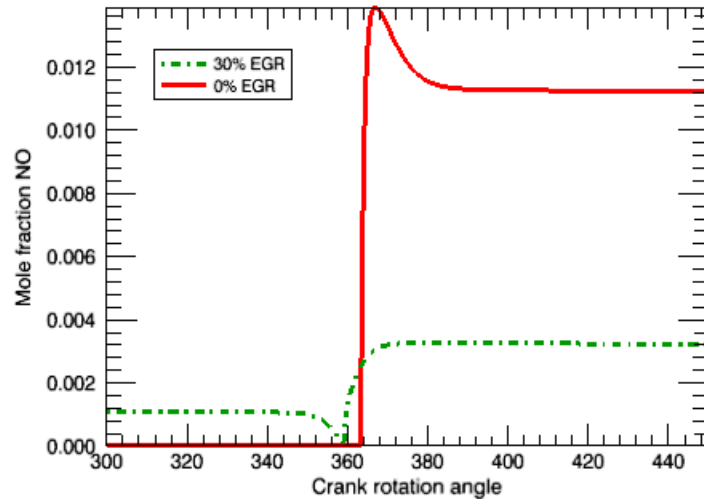
Figure 2-103 Comparison of EGR effect on CO₂ emission. Solid line: no EGR; Dash-dotted line: 30% EGR by mass.

Figure 2-104 Comparison of EGR effect on NO emission. Solid line: no EGR; Dash-dotted line: 30% EGR by mass.



2.6.4 Partially Stirred Reactor for Methane/Air

2.6.4.1 Problem description

In this tutorial, we want to explore effects of imperfect mixing on the exit flow condition from a premixed gas turbine combustor.

When chemical kinetics is the limiting factor of the reacting system under investigation, we would model the reactor as a perfectly stirred reactor (PSR). The perfect mixing of reactants and products inside a PSR is usually accomplished by using mixers or multiple-jet injections. However, a gas-turbine combustor normally

does not have these mixing mechanisms and has to rely on fluid motions, i.e., large-scale eddies and turbulence, to provide the necessary mixing actions. Local turbulence is particularly important as it promotes micro-scale mixing among the gas species.

Although it is adequate in many cases to treat the gas-turbine combustor as a PSR,²⁴ this PSR approach does not always yield proper predictions for the combustor outlet condition. One of the factors that can cause the failure of a PSR approach is the interaction between the turbulence (micro-mixing) and chemical kinetics. If the turbulence is too weak to provide fast mixing among the gas species, the micro-mixing process will interfere with the chemical kinetics. In some cases, when the reactants (non-premixed cases) or the reactants and the products (premixed cases) fail to mix microscopically before they are blown out of the combustor, no combustion zone can be established inside the combustor. The partially stirred reactor (PaSR) model is a tool that can be used to assess the extent of turbulence-kinetics interaction in a gas-turbine combustor or to provide information on how turbulence intensity will affect the combustor.

2.6.4.2 Problem Setup

The project file for this sample problem is located in the ***samples2010*** directory and is called ***pasr_ch4_air.ckprj***. A skeletal methane/air combustion mechanism is used to speed the calculation, since we are interested in knowing whether combustion can be sustained inside the combustor by turbulence mixing.

Molecular mixing is important to this problem despite the fact that the fuel and air are premixed before entering the combustor. For premixed problems, good and fast mixing between the fresh reactants and the burned products is required to anchor the combustion zone inside the combustor. To provide a good starting point for the back mixing, we need to initialize the PaSR with the burned state. This is similar to starting a gas-turbine combustor with a pilot flame. We can use the equilibrium model or the steady state PSR model to obtain the burned state of the premixed fuel-air mixture. Effects of the initial condition on the solutions will be minimal once the simulation time passes the residence time of the combustor.

There are several model parameters that are unique to the PaSR model. First, we need to specify how the PaSR will treat chemical reactions. In the current case, we want to use finite rates defined by the reaction mechanism. Secondly, we have to select a Monte Carlo mixing model and define parameters for the mixing model. The choice of mixing model depends on how we “envision” the mixing process will behave

24. T. Rutar and P.C. Malte, *J of Engineering for Gas Turbines and Power*, **124**:776-783 (2002).

in the combustor. In this case, we choose the modified Curl's model because we think turbulence eddies in our combustor have a relatively large size variation. The mixing time on our panel (0.0001 sec) is actually the mechanical time scale of the turbulence, or the large eddy turnover time. The "factor for mixing models" entry is the scaling factor between the mechanical and scalar time scales and is usually set to 2. We also need to specify the time step size for the Monte Carlo simulation. The time step size should be no greater than the mixing time scale. Finally, define the size of our PaSR simulation. The solution time profiles will be smoother if we use more statistical events, or particles, in the simulation. However, the run time and memory requirement also increase with the number of statistical events in the ensemble.

There are several solvers available for the PaSR model. Usually, we want to pick between the default DDASPK solver and the DVODE solver with backward differencing. The DDASPK solver is more reliable but more time consuming. Here we use the DVODE solver because the chemistry is simple.

In addition to providing the time profiles of the mean and root-mean-squared (rms) values of scalar variables, the PaSR model can generate probability density functions (pdf) of scalars in separate output data files. The pdf profile shows the instantaneous distribution of a scalar at the end of the simulation time. The shape of a pdf profile is a result of the turbulence-chemistry interaction. The pdf will become a delta function (a spike) if the PaSR behaves closely to a PSR. We can also use the pdf's to find out all possible states inside the combustor. Here we would like to examine the pdf of gas temperature at the end of the simulation time. We want the temperature pdf to have a resolution of 100 intervals, or number of bins. The Output Probability Distribution of Scalar tab of the Output Control panel provides the setup parameters for this pdf output, which is set with $T = 100$. The temperature pdf profile will be saved to a file called **pdf_T.plt** and we can import this file to the Post-Processor later.

We want to compare solutions from two cases with different mixing time scales so we can find out how turbulence intensity would affect our premixed combustor. The first case is a relatively strong mixing case with a mixing time of 0.1 msec. The weak mixing case will have a mixing time of 1 msec. After we finish running the first case, we have to rename the solution files, *XMLdata.zip* and *pdf_T.plt*, to **XMLdata_0.1.zip** and **pdf_T_0.1.plt**, respectively, so they will not be overwritten by the second run. To switch to the weak mixing case, we can simply go back to the Reactor Properties panel, C1_ PaSR, and increase the mixing time to 0.001 sec. We can then go to the Run Calculations panel and run the second case.

2.6.4.3 Project Results

The mean and rms gas temperature are shown in [Figure 2-105](#) and [Figure 2-106](#) for mixing times of 0.1 msec and 1 msec. The mean temperature profile of the strong mixing case (mixing time = 0.1 msec) indicates that a combustion zone is established inside the combustor and the outlet temperature is around 1800 K. On the other hand, the mean outlet temperature of the weak mixing case continues to drop because poor mixing between the fresh gas and the burned products fails to stabilize a combustion zone. The rms temperature profile of the weak turbulence case has a higher peak value than that of the strong mixing case. This large temperature variation indicates that part of the gas mixture inside the combustor does not burn in the weak mixing case. As most of the initial burned products get pushed out of the combustor, the statistics contain more and more non-burned events and the temperature variation starts to decrease consistently. Statistics of the strong mixing case are mainly made up of burning states so that the temperature variation is relatively small and stable. Similar trends are also shown by the mean CO mole fraction profiles in [Figure 2-107](#).

Figure 2-105 PaSR Methane/Air—Temperature Comparison

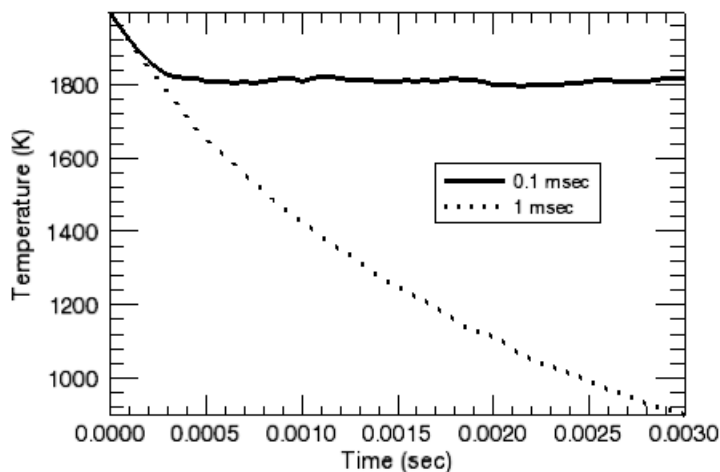


Figure 2-106 PaSR Methane/Air—Temperature Variance Comparison

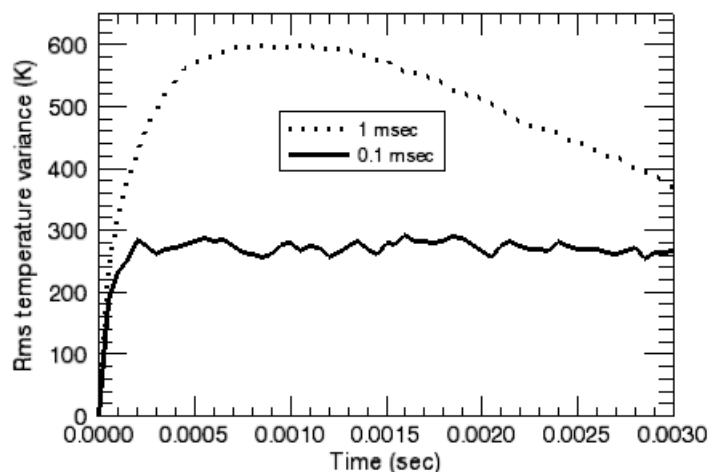
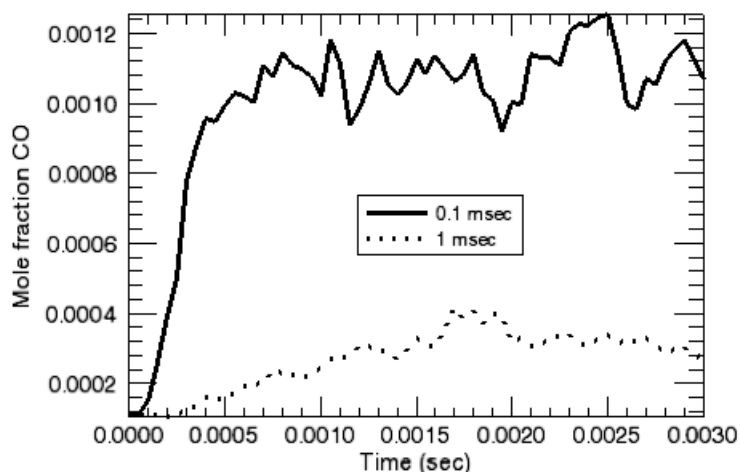


Figure 2-107 PaSR Methane/Air—CO Comparison



Since we requested the temperature pdf to be saved to a data file, we can view the pdf profile by importing it into the Post-Processor. To import the pdf profile generated by the PaSR, we use the **Import** command in the **File** menu of the CHEMKIN Post-Processor. After we select the data file, *pdf_T_0.1.plt*, we should instruct the Post-Processor to skip the first two lines of the text and to read the third line as column titles as shown in [Figure 2-108](#). We also need to set the column delimiter to “space”. We can repeat the same procedures for the second file containing the temperature pdf of the weak mixing case. Once we have both pdf’s imported to the Post-Processor, we can plot these two profiles together for easy comparisons. As shown in [Figure 2-109](#), the pdf of strong mixing case peaks around 2000 K with a small “tail” over temperatures slightly lower than the peak value. We can conclude that a stable combustion zone is established in the strong mixing combustor. The weak mixing case, however, has two peaks in its temperature pdf profile. A smaller peak is located

near 2000 K suggesting there is still some initially burned gas mixture left in the combustor. The large peak of the temperature pdf indicates the combustor most likely has a temperature of 500 K which is the temperature of the inlet gas mixture. Although there might be limited chemical reactions, the slow mixing process cannot sustain a combustion zone inside the combustor.

Figure 2-108 PaSR Methane/Air—Select the Import File Format

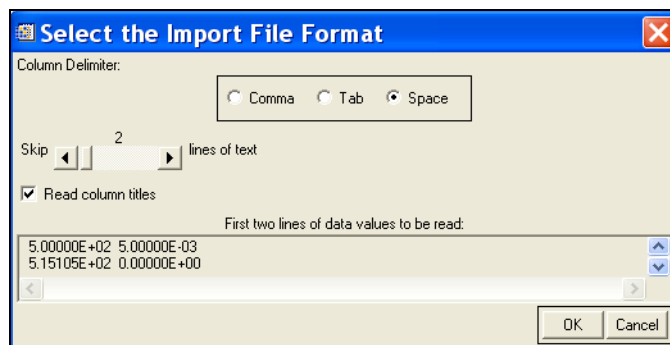
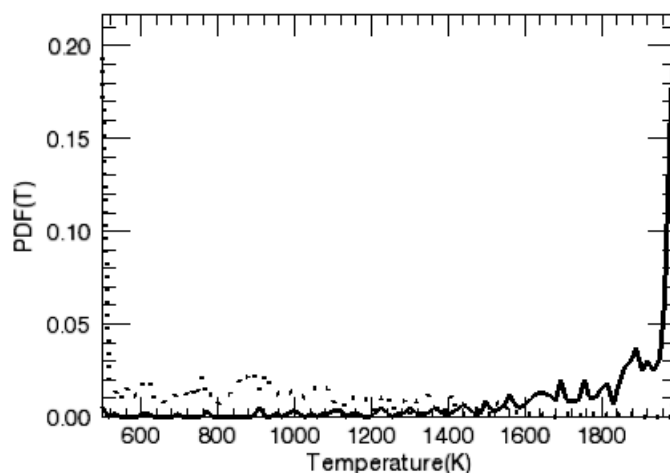


Figure 2-109 PaSR Methane/Air—PDF(T) Comparison



2.6.5 Side Inlet on a Plug Flow Reactor

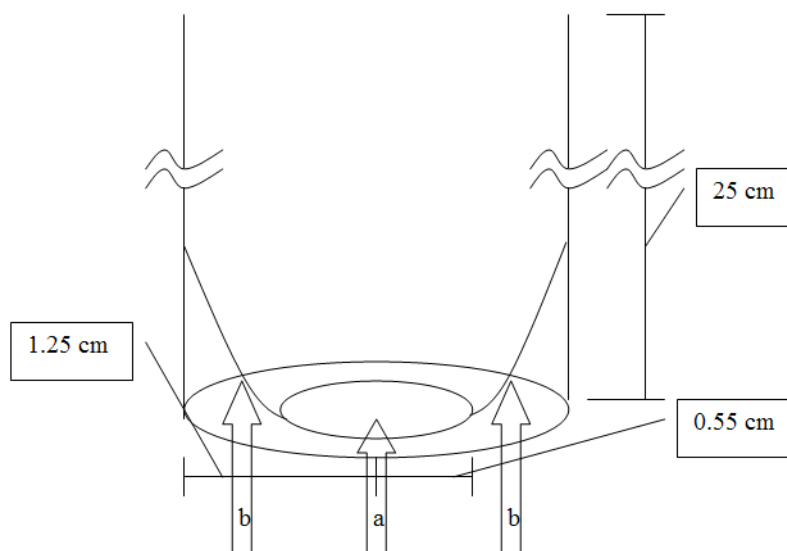
2.6.5.1 Project Description

This tutorial illustrates the use of the side inlet flow into a plug flow reactor, to approximate the effect of a mixing region on product composition. The chemistry used by this project is the Lawrence Livermore National Laboratory NO_x mechanism²⁵. Ammonia as a product of a nitrogen fuel contributes to the production of NO in post-flame oxidation. This model predicts how a mixing region affects the production of NO in a high-temperature oxidizing region that is post-flame.

2.6.5.2 Project Setup

The project file is called *pfr_side_inlet_param_study.ckprj*. All data files are found in the *samples2010\pfr\side_inlet_parameter_study* directory. The simulated model is based on a Lawrence Berkeley National Laboratory experimental setup²⁶. Their report includes a description of a concentric tube, with the ammonia stream in the center, and the oxidizing stream around the edges, as illustrated in *Figure 2-110*.

Figure 2-110 Illustration of the System to be Modeled.



The two streams have the following composition:

Table 2-13 Components in Fuel and Oxidizer Streams

Component	Stream a (fuel)	Stream b (oxidizer)
N ₂	0.974	0.88
CH ₄	2.E-3	0
NH ₃	6.E-4	0
O ₂	0	0.08
H ₂ O	0	0.04

25. Marinov, N. M., Pitz, W. J., Westbrook, C. K., Hori, M., and Matsunaga, N. "An Experimental and Kinetic Calculation of the Promotion Effect of Hydrocarbons on the NO-NO₂ Conversion in a Flow Reactor", Proceedings of the Combustion Institute, Volume 27, pp. 389-396, 1998. (UCRL-JC-129372).

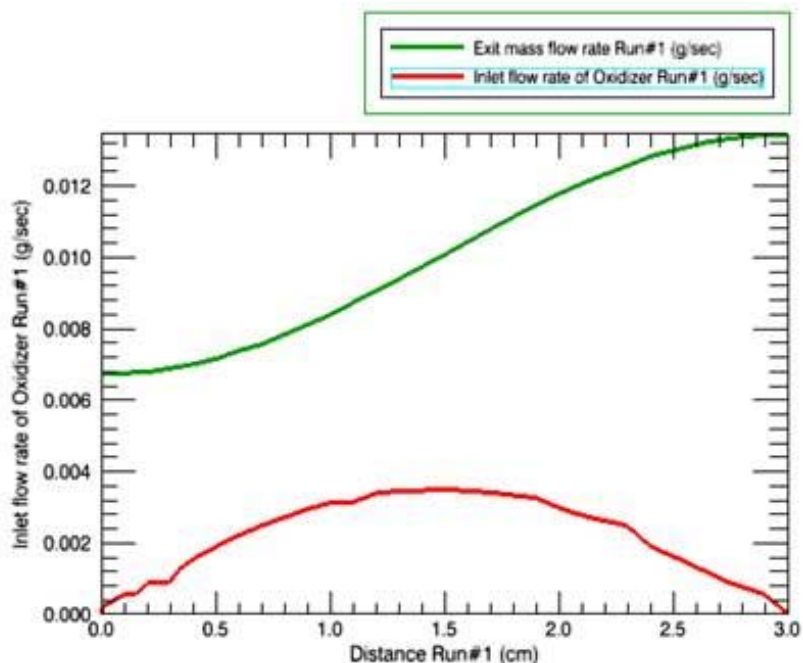
26. Grcar, J. F., Glarborg, P., Bell, J.B., Day, M. S., Loren, A., Jensen, A. D. "Effects of Mixing on Ammonia Oxidation in Combustion Environments at Intermediate Temperatures", Lawrence Berkeley National Laboratory report LBNL-54187.

A length of 3 cm in the mixing region is an estimate based on CFD calculations²⁶ (see p. 133). The temperature of the gas was varied between the range of 1000 to 1500 K in a parameter study. The diameter profile and the flow rate profile vary in the 3-cm mixing region. The fuel and oxidizer streams have a 1:1 flow ratio, with their sum being a value of 2 l/min, which is 16.667 cm³/s for each stream. The oxidizer stream volumetric flow rate is brought up from zero to 16.6667 over the 3-cm mixing region.

2.6.5.3 Project Results

Figure 2-111 shows the increase in mass attributed to the effect of the side inlet flow when the maximum X value in the Post-processor is constrained to 3.0 cm (see the *CHEMKIN Visualization Manual*).

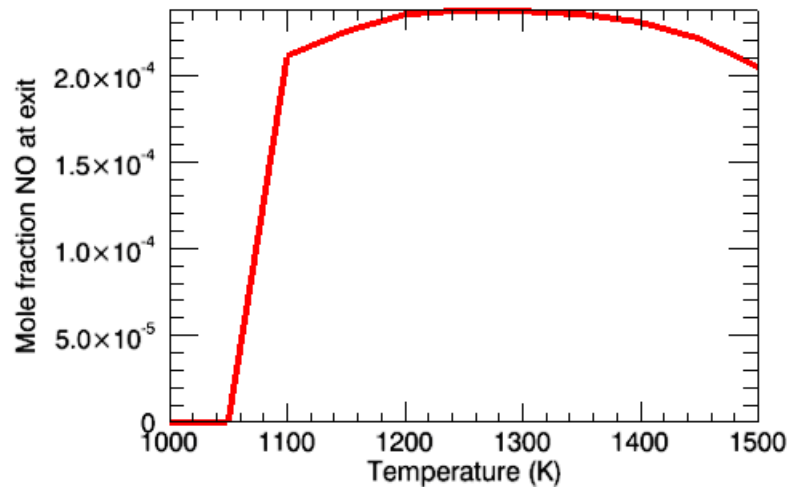
Figure 2-111 Total Flow Growing Directly as a Result of Side Inlet Flow.



At the exit, the predicted NO concentration has a peak near 1250 K, similar to experimental results²⁶.

To create the following plot in the CHEMKIN Post-Processor, select **PFRC1 End Point vs. Parameter** for the **Plot Set** and then select **Mole Fraction NO End Point** for the **Y axis**.

Figure 2-112 Peaking of NO Concentration Dependent on Temperature in a PFR with an Approximated Mixing Region.



Mixing causes a drop in the peak of NO and a lowering shift in the corresponding temperature, similar to the results found in the report. The NO peak shift is attributed to the locations of the reactions in the mixing zone. At temperatures higher than 1300 K, reaction occurs quickly when the oxidizing stream is in low concentrations, thereby decreasing the amount of NO. When the temperature is in the 1200-1300-K range, the reactions occur later in the mixing zone, a location with more oxidizer and consequently more NO. At temperatures lower than 1200 K, the formation of NO is not favored, so the NO concentration drops off. This peak behavior is illustrated in [Figure 2-112](#).

2.6.6 Co-flowing Non-premixed CH₄/Air Flame

2.6.6.1 Problem Description

By default, the cylindrical shear flow reactor model uses the uniform inlet and initial profile for all variables except axial velocity. The default inlet velocity profile is considered to be fully developed, i.e., parabolic. In this example, we will establish a co-annular flow inlet condition by using the user routine option to override the default inlet profiles. Properties of both jets are assumed to be uniform when they enter the reactor so there is a jump in the inlet profiles at the jet interface. A non-premixed flame will be established downstream as fuel and air are mixed due to diffusion. The co-flowing annular jet configuration is shown in [Figure 2-113](#) and properties of the inner (fuel) and the outer (air) jets are given in [Table 2-14](#). The outer wall is adiabatic.

Figure 2-113 Confined Co-flowing Annular Jet Configuration.

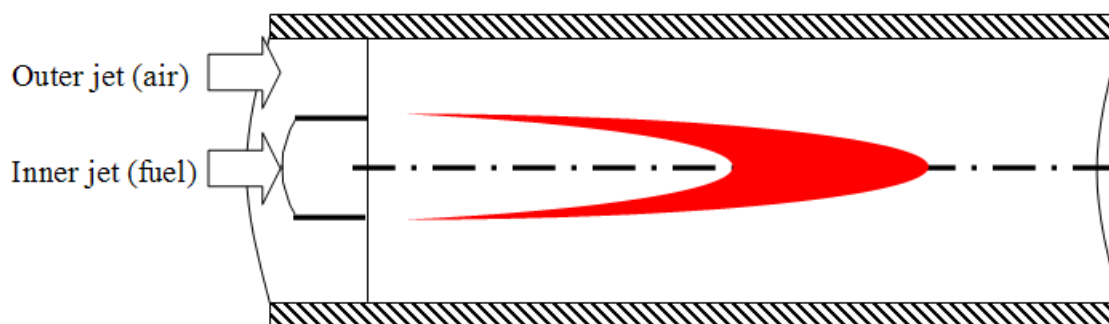


Table 2-14 Properties of the Co-flowing Jets

	<i>Inner Jet (Fuel)</i>	<i>Outer Jet (Air)</i>
Radius (cm)	0.8	4.0
Velocity (cm/sec)	10	25
Temperature (K)	600	1000
H2 Mass Fraction	0.05	0
CH4 Mass Fraction	0.45	0
O2 Mass Fraction	0	0.2329
N2 Mass Fraction	0.5	0.7671

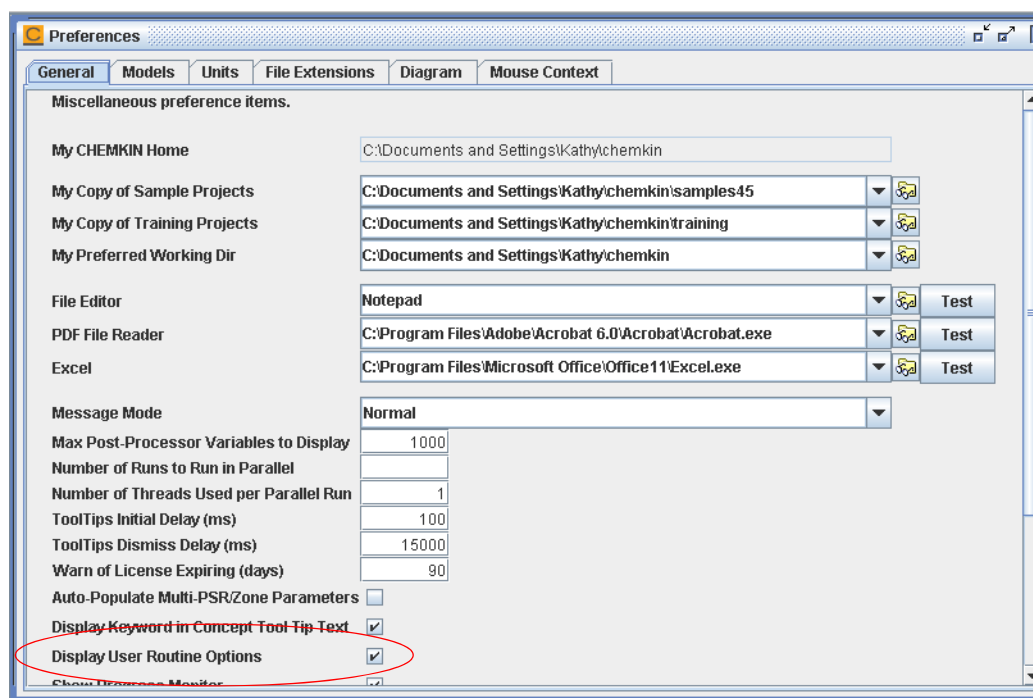
2.6.6.2

Problem Setup

The project file, *cylindrical_shear_flow_profile.ckprj*, is located in the **samples2010** directory. The FORTRAN subroutine used to set up inlet profiles is called `CRUPROF` and can be found inside the user routine file *creslaf_user_routines.f* in the **user_routines** directory. The GRI Mech 3.0, described in [Section 2.9.2](#), is used for the gas phase combustion chemistry. No surface chemistry mechanism is needed because the outer wall is chemically inert.

The user routine options are not shown in the graphical User Interface by default. To make these options available from the User Interface, the Display User Routine Options box in the Preferences panel must be checked. [Figure 2-114](#) shows a typical Preferences panel and the Display User Routine Options is located near the bottom of the panel.

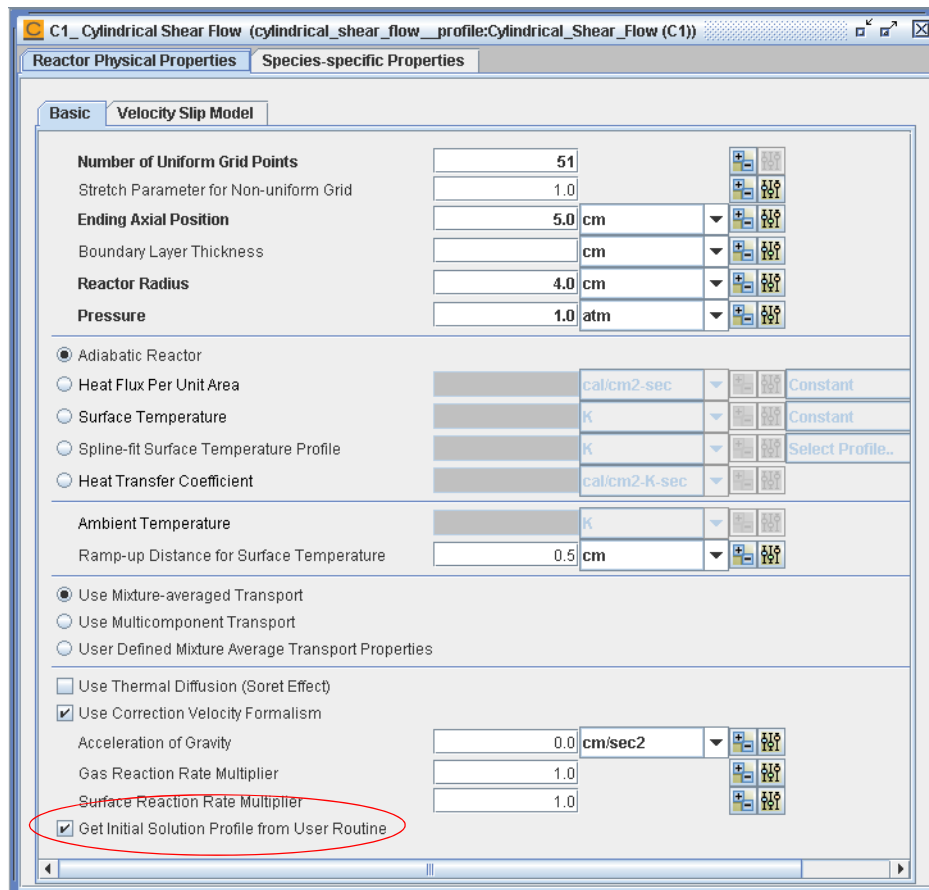
Figure 2-114 Preferences Panel Showing the Display User Routine Options Is Enabled.



Once the Display User Routine Options is enabled, the Get Solution Profile from User Routine option will become available when the Reactor Physical Property panel is opened. The check box for the Get Solution Profile from User Routine option is located near the bottom of the Reactor Physical Property panel as shown in [Figure 2-115](#). Once the box is checked, the reactor model will use the initial profiles defined by the CRUPROF subroutine (in ***chemkin<version>_xxx\user_routines\creslaf_user_routines.f***) instead of the default ones. The other way to activate the CRUPROF subroutine is by including the keyword UPROF in the reactor model input file *cylindrical_shear_flow__profile.inp*. In addition to the user routine option, other reactor parameters such as the number of grid points in the radial direction, reactor pressure, reactor radius (radius of the outer pipe wall), and ending axial position, must be specified in this panel.

The inlet velocity and temperature are entered in the Stream Property Data panel. These two inlet parameters are required even though their values will be overridden by the user routine later. Note that the cylindrical shear flow reactor model will set the outer wall temperature to the inlet stream temperature when the wall is not chemically active (no surface chemistry). If the inlet temperature given in the Stream Property Data panel is different from that of the outer jet (as defined in the user profile routine CRUPROF), a thermal boundary layer will be developed next to the outer wall.

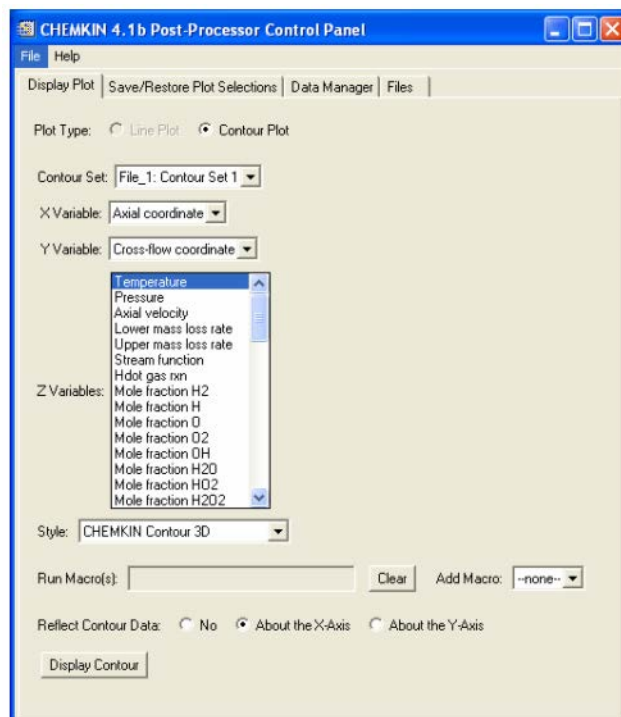
Figure 2-115 Get Initial Solution Profile from User Routine Check box.



2.6.6.3 Project Results

After the simulation has completed successfully, contour plots of solution variables can be visualized in the CHEMKIN Post-Processor. Since this is an axisymmetric problem, the reactor model only solves the top half of the flow domain. To visualize the solutions of the entire physical domain, we can have the CHEMKIN Post-Processor reconstruct contours in the bottom half of the physical domain by “mirroring” the contours with respect to the x-axis. This operation is activated by selecting About the X-Axis under the Reflect Contour Data option, as shown in [Figure 2-116](#).

Figure 2-116 Visualization of Full Computational Domain Can Be Acquired by Selecting Proper Reflect Contour Data Option in the CHEMKIN Post-Processor Panel.



Once the 3-D contour plot of the full computational domain is displayed in a new plot window, we can add a colorbar to label the contours. We first select the 3-D contour plot to be labeled by right-clicking the mouse over the plot. Then, we click on the **Insert** button on the menu bar to make the pull-down list available (see [Figure 2-117](#)). Select **Colorbar** to insert a contour level legend. By default, the colorbar is horizontal and is shown at the middle lower area of the plot. We can customize the colorbar by adjusting the colorbar properties. Double-clicking on the colorbar will open the Colorbar property panel. We will change Orientation from Horizontal to Vertical, set the Text show to True, and type **Temperature (K)** in the text field next to the Title. [Figure 2-118](#) shows the final look of the Colorbar property panel after all the changes. The contour plot will be updated as changes in the Colorbar property panel are made so we do not need to close the property panel. Finally, we can re-position the colorbar on the plot by dragging it with the right mouse button pressed. The finished 3-D temperature contour plot is shown in [Figure 2-119](#). We can print the contour plot directly to a printer or copy-and-paste it to a document.

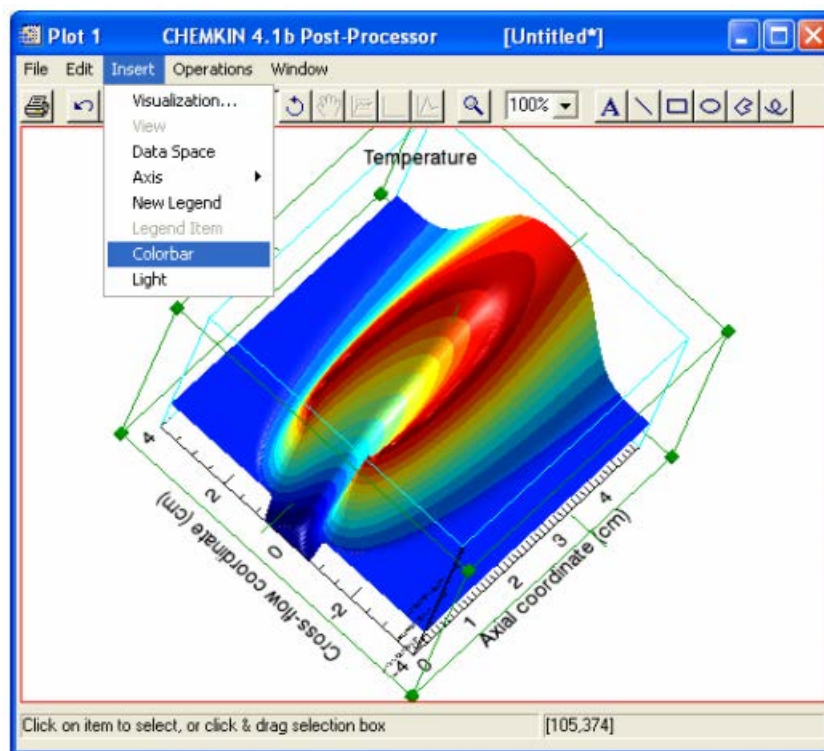
Figure 2-117 Contour Plot Window Showing the Pull-down List Selections of the **Insert** Menu.

Figure 2-118 Colorbar Property Panel.

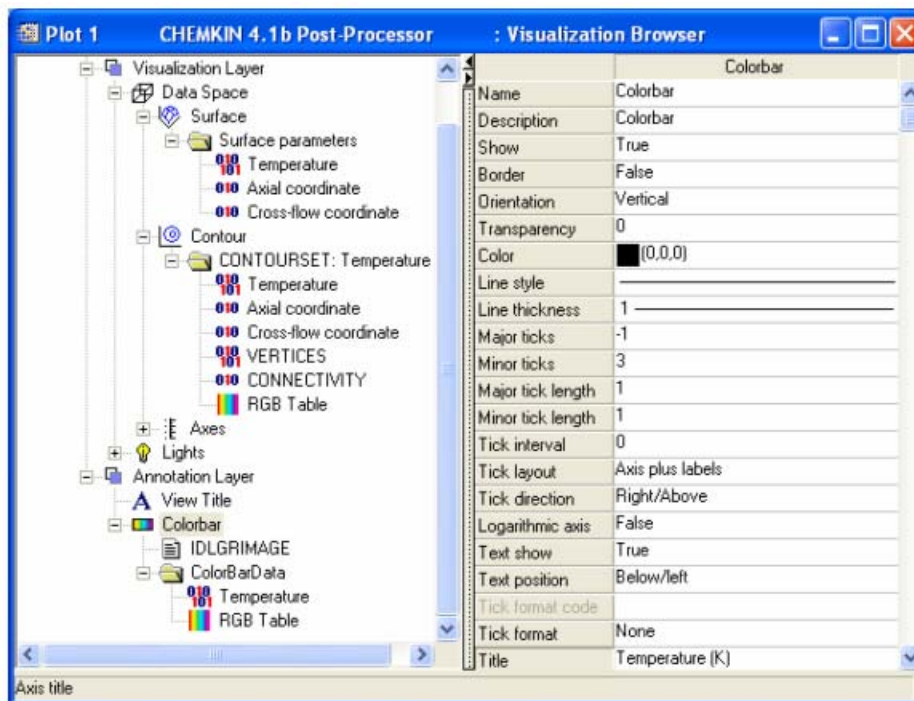
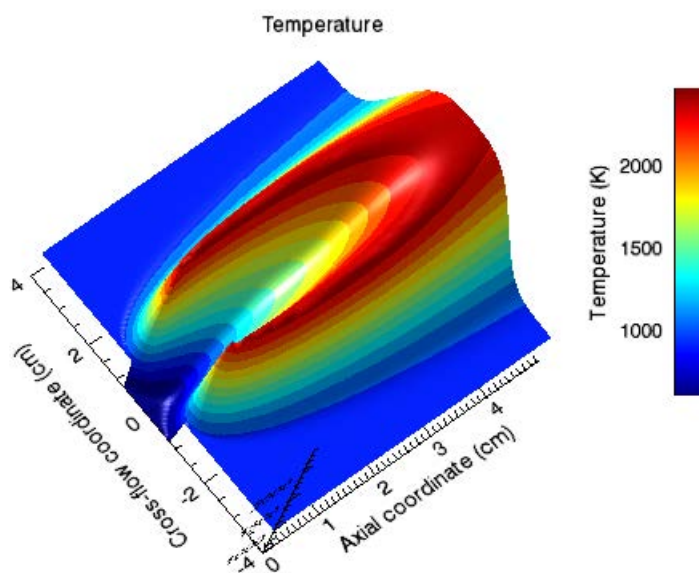


Figure 2-119 Final 3-D Temperature Contours of the Entire Physical Domain with Vertical Contour Legend (Colorbar).



C PRO 2.7

C PRO 2.7.1

Particle Tracking Feature [CHEMKIN-PRO Only]

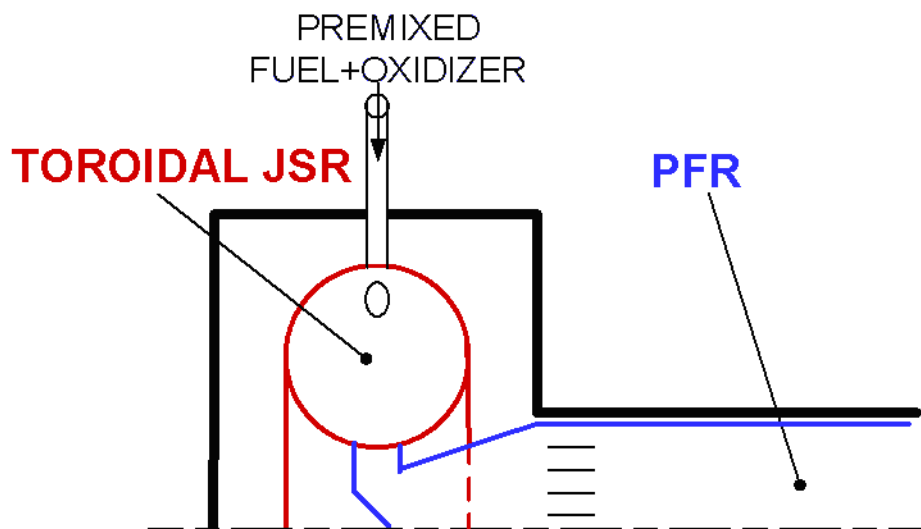
Soot Formation and Growth in a JSR/PFR Reactor [CHEMKIN-PRO Only]

The JSR/PFR system developed at MIT²⁷ provides a good platform for kinetic studies of soot formation and growth because, under the JSR and PFR conditions, the influence of mass diffusion on gas phase species profiles is minimized. The JSR serves as the pre-heat and flame zones of a premixed flame and the PFR is used to simulate the postflame region. From the prospect of model simulation, the JSR/PFR implementation greatly reduces the complexity of the numerical process as well as the run time. A schematic of the JSR/PFR configuration is shown in [Figure 2-120](#).

As an example to assess the performance of the Particle Tracking Feature, modified PSR and PFR models are employed to simulate one of the premixed $C_2H_4/O_2/N_2$ experiments by Marr²⁷. The experimental data include mole fractions of major gas-phase species and PAH's and soot mass concentration at various locations inside the PFR. Therefore, this data set is useful not only to validate the Particle Tracking Feature but to provide insights on the kinetics of nucleation and soot growth surface reactions used to simulate the experiment.

27. J.A. Marr, PhD. Thesis, Dept. of Chemical Engineering, MIT (1993).

Figure 2-120 A schematic of the JSR/PFR reactor configuration used by Marr²⁷



2.7.1.1

Problem Setup

The CHEMKIN project file for this tutorial is named

reactor_network_soot_JSRRPFR.ckprj and is located in the ***samples2010***

directory. The reaction mechanisms for ethylene/air combustion and soot formation and growth are described in [Section 2.9](#).

The JSR/PFR experiment shown in [Figure 2-120](#) can be modeled by one PSR and two PFR's in series. The first PSR is for the upstream (or flame zone) JSR, the following PFR is to model the transition piece between JSR and PFR in the experimental setup, and the last PFR is for the postflame PFR where measurement was performed. The main purpose of the transition PFR is to allow the JSR exhaust to cool down from 1630K to 1620K before entering the test section. The diagram view of this three-reactor network is given in [Figure 2-121](#). Since the Particle Tracking Feature is activated by special keywords in surface reaction mechanism, all soot simulations will need both gas phase and surface chemistry input files. Once the chemistry files have been pre-processed, the Dispersed Phase tab will appear in the Reactor Physical Properties panel. Most parameters for the Particle Tracking Feature can be assigned in this Dispersed Phase tab. Initial conditions of the particle size moments can also be specified here. The initial size moments can be constructed from particle number density alone. Additional particle size information such as particle mass density or particle volume fraction can also be specified. Because the dispersed phase does not exist on the reactor wall, the surface area fraction of the particle material must be set to zero in the Material-specific Data tab. Here, we set Carbon to 0.0 and Wall to 1.0. (Parameters for all materials can be specified on the Reactor Physical Properties tab.)

If particles exist in the inlet streams, their size moments can be provided in the Dispersed Phase tab of the Stream Properties panel.

The values of high particle-size moments can become very large so sometimes the absolute tolerance suitable for species mass fractions might not work well for those high moments. Therefore, the Particle Tracking Feature allows the tolerances for size moments solutions to be given explicitly for the steady state PSR model. The tolerances for particle size moments can be specified in the Solver window, as shown in [Figure 2-123](#).

Once all model parameters, initial/guess conditions and inlet stream properties are set, the JSR/PFR simulation can be launched from the Run Calculations window like any other CHEMKIN project.

Figure 2-121 Diagram View of the CHEMKIN Project Used to Simulate the JSR/PFR Experiment

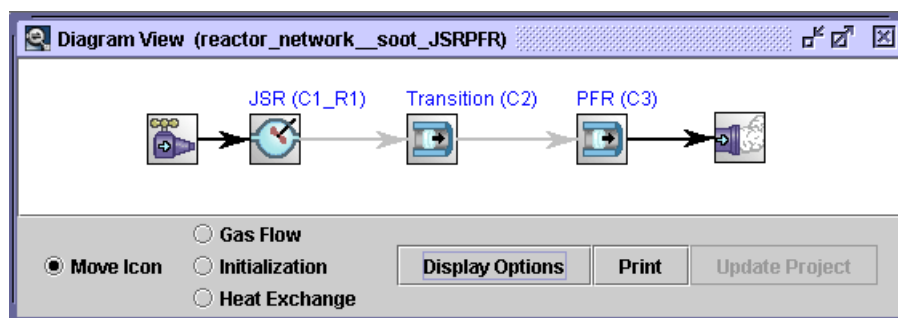
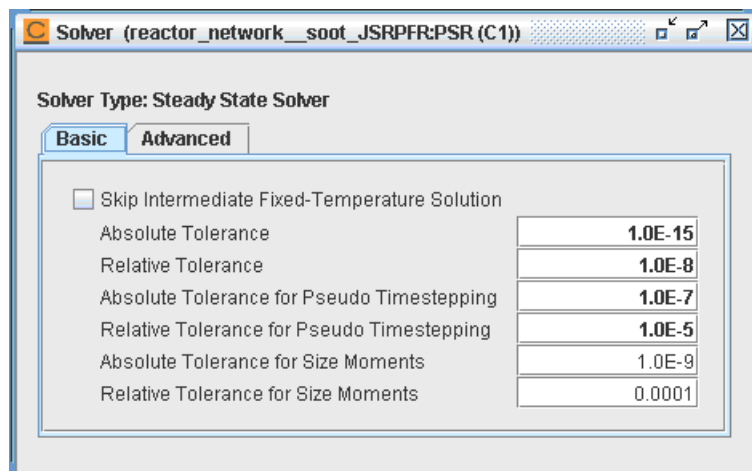


Figure 2-122 Specifying Particle Tracking Feature Parameters and Initial Conditions of Particle Size Moments in the Reactor

The screenshot shows the 'JSR (C1_R1) (reactor_network_soot_JSRRFR:PSR (C1))' window. The 'Dispersed Phase: CARBON' tab is active. The 'Reactor Physical Properties' section includes the following parameters:

- Number of Moments: 3
- Scaling Factor for Moments: 1.0E12
- Scaling Factor for Surface Species: 1.0E12
- Minimum Particle Density: 100 #/cm3
- Critical Particle Class: (empty)
- Minimum Particle Class: (empty)
- Exclude Coagulation of Particles
- Coagulation Collision Regime: Free-molecular
- Coagulation Collision Efficiency: 1.0
- Initial Particle Number Density: (empty) #/cm3
- Initial Particle Volume Fraction: (empty) cm3/cm3
- Initial Particle Mass Density: (empty) g/cm3

Figure 2-123 Tolerances for Particle Size Moments Can Be Given Explicitly in the Solver Window



2.7.1.2 Project Results

Two simulations, one with both H-abstraction-C₂H₂-addition (HACA) and PAH condensation growth reactions and the other with HACA growth reactions only, are performed so that contributions of either soot mass growth mechanism can be identified. When the number of variables available for plotting exceeds a preset limit, the CHEMKIN post-processor presents an option to filter the variables to a smaller number. For example, A1 represents benzene, A2 represents naphthalene, A1C2H represents phenyl acetylene, A4 represent pyrene, and so on.

Results of the $T_{JSR} = 1630K$ and $\Phi = 2.2$ case are presented in [Figure 2-124](#). Use PFR(C3) for analysis. As can be seen from these figures, predictions obtained by the Particle Tracking Feature are in good agreements with experimental data. The Particle Tracking Feature in general slightly underpredicts gas-phase species. There are many factors that can contribute to the discrepancies shown in the figures. For example, Marr did not provide details composition and temperature of the inlet gas mixture to the JSR. Since the temperature of the JSR is maintained by adjusting the N₂ fraction in the inlet gas stream, uncertainties in inlet condition, reactor heat loss, and reactor residence time will surely affect the simulation results in the PFR section behind the JSR.

Comparison of the predicted and measured soot mass concentration profiles in the PFR is presented in [Figure 2-125](#). While the HACA-only mechanism shows an excellent agreement with the data at the PFR inlet, the slope of the soot mass profile predicted by the HACA-only mechanism (dash-dot line) is much smaller than that of the experimental profile. This is an indication that the HACA growth mechanism alone gives a too-slow soot mass growth rate in the post-flame region. Since the present soot model underpredicts C₂H₂ mole fraction in the PFR ([Figure 2-124](#)), it is possible that the lower C₂H₂ concentration leads to lower HACA soot mass growth rate. It is

also possible that another growth mechanism, possibly PAH condensation, might contribute equally to soot mass growth under this condition. The soot mass growth rate predicted by the HACA + PAH mechanism (solid line), on the other hand, shows a much better agreement to the experimental data than the HACA only mechanism does. Since the sticking coefficients of all the PAH considered here are within the range suggested by Marr²⁷, the PAH contribution to soot mass growth should be reasonably predicted by the model. However, the HACA + PAH mechanism does overpredict the soot mass density at the PFR inlet. Note that experimental data indicate that soot mass density increases by about $4 \times 10^{-8} \text{ gm/cm}^3$ for the first 5 mini-seconds in the PFR. Since the residence time in the JSR is about 5 mini-seconds and the temperature in JSR is only 10K higher than that of PFR, the soot mass density at the PFR inlet should be higher than the measured value. Of course, this assessment is based on the assumption that soot particles start to grow once they are created inside the JSR.

The evolution of average soot particle diameter inside the PFR is shown in [Figure 2-126](#). The soot particle diameter increase along the plug flow reactor due to particle coagulation and mass growth. Note that the average particle diameter actually drops a little near the PFR entrance. This signifies that soot nucleation is still occurring as the gas mixture entering the PFR.

Figure 2-124 Comparisons of Mole Fraction Profiles of Selected Gas Phase Species Inside the PFR for the 1630K and $\Phi = 2.2$ Case of the $\text{C}_2\text{H}_4/\text{O}_2/\text{N}_2$ JSR/PFR Experiment by Marr²⁷. Symbols: data; Solid lines: predictions with HACA and PAH condensation growth mechanisms

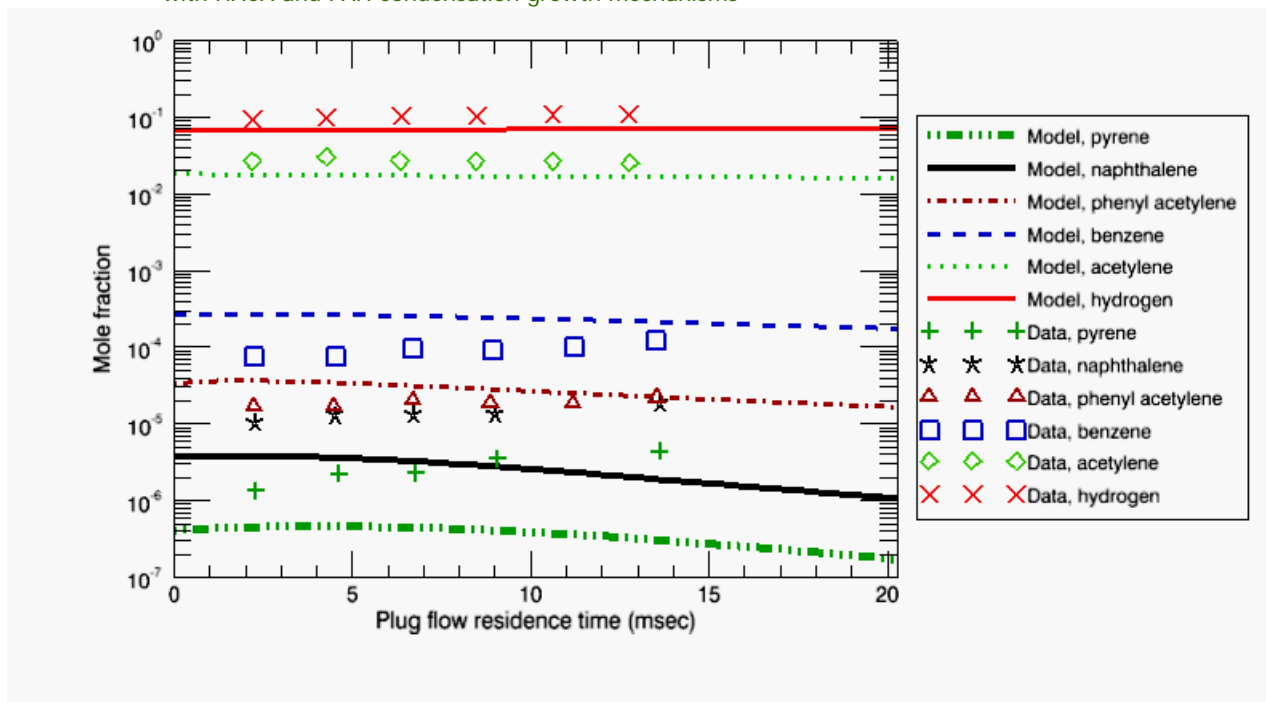


Figure 2-125 Comparisons of Soot Mass Concentration Profiles Inside the PFR for the 1630K and $\Phi = 2.2$ Case of the $C_2H_4/O_2/N_2$ JSR/PFR Experiment by Marr²⁷. Symbols: data; Solid line: prediction with both HACA and PAH condensation growth mechanisms; Dash-dot line: prediction with HACA growth mechanism only

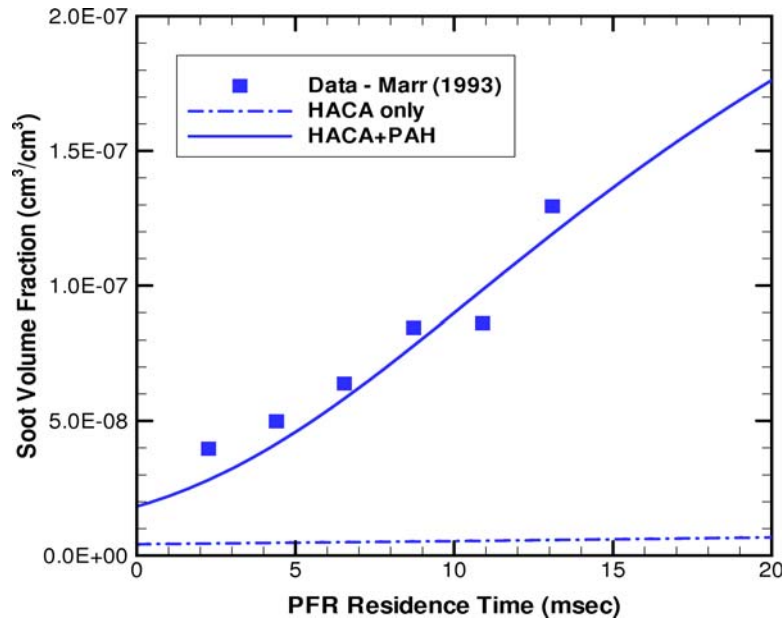
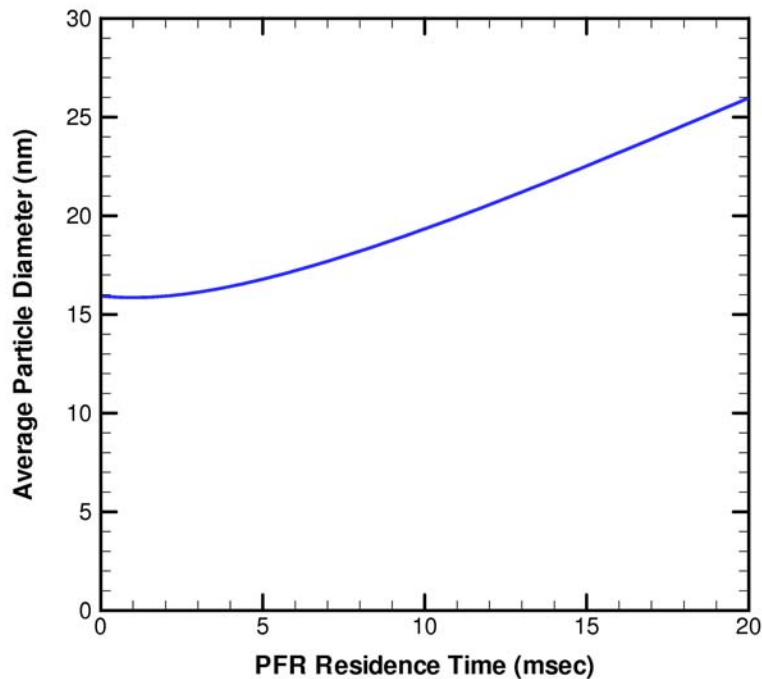


Figure 2-126 The Particle Diameter Evolution Inside the PFR Predicted by the Present Soot Module for the 1630K and $\Phi = 2.2$ Case of the $C_2H_4/O_2/N_2$ JSR/PFR Experiment by Marr²⁷ (see p. 141)





2.7.2 Soot Particles in Flame Simulators [CHEMKIN-PRO Only]

2.7.2.1 Project Description

This tutorial presents the use of Particle Tracking in the Flame-speed Calculator and in the Opposed-flow Flame Simulator. The segregated solution technique described in [Section 18.9](#) of the *CHEMKIN Theory Manual* is used for flame/particle simulations. In this tutorial, however, note that the aggregation model is turned off for this example.

Simulations of flames with particle formation and growth can be CPU-intensive, particularly for sooting hydrocarbon flames. This is due to the relatively large gas-phase mechanisms required to include soot-formation precursors, as well as the added computation of tracking the particle formation, growth, and size distribution. Since most of the computational cost is usually due to the gas-phase reacting-flow solution, a common technique is to solve the gas-phase-only flame simulation first, and then perform the flame-plus-soot simulation by "restarting" from the solved gas-only flame. This approach is recommended for the following types of particle simulations:

1. When the gas-phase mechanism is large.
2. When simulations are being used in parametric analysis that might involve changes to just the surface (soot) chemistry.
3. When difficulties in convergence are encountered for the coupled problem and some experimentation is required with solver parameters.

In general, the default solver settings are satisfactory for most cases. However, convergence problems can occur. For example, convergence can be particularly difficult in cases when the particle-flame interaction is very strong. In general, restarting from the gas-phase solution improves the convergence behavior for the coupled solution and is therefore recommended. In this tutorial we will demonstrate that technique.

2.7.2.2 Project Set-up

The project files for soot simulation with the Flame-speed Calculator and Opposed-flow Diffusion Flames are named as ***flame_speed_soot_particles.ckprj*** and ***opposed-flow_flame_soot_particles.ckprj***, and are located in the ***samples2010*** directory. Both flame simulations use ethylene as the fuel and air as the oxidizer. The gas-phase and surface reaction mechanisms described in [Section 2.9](#) are used. In these simulations, only the HACA (hydrogen abstraction, carbon addition) part of the mechanism is used in the surface chemistry input.

In the Flame-speed Calculator (*flame_speed__soot_particles.ckprj*) project, we consider a freely propagating ethylene (C₂H₄) - air flame with equivalence ratio of 3.0. The computation domain is set between -2 to 5 cm. The inlet gas temperature is set to 300 K and the ambient pressure is 1 atm. An initial temperature profile is selected with fixed temperature of 1200 K located at $x = 0$, thus effectively anchoring the flame at $x = 0$.

For the Opposed-flow Flame simulation (*opposed-flow_flame__soot_particles.ckprj*) project, pure ethylene is on the fuel side and air on the oxidizer side with a separation distance of 1 cm. The velocity from each nozzle is set to 10 cm/s thus giving a global strain-rate of 20 s⁻¹. The gas temperature from both inlets is set to 300 K and ambient pressure is 1 atm.

Both simulations use mixture averaged transport with correction velocity formulation. For the soot particles, we solve for first three moments.

2.7.2.2.1

Controls on the Dispersed Phase Tab

After the chemistry sets have been pre-processed, the Dispersed Phase tab appears in the Reactor Physical Properties panel. This tab contains two sub-tabs: (a) Basic, and (b) Aggregation model. The former can be used to set up all the basic level controls such as number of moments, a switch for including thermophoresis, while the latter is exclusively for the aggregation parameters.

Basic Sub-tab

The particle moments and surface species concentrations span many orders of magnitude. For a typical flame particle simulation, these values when expressed in the units of number/unit volume can be between 0 to 10¹⁶. The usual choice for units of mole/cm³ is often too large and can create problems in ensuring "positivity" for these values. For example, in the double-precision representation of the numbers, near-zero negative values can be on the order of -10 to -20. If the particle moments and surface species concentrations are in "moles/cm³", the zero-th moment can be -10 to -20 at a point in the solution domain. While such a number is clearly of an appropriate order of precision, it means that there are -1000 (= zero-th moment*Avogadro number) particles at that location. To alleviate this difficulty, the two controls, **Scaling Factor for Moments** and **Scaling Factor for Surface Species**, can be used. A value of 10⁹ for these control parameters means CHEMKIN internally uses "nano-moles/cm³" as the unit for moments and surface species concentration. The default values are 10¹². The choice of the scaling factor should be based on some estimate of the maximum value for number density of the particles. In typical flame simulations, this is about 10⁹ to 10¹⁴, leading to the choice of default.

For the opposed-flow sample, a non-default value of $1e+15$ is used for both scaling factors. This choice is motivated by the small amount of soot formed in this flame. Other controls, such as number of moments, coagulation regime, etc., are as explained in [Section 2.7](#).

Aggregation Sub-tab

The aggregation-related parameters are described in the [CHEMKIN Input Manual](#) and [Section 18.8](#) of the [CHEMKIN Theory Manual](#).

2.7.2.2.2

Solver Options

The segregated solution scheme used in flame-particle simulations checks iteration convergence by monitoring the differences in the gas-phase mole fractions. The corresponding convergence criterion is given by the parameter **Absolute Tolerance in Segregated Scheme** on the Basic tab of the Solver options panel. Specifically, after updating the particle source terms the gas-phase equations are solved and the resulting mole fractions are compared against those obtained from the previous iteration. If the maximum absolute change in the mole fraction is below the convergence parameter, the iterations stop and the solution is complete; otherwise new particle source terms are computed and the procedure is repeated.

Advanced Solver Options Tab

Similar to the small negative "floor" value specified for the gas-phase species mole fractions, there are two options available for setting bounds: **Minimum Bounds on Surface Species Concentration** and **Minimum Bounds on Particle Moments**. The default value for both these controls is zero. While it is acceptable to set the former to a small negative number, the particle moments should *not* be set to a negative number. This restriction is not only due to the physical constraint but also due to the fact that a logarithmic interpolation scheme is used when computing the fractional moments. The lower bound on the zero-th moment, i.e., number density, is fixed at zero. The bound control thus applies only to higher moments. Also note that these values are applied to the "scaled" variables, i.e., to the actual solution variable and not to the mole/cm³ or number/cm³ values. For example, if the scale factor is specified as $1.0E+09$, then for the value of $-1.0E-06$ for the lower bound, the search can explore a solution space with -10^{-6} nanomoles.

The maximum number of iterations performed by the segregated scheme is controlled by the parameter **Maximum Number of Iterations in Segregated Scheme**. The default value of this parameter is 100.

2.7.2.3 Monitoring Convergence

A text output file named "SgConvergence.out" is written in the output directory. The data in this file consists of 4 columns: (1) iteration number, (2) absolute value of the maximum difference in the mole fraction, (3) the gas-phase species index for which the maximum difference happens, and (4) the grid-point number where this happens.

This output can be useful in a variety of ways; for example to detect which species is most sensitive to particle interactions or to monitor if the convergence is stalling.

While the former can shed some light on the reaction mechanism, the latter typically happens when the grid is not sufficiently fine and/or the absolute convergence tolerance on the gas-phase species is not tight enough. A tight tolerance is required; for example, in the opposed-flame example in this tutorial, the absolute tolerance is set to 1.e-12.

2.7.2.4 Project Results

As mentioned earlier, the surface mechanism used in these simulations is the HACA soot-growth mechanism and thus soot growth by reactions with aromatic species is not considered. For the Flame-speed simulation, soot oxidation by hydroxyl radical (OH) is included. Following the general guidelines in these examples, a parametric analysis can be conducted to understand and evaluate various soot mechanisms and individual reactions.

2.7.2.4.1 Flame-speed Calculator with Particle Formation and Oxidation Simulation

[Figure 2-127](#) shows particle volume fraction and temperature as a function of distance for the ethylene-air premixed flame ($\phi = 3.0$). It can be seen that while the flame is located at around $x = 0.0$ cm, the particle nucleation and growth continues in the post-flame region. Considering the slope of the volume fraction profile at the downstream side, the computation domain may be extended further so that the gradient vanishes smoothly. [Figure 2-128](#) shows, along with the particle number density, the mole fractions of the gas-phase precursor, pyrene (A4), the species that contributes to growth, acetylene (C_2H_2), species that reacts with particle surface (H), and species that consumes the particle (OH). Since, as per the reaction mechanism, A4 is responsible for soot nucleation, the shapes of particle number density profile and pyrene profile are qualitatively similar. Acetylene, in addition to coagulation, increases the size of soot particles by attacking the 'open sites' on the particle surface. It is also interesting to note that A4 and OH mole fractions are of the same order of magnitude in the post-flame region. Using the rates of production and reaction progress variables, further analysis can be conducted to evaluate competition between the soot nucleation and oxidation reactions.

Figure 2-127 Distance vs temperature and particle volume fraction

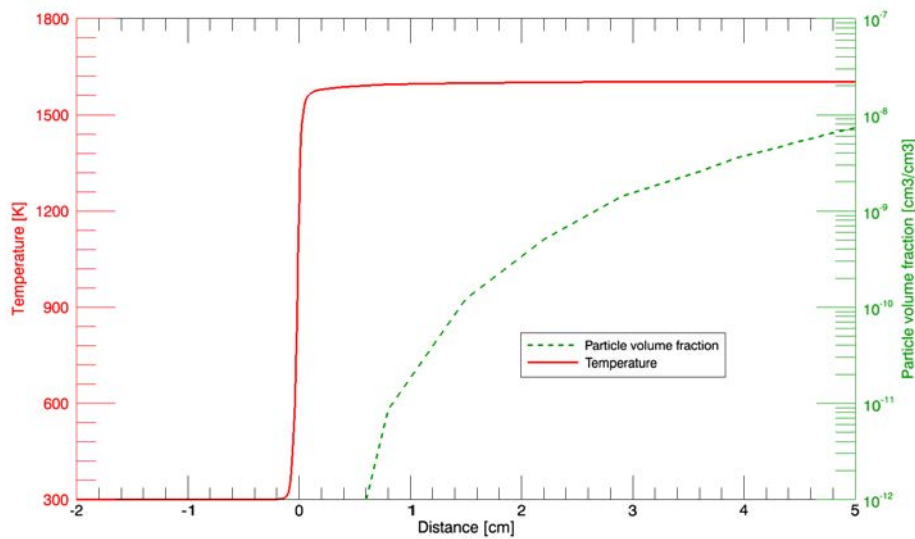
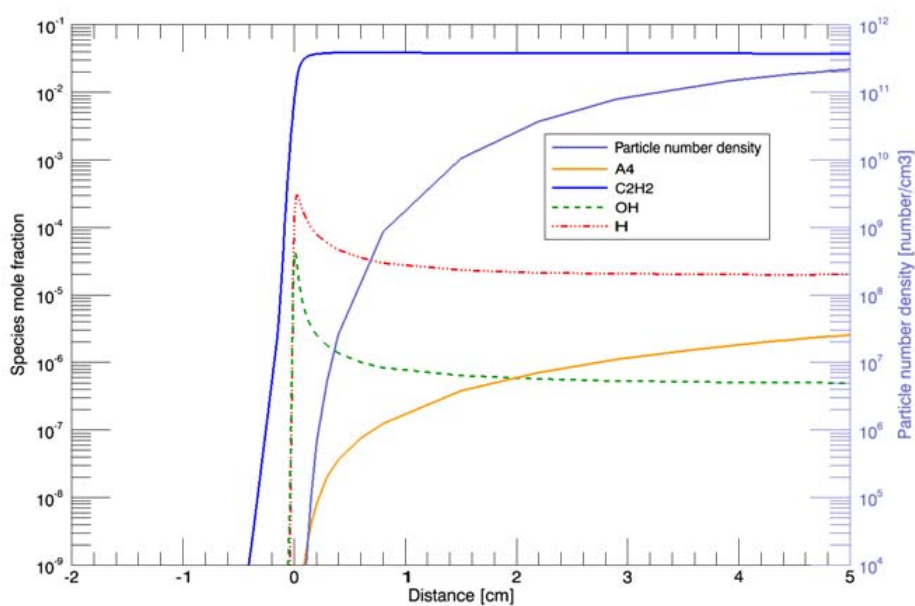


Figure 2-128 Distance vs species mole fraction and particle number density



2.7.2.4.2

Opposed-flow Diffusion Flame Simulation with Soot Formation Simulation

In general, for soot studies, the opposed flow diffusion flames can be classified in two types: (i) Soot formation (SF) and (ii) Soot formation-oxidation (SFO). Depending on the composition of reactants in the fuel and oxidizer nozzles, the flame may be located on the either side of the stagnation plane. When the flame is on the oxidizer side, as in this example, the soot particles that nucleate and grow are convected away from the flame towards the stagnation plane and thus cannot oxidize. The HACA mechanism alone is therefore a reasonable model for the soot surface reactions in these flames.

[Figure 2-129](#) shows computed profiles of particle volume fraction and temperature. As expected, the flame is situated on the oxidizer side of the stagnation plane at about 6 mm from the fuel inlet whereas the particle number density shows a peak at about 4 mm from the fuel inlet. The temperature of the "sooting zone" is about 1200 K. As seen from [Figure 2-130](#), the particle number density practically vanishes at the flame location and the profile is mono-modal. (In contrast, a bimodal behavior is expected from SFO flames.) Although the OH radical peaks away from the particle number density peak as expected, thus having minimal effect on soot oxidation, the predicted soot volume fraction is still quite small. This suggests that HACA mechanism alone may not be sufficient to capture soot growth in this case and one may have to use a PAH condensation model and/or soot formation from acetylene.

Figure 2-129 Distance vs Temperature and Particle volume fraction

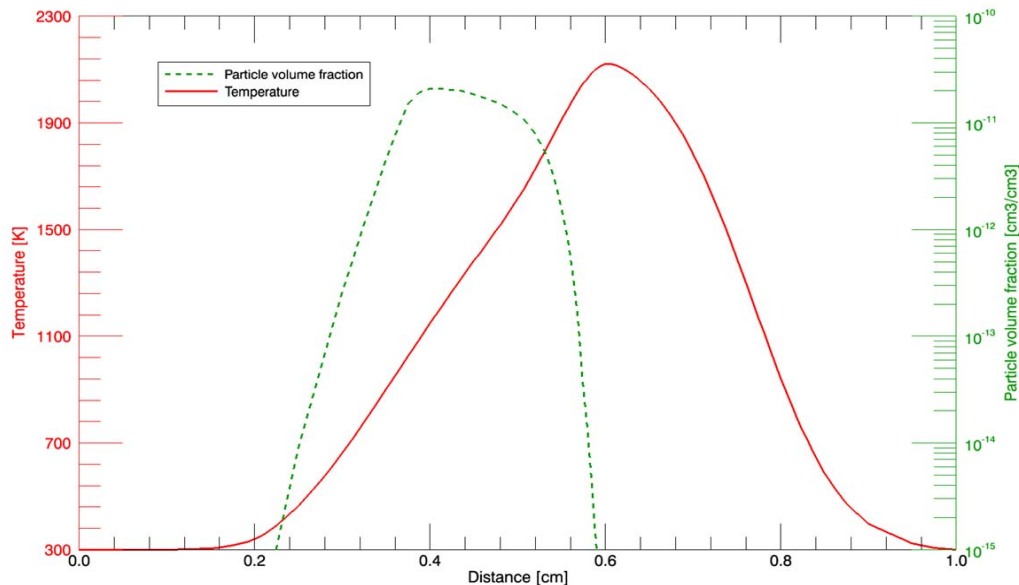
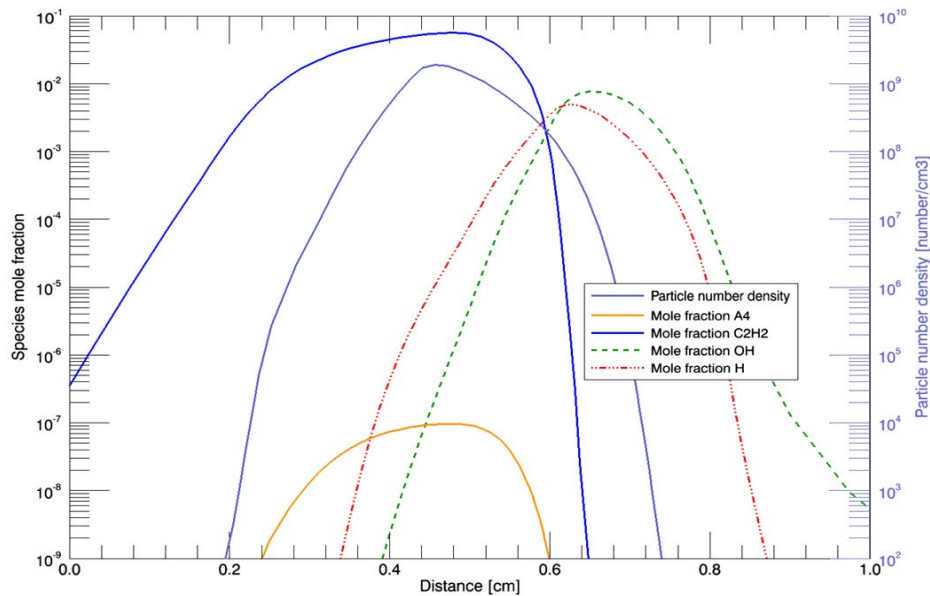


Figure 2-130 Distance vs species mole fraction and particle number density



2.7.2.5

Concluding Remarks

The purpose of these examples is to demonstrate techniques for applying Particle Tracking Feature to simulate soot formation in pre-mixed and opposed-flow flames. The area of soot nucleation, growth, and destruction is still the subject of research, such that the mechanisms and values of the rate parameters have a lot of uncertainty. The Particle Tracking Feature can be used to perform systematic parametric analysis to better understand soot formation pathways and also to provide engineering estimates of related quantities.



2.7.3

Sectional Method for Particle-Size Distribution with Pre-mixed Laminar Burner-Stabilized Stagnation Flame [CHEMKIN-PRO Only]

2.7.3.1

Project Description

As shown in [Figure 2-131](#), in the cases of CHEMKIN-PRO reactor models that support the Sectional Method and the Particle Tracking feature, radio buttons on the Reactor Properties tab provide a choice between the Moments Method and Sectional Method. Selecting the Sectional Method means that the segregated solver computes the solution by sequentially solving the gas-phase equations followed by the sectional equations along with the surface species.

2.7.3.2 Project Setup

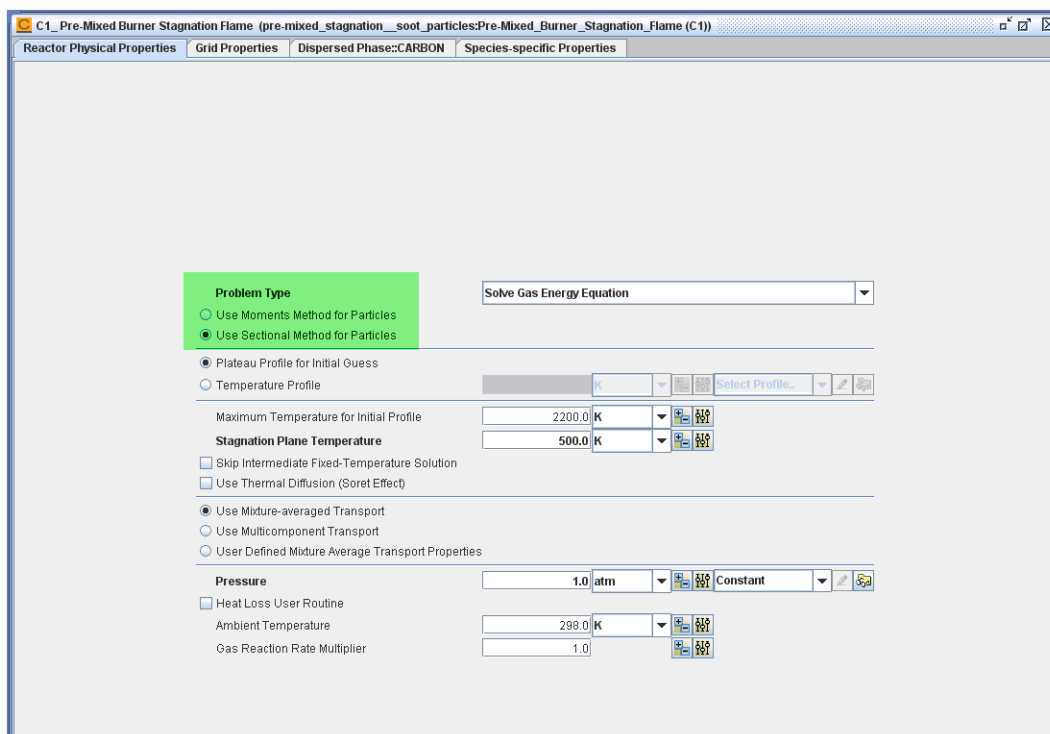
The project file is named *pre-mixed_stagnation__soot_particles.ckprj* and is located in the *samples2010* directory. The corresponding input and chemistry set files are located in the *samples2010\pre-mixed_stagnation\soot_particles* directory. The project is set up to represent roughly the flame facility at the University of Southern California (USC)²⁸, where extensive soot measurements are being conducted. For this tutorial, as in [Section 2.7.2](#), only the HACA (H-Abstraction-Carbon-Addition) part of the surface reaction mechanism (described in [Section 2.9](#)) is used. The fuel is ethylene, the equivalence ratio is about 2.067 and fuel-oxygen mixture is diluted with argon. The burner inlet velocity is set to 15 cm/s at an inlet temperature of 400 K. The stagnation plane (wall) temperature is set to 500 K and is located at 1 cm from the inlet. The ambient pressure is set to 1 atm for the atmospheric flame facility. The simulation uses mixture-averaged transport, which is a good approximation for most hydrocarbon fuels. The adaptive grid control parameters for gradient and curvature are set to 0.2 and 0.4, respectively. This setting gives reasonable resolution while keeping the computational cost small.

2.7.3.2.1 Selecting the Sectional Method

As shown in [Figure 2-131](#), in the cases of simulators CHEMKIN-PRO reactor models that support the Sectional Method and the Particle Tracking module, radio buttons on the Reactor Properties Tab provide the choice between the Moments Method and Sectional Method. Selecting the Sectional Method currently means: (a) both the Moments Method and Sectional Method are used, and (b) the segregated solver computes the solution by sequentially solving the gas-phase, the moments, and the Sectional Method. The coupling between the gas-phase and the particles is through the Moments Method equations.

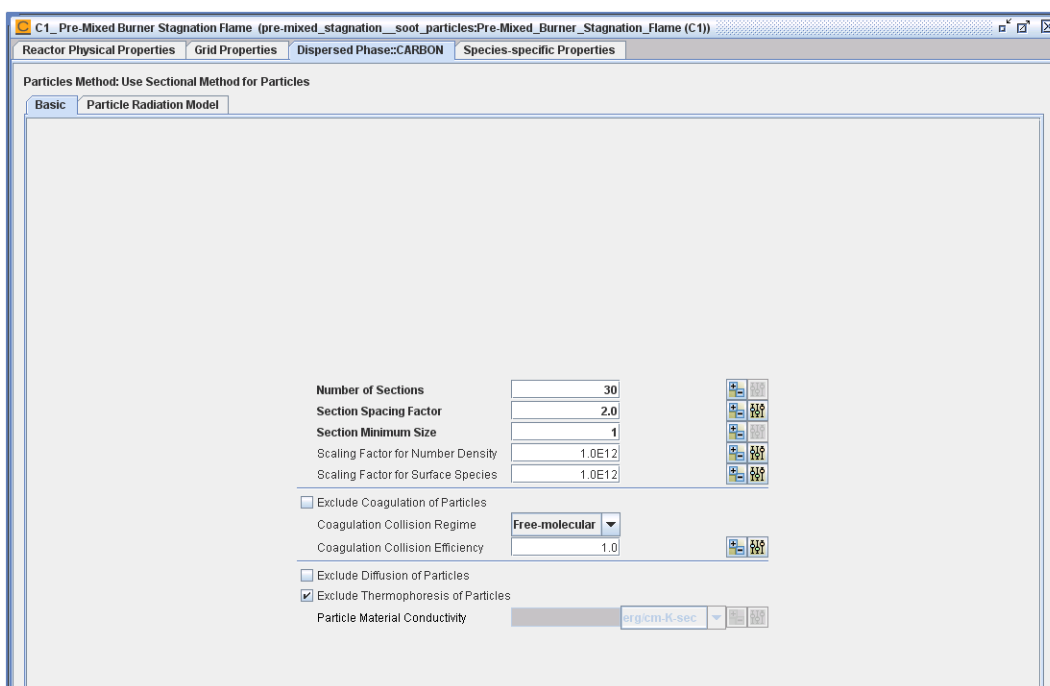
28. Wang, Hai, Personal communication, 2010.

Figure 2-131 Selecting the Sectional Method on the Reactor Physical Properties tab.



The appearance of the Dispersed Phase tab is controlled by the existence of a DISPERSED phase material in the surface chemistry file of the chemistry set defined for the project. When the Sectional Method is selected, this panel appears as shown in [Figure 2-132](#).

Figure 2-132 Appearance of the Dispersed Phase tab when the Sectional Method is selected.



2.7.3.2.2 Description of Input for the Sectional Method

The Sectional Method has three mandatory inputs, which control the range of particle sizes used by the simulation. These inputs are (a) number of sections, (b) spacing factor, and (c) section minimum size. The spacing factor is a geometric control of the relative sizes of the sections or "bins" used for tracking particle units (monomers). For example, the representative particle size in the $(n+1)^{\text{th}}$ section is the spacing factor times the representative particle size in the n^{th} section.

The sections consider particle units or monomers. For example, for soot defined by carbon atoms the possible "particles" may be defined to start from a single carbon atom in the bulk phase even if the nucleation reaction(s) have a higher inception class (i.e., the nucleated particle has more than one carbon atom). In the soot-formation mechanism used in this tutorial, there is one nucleation reaction and it yields particles with 32 atoms (monomers) in it. The spacing factor of 2 then means that the nucleated particles go in the 6th section. If the nucleated particles were then allowed to be etched away (by including reducing reactions in the mechanism), then sections 1 through 5 could have non-zero particle number density. Since there are no reducing reactions in the mechanism used in this tutorial, the minimum section size can be set to 6, but for general demonstration purposes it is set to unity. Note that the minimum size must be set to unity whenever there are bulk-etching reactions in the particle surface chemistry mechanism.

For a given simulation, the setting of these parameters is influenced by the size range of particles expected to form and/or permitted by the model approximations. For example, for the particle models implemented in the Particle Tracking module, the diameter of the largest particle formed should not be greater than about $1\ \mu\text{m}$; which is the resolution with which the gas-phase solution of the reacting flow is typically computed. For this tutorial, the number of sections used is 30, which, with a spacing factor of 2 and 0.2765 nm for the diameter of a single C(B) atom, gives, means that the representative particle diameter in the 30th section is approximately equal to 225 nm. While this is sufficient for the present simulation, the computed particle number density in the largest section must be checked after the simulation to verify that it vanishes smoothly at each grid point in the computational domain.

The input for scaling factors, coagulation regime and efficiency is kept at its default values. The scaling factors for moment and surface species are set to 1E+14. Particle thermophoresis is excluded in this tutorial. When it is included, the input for the particle material's thermal conductivity should also be specified.

2.7.3.3 Project Results

When the Sectional Method is included in the simulation, the following variables become available during post-processing: (a) the number density for each section, (b) the average properties predicted using the sectional data, and (c) the particle-size distribution function (PDF) at each grid-point. The experimental data on particles is usually in the form of a PDF and the form $(dN/d\text{Log}D)$ reported by the Sectional Method matches that reported in the literature. To distinguish between the average properties computed using the Moments Method used alone and Sectional Method, the latter results include "total_(section)" in the name. For example, total_(section)_number_density gives the total particle number density calculated by the Sectional Method.

As mentioned above, this project allows no particles in the first 5 sections since there is no oxidation reaction in the surface mechanism. These values are filtered out by the Post-processor, as with all zero-value arrays.

Figure 2-133 is a plot of temperature and mole fraction of pyrene (A4), which is the nucleating species, as a function of distance. Since the inlet velocity is about a factor of 10 smaller than the laminar burning speed for the mixture at the inlet conditions, the flame is attached to the burner. The presence of a wall creates a colder boundary layer near that wall. It can also be seen that the mole fraction of A4 has a negative slope in the region near the wall.

Figure 2-133 Sectional Method plot of temperature and mole fraction of pyrene (A4).

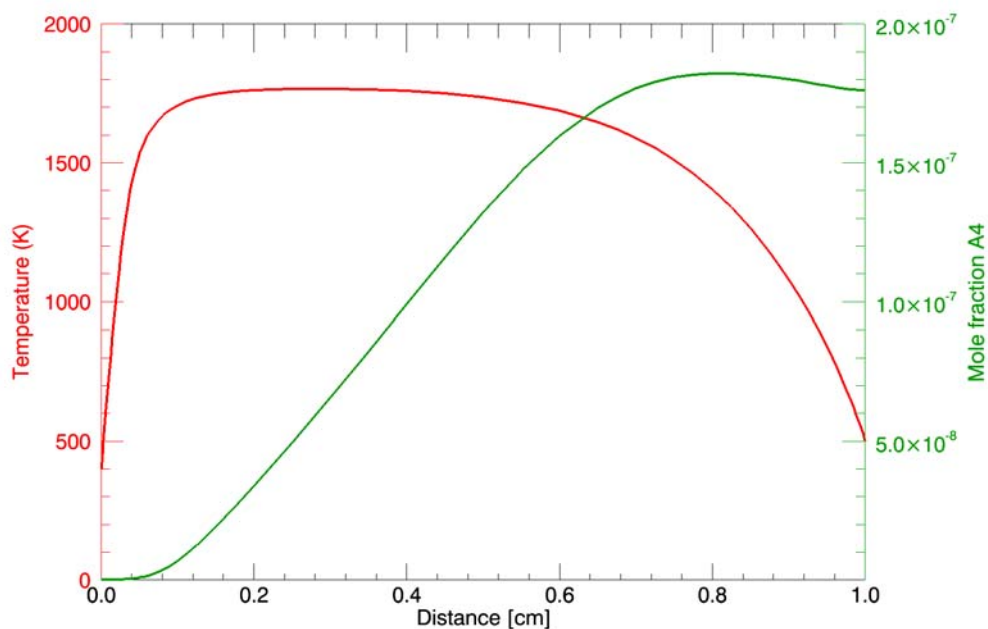


[Figure 2-134](#) and [2-135](#) show the particle-size distribution and the PDF as a function of distance. This plot is created by selecting the sectional data vs. section property for the **Plot Set** textbox in the Post-processor control panel and then choosing **section diameter** for the X-axis. The nucleation reaction in the mechanism used here creates particles of diameter about 0.87 nm. Since smaller particles are not present, the curves in [Figure 2-134](#) and [2-135](#) start somewhat abruptly at the corresponding point. The presence of the cold wall (distance = 1 cm) enhances particle production, as seen by an increase in the number density of smaller particles near the wall.

Figure 2-134 Particle-size distribution as a function of distance.

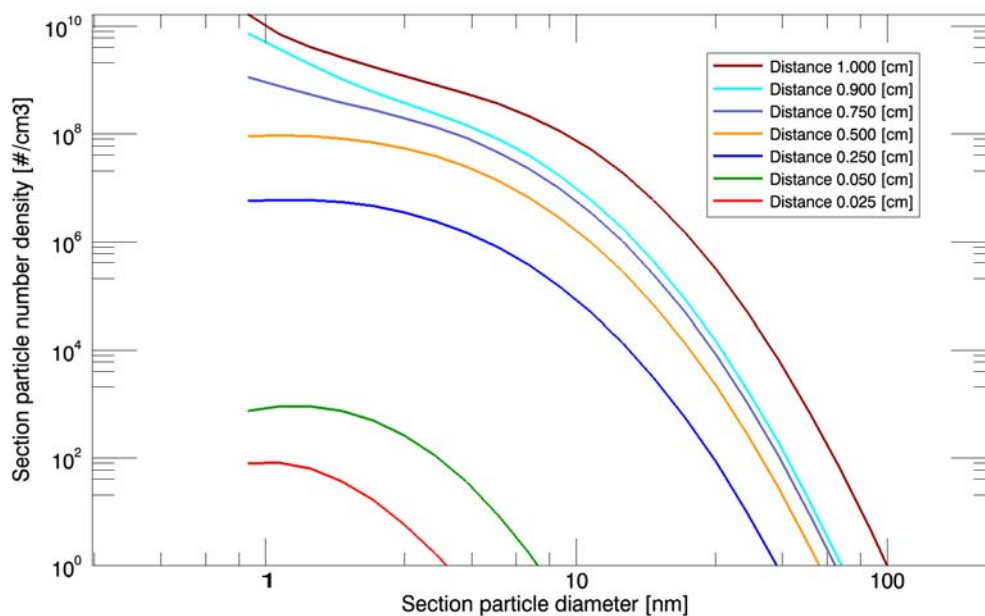
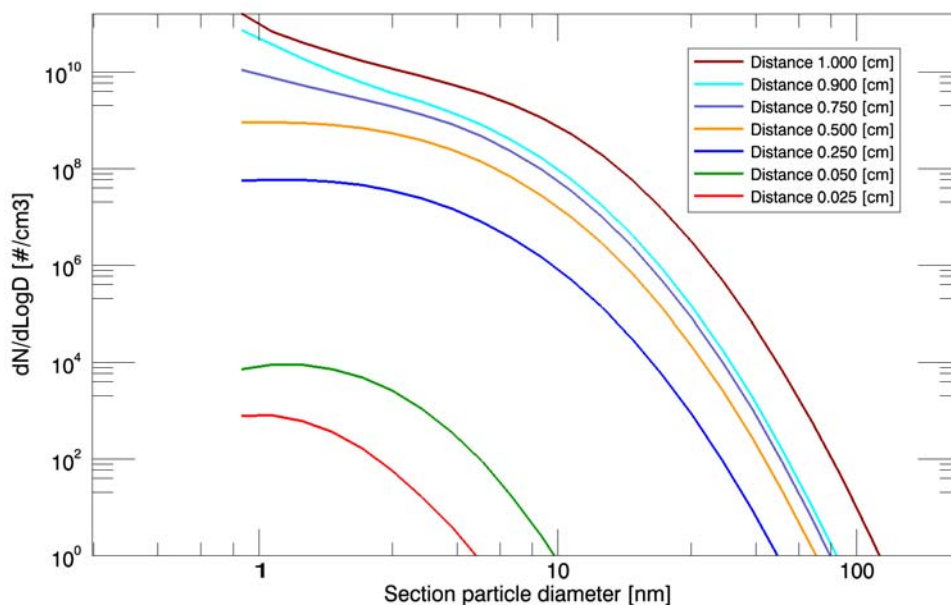


Figure 2-135 PDF as a function of distance



2.7.4 Simulating Particle-Size Distributions in a Burner-Stabilized Stagnation Flame

When simulating particle-size information in flames in CHEMKIN-PRO, you have a choice of using the Moment Method, which provides statistical information about the size distribution and mean particle properties, or the Sectional Method, which predicts the size distribution directly. These particle simulation options are part of the Particle Tracking module that is included with CHEMKIN-PRO. In describing the formation and growth of particles in flames, it is often important to include the effects of particle aggregation. In this tutorial we apply the use of particle aggregation with the Sectional Model method for simulating soot-particle size distributions in a flame. The flame considered is a burner-stabilized premixed flame that impinges on a stagnation surface; this is modeled using the Burner-Stabilized Stagnation Flame reactor model.

For flame simulations using the Sectional Model, the aggregation model employed is the so-called *Simple Aggregation Model*, which is described in detail in the CHEMKIN *Theory Manual*. This form of the aggregation model is particularly useful when the data for characteristic fusion time is not well known, which is the case for many particle materials of practical interest; most notably for carbon-based soot formed in flames and combustion engines. For such systems, it is often easier to define a limiting size for the primary particles in the system. This limiting size (diameter) is

dictated by the competition between collisions among the aggregates and fusion/coalescence of individual aggregates that lead to spherical particles. When collisions happen too quickly or fusion takes long time, a given aggregate cannot coalesce and the primary particle size appears to reach a limit.

In the flame systems, then, the aggregates are modeled as either pure aggregates consisting of primary particles of a fixed (limited) size or as completely coalesced spheres with sizes less than or equal to the limiting size. In this tutorial, we describe the setup and analysis of a flame with particles, considering this simplified representation of particle aggregation for sooting flame conditions.

2.7.4.1 Project Setup

The project set-up is almost identical to the previous one ([Section 2.7.3](#)) except that the following changes are made: The project file is named ***pre-mixed_stagnation_soot_aggregation.ckprj*** (it is located in the ***samples2010*** directory and the corresponding input and chemistry set files are located in the ***samples2010\pre-mixed_stagnation\soot_particles*** directory); the inlet velocity, the separation distance, and inlet equivalence ratio are increased to **25** cm/s, **b** cm, and **2.2**, respectively. For these conditions, the particle size distribution (PSD) shows much more pronounced bimodality than that shown by the PSD obtained for the conditions from the project in [Section 2.7.3](#). The effect of using the simple aggregation model is hence illustrated better with the new set of conditions used in this tutorial.

Since larger particles may form at these simulation conditions, the number of sections used is increased to 45. In addition, the transition regime is selected for collisions. The corresponding collision kernel (CHEMKIN [Theory Manual Equation 18-131](#)) is applicable over the entire range of particle Knudsen number.

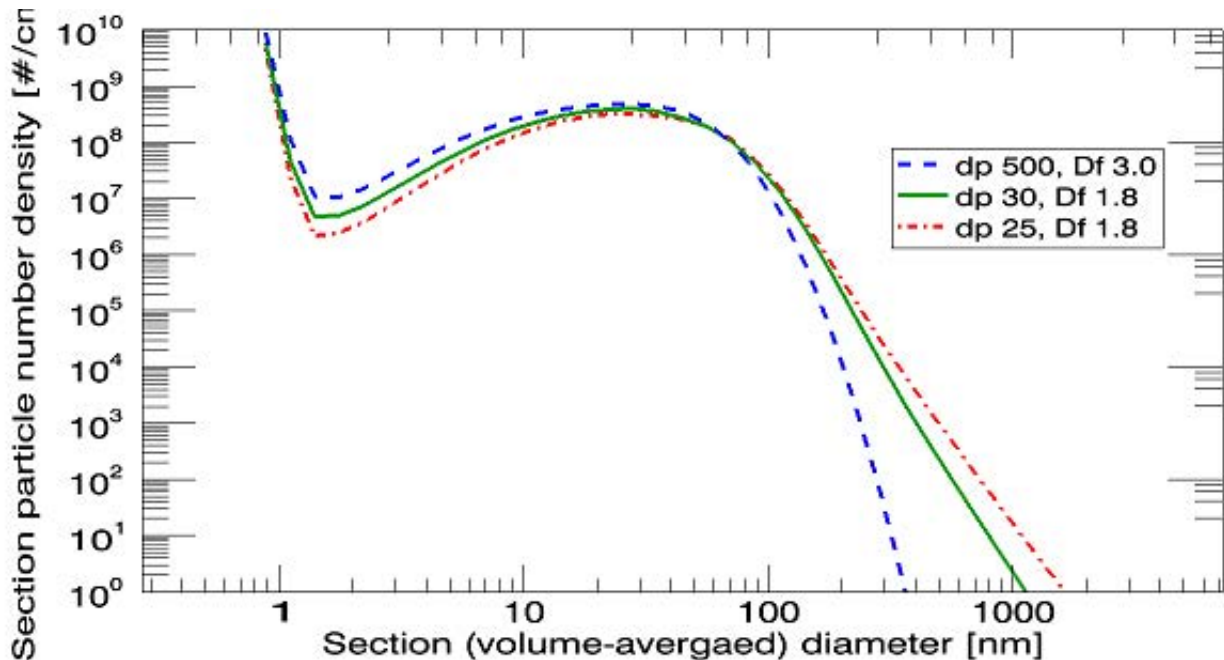
The Aggregation properties are entered on a sub-panel within the "Dispersed Phase::CARBON" tab in the reactor properties node of the project tree. On the Aggregation sub-panel, the **Simple Model** option is selected. The two user-input parameters are: the fixed (limiting) primary particle diameter and the fractal dimension of the aggregate. The fractal dimension of **3.0** implies a spherical particle. If the fixed primary particle diameter were set to a value larger than the largest particle that can form in the system, the simple aggregation model would yield the same results as if the aggregation model were turned off. In this way, we can look at the limiting case and compare this to other cases to see the effects of aggregation.

We set up a parameter study to explore the effects of the aggregation model. The fixed primary particle diameter and fractal dimension are set to **500 nm** and **3.0**, respectively, for the last run. For the first two runs, the fractal dimension is set to **1.8**, indicating cluster-cluster aggregation, while the fixed primary particle diameter is varied between **30 nm** and **25 nm**.

2.7.4.2 Project Results

Figure 2-136 shows the particle number density distributions obtained at the stagnation plane as a function of the section (volume-averaged) diameter for all three parameter studies. In the figure legend, *dp* indicates the fixed primary particle diameter in nanometers and *Df* indicates the fractal dimension. The effect of aggregation can be easily seen. As mentioned above, the complete instantaneous coalescence to spherical particles is mimicked by the last run (the dotted line). Comparing this to the other runs, we can see that the smaller particles are “scavenged” by the larger ones more effectively when the aggregation model is active. This can be attributed to the higher collision diameter of aggregates. The scavenging effect increases as the limiting primary particle size is decreased.

Figure 2-136 Particle-size distribution at the stagnation plane for three conditions imposed by the parameter study.





2.7.5 Detailed Particle Aggregation in a Batch Reactor [CHEMKIN-PRO Only]

2.7.5.1 Project Description

This tutorial describes how to use the particle-aggregation model, when using the Sectional Method in the Particle Tracking feature for computing the particle size distributions in a batch reactor. As discussed in the CHEMKIN *Theory Manual*, the Sectional Method in the CHEMKIN-PRO Particle Tracking feature offers two ways (models) to incorporate the effect of aggregation on particle size distribution for 0-D and plug-flow reactor models in CHEMKIN-PRO. These options are the "simple" and "complete" aggregation model. The "complete" model requires knowledge of the characteristic fusion time for the particle material system being studied. In this tutorial, we simulate formation of titania (TiO_2) particles by oxidation of titanium tetrachloride (TiCl_4). Since the characteristic fusion time data is available for TiO_2 , the complete aggregation model is used.

2.7.5.2 Project Setup

The project file is named ***closed_homogeneous_particle_aggregation.ckprj*** and is located in the ***samples2010*** directory. The corresponding input and chemistry set files are located in the ***samples2010\closed_homogeneous_particle_aggregation*** directory.

This tutorial models a constant-pressure and given-temperature batch reactor. The pressure is set at 1 atm and a piecewise temperature profile as a function of time is imposed on the closed system. The end time for the simulation is 1 s. The initial gas-phase reactant mixture contains pure oxygen (O_2) as the oxidizer and titanium tetrachloride (TiCl_4) as the precursor. For the TiCl_4/O_2 system, it is assumed that the titania particles are nucleated by single-step oxidation of TiCl_4 . The rate of this reaction is assumed to be only dependent on the amount of precursor. The initial mixture consists of 10 moles of O_2 and 10^{-4} moles of TiCl_4 .

2.7.5.2.1 Setting Sectional Method Inputs

For CHEMKIN reactor models that support the Particle Tracking feature and the Sectional Method, radio buttons on the Reactor Properties tab provide a choice between the Moments Method and Sectional Method. This choice is available when the preprocessed chemistry set contains DISPERSED phase material in the surface reaction mechanism. Based on the choice of particle tracking method selected, the Dispersed Phase tab contains appropriate input controls.

2.7.5.2.2 Selecting the Number of Sections and Section Spacing

The number of sections used in the Sectional Method should be large enough that vanishingly small number densities are obtained in the last sections, i.e., in the sections with the largest particles. The number of sections is hence decided based on an estimate of the size of the largest particle that can be formed in a given the system. While the exact value is not known *a priori*, most reacting particle-flow mixtures of interest do not involve particles of size greater than a micron in diameter. In this tutorial, 40 sections are used with a section-spacing factor of 2. The section minimum size is set to unity since the nucleation reaction produces monomers of titania. Since the diameter of the titania monomer is about 0.4 nm, 40 sections with a spacing factor of 2 gives aggregates of about a 3 micron volume-equivalent spherical diameter. This is sufficient for this system.

As sub-micron-size particles are typically expected for most reacting flow particulate systems, the free-molecular collision regime is usually appropriate to model particle collisions. This is also true for the system considered in this tutorial. The corresponding collision kernel for the free-molecular regime has a simple mathematical form, as given by [Equation 18-129](#) in the [CHEMKIN Theory Manual](#). However, for illustrative purposes, we select the transition collision regime for this tutorial since it is applicable to both free molecular and continuum regimes and in some cases you may not know the regime in advance of the simulation. The collision kernel for the transition regime is given by [Equation 18-131](#) in the [CHEMKIN Theory Manual](#). Since the collision kernel expression for the transition regime needs the viscosity of ambient gas, we provide viscosity parameters for the power law fit for oxygen. Note that the computational cost of using the transition regime collision kernel is generally higher than when using the kernels of either free-molecular or continuum regime. (Note that the gas viscosity is also required to specify the collision kernel for the continuum regime, as given by [Equation 18-130](#) in the [CHEMKIN Theory Manual](#).)

2.7.5.2.3 Setting Aggregation Model Inputs

The aggregation sub-tab in the Dispersed Phase panel provides the option to turn ON the aggregation model (OFF is the default). When turned on, you can select either the Simple or Complete aggregation formulation. For this tutorial, the complete aggregation model is selected. The characteristic fusion time for titania is given by²⁹

29. Xiong, Y., and Pratsinis S. E., "Formation of Agglomerate Particles by Coagulation and Sintering", *Journal of Aerosol Science and Technology*, **24**: 301 (1993).

Equation 2-1

$$\tau = 8.3 \times 10^{16} T \exp\left(\frac{3700}{T}\right) d_p^4$$

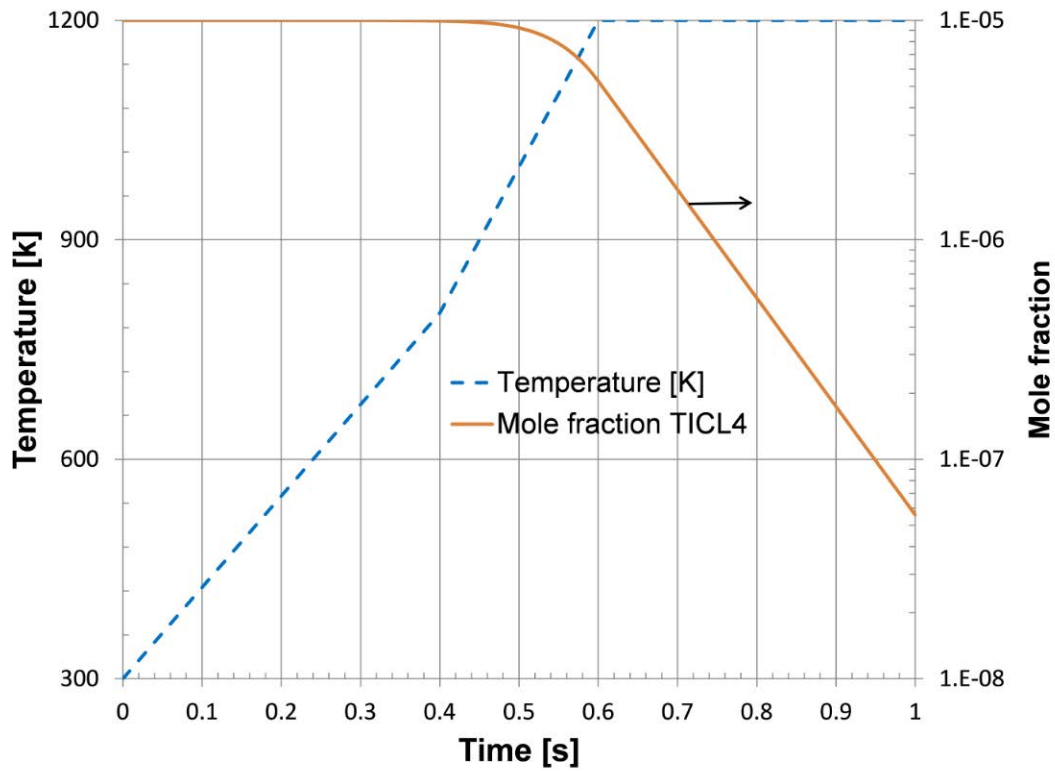
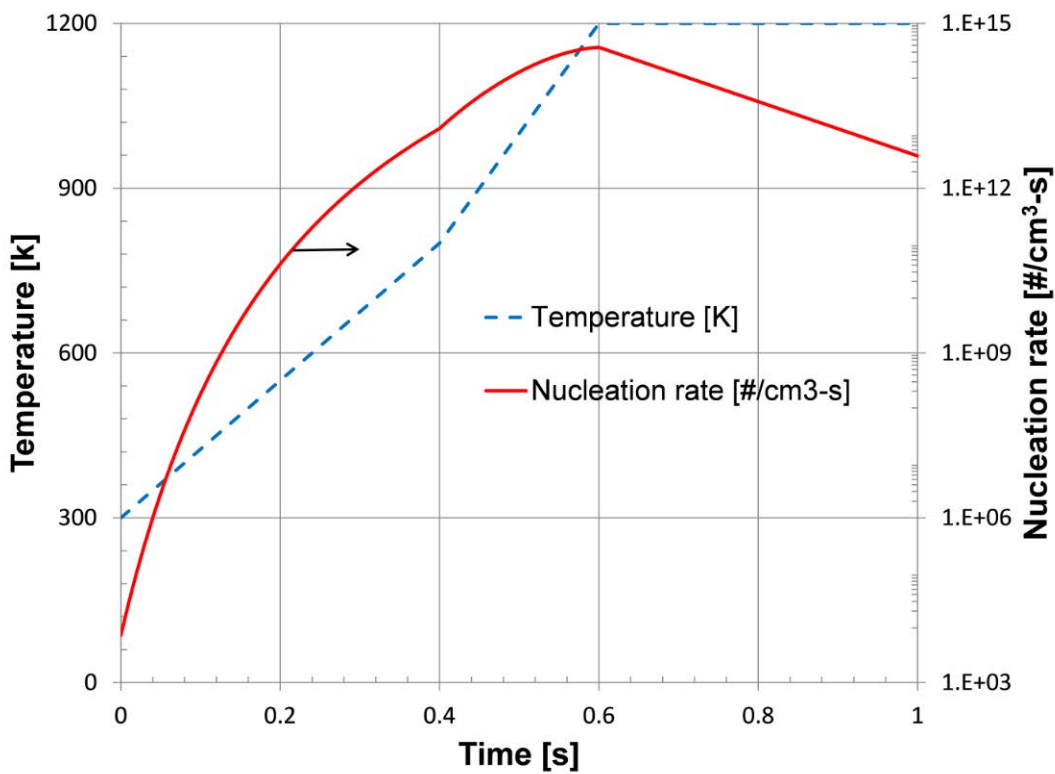
In [Equation 2-1](#), the primary particle diameter (d_p) is in units of cm while the characteristic fusion time (τ) is in s. As indicated by [Equation 18-92](#) from the CHEMKIN [Theory Manual](#), it can be noted that the characteristic fusion time indicates the time required to reduce by 63% the excess surface area of an aggregate over that of an equal mass (volume) spherical particle.

The input parameter threshold to include the fusion effect performs the task of limiting the value of fusion rate. Aggregates with small primary particle diameter coalesce very rapidly and the characteristic fusion times can be on the order of microseconds or smaller. Resolving aggregation of such small particles is unnecessary and can force very small integration time steps. The default value of this threshold parameter is 1 microsecond, which is adequate for most cases. For this tutorial, by setting τ equal to 1 microsecond in [Equation 2-1](#), it can be seen that aggregates with primary particle diameters of less than 1.5 nm will coalesce by 63% within 1 microsecond at the highest temperature (1200K), where fusion is the fastest. Considering that the diameter of the titania monomer is about 0.4 nm, particles of 1.5 nm are indeed small (would fall within the first 5 to 8 sections with a spacing factor of 2). Thus the default value is satisfactory.

The fractal dimension of aggregates is set to 1.8, indicating cluster-cluster aggregation.

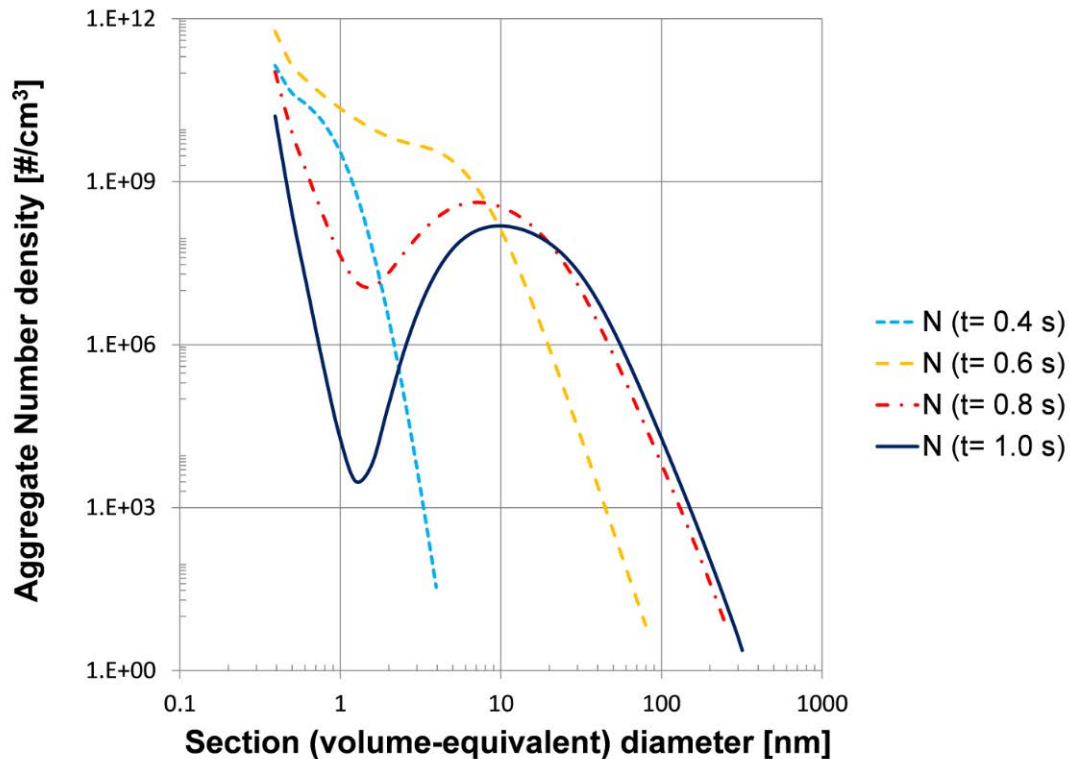
2.7.5.3 Project Results

[Figure 2-137](#) and [Figure 2-138](#) show the imposed temperature profile along with the mole fraction of the precursor (TiCl_4) and the nucleation rate of TiO_2 monomers as a function of time, respectively. As expected, due to the first-order dependence of the nucleation reaction on the concentration of TiCl_4 , the decay of the precursor is exponential once a critical temperature is reached. The nucleation rate peaks at around 0.6 s. We note that nucleation is active throughout the entire duration of the simulation.

Figure 2-137 Imposed temperature profile with the mole fraction of the precursor TiCl_4 .Figure 2-138 Imposed temperature profile with the nucleation rate of the precursor TiCl_4 .

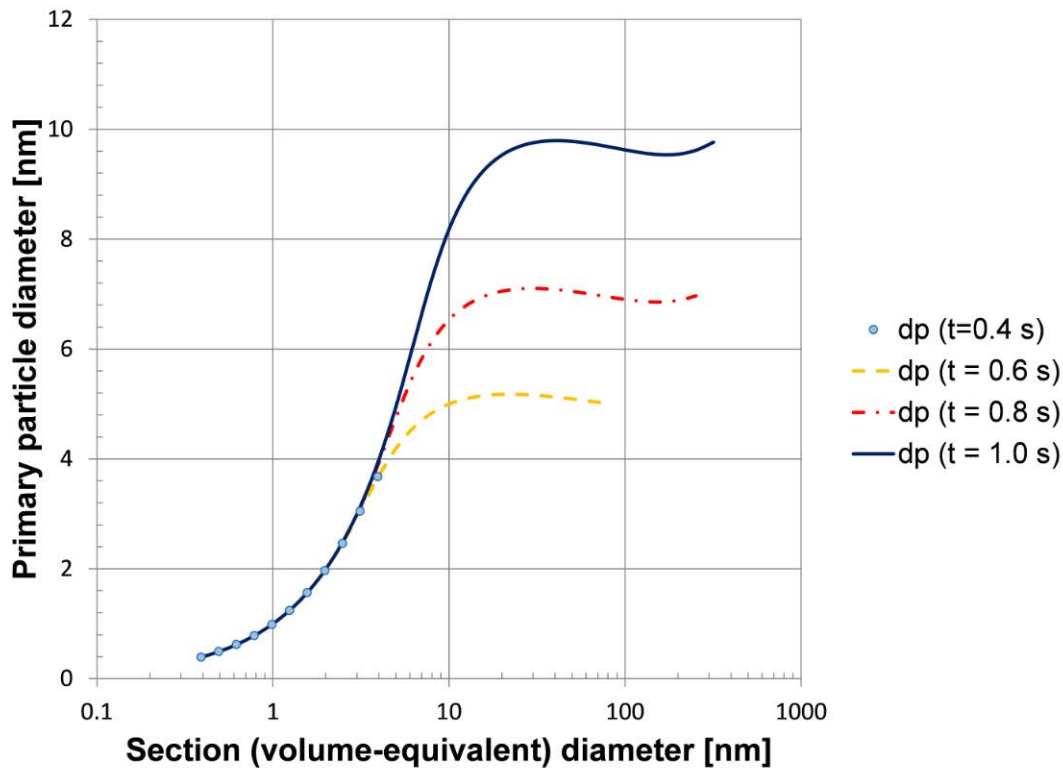
Shown in [Figure 2-139](#) is the aggregate number density as a function of the volume-equivalent section diameter. At $t = 0.4$ s, the particle size distribution is almost unimodal. As the nucleation slows down the bimodal shape of the distribution becomes evident as seen from curves corresponding to $t > 0.6$ s.

Figure 2-139 Complete Aggregation - Aggregate number density as a function of the volume equivalent section diameter.



Plotted in [Figure 2-140](#) is the evolution of primary particle diameter. The primary particle diameter is computed using [Equation 18-96](#) from the [CHEMKIN Theory Manual](#). At $t = 0.4$ s all aggregates are small: volume equivalent diameter is less than 5 nm. Consequently, all are almost completely coalesced spheres. Thus, the number of primary particles per aggregate is close to unity and the primary particle diameter is the same as the volume equivalent diameter. (In the plot, the series for $t = 0.4$ is shown as points only in order to distinguish it from the data points of other series.)

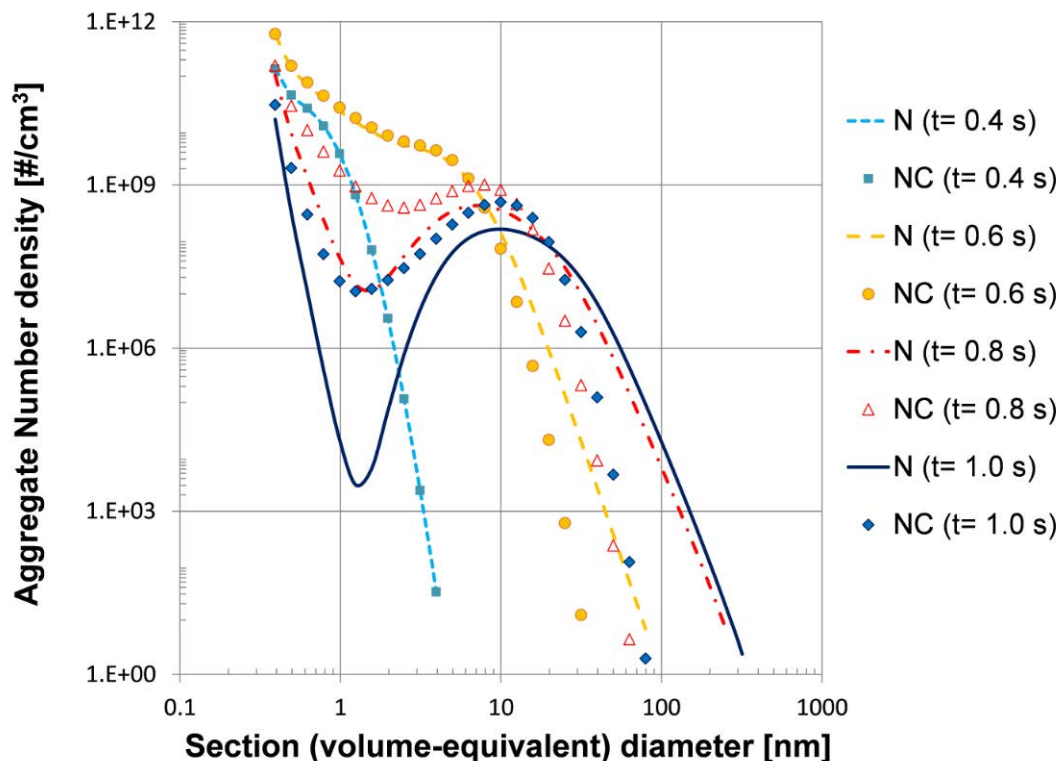
Figure 2-140 Evolution of the primary particle diameter.



Since the rate of fusion is quite high for aggregates with small primary particles, this condition (i.e., completely coalesced aggregates) stays true at all times for small aggregates. For larger aggregates, the primary particle diameter clearly shows a limiting value. This suggests that the rate of fusion cannot keep up with the rate of collisions between the aggregates. (This fact, that a limiting primary particle size can exist, illustrates the motivation behind a simple aggregation model. Please see the CHEMKIN *Theory Manual, Simple Aggregation Model* in [Chapter 18](#).)

To see the effect of aggregation, the simulation can be repeated with the aggregation model turned off. Shown in [Figure 2-142](#) are the number density distributions obtained without aggregation. As expected, the aggregate distribution does not differ much between instantaneous coalescence (aggregation model turned-off) and finite rate fusion. Divergence in the responses of the two models occurs as nucleation slows down and/or larger particles are formed. The instantaneous coalescence shows a gradual shift to a self-similar distribution through a bimodal distribution.

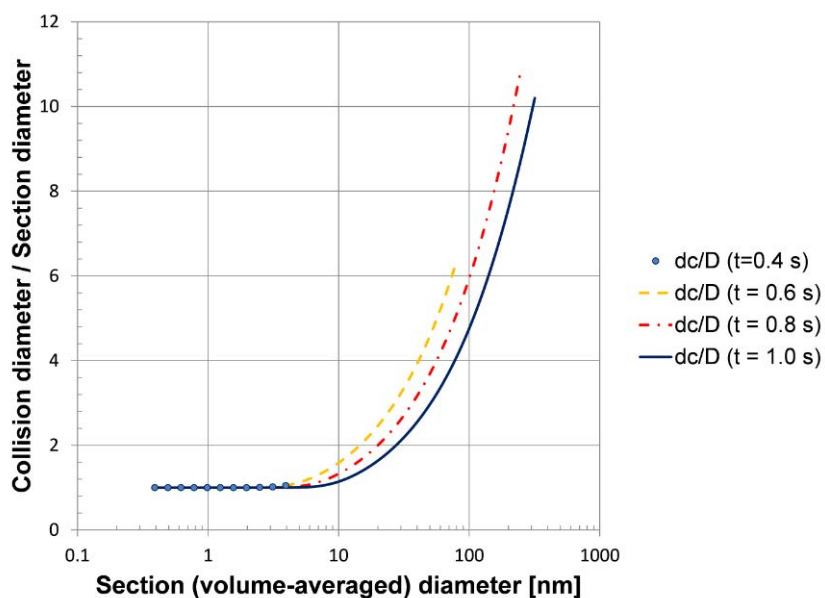
Figure 2-141 Number density distributions obtained without aggregation.



For a finite rate of fusion as given by [Equation 2-1](#), small particles are depleted much more quickly owing to the larger (than volume-averaged) collision diameters of bigger aggregates. This “scavenging effect” is clearly seen at $t = 1$ s. As the nucleation rate slows down, the number density of particles in certain (volume equivalent) diameter ranges start to vanish. Since the nucleation is not completely stopped, particles of the smallest size are still produced in significant enough numbers and the distribution may eventually develop a gap/discontinuity.

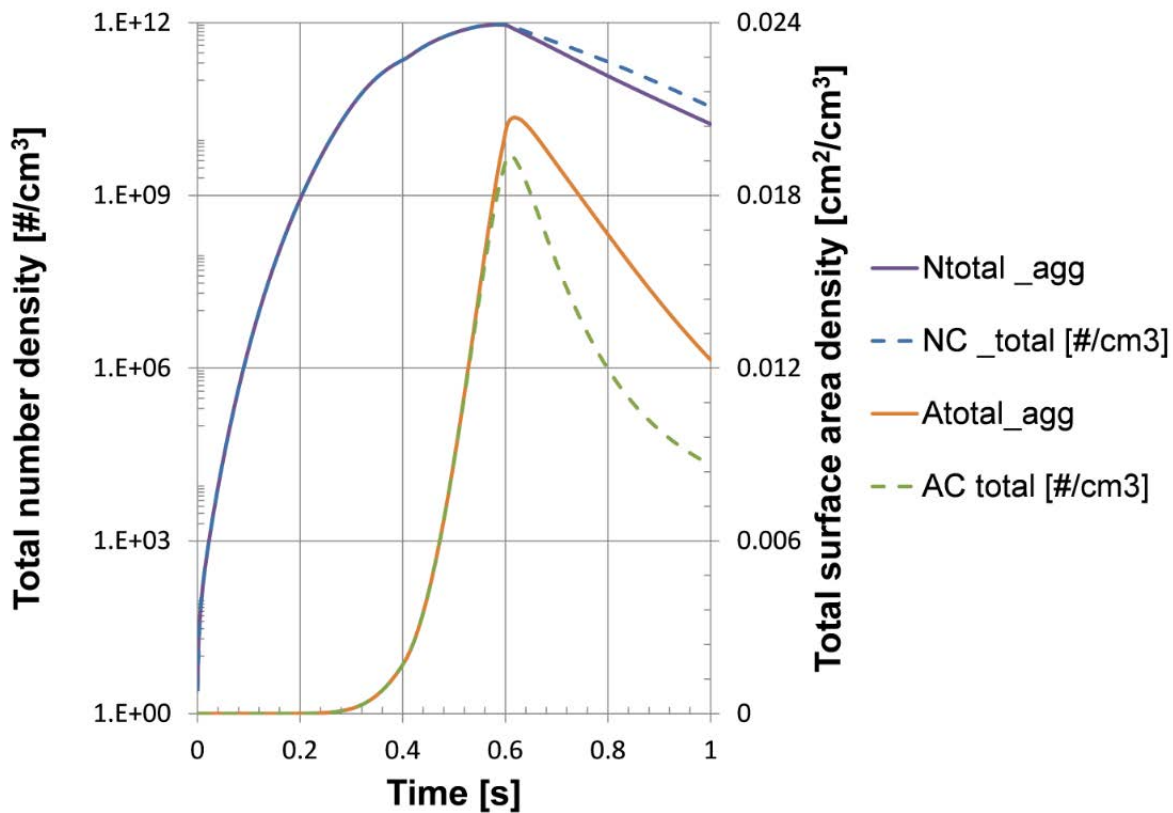
[Figure 2-142](#) shows the collision diameter as a function of (volume equivalent) section diameter. It can be seen that the ratio of collision diameter to volume-equivalent diameter is greater than unity; approaching an order of magnitude for aggregates with 100 nm and higher volume-equivalent diameter.

Figure 2-142 Collision diameter as a function of (volume equivalent) section diameter.



Shown in [Figure 2-143](#) is the comparison of the total particle number and surface area densities as a function of time with and without aggregation model. As expected, there is very little difference when nucleation is more dominant ($t < 0.6$ s). However, the number density predicted with finite rate of fusion (aggregation model turned on) is a factor of 3 smaller and the surface area is a factor of 2 than that predicted when the aggregation model is not used. Thus, when reliable data for fusion time is available, the complete aggregation model with the Particle Tracking feature can be used to guide design in particle production processes.

Figure 2-143 Comparison of the total particle number and surface area densities as a function of time with and without aggregation model



2.8

Uncertainty Analysis [CHEMKIN-PRO Only]

2.8.1

Uncertainty Analysis of NO_x Emissions [CHEMKIN-PRO Only]

Emission studies have become a vital part of the design and analysis of gas-phase combustion processes, because of the increasingly stringent requirement imposed by government regulations. The emission standard of NO_x by combustion processes is approaching the ppm (parts per million) level. However, the combustion processes in general demonstrate variations in operating conditions due to the very nature of these processes. These variations can induce uncertainties in the level of NO_x emission. It is therefore necessary to account for these uncertainties during the design and analysis of the combustion processes to make sure the emission level is still within the regulatory requirements. Uncertainty analysis can be performed to study the effect of variations in the operating conditions on the NO_x emission level.

In this tutorial, we apply an uncertainty analysis to investigate the effects of heat loss and equivalence ratio for the NO_x emission level of a perfectly stirred reactor. The associated project file is called ***psr_NOx_uncertainty_analysis.ckprj***. The chemistry-set files used for this sample problem are located in the ***psr/NOx_uncertainty_analysis*** folder of your CHEMKIN ***samples2010*** directory. For the gas-phase kinetics, we employ the GRI gas-phase mechanism and thermodynamic data for methane combustion. This mechanism contains NO_x chemistry in methane combustion.

We choose to study the effect of the variations in heat loss from the wall of the reactor and the equivalence ratio (i.e., fuel/air ratio) for the NO_x emission of a perfectly stirred reactor. These operating conditions are selected because (1) the exact heat loss from the wall of the reactor/combustor is often unknown in the combustion industry (2) non-perfect mixing in the combustion processes often lead to pockets of very fuel-rich or fuel-lean reactant mixtures, thus making the overall reactant fuel/air ratio uncertain.

An uncertainty analysis has already been set up for heat loss and equivalence ratio in the ***psr_NOx_uncertainty_analysis*** project. To see how this is done, double-click the C1_PSR node on the project tree to open the Reactor Physical Properties panel, as shown in [Figure 2-144](#). Click on the Setup Uncertainty Analysis button (i.e. with icon ) next to the Heat Loss parameter of the reactor to view the uncertainty analysis setup, as shown in [Figure 2-145](#). We are using the normal (Gaussian) probability density function to represent the uncertainty in the heat loss because of the lack of more specific information available. The mean value of the distribution is the nominal value of heat loss in the reactor and the standard deviation is assumed to be 1.0 cal/sec or 20% of the mean value for this analysis. You can view the uncertainty setup of the equivalence ratio by double-clicking the C1_Inlet1 node on the project tree and then clicking on the Species-specific Properties tab. We are using the normal distribution for the equivalence ratio too but we are assuming a much smaller standard deviation in the analysis. We use the final mole fraction of NO in the reactor as the uncertain output in the NO_x emission study.

Figure 2-144 Setting Up an Uncertainty Analysis for Heat Loss

C1_PSR (psr_NOx_uncertainty_analysis:PSR (C1))

Reactor Physical Properties Species-specific Properties

Problem Type: Solve Gas Energy Equation

Steady State Solver

Transient Solver

End Time: 0.02 sec

Residence Time: 0.0035 sec

Temperature: 1800.0 K

Pressure: 1.0 atm Constant

Volume: 15.8 cm3 Constant

Heat Loss: 5.0 cal/sec Constant

Heat Transfer Coefficient: cal/cm2-K-sec

Ambient Temperature: K

Figure 2-145 Setting Up the Uncertainty Distribution for Heat Loss

Uncertainty Analysis for PSR (C1) :: C1_PSR :: Heat Loss

Heat Loss :: C1_PSR :: PSR (C1)

Nominal Value = 5.0 cal/sec

Select Unit: cal/sec

Probability Density Function: Normal



Mean Value: 5.0

Standard Deviation: 1.0

Relative Standard Deviation

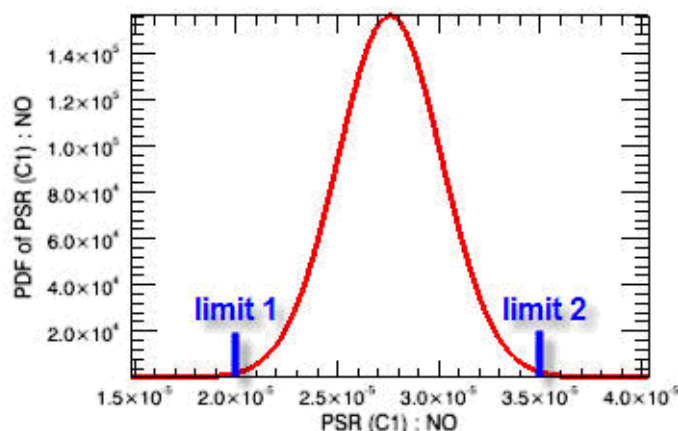
Clear Done

Run the uncertainty analysis by selecting all of the runs in the Running Uncertainty Analysis panel and clicking the Run Selected button. Once they are done, click the Do Analysis button to perform the uncertainty analysis for the NO_x emission level and perform the variance analysis to determine the contribution to the uncertainty in NO_x emission from the variations in heat loss and equivalence ratio. A text file is displayed to show the summary of the analysis. From Section 2, Error Analysis, you can see that the accuracy of the uncertainty model is high in the predictions of NO_x emission level. From Section 3, Variance Analysis, you can see that the uncertainty in the NO_x emission level is quite moderate, since the standard deviation of the NO_x emission level is about 10% of the mean value. The more interesting results from the variance

analysis is that the smaller variation in the equivalence ratio has much more impact on the uncertainty of the NO_x emission level than the much larger variation in the heat loss. This indicates that the variation in the equivalence ratio is more important to maintain the required level of NO_x emission in this perfectly stirred reactor.

Further analysis of the NO_x emission can be achieved by examining the probability density function (pdf) of NO . Click the **View PDF** button and select to view the pdf of NO , as shown in [Figure 2-146](#). The pdf of NO shows the distribution of the NO emission given the variations in the heat loss and equivalence ratio of the reactor. From the pdf, we can conclude that the most likely emission level of NO is between $2.3\text{E-}5$ (23 ppm) and $3.2\text{E-}5$ (32 ppm). If the emission requirement is $2.0\text{E-}5$ (20 ppm) (i.e., limit 1), the likelihood of the NO emission to be below this level is minimal, since most portion of the pdf curve lies above the level of limit 1. If the emission requirement is $3.5\text{E-}5$ (35 ppm) (i.e. limit 2), it is almost certain that the NO emission will satisfy this requirement, regardless of the variations in the heat loss and equivalence ratio of the reactor.

Figure 2-146 Probability Density Function of NO



2.9 Chemistry Sets

In this section we provide a brief description of and references for the chemistry mechanisms employed in [Chapter 2](#).

2.9.1 Hydrogen/Air

The chemistry sets used to describe the combustion of hydrogen in air are provided for the purposes of illustration only. These are slight variations of early work done at Sandia National Laboratories, and are out-of-date. The gas-phase kinetics input files are relatively simple. They generally contain 3 elements H, O and N or Ar, and 9 gas-

phase species: H₂, H, O₂, O, OH, H₂O, HO₂, H₂O₂ and N₂ or Ar, with about 18-20 reactions. Nitrogen is generally present as N₂ only, where it does not participate in any chemical reactions (i.e., NO formation is not included). Pressure dependencies for reaction rates are not explicitly treated, although there are enhanced collision efficiencies for some reactions.

2.9.2 Methane/Air

Two somewhat different chemistry sets are used in the user tutorials to describe the combustion of methane in air or oxygen. One is the full version of GRImech 3.0,³⁰ which includes the reactions leading to NO_x formation. The other is a smaller reaction mechanism, which is used for the purposes of illustration in cases where reducing computation time is helpful.

2.9.2.1 GRImech 3.0

GRImech version 3.0 is a relatively well-tested reaction mechanism that was developed under the auspices of the Gas Research Institute. This reaction mechanism, consisting of gas-phase chemistry, thermodynamic, and transport data files, is provided as one of the default chemistry sets in CHEMKIN in the system data folder. A detailed description of the development and extensive validation of this mechanism is available.

The gas-phase kinetics input file contains 5 elements, C, H, O, N and Ar, 53 chemical species, and 325 reactions. The reaction mechanism describes the combustion of methane and smaller species such as hydrogen, as well as the formation of nitrogen oxide pollutants. Most of the reactions are reversible; only a small number of irreversible reactions are included. Many of the reactions have explicit descriptions of their pressure-dependencies, using the Troe formulation and including enhanced collision efficiencies for particular species.

2.9.2.2 Reduced Mechanism

This smaller reaction mechanism is from early work at Sandia National Laboratories and is given for purposes of illustration only. The gas-phase kinetics input file contains 4 elements, C, H, O, and N, 17 chemical species, and 58 reversible reactions. The reaction mechanism describes the combustion of methane and smaller species such as hydrogen, but nitrogen is present as N₂ only, and does not participate in any chemical reactions. There is no explicit treatment of pressure-dependencies for reaction rates, although there are enhanced collision efficiencies for some reactions.

30. <http://www.me.berkeley.edu/gri-mech/>.

2.9.3 NO_x and CH_4 , C_2H_4 , C_2H_6 , C_3H_6 , and C_3H_8

This reaction mechanism is made available by Lawrence-Livermore National Labs. The gas-phase kinetics input file contains 5 elements, Ar, C, H, O, and N, 126 chemical species, and 638 reversible reactions. The chemical kinetic mechanism was validated to describe the promotion effect of hydrocarbons (methane, ethane, ethene, propene and propane) on NO to NO_2 conversion in an atmospheric flow reactor. The NO level was 20 ppm and the hydrocarbon level was 50 ppm. The flow reactor temperature ranged from 600 to 1100 K.

2.9.4 Propane/Air

This mechanism is the result of work at the Center for Energy Research (CER), University of California, San Diego. It consists of 46 species and 235 reactions. The elements constituting the species are N, H, C, O, Ar, and He. The thermodynamic and transport data in this chemistry set are included from the same source. All reactions are reversible, and some of the reactions include pressure-dependencies on the rate constant using the Troe formulation (see [Equation 3-27](#) in the *CHEMKIN Theory Manual*). Enhanced collision efficiencies are used for some reactions. The references for the reaction rate parameters as well as for thermodynamic and transport data can be obtained from the CER website:

<http://www-mae.ucsd.edu/~combustion/cermech/>

2.9.5 Ethylene/Air Combustion and Soot Formation and Growth

2.9.5.1 Combustion Mechanism and Soot Nucleation Reaction

The C_2H_4 -air combustion mechanism of Appel et al.³¹ is provided with this chemistry set. This reaction mechanism consists of 101 species and 543 reactions which include PAH growth reactions up to pyrene, A4.

According to Frenklach and coworkers^{31,32}, soot particles are created by the dimerization of pyrene molecules and to represent this, a single nucleation reaction is included in this chemistry set. The kinetic parameters of the soot nucleation reaction were derived by matching the nucleation-only soot mass concentration prediction to measurements³³, and are shown as follows

31. J. Appel, H. Bockhorn, and M. Frenklach, *Combust. and Flame*, **121**:122-136 (2000).

32. M. Frenklach and H. Wang, in *Soot Formation in Combustion: Mechanisms and Models*, H. Bockhorn (Ed.), Springer-Verlag, pp. 165-192 (1994).

33. C.-P. Chou, D. Hodgson, M. Petrova, and E. Meeks, "Modeling Soot Growth and Activity with Heterogeneous Kinetics and Method of Moments," 5th U.S. Combustion Meeting, Combustion Institute, San Diego, CA, 2007.

```
(S1) 2A4=>32C(B)+20H(S)+28.72(S) 9.0E09 0.5 0.0
```

The A-factor computed from the collision frequency between A4 molecules is of the order of 10^{12} and is much larger than the one used in the above nucleation reaction, which suggests that about one in 1000 collisions results in a nucleation event.

2.9.5.2 Soot Mass Growth Reactions

One of the advantages of the Particle Tracking module is that soot mass growth and oxidation reactions can be provided as regular surface reactions. For example, the H-Abstraction- C_2H_2 -Addition (HACA) soot growth sequence proposed by Frenklach and coworkers^{31,32} can be given as:

```
(S2) H+H(S)=>(S)+H2 4.20E13 0.0 13000.0
(S3) H2+(S)=>H(S)+H 3.90E12 0.0 9320.0
(S4) H+(S)=>H(S) 2.00E13 0.0 0.0
(S5) H(S)+OH=>H2O+(S) 1.00E10 0.734 1430.0
(S6) H2O+(S)=>OH+H(S) 3.68E08 1.139 17100.0
(S7) C2H2+(S)=>H(S)+2C(B)+H 8.00E07 1.56 3800.0
```

Each sweep of the HACA growth sequence will increase the soot particles by two classes.

Marr²⁷ (see p. 141) suggested that PAH condensation on the soot particle surface can have significant contribution to soot mass growth in a post-flame zone. He also found from his experimental study that the collision efficiency of PAH condensation is of the order of 0.1. Since a description of how PAH species interact with a soot particle is not readily available, the PAH condensation reactions used in the simulation are estimated. Only condensations of major PAH species in the gas mechanism are considered. The reaction orders are determined by fitting the experimental data while keeping the sticking coefficients to be on the order of 0.1. Basically, the PAH condensation reactions used here are designed to increase soot particle mass in two ways: they grow the soot particle by the addition of PAH species and they remove some H atoms (H(S)) on the soot particle surface so that the more effective soot growth reaction, C_2H_2 addition (S7), can proceed at a greater rate.

(S8)	A1+6H(S) =>6C(B) +6(S) +6H2 FORD/H(S) 1.0/ FORD/(S) 1.0/ DCOL/2.46E-8/ STICK	0.2	0.0	0.0
(S9)	A1C2H+6H(S) =>8C(B) +6(S) +6H2 FORD/H(S) 2.0/ DCOL/2.46E-8/ STICK	0.21	0.0	0.0
(S10)	A2+16H(S) =>10C(B) +16(S) +12H2 FORD/H(S) 2.0/ DCOL/4.92E-8/ STICK	0.1	0.0	0.0
(S11)	A2R5+16H(S) =>10C(B) +16(S) +11H2+C2H20.1 FORD/H(S) 2.0/ DCOL/4.92E-8/ STICK		0.0	0.0
(S12)	A3+20H(S) =>14C(B) +20(S) +15H2 FORD/H(S) 2.0/ DCOL/4.92E-8/ STICK	0.1	0.0	0.0
(S13)	A4+20H(S) =>16C(B) +20(S) +15H2 FORD/H(S) 2.0/ DCOL/4.92E-8/ STICK	0.1	0.0	0.0

Expressing the soot growth sequence as a chain of surface reactions has other advantages. As part of the surface mechanism, it is easy to check for the conservation of elements and to perform sensitivity analysis on these reactions. Furthermore, as information about certain reactions, such as PAH condensation, becomes available from surface-science experiments, utilization of such information would be straightforward.

2.9.5.3 Soot Oxidation Reaction

Once soot particles are created in the flame zone, they start interacting with the surrounding gas mixture and with one another. Therefore, if oxidizers such as O, OH, and O₂ are available in the local gas mixture, the soot particles are also subjected to oxidation. Neoh et al.³⁴ found that the most effective soot oxidizer in the flame zone is OH and determined that the collision efficiency (or sticking coefficient) for the OH oxidation reaction is 0.20. For simplicity, the current mechanism only includes soot oxidation due to OH using this rate:



2.9.6 C2_NOx Mechanism

The C2_NOx mechanism was developed at Reaction Design. This reaction mechanism, consisting of gas-phase chemistry, thermodynamic, and transport data files, is provided as one of the default chemistry sets in CHEMKIN-PRO in the system data folder. It describes oxidation of hydrogen, methane, and ethane over a broad range of temperature and pressure and includes NO_x chemistry.

The mechanism is based on a literature mechanism for oxidation of model-fuel components³⁵. Many reactions in the base mechanism have been updated based on most recent kinetic studies. Reaction sub-mechanisms have been updated based on recent studies on hydrogen³⁶ and methane³⁷ oxidation. The chemically activated reaction of ethyl radical with molecular oxygen has also been updated based on Naik and Dean³⁸. The base high-temperature NO_x chemistry is from the GRI-mech 3.0 mechanism (see [Section 2.9.2.1](#)). Recently, researchers have identified the mutual sensitization effect of NO_x on hydrocarbon oxidation at lower temperatures. The

34. K.G. Neoh, J.B. Howard, and A.F. Sarofim, in *Particulate Carbon Formation During Combustion*, D.C. Siegl and G.W. Smith (Eds.), Plenum Publishing Corp., pp. 261-282 (1981).

35. Naik, C.V., et al., *Detailed Chemical Kinetic Modeling of Surrogate Fuels for Gasoline and Application to an HCCI Engine*. Society of Automotive Engineers, 2005. SAE 2005-01-3741.

36. O'Conaire, M., et al., *A Comprehensive Modeling Study of Hydrogen Oxidation*. Int. J. Chem. Kinet., 2004. 36: p. 603-622.

37. Petersen, E.L., et al., *Methane/Propane Oxidation at High Pressures: Experimental and Detailed Chemical Kinetic Modeling*. Proceedings of the Combustion Institute, 2007. 31: p. 447-454.

38. Naik, C.V. and A.M. Dean, *Detailed Kinetic Modeling of Ethane Oxidation*. Combustion and Flame, 2006. 145: p. 16-37.

current mechanism includes the most recent pressure-dependant NO_x -hydrocarbon reactions from Rasmussen³⁹. Reactions pertaining to NO_x chemistry in the intermediate temperature region has also been updated based on the review of Dagaut, Glarborg et al.⁴⁰

The final pressure-dependant mechanism contains 99 chemical species and 693 elementary reactions that describe hydrocarbon oxidation chemistry as well as NO_x chemistry over broad range of temperatures and pressures. Most of the reactions are reversible and many of the reactions have explicit descriptions of their pressure-dependencies, using the TROE and PLOG formulation and including enhanced collision efficiencies for particular species.

39. Rasmussen, C.L., A.E. Rasmussen, and P. Glarborg, *Sensitizing Effects of NO_x on CH_4 Oxidation at High Pressure*. Comb. Flame, 2008. 154(3): p. 529-545.

40. Dagaut, P., P. Glarborg, and M.U. Alzueta, *The Oxidation of Hydrogen Cyanide and Related Chemistry*. Progress in Energy and Combustion Science, 2008. 34: p. 1-46.

3 Catalytic Processes

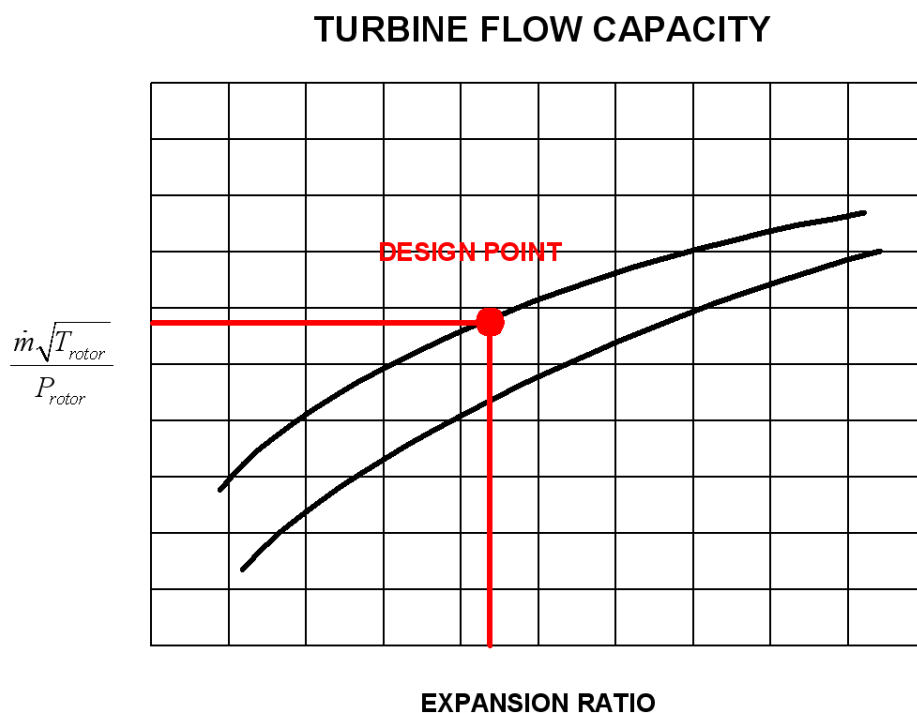
3.1 Catalytic Combustors, Converters and Aftertreatment

3.1.1 Two-Stage Catalytic Combustor

3.1.1.1 Problem Description

For this problem, we need to design a virtually zero- NO_x combustor for a sub-scale test unit of our micro-turbine system. This new combustor must also match several gas turbine inlet specifications to optimize the overall system performance under full-load, steady-state operation. A typical gas turbine flow capacity chart is shown in [Figure 3-1](#). The combustor-related design specifications normally include total mass flow rate of the gas turbine system and the turbine rotor inlet temperature, TRIT.

Figure 3-1 Turbine Flow Capacity



The basic rule for minimizing NO_x emissions from a gas turbine combustor is to keep the gas temperature low by operating the combustor under ultra-lean conditions. However, if the fuel-air ratio gets too low, the combustor will run into flame stability problems. We decide to work around the flame stability issue with the implementation of a catalytic combustor. A catalytic combustor produces essentially no NO_x and can convert very lean fuel-air mixtures at relatively low temperatures. There are some disadvantages of a catalytic combustor, though. For instance, the honeycomb monolith introduces a large pressure drop and the thermal mass of the honeycomb material can slow down the catalytic combustor's response to changes in operating conditions. The precious metals used as catalysts are usually very expensive (Pt \$870/oz, Pd \$230/oz) and, to prolong the lifetime of the catalyst, the maximum operating temperature is much lower for catalytic combustors than for homogeneous (gas-phase only) combustors. To raise the catalytic combustor exit gas temperature (< 1200 K) to the desired TRIT (~1475 K), a second stage combustor must be added and it has to be a homogeneous combustor. We expect that almost all NO_x emission from this two-stage combustor system will come from the homogeneous combustor. Fortunately, the gas mixture entering the homogeneous combustor is already at an elevated temperature, we can try to push the fuel-air ratio as lean as possible to minimize NO_x generation without getting into flame stability issues. If the exit temperature of the second combustor becomes too high for the turbine rotor, a third stage can be added to cool the gas down with excess air.

3.1.1.2 Problem Setup

The CHEMKIN project file for this tutorial problem is called ***reactor_network_two_stage_catalytic_combustor.ckprj*** located in the default sample directory. We are going to use methane as the main fuel in our micro-turbine combustor system, so we choose GRI Mech 3.0, as described in section [Section 2.9.2](#), to handle the gas phase combustion and, for the catalytic combustion, the surface reaction mechanism developed by Deutschmann *et al.*⁴¹ for methane oxidation on platinum catalyst, as described in section [Section 3.3.1](#), is employed. The chemistry set, ***reactor_network_two_stage_catalytic_combustor.cks***, which includes the gas phase (GRI methane oxidation mechanism) and surface (Deutschmann's methane/platinum catalytic oxidation mechanism) reactions can be found in the working directory ***samples2010\reactor_network\two_stage_catalytic_combustor***. Since we will use only the perfectly stirred reactor (PSR) and plug flow reactor (PFR) in our model, we do not need any transport data.

Before building a model for our combustor system, we need to find out all the important parameters of the system. The total mass flow rate of our sub-scale micro-turbine system has to match the gas-turbine design point, which, in our case, is 980 g/sec. Since this designed flow rate is too large to be handled by a single combustor, we divide the flow evenly into 6 identical combustor units in parallel and merge them before entering the gas turbine. We set the mass flow rate of each catalytic combustor to 127 g/sec so that there is about 21.5% (or 35 g/sec) excess air per combustor for liner cooling and downstream dilution. Methane and compressed air are pre-mixed before entering the catalytic combustor. We keep the fuel-air mixture very lean so it will not ignite before reaching the catalytic combustor. The gas temperature and pressure at the inlet of the catalytic combustor are 715 K and 3.75 atm, respectively. The inlet gas temperature is higher than that of a homogeneous combustor. We have to use a higher inlet gas temperature to ensure a light-off (or surface ignition) on the catalyst surface. Note that we could lower the inlet temperature if a palladium-based catalyst were used or if a small amount of hydrogen were added to the fuel. However, at this point, we consider methane as the only fuel component.

The catalytic combustor is 10 cm in diameter and 10 cm long. It consists of a metal outer liner providing structure support and a honeycomb monolith core. The catalyst is coated on all internal surfaces of the monolith. The cell density of the honeycomb monolith we selected is 400 cpsi (cells per square-inch) and the cell wall thickness is 0.18 mm. The pressure drop across the monolith is determined to be 0.064 psi/cm for the given flow rate. 5.2 grams of platinum are wash-coated onto the internal surfaces

41. Deutschmann *et al.*, *Proceedings of Combustion Institute*, **26**:1747-1754 (1996).

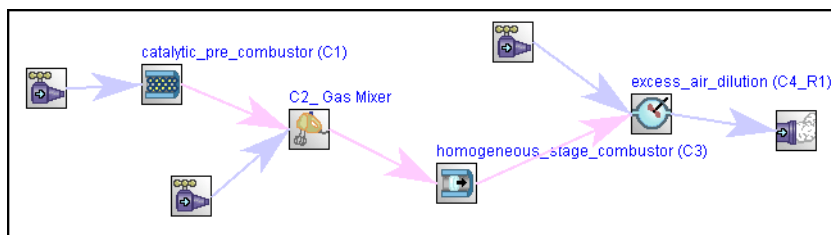
of the honeycomb monolith. The metal surface area is $189 \text{ m}^2/\text{g}$ and the metal dispersion is 70%. Based on the inlet stream properties, mass flow rate, and the geometry of the honeycomb monolith, we find that the inlet velocity of the catalytic combustor should be 1200 cm/sec.

Since we want to make the catalyst last longer to reduce operating costs, we need to keep the catalyst surface below its maximum operating temperature. Theoretically the maximum surface temperature in the catalytic combustor should not exceed the adiabatic flame temperature of the inlet gas mixture. In other words, we can determine the maximum equivalence ratio of the fuel-air mixture entering the catalytic combustor by comparing the adiabatic flame temperatures against the maximum catalyst operating temperature. The adiabatic flame temperature of a given equivalence ratio can be easily obtained by using CHEMKIN's Equilibrium Reactor Model. Of course, the minimum equivalence ratio of the inlet fuel-air mixture is the one below which no light-off is observed on the catalyst surface. Accordingly, we set the equivalence ratio to 0.185.

With all the basic information defined, we are ready to build a simple reactor network model for our two-stage combustor system. We choose the Honeycomb Monolith Reactor Model to represent the first-stage catalytic combustor and a Plug Flow Reactor Model for the second-stage homogeneous combustor. Since all of the initial fuel is expected to be consumed by the catalytic combustor, we have to inject additional fuel to the second-stage homogeneous combustor. To achieve this, we need to add a gas mixer between the Honeycomb Monolith Reactor and the Plug Flow Reactor in our reactor network model. A fourth reactor, which can be either a PSR or a PFR, is added after the PFR (the homogeneous combustor) to simulate the post-flame flow in transition to the gas turbine and to allow the introduction of excess air to cool down the flue gas if needed. [Figure 3-2](#) shows the “diagram” of our combustor system model that comprises four reactor clusters. We will run these clusters in sequence.

Temperatures of both the additional fuel and the excess air are assumed to be the same as the inlet temperature of the catalytic combustor. The mass flow rate of excess air is the difference between the design flow rate of the gas turbine and the exit mass flow rate of the homogeneous combustor. The amount of fuel added to the homogeneous combustor should be able to raise the gas temperature high enough so that, after excess air dilution, the gas temperature can still meet the required TRIT. After a few iterations, we find the additional fuel mass flow rate is 1.5 g/sec.

Figure 3-2 Two-Stage Catalytic Combustor—Diagram View



Now we can further set up our combustor system model by providing proper information on each input panel. The catalyst properties and the honeycomb monolith geometry are entered on two special sub-tabs (please see [Figure 3-3](#) and [Figure 3-4](#)). To find these two special sub-tabs, go to the Honeycomb Monolith Reactor's Catalytic Pre-combustor (C1_) panel and click on the Honeycomb Monolith tab.

Figure 3-3 Catalytic Pre-combustor (C1_)—Honeycomb Monolith, Catalyst sub-tab

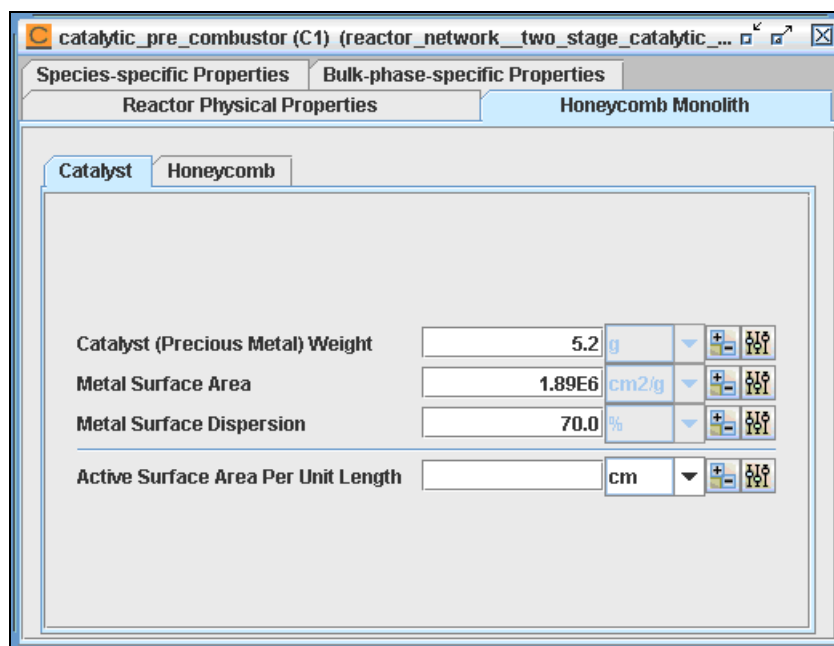
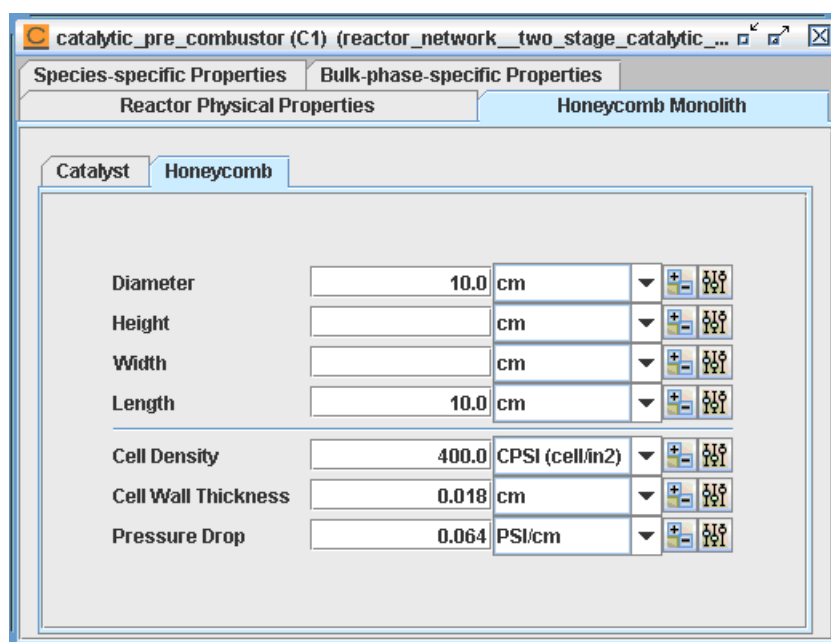
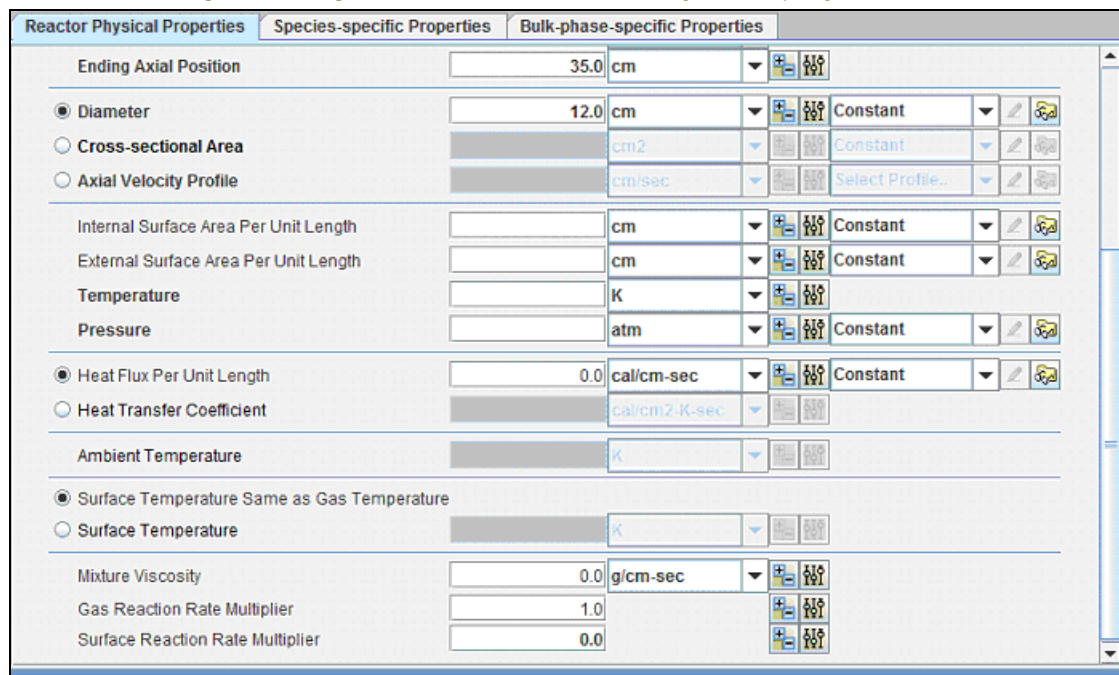


Figure 3-4 Catalytic Pre-combustor (C1_)—Honeycomb Monolith, Honeycomb sub-tab



Since there is no surface reaction in the homogeneous combustor and the post-flame mixer, we need to turn the surface chemistry calculations off in our reactor models. There are several methods to make the models ignore the surface chemistry. Here we choose to set the surface reaction rate multiplier to 0.0, using the parameter at the bottom of the Reactor Physical Property tab as shown in [Figure 3-5](#).

Figure 3-5 Homogeneous Stage Combustor (C3_)—Reactor Physical Property



3.1.1.3 Project Results

We have to run the reactor clusters in order because calculations of later clusters require information from the solution of the previous cluster. After finishing all four cluster runs, we want to see if the predicted mass flow rate and gas temperature at the exit of the last (fourth) reactor cluster match the gas turbine design point targets. The predicted mass flow rate of each combustor system, which is 1/6 of the total mass flow rate, and the turbine rotor inlet temperature can be found from the output file from the last cluster run (see [Figure 3-4](#)).

Figure 3-6 Two Stage Catalytic Combustor—Excess_Air_Dilution (Cluster 4) Output Results

TWOPNT: FINAL SOLUTION:

```

=====
                        PSPRNT: Printing of current solution from TWOPNT:
=====

RESIDENCE TIME                2.0000E-03  SEC
MASS FLOW RATE                1.6344E+02  GM/SEC
PRESSURE                      3.706      ATM
MASS DENSITY                  8.9763E-04  GM/CM^3
VOLUME                       364.2     CM^3
TOTAL MASS                    0.3269    G
TOTAL SURFACE AREA            0.000    CM^2
TOTAL SURFACE TO VOLUME RATIO 0.000    CM-1
GAS CHEM HEAT PRODUCTION     2.4785E-02  CAL/S/CM^3
TEMPERATURE (INLET: C4_Inlet1) 715.0000  K
TEMPERATURE (INLET: homogeneous_stage_combustor_(C3)_to_excess_air_dilution_(C4_R1)) 1604.8328  K
TEMPERATURE                   1431.7571  K
SURF TEMP, CATALYST           1431.7571  K (same as gas temp)
HEAT LOSS, CATALYST           0.000     CAL/SEC
SURF CHEM HEAT PRODUCTION,
CATALYST                      0.0000E+00  CAL/S/CM^2

EXIT    GAS PHASE MOLE FRACTIONS

H2      = 2.4345E-07      H      = 6.4644E-09      O      = 1.2175E-06
O2      = 0.1415        OH     = 4.3863E-05      H2O    = 6.1973E-02
HO2     = 1.7455E-07    H2O2  = 2.1735E-08      C      = 2.7918E-29
CH      = 6.7819E-26    CH2   = 1.8560E-21      CH2(S) = 2.5248E-23
CH3     = 3.7230E-20    CH4   = 8.2935E-20      CO     = 6.7122E-07
CO2     = 3.0997E-02    HCO   = 1.5349E-17      CH2O   = 5.8356E-19
CH2OH   = 4.2927E-24    CH3O  = 1.6348E-23      CH3OH  = 3.0972E-20
C2H     = 1.2566E-22    C2H2  = 1.3749E-17      C2H3   = 5.2738E-26
C2H4    = 4.7943E-25    C2H5  = -4.6945E-30     C2H6   = -3.4532E-28
HCCO    = 1.4424E-21    CH2CO = 1.4861E-18      HCCOH  = 3.2210E-15
N       = 1.6160E-15    NH    = 1.6167E-15      NH2    = 1.1761E-14
NH3     = 1.9500E-13    NNH   = 2.5377E-14      NO     = 2.1761E-07
NO2     = 2.4198E-09    N2O   = 2.8742E-07      HNO    = 5.3606E-14
CN      = 1.0374E-19    HCN   = 3.2462E-14      H2CN   = 1.6896E-23
HCNN    = 8.5484E-28    HCNO  = 3.0537E-12     HOCN   = 7.9801E-13
HNCO    = 1.0132E-12    NCO   = 4.8094E-15     N2     = 0.7655
AR      = 0.000        C3H7  = 9.2007E-37     C3H8   = 1.0914E-37
CH2CHO  = 9.6703E-26    CH3CHO = 3.8498E-28

Volatile Organic Compounds (ppm): 4.9039E-06
Unburned Hydrocarbons      (ppm): 2.7620E-11

CO      (ppmvd) : 0.7156
NO      (ppmvd) : 0.2320
NOx     (ppmvd) : 0.5410
CO      (ppmvd 15% O2) : 0.7256
NO      (ppmvd 15% O2) : 0.2352
NOx     (ppmvd 15% O2) : 0.5486

```

```

SURFACE SITE FRACTIONS IN SURFACE PHASE, PT_SURFACE
Site density = 2.7063E-09 mole/cm^2
Standard State Site density = 2.7063E-09 mole/cm^2
Rate of change of site density = 0.000 mole/(cm^2*sec)

PT(S)      = 9.0909E-02      H(S)      = 9.0909E-02      H2O(S)     = 9.0909E-02
OH(S)      = 9.0909E-02      CO(S)     = 9.0909E-02      CO2(S)    = 9.0909E-02
CH3(S)     = 9.0909E-02      CH2(S)s   = 9.0909E-02      CH(S)     = 9.0909E-02
C(S)       = 9.0909E-02      O(S)      = 9.0909E-02

BULK PHASE MOLE FRACTIONS AND ACTIVITIES IN BULK PHASE, PT_BULK
Linear growth rate of this bulk phase = 0.000 cm/sec
Total growth rate of this bulk phase = 0.000 gm/sec
Density of the bulk phase = -1.000 gm/cm^3
Average molecular weight of bulk phase = 195.1 gm/mole

Species Name  Mole_frac  Activity  Density  -----Growth Rate-----
              (gm/cm^3)  mole/(cm^2*sec)  gm/(cm^2*sec)  cm/sec  (microns/hr)
PT(B)        = 1.000    1.000    -1.000    0.000    0.000    0.000    0.000
=====

```

The predicted mass flow rate for each combustor is 163.4 g/sec so the total mass flow rate is 980.4 g/sec (= 6*163.4). The predicted exit gas temperature, TRIT, is 1432 K. Both values are very close to the targets. Since our goal is a zero-NO_x combustor, we want to find out NO, NO₂, and N₂O emissions from our new combustor. The solution shows the mole fractions of NO, NO₂, and N₂O are 0.22 ppm, 0.003 ppm, and 0.27 ppm, respectively. All these concentrations are below 1 ppm and are not detectable by instruments. Before we can say a job well done, we need to check on CO and UHC (unburned hydrocarbon) emissions as well. Sometimes CO and UHC concentrations increase when we try to minimize NO_x formation. Our model indicates our combustor has sub-ppm CO emission (~0.7 ppm) and essentially no UHC.

We are also interested in knowing how the gas temperature varies inside the combustor system and whether the maximum temperature inside the catalytic combustor exceeds its safe operating temperature. We can use the CHEMKIN Post-Processor to obtain profiles along the two-stage combustor for quick visual confirmation. We only need to load solutions of the first (catalytic combustor) and the third (homogeneous combustor) clusters into the CHEMKIN Post-Processor because the other two clusters yield a single solution point each. The “axial” profiles of gas temperature, pressure, and mole fractions for CH₄, CO and NO are shown in the following figures.

Figure 3-7 Two Stage Catalytic Combustor—Temperature Comparison

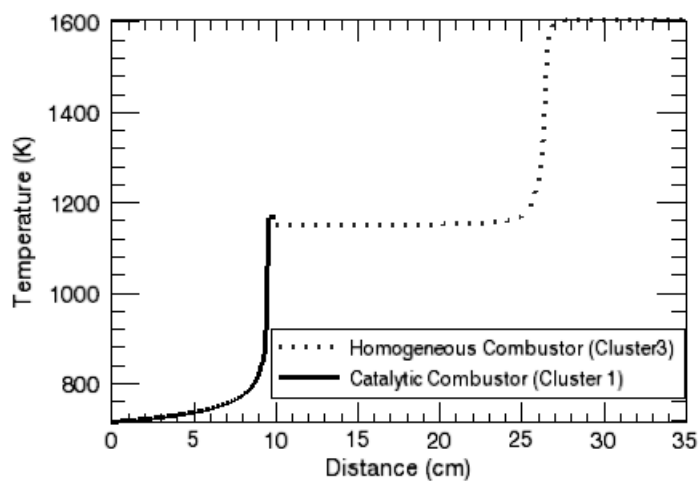


Figure 3-8 Two Stage Catalytic Combustor—Pressure Comparison

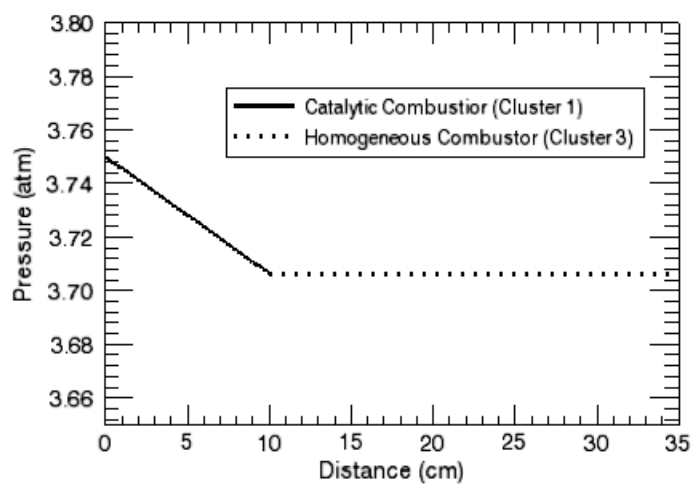


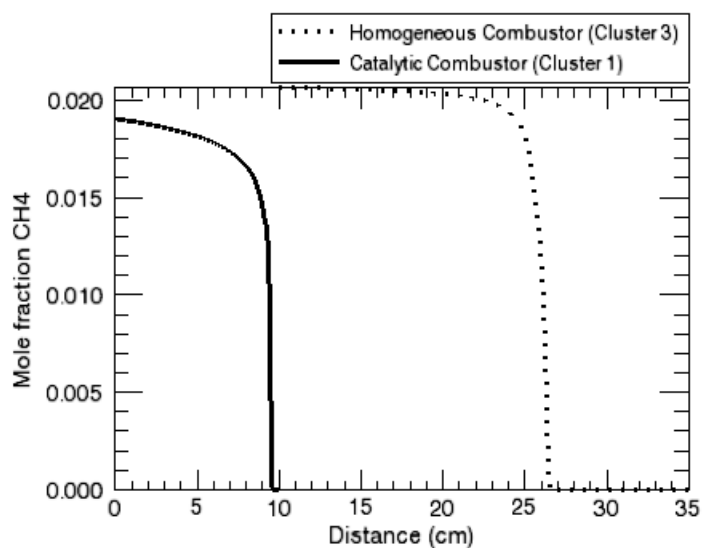
Figure 3-9 Two Stage Catalytic Combustor—CH₄ Comparison

Figure 3-10 Two Stage Catalytic Combustor—CO Comparison

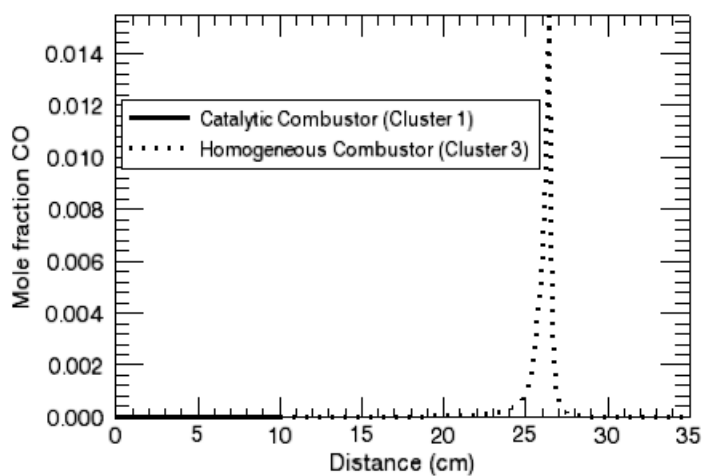
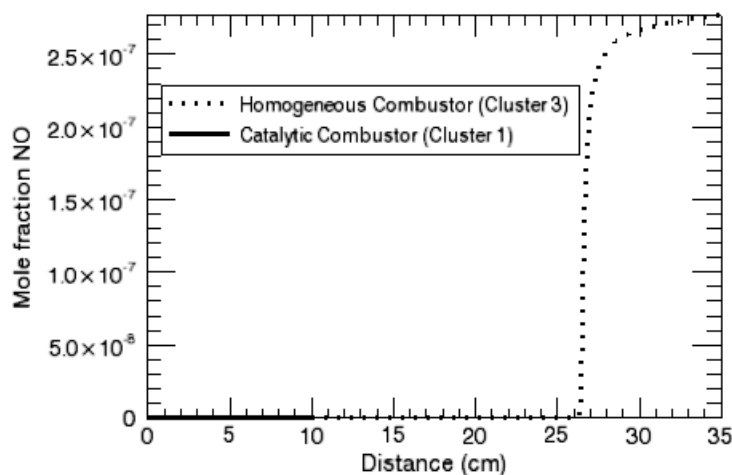


Figure 3-11 Two Stage Catalytic Combustor—NO Comparison



The temperature profile ([Figure 3-7](#)) indicates that the gas temperature is increased in two steps. The catalytic combustor has a lower operating temperature and only raises the gas temperature to about 1100 K. The homogeneous combustor, which can operate at higher temperatures, further raises the gas temperature to more than 1600 K before the excess air cools the gas mixture down to the target TRIT at about 1450 K. The CO profile ([Figure 3-10](#)) has a spike inside the homogeneous combustor corresponding to the gas-phase ignition and all CO generated is later consumed in the post-flame region. The model also predicts that NO_x is formed after gas-phase ignition and, unlike CO, its concentration continues to grow in the post flame region.

Note that this project only addresses the limitation posted by chemical kinetics. Mass transport, i.e., diffusion and turbulence mixing, can become the limiting factor in determining the performance of this gas combustor system. At high pressure, species transport between the bulk gas and the active surface can be the rate-limiting factor for the catalytic combustor. Poor molecular diffusion at high pressure could also affect the homogeneous combustor. When the mixing between injected fuel and oxygen in the hot gas slows down, the ignition distance becomes longer and could even cause flame-out in the homogeneous combustor. The tutorial in [Section 2.6.4](#) addresses some of these issues.

3.1.2 Engine Exhaust Aftertreatment with a Transient Inlet Flow

3.1.2.1 Project Description

This user tutorial demonstrates how you can employ a user-defined subroutine to read in transient engine-out data to set dynamic inlet conditions for an engine-exhaust aftertreatment simulation. In this sample, the engine-out conditions as a function of time are stored in a tab-delimited text file. A user-editable subroutine is provided that

reads the contents of this file and extracts from it the time-dependent inlet composition, temperature, and instantaneous flow rate into a transient perfectly stirred reactor model. The reactor approximates a 3-way catalytic converter, designed to convert NO_x, CO, and un-burned hydrocarbons (UHCs) through catalytic surface reactions on a platinum/rhodium catalyst. For this sample, gas-phase chemistry is neglected due to the dominance of the surface conversion reactions. This sample user routine is already compiled and linked into the standard installation, such that it can be run from the CHEMKIN Interface without the need of a FORTRAN compiler. Modifying the behavior of the sample user routine will require access to an a compatible FORTRAN compiler on the computer where CHEMKIN is installed. With the pre-compiled routine, however, you can change the numerical values of the engine-out data that is read by the user routine.

3.1.2.2 Project Setup

The project file is called *psr_aftertreatment.ckprj*. Catalytic conversions of NO_x, CO, and UHCs are modelled by the Pt/Rh three-way catalyst surface mechanism described in [Section 3.3.2](#). The data files used for this sample are located in the *samples2010\psr\aftertreatment* directory. This reactor diagram contains only one gas inlet and one perfectly-stirred reactor model. The sample user subroutine that is used to define the inlet is provided in the standard CHEMKIN installation location, in the *user_routines* sub-directory. The FORTRAN subroutine is named `USRINLET` and is included in the file *aurora_user_routines.f*. The subroutine is discussed in more detail below.



Before running this sample problem from the CHEMKIN Interface, the Display User Routines box on the General tab of the User Preferences panel must be checked. Open the Preferences panel from the **Edit** menu.

3.1.2.2.1 Reactor and Inlet Settings

On the Reactor Physical Properties tab of the C1_PSR panel, first the problem type is selected as Solve Gas Energy Equation while selecting the Transient Solver. In this case, the reactor volume is the void volume in the converter honeycomb or porous media, estimated here as 1400 cm³ for the entire length of the converter. Similarly, the reactive (internal) surface area within the converter is estimated based on the void geometry to be 59000 cm². No residence time is input because the volume and flow rates are specified. The initial temperature (296.15 K) is input, along with the pressure (1 atm), and the fact that the system is treated as adiabatic (no heat loss).

On the Species-specific Properties tab of the C1_ PSR panel, the initial conditions of the converter system, prior to the exhaust gas flowing through the system, are assumed to be air and are input on the Initial Gas Fraction sub-tab. The surface site fractions are estimated based on understanding of the surface conditions or on initial tests of the mechanism. A user-supplied initial guess can sometimes aid convergence; if it is not specified CHEMKIN will assume a uniform distribution of sites. In this case, we specify O(S) as the dominant site at the start for the platinum portion of the catalyst and CO(S1) for the rhodium portion. These site species are set to 1.0 on the Surface Fraction sub-tab to provide the initial conditions for the catalyst surface.

The gas inlet has been given a name that reflects its function, **engineout**. On the Stream Properties Data tab of the engineout panel, the Use Inlet User Routine option is selected, which indicates that information about the gas inlet composition, flow rate and temperatures should be obtained from the user inlet routine. The user routine pre-packaged with CHEMKIN reads a text file. The name of this file, **engineout.txt**, is set in the FORTRAN subroutine. The inlet conditions, some of which are shown in [Table 3-1](#), are representative of measurements that might be taken during an engine test, where engine load and therefore exhaust flow rates and composition vary as a function of time. In this case, mole fractions for only a few species are provided (CO, NO, UHCs, and O₂). We will assume that the balance of the gas can be represented by N₂ and that C₃H₆ will chemically represent the UHCs. On this panel, the **Use SCCM for User Inlet Routine** box is also checked to indicate that flow rates are given in volumetric flow units, rather than mass flow units.

On the Basic tab of the Solver panel, the end time of the simulation is set to 100 sec. Although the input data file extends to longer times, this is sufficient for this demonstration. The maximum Solver Time Step is set to 1 msec, the Time Interval for Printing the solution to the text output file is set to 10 sec, and the Time Interval for Saving Data is set to 1 sec. There are no inputs on the Output Control or Continuations panels for this problem.

Table 3-1 Excerpt of Data Representing Engine-out Test Measurements

<i>Time(s)</i>	<i>InletT(C)</i>	<i>Flow(SLM)</i>	<i>C_{3xx}(ppm)</i>	<i>CO(ppm)</i>	<i>CO₂(ppm)</i>	<i>NO_x(ppm)</i>	<i>O₂(ppm)</i>
0	23.9	87.08	924	4341	22764	38	127856
0.5	25	85.49	1238	23557	49535	127	77187
1	20.1	27.15	1369	36212	66499	126	50914
1.5	22.6	81.89	1267	37984	80793	118	28314
2	39.1	81.2	1176	29212	95735	92	14359

Table 3-1 Excerpt of Data Representing Engine-out Test Measurements (Continued)

<i>Time(s)</i>	<i>InletT(C)</i>	<i>Flow(SLM)</i>	<i>C_{3xx}(ppm)</i>	<i>CO(ppm)</i>	<i>CO₂(ppm)</i>	<i>NO_x(ppm)</i>	<i>O₂(ppm)</i>
2.5	66.2	83.17	1016	18119	104492	89	9577
3	88.2	86	999	10391	110148	108	7744
3.5	111.3	87.08	912	5786	111276	101	13012
4	125.4	85.42	877	3663	112346	111	8645
4.5	141.2	82.53	843	2532	111864	104	11867
5	163	81.1	808	1967	111803	110	16508
5.5	175.2	82.43	681	1619	111685	101	12255
6	189.8	85.28	756	2224	110433	119	15728
6.5	208.9	87.06	825	6022	108765	207	7865
7	218.2	86.12	825	11532	107414	366	12835
7.5	230.6	83.34	732	9837	105707	440	20696
8	244.3	81.27	857	5259	102752	446	24211
8.5	251.6	193	957	2823	100132	381	28629
9	272.1	374.28	991	2942	99228	354	28534
9.5	297.4	479.67	864	2355	101356	331	28906
10	313.6	483.61	851	1514	103822	309	29511
10.5	333.2	431.87	796	1343	105570	276	23807
11	347	388.16	788	1251	106826	241	26600
11.5	349.6	344.94	868	910	106112	207	26409

3.1.2.2.2 Details of the User Routine

The subroutine for the user-defined inlet is reproduced in [Figure 3-12](#). The data in [Table 3-1](#) has units of parts-per-million for species composition, standard liters per minute for flow rate, and degrees Celsius for temperature, which are not the standard units used by the CHEMKIN software. The user routine must therefore perform necessary conversions before providing the data to the PSR program executable. It is also responsible for interpolating between data points for each time value needed during the time integration. At each time step during the transient simulation, the PSR program will call `USRINLET`. Parameters needed by the `USRINLET` subroutine are passed in through integer and real workspace arrays called `IINWRK` and `RINWRK`, respectively. The comments at the top of the code explain what parameters are stored in these arrays.

The sample `USRINLET` code in [Figure 3-12](#) reads in data from a file on the first call, as determined when the time is equal to the starting time of the simulation. In this section, the routine uses the CHEMKIN library routine `CKCOMP` to find the location of a given species name in the gas-phase species array (`KNAMES`). Conversion from Celsius to Kelvin and from parts-per-million to mole fraction are performed as the data is read and stored on the first call. On subsequent calls, the data is accessed from memory (stored in a FORTRAN common block), and values are interpolated for the specified simulation time. The interpolation uses the CHEMKIN GAS-PHASE KINETICS library routine `CKBSEC` to linearly interpolate between the data points. Before returning, the routine converts the flow rate from standard liters per minute (slm) to standard cubic centimeters per minute (sccm). Note that the routine could have been written to return mass flow rate in units of g/sec. In this case, however, CHEMKIN Interface inputs tell the program to expect user-defined flow rates in units of sccm.

Figure 3-12 Sample USRINLET Subroutine for User-Defined Transient Inlet Conditions

```

      SUBROUTINE USRINLET (LIUIN, IINWRK, LRUIN, RINWRK, INAME, KNAMES,
      1 FLRT, TINL, TEIN, XIN)
!DEC$ IF DEFINED (DLLEXPORT)
!DEC$ ATTRIBUTES DLLEXPORT :: USRINLET
!DEC$ ENDIF
C This is a USER SUBROUTINE for defining Inlet properties
C as an arbitrary function of time.
C Use of this subroutine is controlled by the PSR program
C keyword, USRIN, as described in the CHEMKIN Input Manual.
C
C The subroutine USRINLET is used to supply values of
C   FLRT - Real scalar, Mass flow rate in g/s
C           (or if SCCM are the preferred units,
C           use keyword LFPSC in addition to USRIN)
C   TINL - Real scalar, Inlet temperature (K)
C   TEIN - Real scalar, Inlet electron temperature (K)
C   XIN(*) - Real array, Gas-phase reactant composition of
C            the inlet (mole fraction);
C            The length of this array is *exactly* KKGAS,
C            the number of gas-phase species in the problem.
C and the user may set the Integer flag
C   IINWRK(1) - if 0, inlet parameter setting was successful,
C               else, there was a problem, so discontinue calculations
C
C Given the following data:
C
C   LIUIN - Integer scalar, length of some Integer workspace
C   IINWRK(*) - Integer workspace array, containing
C   IINWRK(2), LOUT - if positive, the unit number of an open output file
C   IINWRK(3), IPSR - PSR index number
C   IINWRK(4), IINL - Index number of an Inlet of IPSR
C   IINWRK(5), KKGAS- Gas-phase species count
C   IINWRK(6), LENRGY-If 0, then inlet temperature TINL is fixed,
C               else TINL must be supplied here
C   IINWRK(7), LENRGE-If 0, then inlet electron temperature TEIN is fixed,
C               else TEIN must be supplied here
C
C   LRUIN - Integer scalar, length of some Real workspace
C   RINWRK(*) - Real workspace array, containing
C   RINWRK(1), TSTART - Initial time (sec.) of calculation
C   RINWRK(2), TIM - Current time (sec.)
C
C   INAME - Character-string Inlet name
C   KNAMES- Character-string array, Gas-phase species names
C*****
IMPLICIT DOUBLE PRECISION (A-H, O-Z), INTEGER (I-N)
include 'user_routines_interface.inc'
PARAMETER (PATM = 1.01325D6, TSTD=273.15, ZERO=0.0D0)
C Variables passed in from calling routine
DIMENSION IINWRK(LIUIN), RINWRK(LRUIN)
CHARACTER*16 INAME, KNAMES(*)
C Arrays returned by this user routine
DIMENSION XIN(*)
C Local variables:
CHARACTER*80 MYFILE
PARAMETER (MYFILE = 'engineout.txt', LUNIT=33,
      1 MXPTS=10000, MXSPEC=6)
C Local storage space for variables
CHARACTER*16 MYSPEC(MXSPEC)
CHARACTER*80 HEADER
LOGICAL LENRGY, LENRGE
DIMENSION PPM(MXSPEC)
COMMON/USRINL1/ MAPSP(MXSPEC), NPTS
COMMON/USRINL2/ TIMEPT(MXPTS), SLMPT(MXPTS), XINPT(MXPTS, MXSPEC),
      1 TPT(MXPTS)
EXTERNAL CKUFIRST
SAVE IFIRST
DATA IFIRST/0/
C
C set error flag
IINWRK(1) = 0
C set local variables from workspace data provided
LOUT = IINWRK(2)
C acknowledge that USRINLET has been applied
IF (IFIRST .EQ. 0) CALL CKUFIRST (IFIRST, LOUT, 'USRINLET')
C

```

```

IPSR = IINWRK(3)
IINL = IINWRK(4)
KKGAS= IINWRK(5)
LENRGY=IINWRK(6).GT.0
LENRGE=IINWRK(7).GT.0
C
TSTART=RINWRK(1)
TIME  =RINWRK(2)
C
C Initialize returned variables
FLRT = 0.0
TINL = 298.D0
TEIN = 298.D0
DO K = 1, KKGAS
  XIN(K) = 0.0D0
ENDDO
C
C First time in, read in all the points so we don't have to do
C IO on each call. Interpolate from saved points thereafter
C IF (TIME .EQ. TSTART) THEN
C   Open and read the time-date file
C   Store points in arrays for access/interpolation at later times
C   IOS = 0
C   OPEN(LUNIT, FILE=MYFILE, FORM='FORMATTED', STATUS='OLD',
1     IOSTAT=IOS)
C   Check that file open was successful, if not return with error
C   IF (IOS .NE. 0) GO TO 1000
C
C   Map input species to CHEMKIN names and find indices
C   MYSPEC(1) = 'C3H6'
C   MYSPEC(2) = 'CO'
C   MYSPEC(3) = 'CO2'
C   MYSPEC(4) = 'NO'
C   MYSPEC(5) = 'O2'
C   MYSPEC(6) = 'N2'
C   DO MYK = 1, MXSPEC
C     CALL CKCOMP(MYSPEC(MYK),KNAMES,KKGAS,INDX)
C     IF (INDX .GT. 0 .AND. INDX .LE. KKGAS) THEN
C       MAPSP(MYK) = INDX
C     ENDIF
C   ENDDO
C   Read in the arrays of available information
C   In this case file format is as follows:
C   Time (s), T(C), Flrt (SLM), C3H6 (ppm), CO (ppm), CO2 (ppm), NO (ppm), O2 (ppm)
C   READ(LUNIT, '(A)', END=800, ERR=1000) HEADER
C   NPTS = 0
C   DO I = 1, MXPTS
C     READ(LUNIT, *, END=800, ERR=1000)
1     TIMEPT(I), TCELS, SLM, (PPM(K), K=1, MXSPEC-1)
C     NPTS = NPTS + 1
C     TPT(I) = TCELS + 273.15D0
C     SLMPT(I) = SLM
C     XSUM = 0.0D0
C     DO MYK = 1, MXSPEC-1
C       XINPT(I,MYK) = PPM(MYK) * 1.D-6
C       XSUM = XSUM + XINPT(I,MYK)
C     ENDDO
C     Set fraction of N2 = 1 minus the sum of others
C     XREM = 1.0D0-XSUM
C     XINPT(I, MXSPEC) = MAX(XREM, ZERO)
C     Note: if XSUM > 0.0, AURORA will normalize so that sum = 1
C   ENDDO
800  CONTINUE
C   IF (NPTS .EQ. 0) GO TO 1000
C   CLOSE(LUNIT)
C ENDIF
C
C Interpolate data for input time and perform units conversions
C XSUM = 0.0
C DO MYK = 1, MXSPEC-1
C   XIN(MAPSP(MYK)) = CKBSEC(NPTS, TIME, TIMEPT, XINPT(1, MYK))
C   XSUM = XSUM + XIN(MAPSP(MYK))
C ENDDO
C XREM = 1.0-XSUM
C XIN(MAPSP(MXSPEC)) = MAX(XREM, ZERO)
C SLM = CKBSEC(NPTS, TIME, TIMEPT, SLMPT)
C Convert from SLM to SCCM
C FLRT = SLM * 1000.D0
C IF (LENRGY) THEN
C   Set the gas inlet temperature
C   TINL = CKBSEC(NPTS, TIME, TIMEPT, TPT)

```

```

        ENDIF
        IF (LENRGE) THEN
C      Set the electron inlet temperature
          TEIN = TINL
        ENDIF
        RETURN
C
1000 CONTINUE
        IF (IOS .NE. 0) THEN
          WRITE (LOUT, *) ' ERROR...OPEN failure on inlet data file'
          CALL CKWARN(2)
        ELSE
          WRITE (LOUT, *) ' ERROR...READ failure on inlet data file'
          CALL CKWARN(2)
          CLOSE (LUNIT)
        ENDIF
        IINWRK(1) = 1
C
        RETURN
      END

```

3.1.2.3

Project Results

[Figure 3-13](#) shows molar conversions for C_3H_6 , CO, NO as a function of time. Note that "molar conversion" variables must be selected on the Select Post-Processing Variables panel in order for molar conversion variables to be available for plotting. The effectiveness of conversion can also be viewed by comparing the inlet mole fraction to the outlet mole fractions, as shown in [Figure 3-14](#) for C_3H_6 or by looking at the calculated conversion efficiencies directly. These figures clearly show that C_3H_6 and CO are converted more effectively than NO under these conditions. Early in the simulation, the conversion rates are low for all of these species. Although at $t = 0$, the calculated molar conversion is 100%, this is simply due to setting the initial conditions in the reactor to pure air, which determines the initial exit flow. At certain times the calculated conversion rates for CO and NO actually go negative. This results from the fact that CO and NO can be formed on the surface and thus can be "produced" as the state of the surface changes. [Figure 3-15](#) shows inlet and exit gas temperatures as a function of time. Temperatures show that the gas heats up relative to the inlet gas due to exothermic surface reactions. The catalyst does not become effective until it reaches a temperature above about 600 K, which is consistent with the work reported by Chatterjee et al.⁴²

42. D. Chatterjee, O. Deutschmann and J. Warnatz, "Detailed Surface Reaction Mechanism in a Three-way Catalyst," *Faraday Discussions*, **119**:371-384 (2001).

Figure 3-13 Engine Exhaust Aftertreatment—Molar Conversion Rates

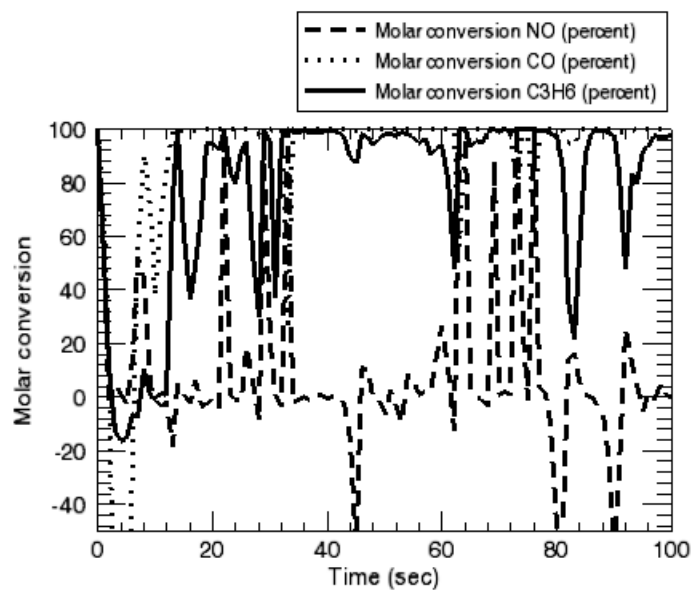


Figure 3-14 Engine Exhaust Aftertreatment—Mole Fractions

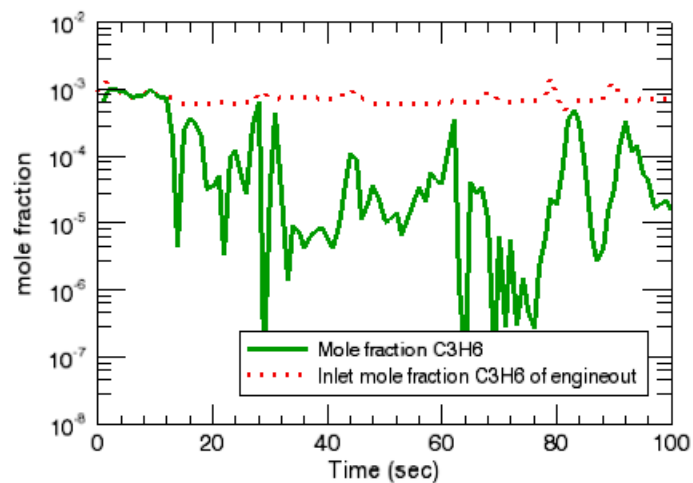
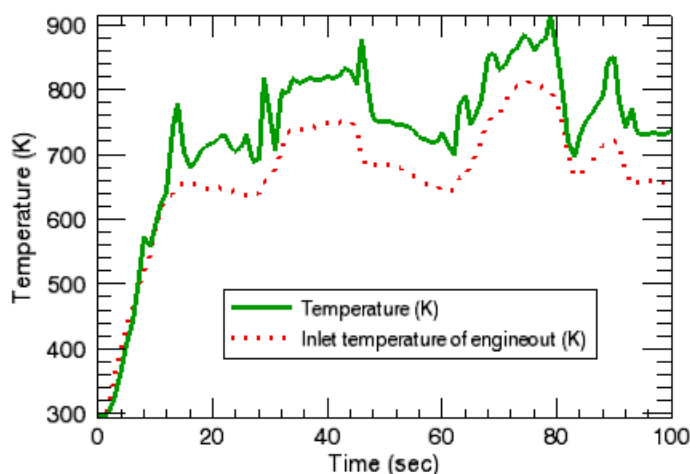


Figure 3-15 Engine Exhaust Aftertreatment—Gas Temperatures



3.2 Parameter Studies

3.2.1 Parameter Study Facility for Surface Chemistry Analysis

The science of surface chemistry has undergone rapid development in recent years, and there is a trend towards use of more detailed “microkinetic” models, especially in the field of catalysis. However, compared with gas-phase combustion problems, surface reaction mechanisms often contain larger uncertainties in reaction-rate coefficients that must often be estimated by semi-empirical methods. For this reason, and because there are variabilities in the catalyst properties, it is often necessary to adjust kinetic parameters to model a specific catalytic system. Thus it is of interest to see how uncertainties that exist in surface mechanisms affect predicted modeling results. Performing a parameter study, which varies reaction-rate parameters for key reactions in the system, is one way to analyze these effects.

In this tutorial, we apply a parameter study to investigate the effects of one reaction rate coefficient for a simulation involving catalytic oxidation of methane on a platinum catalyst. The associated project file is called

honeycomb_monolith_reaction_rate_param_study.ckprj. The chemistry-set files used for this sample problem are located in the

honeycomb_monolith/reaction_rate_param_study folder of your CHEMKIN ***samples2010*** directory. For the gas-phase kinetics, we employ the GRI gas-phase mechanism and thermodynamic data for methane combustion. For the catalytic surface-chemistry that describes the oxidation of methane on a platinum catalyst, we

use the surface chemistry mechanism reported by Chou, et al.⁴³ In this example's reactor model, we focus on the first stage (Honeycomb Catalytic Reactor) of the Two-stage Catalytic Combustor Sample (*reactor_network_two_stage_catalytic_combustor.ckprj*).

3.2.1.1 Determining Influential Reactions with Sensitivity Analysis

We first intend to study those surface reactions that will be the most influential to our output parameters of interest for the conditions in this sample. Since this is a catalytic combustion case, where the catalytic stage serves to preheat the gas, the reactor temperature is of interest. We therefore first run a sensitivity analysis in order to determine the sensitivity of Temperature to the Arrhenius pre-exponential factors (A-factors) of the various reaction-rate constants. In order to accomplish this, first open the *honeycomb_monolith_reaction_rate_param_study* project and pre-process the chemistry set. Then look at the nominal case, which is set up in the Reactor and Inlet panels and which can be run from the Run Calculations node on the project tree.

Follow the steps below to run the sensitivity analysis.

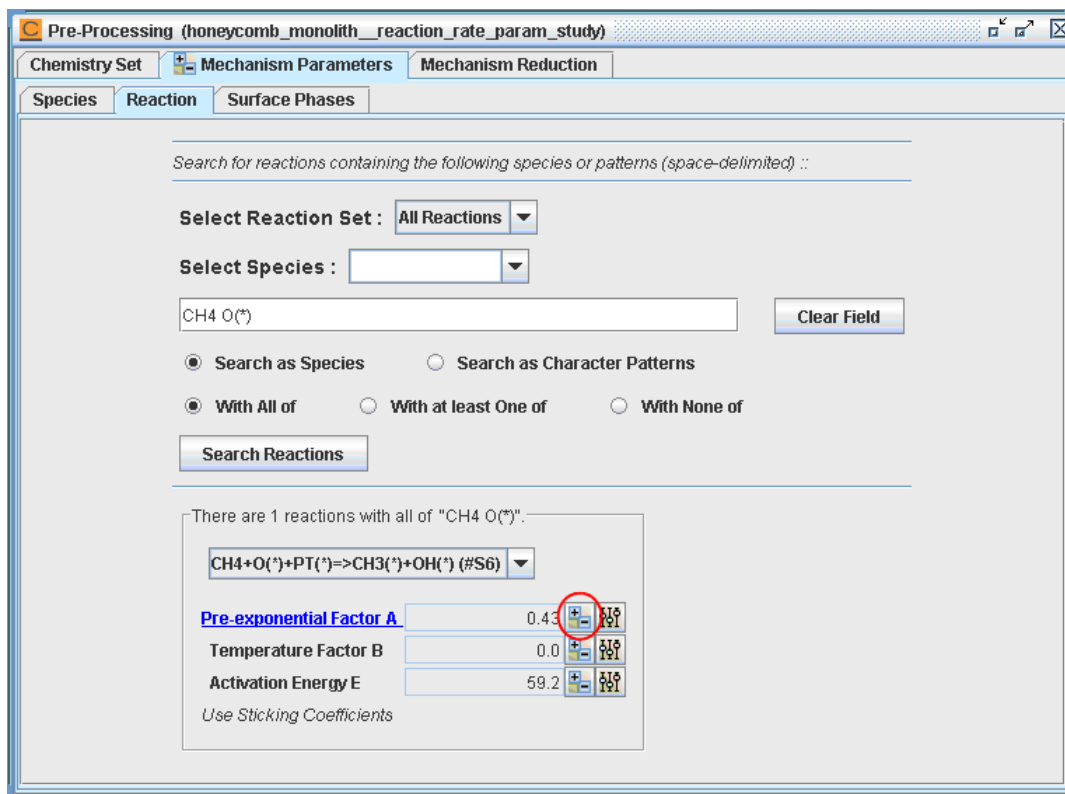
1. Double-click on the Output Control in the Open Projects tree.
2. On the Output Control tab's Basic sub-tab, select **Temperature A-factor Sensitivity**.
3. Open the Run Calculations panel, notice that Parameter Study is selected, and click the **Begin** button.
4. Answer the prompt about number of parallel runs and click **OK**. Note that the number of runs for parallel can be changed later by editing the user Preferences (see [Getting Started with CHEMKIN](#)).
5. Once the Parameter Study has completed successfully, the Analyze Results panel displays. Select to Plot Results and click the **Next Step** button.
6. In the Post-Processor control panel, set **Plot Type** to **Line Plot** and use the pull-down menu to select **File_1: Honeycomb MonolithC1:sensitivity for solution no 1**.
7. Select **Distance** for the X Variable and select as Y Variables all of the surface reaction sensitivities that are listed. (To select multiple variables, hold down the Ctrl key while clicking each variable.)
8. Click on **Display Plot**.

43. C.-P. Chou, J.-Y. Chen, G. H. Evans and W. S. Winters, *Combustion Science and Technology*, **150**:27 (2000).

From the plot results, you should see that Surface reactions #1, ($\text{O}_2 + 2\text{PT}^* \rightarrow \text{O}^* + \text{O}^*$) and #6, ($\text{CH}_4 + \text{O}^* + \text{PT}^* \rightarrow \text{CH}_3^* + \text{OH}^*$), are particularly important in determining the resulting temperature. In the case of both of these reactions, the A-factors are actually sticking coefficients as indicated by the keyword `STICK` in the surface-chemistry file.

It is now of interest to vary the sticking coefficients for these rates one by one, and see how such variations will affect predicted temperature profiles in the reactor. A Parameter Study has already been set up to do this in the **honeycomb_monolith_reaction_rate_param_study** project. To see how this is done, go to the Mechanism Parameters tab in the Pre-processing panel. On the Reaction sub-tab, select COMBUST (which is the name of our surface material, so we're selecting reactions related to this material only) from the pull-down menu of the Select Reaction Set and click on the Search Reactions button. The results are reported in the drop-down list at the bottom of the panel. The first reaction to show up in the pull-down window under the **Search Reactions** button is highlighted in blue, indicating that a parameter study has been set up for this reaction rate constant. Click on the **Setup Parameter Study** button next to the **Pre-exponential Factor A** value for this reaction to view the Parameter Study Setup, as shown in [Figure 3-16](#).

Figure 3-16 Setting Up a Parameter Study for Sticking Coefficients vs. Predicted Temperature Profiles

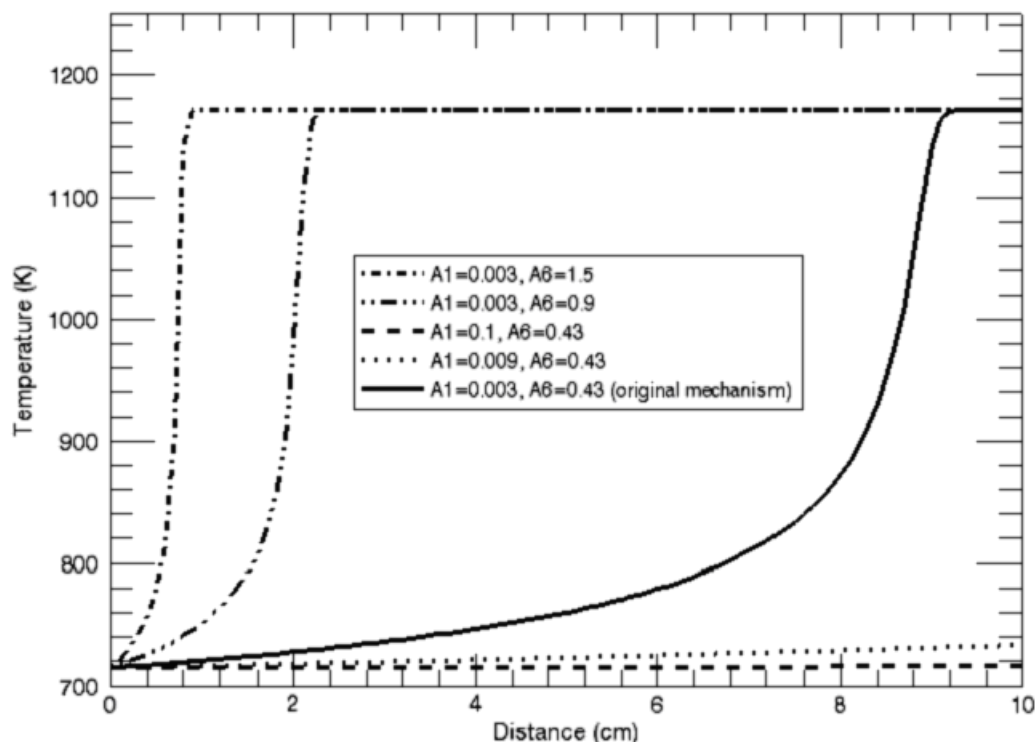


3.2.1.2 Viewing Results with the Post-Processor

Run the Parameter Study by selecting all of the runs in the Run Parameter Study window and clicking the **Post-Process** button. Once in the Post-Processor control panel, select **Line Plot** for **Plot Type**. Under **Plot Set**, select **Solution no 1**. Ctrl-click all of the temperature profiles for each of the Parameter Study runs as the **Y Variables**. Click on **Display Plot**.

Figure 3-17 demonstrates the results of the Parameter Study displayed by the CHEMKIN Post-Processor. The results clearly indicate that if we keep the sticking coefficient of reaction 1 constant, and increase the sticking coefficient for reaction 6, the ignition occurs much sooner and the maximum combustion temperature is reached almost as soon as the reactants enter the catalytic reactor. This makes sense, because reaction 6, $\text{CH}_4 + \text{O}^* + \text{PT}^* \rightarrow \text{CH}_3^* + \text{OH}^*$, is a branching reaction that liberates radicals CH_3 and OH , thus rapidly increasing the radical pool that in turn is responsible for catalytic light-off. On the other hand, increasing the sticking probability of the $\text{O}_2 + 2\text{PT}^* \rightarrow \text{O}^* + \text{O}^*$ reaction delays ignition probably because it is competing with the adsorption of CH_4 on open sites.

Figure 3-17 Varying Rate Constants of Reactions 1 and 6.



3.3 Chemistry Sets

In this section, we discuss briefly the chemistry sets used in [Chapter 3](#) and provide references for further study.

3.3.1 Methane Oxidation on Pt

Two projects in this chapter involve methane oxidation on a platinum surface. This demonstrates that the gas-phase mechanism does not need to align to a particular surface mechanism by implementing two different surface mechanisms to describe the same surface process – methane oxidation on a platinum (Pt) surface.

The chemistry set of the two-stage catalytic combustor project ([Section 3.1.1](#)) uses a slightly altered version of the surface mechanism published by Deutschmann et al.⁴¹ (see p. 183) in 1996 and put into CHEMKIN format by L. Raja. A different surface mechanism developed by Chou et al.⁴³ (see p. 201) in 2000 is employed by the Parameter Study Facility for the surface chemistry analysis project ([Section 3.2.1](#)).

If gas-phase reactions are expected to be important, any reaction mechanism describing the gas-phase kinetics for methane oxidation chemistry can be used, but Pt needs to be added to the element list. In both projects, an altered version of the GRMech 3.0 is provided as an example. In the case of a simulation where it is known that gas-phase chemistry is not important, a simple gas-phase chemistry input file can be used that only defines the elements and species that are included in the SURFACE KINETICS input file.

The SURFACE KINETICS input file for Duetschmann's mechanism describes chemistry occurring on one material called CATALYST that has one site type called PT_SURFACE. The PT(B) bulk material is defined, but does not participate in any reactions, as neither etching or deposition of platinum occurs in this system. The surface site can be occupied by any of 11 surface species, where PT(S) is the open platinum site, and the other surface species represent H, C or O atoms, CO, CO₂ or H₂O molecules, OH, CH₃, CH₂, or CH radicals adsorbed on the platinum surface atom. Note that GRMech has already used the symbol CH₂(S) to represent gas-phase methylene radicals in the singlet electronic state, such that adsorbed methylene radicals have been given the symbol CH₂(S)s. Thermochemical data for surface species are included in the surface kinetics input file, and have been defined using PT(S) as the reference point. There are 22 surface reactions, some reversible and some irreversible. These reactions include simple and dissociative adsorption

reactions, as well as simple and associative desorption reactions, plus reactions between adsorbed species. Some reactions are described in terms of sticking coefficients, a few reactions have reaction-order overrides, and in two cases, the activation energy for an adsorption reaction varies with surface coverage.

The surface mechanism published by Chou et al. in 2000 describes the oxidation of methane on the surface of a supported platinum catalyst under fuel-lean conditions. The surface reactions take place on the PT_POLY surface phase (site type) of the material. Bulk species PT(B) and surface species PT(*) represent the platinum atom covered by a surface species and the bare surface platinum atom (or open surface site), respectively. There are 9 other surface species that can exist on the platinum surface (H, C, O, CO, H₂O, OH, CH₃, CH₂, and CH), and their thermodynamic data are provided in the SURFACE KINETICS input file. Since definitions of these surface species (given as part of their thermochemical data) do not contain a platinum atom, the PT(B) bulk species in Chou's mechanism must participate in some of the surface reactions so that these reactions are balanced. The conservation of platinum atom is important because, as a catalyst, platinum should not be created or consumed by the surface reactions. Chou's surface mechanism consists of 23 irreversible reactions. These reactions describe simple and dissociative adsorption of reactants, simple and associative desorption of products, and reactions between adsorbed species. Some adsorption rates are given in terms of sticking coefficients.

3.3.2 Pt/Rh Three-way Catalyst

This chemistry set describes several processes that occur on a platinum/rhodium “three-way” catalyst. These processes are: the oxidation of unburned bicarbonates (represented by C₃H₆) on Pt, the reduction of NO on Pt, the reduction of NO on Rh, and the oxidation of CO on Rh. This reaction mechanism is based on the published work of Chatterjee, *et al.*⁴⁴ in 2001. This reaction mechanism was developed for a surface made of 75% Pt and 25% Rh, and should be considered valid only for this composition. In particular, the coverage dependent activation energies have been scaled for that Pt/Rh ratio.

Gas-phase kinetics is ignored in this chemistry set. The GAS-PHASE KINETICS input file, therefore, includes 6 elements: O, H, C, N, Rh and Pt; 9 species: O₂, C₃H₆, H₂, H₂O, CO₂, CO, NO, NO₂, and N₂; and no reactions.

44. D. Chatterjee, O. Deutschmann and J. Warnatz, “Detailed Surface Reaction Mechanism in a Three-way Catalyst”, *Faraday Discussions*, **119**:371-384 (2001).

The SURFACE KINETICS input file describes chemistry occurring on one material called 3WAYCATALYST that has two site types each representing one of the metals, called PLATINUM and RHODIUM. The PLATINUM site can be occupied by any of 18 surface species, of which Pt(S) is the open site, and one of which, the C3H6(S) species, occupies two sites. The RHODIUM site has simpler chemistry with only 5 surface species, of which Rh(S1) is the open site. Thermochemical data are provided for some of the surface species, but others have placeholder values. All surface reactions are irreversible, such that none of the thermochemical data are used to obtain rates for reverse reactions. The PLATINUM site in this reaction mechanism has a site density of $2.04\text{E-}9$ moles \cdot cm⁻², which is close to the number of $2.717\text{E-}9$ moles \cdot cm⁻² that is obtained from the density and molecular weight of solid platinum. This indicates that the creators of this mechanism chose to describe some of the effects of the high-surface-area nature of the catalyst material by increasing the site density, rather than by increasing the effective surface area for chemistry. This aspect should be kept in mind in applying this mechanism to other systems.

The oxidation of C₃H₆ (or UHCs) on platinum is described in 47 irreversible reactions that include simple and dissociative adsorptions, simple and associative desorptions, plus reactions between adsorbed species. The latter include decomposition of adsorbed hydrocarbon species by hydrogen transfer to Pt(S) species, as well as various oxidation reactions for adsorbed hydrocarbon species ranging from a global description of C3H5(S) oxidation to more step-wise oxidation reactions for other hydrocarbon fragments. NO reduction on platinum is described in 5 reactions, while NO reduction and CO oxidation on rhodium are described in another 9 reactions, each involving adsorptions, desorptions and reactions among adsorbed species. Some reactions are described in terms of sticking coefficients, a few reactions have reaction-order overrides, and in several cases, the activation energy for a reaction varies quite strongly with the extent of coverage of the surface by one or more species.

4 Materials Problems

4.1 Chemical Vapor Deposition

A number of CHEMKIN Reactor Models can be used for CVD simulations. Thermal CVD processes generally involve furnaces or heated surfaces. Simulations of CVD processes, therefore, often treat the temperature of the reactor or deposition surfaces a fixed, experimentally determined input parameter, rather than a quantity that is obtained by solving an energy equation. The surface temperature is usually assumed to be equal to the temperature of the adjacent gas, except for processes performed at very low pressures. Many CVD processes also have fairly long run times compared with startup and end-of-process transients, such that a steady-state simulation is often a good representation of a CVD process.

Generally, a low-dimensional simulation, such as an Equilibrium calculation or a PSR simulation, will be used to assess the chemistry, and possibly to simplify a reaction mechanism before using it in higher-dimensional simulations. A multiple-phase equilibrium calculation can be used to determine the maximum possible deposition rate for a certain gas mixture, pressure and temperature. In a PSR simulation of a CVD process, the assumption is made that the chemical kinetics are rate limiting rather than mass transport effects or the inlet reagent supply rate. Higher dimensional simulations allow evaluation of the relative effects of chemical kinetics and mass transport. The reactor models in the CHEMKIN software can be used to simulate a number of reactor geometries used for CVD. The Plug Flow Reactor and Cylindrical Shear Flow Reactor Models can be used to model tube-furnace CVD systems, while the Planar Shear Flow Reactor can be used to model horizontal flow CVD systems. The Stagnation Flow Reactor Model can simulate a vertical showerhead system, while the Rotating Disk Reactor Model is for reactors in which high-speed rotation of the plate dominates the gas flow field. There are also specialized models for the thermal analysis and modeling of the multi-wafer batch low-pressure CVD furnaces used in the fabrication of microelectronic devices.

4.1.1 Equilibrium Analysis of Chlorosilane CVD

4.1.1.1 Project Description

This user tutorial presents a multi-phase equilibrium calculation of the Si-Cl-H system. A constant pressure and temperature equilibrium calculation gives the maximum amount of solid product that could be formed in the absence of kinetic or transport limitations. This can be a valuable screening tool in choosing operating conditions for a CVD process. In this case, adding HCl to a mixture of SiCl_3H , H_2 , and solid silicon alters the Si/Cl ratio in the system enough to change the equilibrium composition from one that would result in deposition of more solid Si, to one that would result in etching.

4.1.1.2 Project Setup

The project file is called ***equilibrium__siclh_cvd.ckprj***. The data files used for this sample are located in the ***samples2010\equilibrium\siclh_cvd*** directory. This diagram contains only one Equilibrium calculator.

The equilibrium calculation only needs a list of species with their thermodynamic data; a reaction list is not needed. It is important to include all likely radical species as well as the desired and undesired product species in the calculation. It is generally better to include some unimportant species than to leave out ones that turns out to be important. The *chem.inp* file includes 3 elements and 22 gas-phase species and no reactions. This file contains more species than the trichlorosilane CVD chemistry set described in [Section 4.4.3](#). In the interest of completeness, a number of species such as SiH_4 or atomic Cl were added that are not expected to be important at standard CVD conditions, but that might be more important under different conditions. The *surf.inp* file includes only solid silicon in the bulk (condensed) phase.

Setting up this problem first involves the C1_ Equilibrium panel. The problem type, temperature (1400 K) and pressure (1 atm) are entered on the Reactor Physical Property tab. The starting composition is entered on the Reactant Species tab. Starting with a molecular mixture will give the same equilibrium composition as starting with elemental Si, H, and Cl with the same Si/Cl and H/Cl ratios. The Continuations panel is used to specify three additional simulations where increasing amounts of HCl are added, replacing some of the hydrogen carrier gas. All components of the starting mixture have been re-entered, because the composition must be entered as a set.

4.1.1.3 Project Results

Figure 4-1 shows the initial and equilibrium amounts of solid silicon for an initial mixture of 10% (by volume) SiCl_3H in hydrogen with increasing amounts of HCl at 1 atm total pressure and 1400 K. With no added HCl, the equilibrium mole fraction of solid silicon is larger than the initial amount, indicating that this gas mixture is likely to result in the deposition of silicon. As the HCl content increases, the mole fraction of Si(B) expected at chemical equilibrium decreases below the initial mole fraction. This initial gas mixture is thus expected to result in etching, rather than deposition of Si under these conditions. This primarily results from the decreasing Si/Cl ratio in the system. As shown in *Figure 4-2*, the most prevalent gas-phase species at equilibrium are the hydrogen carrier gas and various chlorinated silicon species. Increasing the relative amount of Cl in the system favors the formation of these gas-phase species.

Figure 4-1 Chlorosilane CVD—Equilibrium Calculations

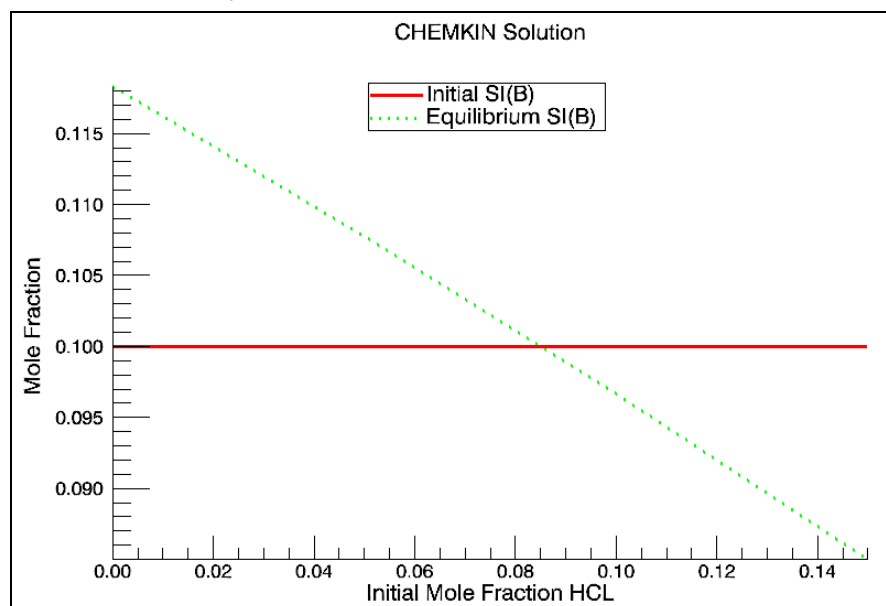
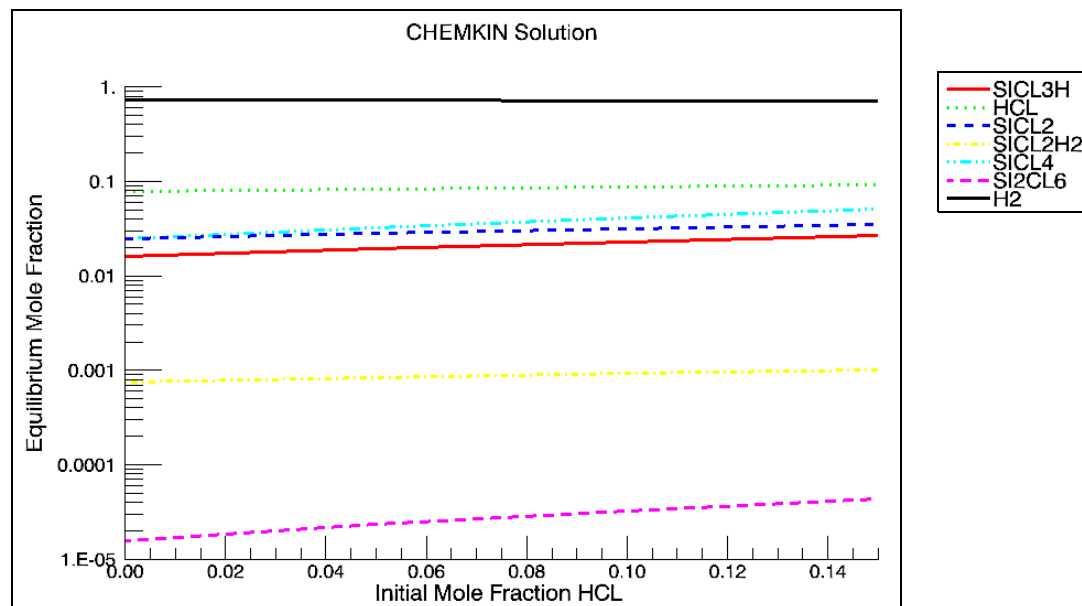


Figure 4-2 Chlorosilane CVD—Mole Fractions



4.1.2 PSR Analysis of Steady-state Thermal CVD

4.1.2.1 Project Description

This user tutorial presents a model for the CVD of silicon nitride in a steady-state PSR, using the chemistry set described in [Section 4.4.1](#). The process operates at a low pressure of 1.8 Torr, and a high temperature of 1440 C, which makes it reasonable to approximate this system as a PSR. In the PSR model, the CVD reactor is described using a volume, surface area, and gas flow rate. This is a fixed-temperature simulation that uses continuations to see the effects of changing the SiF_4/NH_3 ratio in the input gas. It also uses sensitivity and rate-of-production (ROP) options to analyze the chemistry occurring in the system.

4.1.2.2 Project Setup

The project file is called *psr_cvd.ckprj*. The data files used for this sample are located in the *samples2010\psr\cvd* directory. This reactor diagram contains only one inlet, one Perfectly Stirred Reactor, and an output Product icon.

The inlet flow rate (11300 sccm, standard cubic centimeters per minute) is input on the Stream Property Data tab of the Inlet Stream panel. The inlet gas composition is input on the Species-specific Property tab of the Inlet Stream panel.

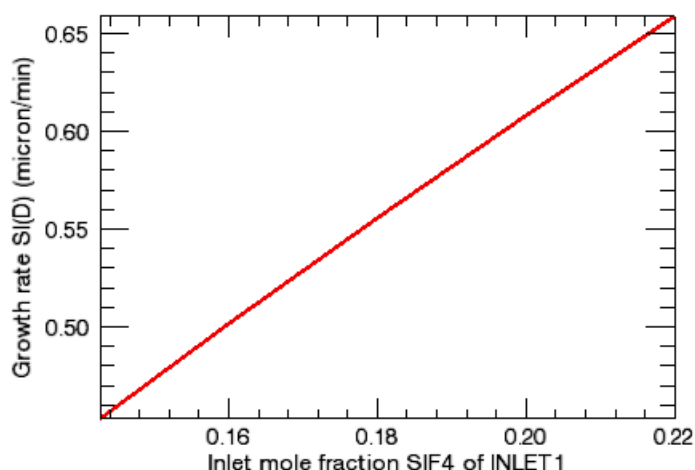
The constant reactor temperature (1440 C), pressure ($2.368\text{E-}3$ atm), volume, and internal surface area are input on the Reactor Physical Property tab of the (C1_) PSR panel. In this sample problem, no estimated gas mole fractions are input on the Initial Gas Fraction sub-tab of the Species-specific tab of the (C1_) PSR panel. This is not a restart problem, so the absence of a solution estimate for the gas-phase species causes the equilibrium composition to be calculated at 1713 K and used as a starting point for the iterations. However, solution estimates for the surface site concentrations and bulk phase activities are input on the corresponding sub-tabs of the Species-specific tab of the (C1_) PSR panel. The Bulk-phase-specific Data tab of the (C1_) PSR panel does not have input values because this is a deposition rather than an etching system.

The Output Control tab of the Output Control panel specifies that a threshold of 0.001 should be used for filtering A-factor sensitivities, while a threshold of 0.01 should be used for ROP. These are the default values in determining what gets printed in the output file and saved in the XML Solution File. The check box for indicating that growth rate sensitivities should be calculated and saved is on this tab, as are similar boxes to choose that sensitivities or ROP for all species should be calculated and stored. These latter options should be used with care for large mechanisms, as they can result in very large output and solution files. The Species Sensitivity and ROP tab allows the user to specify that sensitivities should be calculated and saved for only particular species, in this case HF, SiF₄ and NH₃. Also on this table are choices for printing ROP information for particular species in the output file. The Continuations panel has input specifying four more simulations to be done with increasing SiF₄/NH₃ ratios.

4.1.2.3 Project Results

Figure 4-3 shows that the predicted deposition rate increases with increasing SiF_4/NH_3 ratio, as expected under these conditions of excess ammonia. Although this particular plot shows the growth rate of Si(D), choosing to plot the growth rate of N(D), BULK1 or BULK2 would give essentially the same result.

Figure 4-3 Steady-state Thermal CVD—Deposition Rate vs. SiF_4 Mole Fraction



In studying a CVD system, it is often useful to know the relative importance of gas-phase and surface reactions. For this system, the model shows that very little gas-phase decomposition occurs under these conditions. *Figure 4-4* shows the total rates of production (ROPs) for SiF_4 and NH_3 due to gas-phase and surface reactions. In these cases, the negative numbers indicate that these are really loss rates rather than production rates. However, these results clearly show that surface reactions (rather than gas reactions) dominate the decomposition of these starting materials.

Sensitivity analysis gives complementary information to the ROP analysis. *Figure 4-5* shows the silicon nitride growth rate is most sensitive to surface reaction #2, which is the reaction of SiF_4 at the surface. *Figure 4-6* shows that the $\text{NH_NH}_2(\text{S})$ site fraction is much larger than the site fractions of the other surface species.



Include variables from other plot sets by checking the box on the Post-Processor Control Panel:

Include Variables from Other Plot Sets:

Figure 4-4 Steady-state Thermal CVD—ROP Comparison

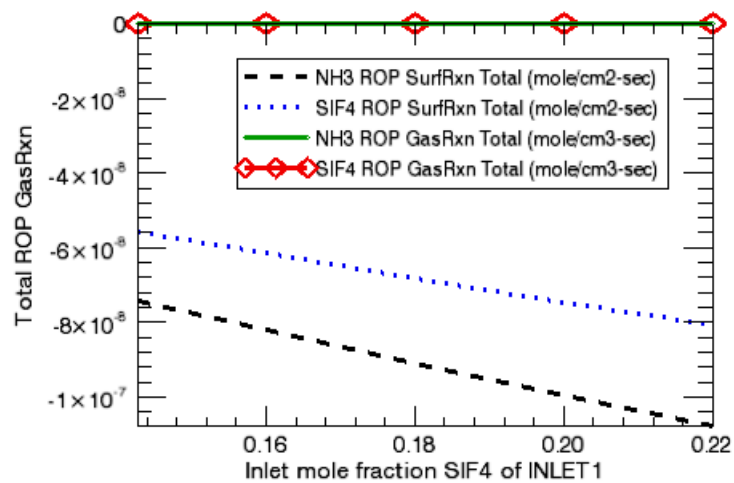


Figure 4-5 Steady-state Thermal CVD—Growth Rates

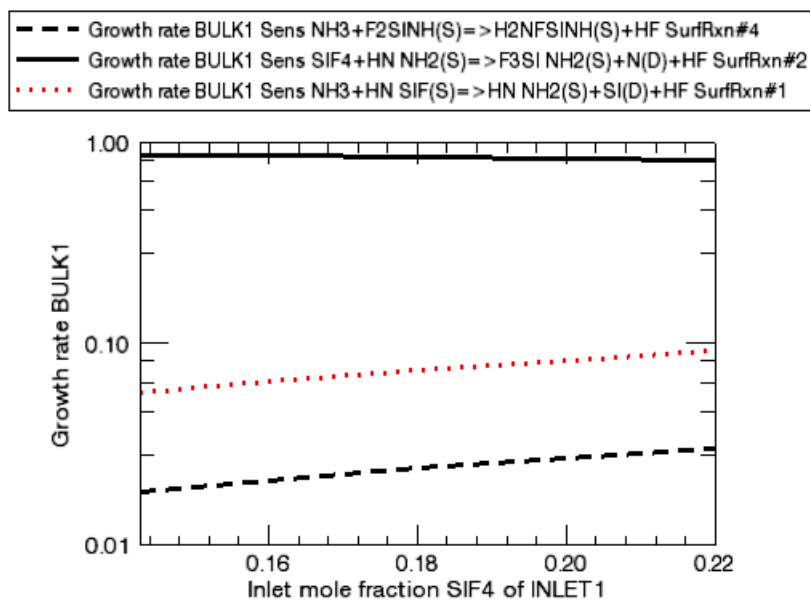
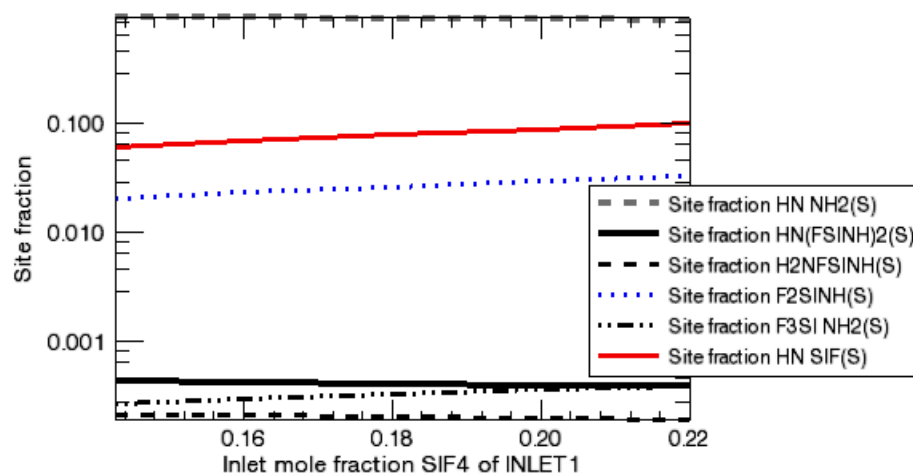


Figure 4-6 Steady-state Thermal CVD—Site Fractions



4.1.3 Approximations for a Cylindrical Channel Flow

4.1.3.1 Project Description

This user tutorial explores three ways of modeling steady-state CVD in a cylindrical flow reactor, and compares the results of the levels of approximation. This project uses the silicon nitride CVD chemistry set described in [Section 4.4.1](#). The three approximations used are, in order of increasing simplification, Cylindrical Shear-layer Flow Reactor, Plug Flow Reactor, and a series of Perfectly Stirred Reactors.

4.1.3.2 Project Setup

This project file is an example of a project that contains multiple sub-projects. It is called ***multiple_models_channel_flow_approximations.ckprj***. The data files used for this sample are located in the ***samples2010\multiple_models\channel_flow_approximations*** directory. The first reactor diagram contains one inlet and a network of 10 sequential PSRs. The other two reactor diagrams in this project are simple ones that contain only one inlet and either a Plug Flow or a Cylindrical Shear-Flow Reactor Model.

4.1.3.2.1 Cylindrical Shear-Flow Reactor

The properties of the inlet gas are described on the R1_IN1 panel. The inlet gas temperature and mass flow rate are input on the Stream Property Data tab. The mass flow rate is the maximum gas-phase velocity at the inlet. For this problem, which is in cylindrical coordinates, the average velocity equals one half of the maximum velocity of the assumed parabolic velocity profile. The composition of the inlet gas is input on the Species-specific Property tab of the R1_IN1 panel. This example uses mole fraction, but the user may choose to input these values in mass fractions instead.

Parameters describing the reactor geometry and wall temperature are entered on the Reactor Physical Property tab of the C1_ Cylindrical Shear Flow panel. The temperatures for the wall are input on this tab. In this case, the inlet gas temperature is equal to the wall temperature, so there is no need to provide transitioning parameters. The pressure, grid parameters, as well as the use of multicomponent diffusion and thermal diffusion (the Soret effect) are specified on this tab. To be consistent in our approximation to the Plug Flow as well as to the multiple PSR examples, the Boundary Layer Thickness has been set to 0.01 cm, to provide an initially flat velocity profile. The Species-specific Data tab allows the specification of initial guesses for the gas composition adjacent to the surface, which is not used in this example, as well as estimated values for the surface site fractions and bulk activities, which are provided. A good initial guess for these values is very helpful in attaining convergence.

No values are entered on the Solver panel; the default tolerance values are used. The Output Control panel has been used to specify that the text output file should have solution data printed every 1 cm.

4.1.3.2.2 **Plug Flow Reactor**

The properties of the inlet gas are described on the R1_IN1 panel. The inlet mass flow rate is input on the Stream Property Data tab. The composition of the inlet gas is input on the Species-specific Property tab of the R1_IN1 panel. This example uses mole fractions, but the user may choose to input these values in mass fractions instead.

Parameters describing the reactor geometry and gas temperature are entered on the Reactor Physical Property tab of the C1_ PFR panel. The problem type and pressure are also specified on this tab. The Species-specific Data tab allows the specification of initial guesses for the surface site fractions and bulk activities. No values are entered on the Solver panel, except to specify that the text output file should have solution data printed every 1 cm.

4.1.3.2.3 **Perfectly-stirred Reactor Network**

As for the other sub-projects, the properties of the inlet gas for the series PSR project are described on the R1_IN1 panel. The mass flow rate is input on the Stream Property Data tab. The composition of the inlet gas is input on the Species-specific Property tab of the R1_IN1 panel.

This sub-project contains a series of 10 identical PSR reactors, so in this case, the C1_Rx PSR (where $x = 1 - 10$) panels have no entries. Instead, the properties of these reactors are input on the C1 Cluster Properties panel. Cluster properties will apply to all PSRs in the cluster unless overridden in the individual reactor panels.

Parameters describing the problem type, reactor geometry, pressure, and gas temperature are entered on the Property for All Reactors tab of the Cluster Properties panel. The Species-specific Data for All Reactors tab allows the specification of initial guesses for the gas composition, which are not used in this example, as well as estimated values for the surface site fractions and bulk activities, which are used. A good initial guess for these values is very helpful in attaining convergence. There are no entries on the Solver, Output Control, or Continuations panels; all the default values are used.

4.1.3.3

Project Results

Figure 4-7 shows a contour plot of the SiF_4 mole fractions as a function of radial and axial position in the shear flow simulation. There is a minor degree of radial non-uniformity for this reactant species, as a result of chemical reactions consuming SiF_4 at the wall. *Figure 4-8* shows SiF_4 mole fraction as a function of axial distance for all three simulations. The mole fraction for the centerline is higher than that for the upper-wall in the shear-flow simulation, as expected, and these results bracket the results from the plug-flow and series-PSR simulations. Although not shown, the area-averaged value for the SiF_4 mole fraction from the shear-flow simulation agrees well with the results from the other two simulations.

Figure 4-7 Cylindrical Channel Flow—Shear-flow Simulation of SiF_4 Mole Fractions

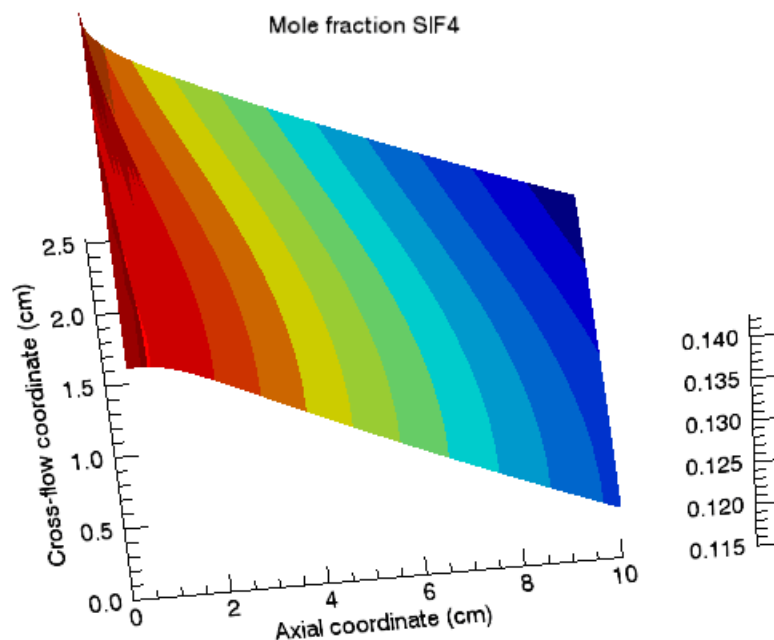


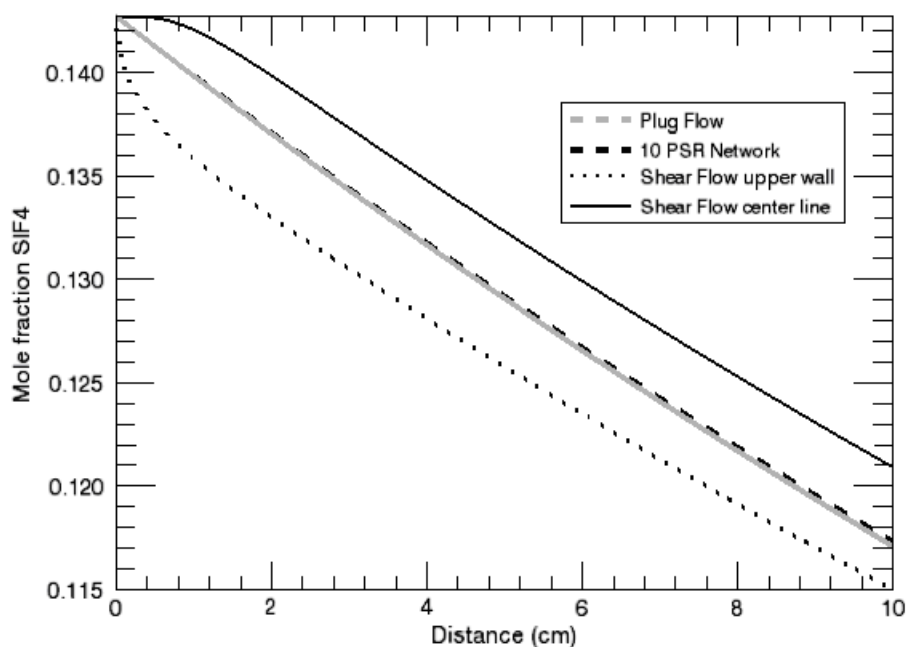
Figure 4-8 Cylindrical Channel Flow—SiF₄ Mole Fractions Comparison

Figure 4-9 shows the silicon nitride deposition rates from these three simulations. The predictions from the plug-flow and series-PSR simulations are nearly identical, with the shear-flow simulations results being somewhat lower. Although there is some differences in the axial gas velocities shown in *Figure 4-10* for the shear-flow and plug flow simulations, the difference in deposition rates mostly results from the lower reactant concentrations at the surface in the higher-dimensional simulations. The series of 10 PSR reactors and the Plug Flow simulations represent comparable levels of approximation to the channel flow. As the Plug Flow simulation actually runs faster, it would be the recommended reactor model to use in developing chemical mechanisms, or for exploring general trends for these conditions. However, the series-PSR approach has the advantage that it can approximate transient flow, as well as steady-state flow, in a channel. The deposition rate is affected by mass-transfer in this case, so the higher-dimensionality shear-flow simulations would be used for final mechanism adjustment and reactor design simulations.

Figure 4-9 Cylindrical Channel Flow—Deposition Rates Comparison

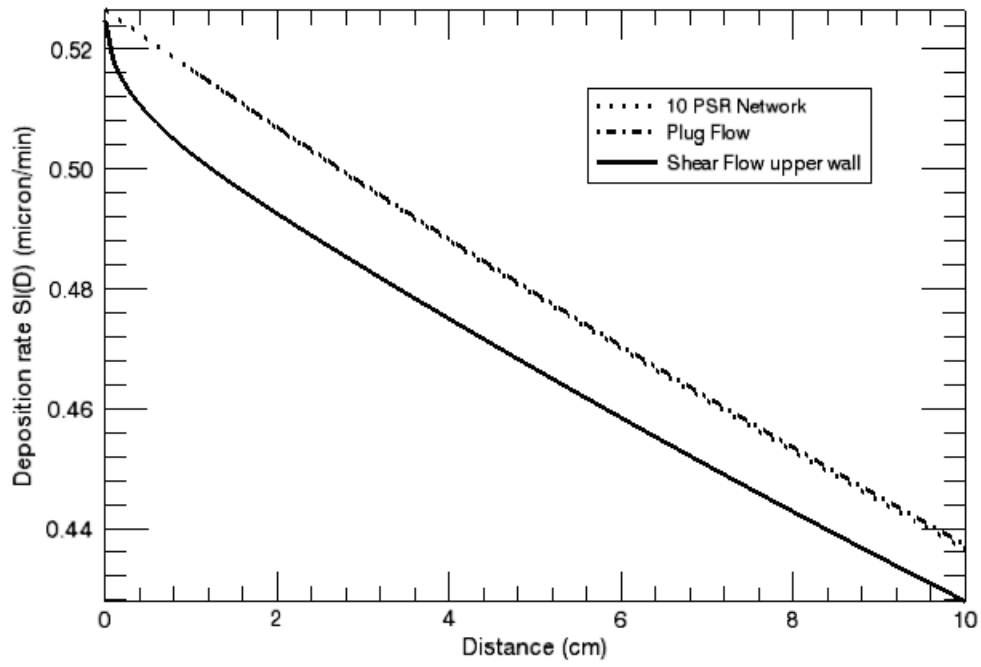
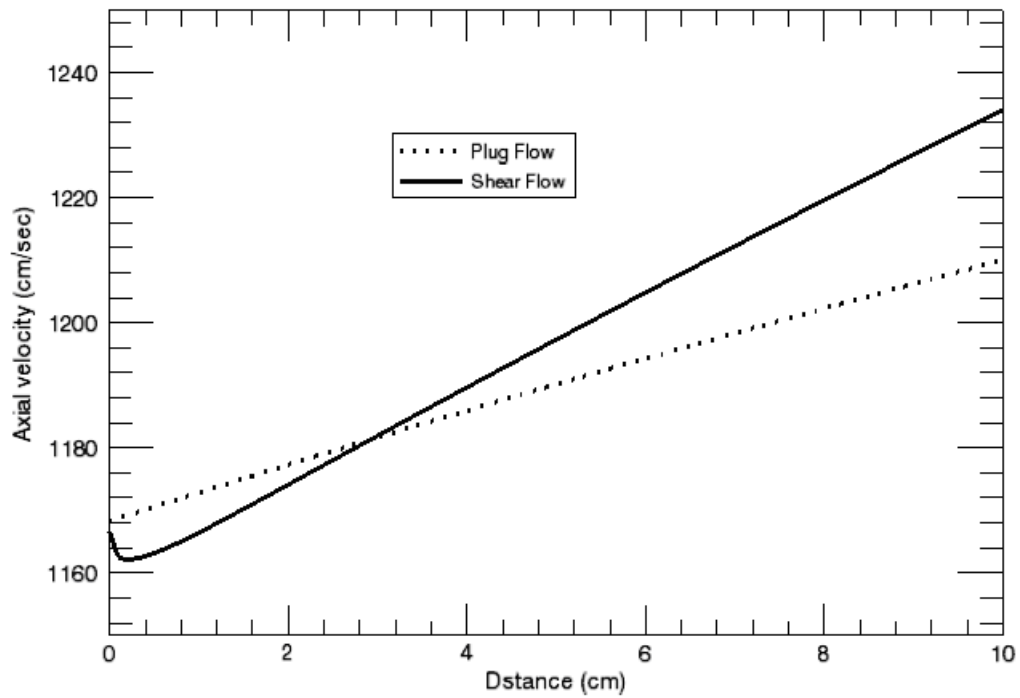


Figure 4-10 Cylindrical Channel Flow—Axial Gas Velocities Comparison



4.1.4 Deposition in a Rotating Disk Reactor

4.1.4.1 Project Description

This user tutorial presents a model for the CVD of silicon from silane in a steady-state rotating disk reactor using the chemistry set described in [Section 4.4.2](#). This is a fixed-surface temperature simulation that represents the experimental rotating-disk reactor used by Ho, Coltrin and Breiland,⁴⁷ (p. 247) with the conditions corresponding to *Figure 4* in that paper. The inlet gas is a dilute mixture of silane in helium. The use of a helium carrier gas, rather than hydrogen, favors the gas-phase decomposition reactions of silane. For this case, a surface temperature of 923 K (650° C) is used. This example has two continuations, where the silane partial pressure is increased.

4.1.4.2 Project Setup

The project file is called ***rotating_disk_sih4_cvd.ckprj***. The data files used for this sample are located in the ***samples2010rotating_disk\sih4_cvd*** directory. This reactor diagram contains only one inlet and one rotating-disk CVD reactor.

The properties of the inlet gas are described on the C1_Inlet panel. The inlet gas temperature is input on the Stream Property Data tab. An inlet gas velocity is usually not entered for a steady-state rotating disk simulation, as it is calculated from the spin rate, pressure, and gas-properties, but the user may override this value on the Reactor Physical Property tab, Basic sub-tab, if desired. The composition of the inlet gas is input on the Species-specific Property tab of the C1_Inlet panel. Note that the mole fractions do not add up to one, as the partial pressures (in Torr) have actually been entered. This is permitted, as the program will normalize the gas composition internally if the user does not do so in the CHEMKIN Interface. The Continuations panel is used to input the new compositions of the reactant gas mixture for the second and third simulations in this sample project.

Parameters describing the reactor conditions are entered on the Reactor Physical Property tab, Basic sub-tab of the C1_Rotating Disk panel. The choice of a steady-state simulation solving the gas energy equation is entered here, as well as the use of multicomponent diffusion and thermal diffusion (the Soret effect). The temperature for the deposition surface (923 K), pressure (200 Torr), and disk rotation rate (450 rpm) are input on this tab. The other sub-tabs on the Reactor Physical Property tab are for options that are not used in this example. The Initial Grid Property tab of the Reactor Physical Property tab allows specification of the locations of the deposition surface ($x = 0$, default) and the end axial location where the gas enters (6.2 cm). Grid parameters are specified on this tab. This reactor model includes adaptive gridding, and the use of a relatively-low value for the initial number of grid points is recommended. The Species-specific Data tab allows the specification of initial

guesses for the gas composition at the inlet, adjacent to the surface, or maximum mole fractions for intermediate species, none of which are used in this example. However, estimated values for the surface site fractions and bulk activity are provided. A good initial guess for these values can be very helpful in attaining convergence.

4.1.4.3 Project Results

Figure 4-11 shows the axial, radial and circumferential velocity components for the rotating disk reactor as a function of height above the surface. The deposition surface is at the origin, and the gas enters at $x = 6.2$ cm with an axial velocity of -12.4 cm/sec and zero radial and circumferential velocity components. As the gas approaches the rotating surface, the axial velocity initially increases slightly then decreases while the radial and circumferential velocity components increase. At the surface, the axial and radial velocity components are zero, and the circumferential velocity matches that of the disk (in radians/sec), as expected.

Figure 4-11 Deposition in a Rotating Disk—Gas Velocity Components

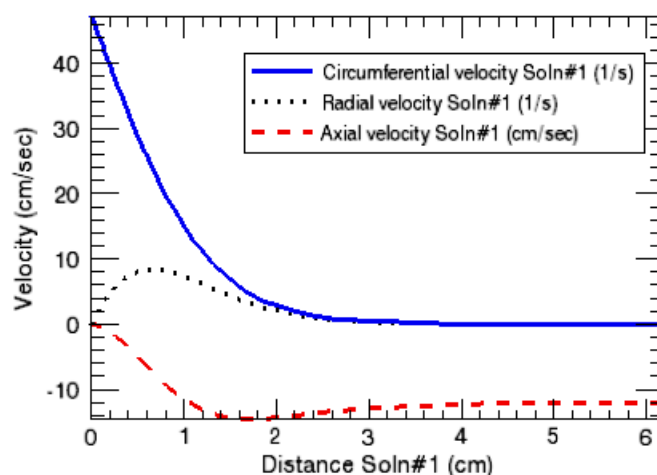


Figure 4-12 shows predicted mole fractions for the various silicon hydrogen species as a function of distance above the surface (the helium carrier gas is not included), again for the first simulation in the project. The composition at the grid point with largest x value is constrained to that of the inlet gas (silane and helium only). The other grid points show varying amounts of product and reactive intermediate species that are formed by gas-phase and surface reactions. Si atoms are present in very low amounts (mole fractions $\sim 10^{-12}$), but can easily be detected by laser-induced fluorescence techniques, so they are kept in the mechanism. You can choose concentration units for species composition in the Species/Variables tab of the Select Results to Load panel when the Post-Processor is first launched. This yields the results shown in *Figure 4-13*, illustrating that Si atom concentrations increase with increasing silane concentration, as expected. The profiles of the Si atom

concentrations are shown as a function of distance above the surface for different starting silane partial pressures: #1 = 0.11 Torr, #2 = 0.34 Torr, #3 = 0.67 Torr. The curves in this figure suggest that the profiles might also be changing shape. This is confirmed in [Figure 4-14](#), which was made by exporting the simulation results, normalizing and plotting experimental results from Ho, Coltrin and Breiland (see [Figure 4](#) of referenced paper)⁴⁷ (p. 247) in third party software. It shows that: a) Si atom profiles are experimentally observed to be narrower for higher silane concentrations, and b) this reaction mechanism reproduces this observation. Comparisons between the model and this experimental data set shown that the original reaction proposed for Si atom formation, the collisionally-induced decomposition of SiH₂, could not account for the experimental observations. Two other reactions, H₃SiSiH ↔ Si + SiH₄ and Si + Si₂H₆ ↔ H₃SiSiH + SiH₂, are instead the primary reactions involving Si atoms.

Figure 4-12 Deposition in a Rotating Disk—Mole Fractions

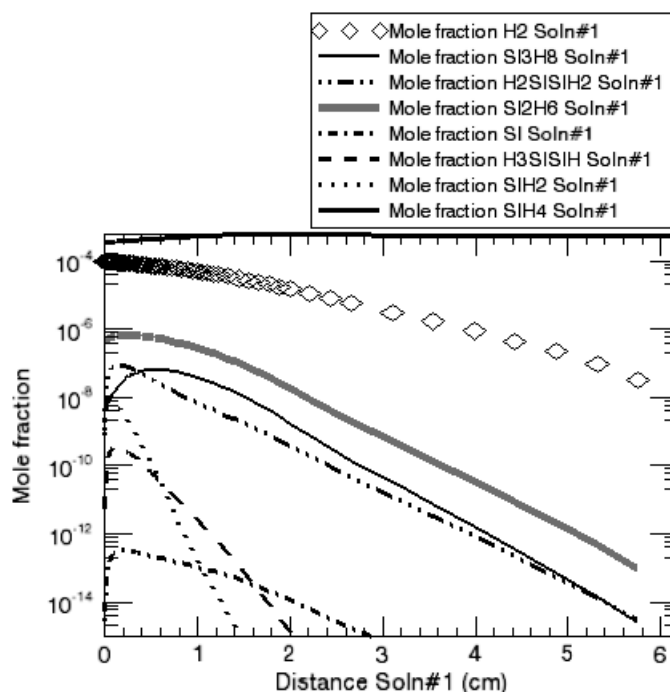


Figure 4-13 Deposition in a Rotating Disk—Si Atom Concentrations

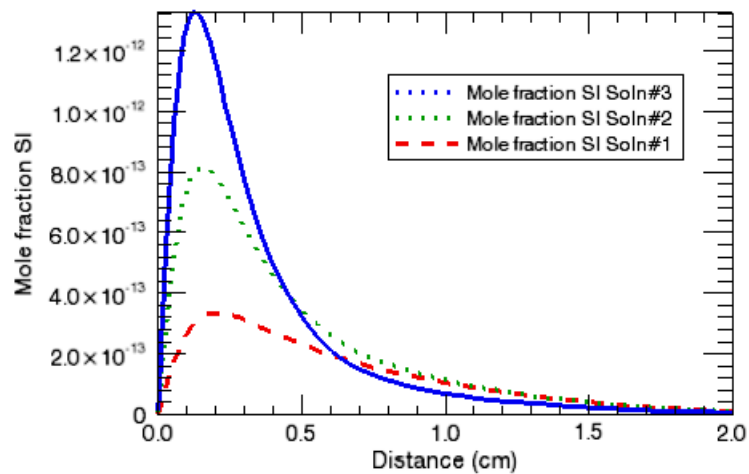
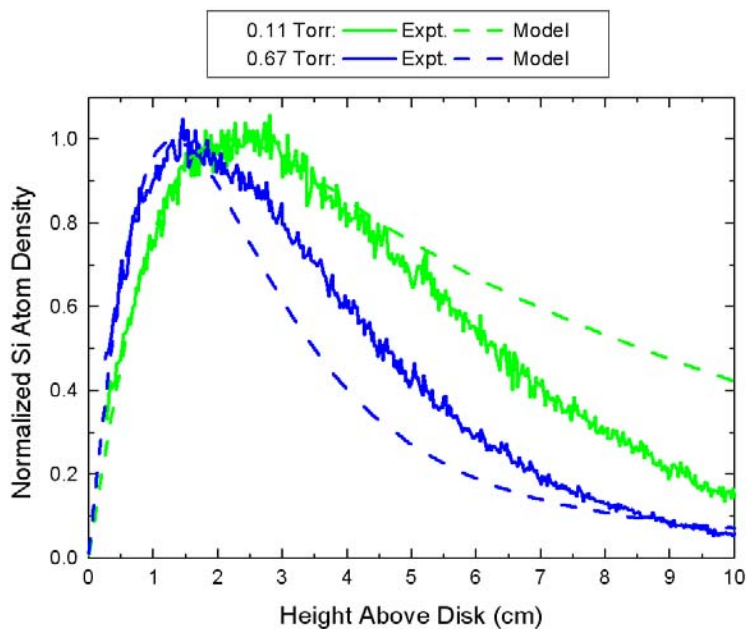


Figure 4-14 Deposition in a Rotating Disk—Experimental Data



4.1.5 Trichlorosilane CVD in Planar Channel Flow Reactor

4.1.5.1 Project Description

This user tutorial presents a model for the CVD of silicon in a steady-state planar shear-layer flow reactor using the chemistry set described in [Section 4.4.3](#). The process operates at atmospheric pressure, and a relatively high temperature (1398 K). This is a fixed-temperature simulation that represents a horizontal cross-flow reactor of the type used to deposit epitaxial silicon layers. In this case, the upper wall temperature is held at a temperature (773 K), which is significantly lower than the deposition substrate, but higher than the inlet gas temperature (623 K).

4.1.5.2 Project Setup

The project file is called *planar_shear_flow__tcs_cvd.ckprj*. The data files used for this sample are located in the *samples2010\planar_shear_flow\tcs_cvd* directory. The reactor diagram contains one inlet, one planar shear-flow reactor, and an outlet.

The properties of the inlet gas are described on the C1_Inlet panel. The inlet gas temperature and inlet gas velocity are input on the Stream Property Data tab. The Axial Velocity should be the maximum gas-phase velocity at the inlet. For this problem, which is in cartesian coordinates, the average velocity equals two-thirds of the maximum velocity of the parabolic velocity profile. The composition of the inlet gas is input on the Species-specific Property tab of the C1_Inlet panel.

Parameters describing the reactor geometry and wall temperatures are entered on the Reactor Physical Property tab of the C1_Planar Shear Flow panel. The temperatures for the upper wall and deposition surface (lower wall) are input on this tab, as well as an optional parameter specifying the distance over which the wall temperatures are smoothly transitioned from the inlet gas temperature to the desired wall temperature. The pressure, grid parameters, as well as the use of multicomponent diffusion and thermal diffusion (the Soret effect) are specified on this tab. The Species-specific Data tab allows the specification of initial guesses for the gas composition adjacent to the surface, which is not used in this example, as well as estimated values for the surface site fractions and bulk activities, which are provided. A good initial guess for these values is very helpful in attaining convergence.

On the Basic tab of the Solver panel, the text output file has been specified to have solution data printed every 1 cm along the channel.

4.1.5.3 Project Results

The gas temperatures in [Figure 4-15](#) show that the gas heats up substantially near the deposition surface, with the hot zone expanding with axial distance, as expected. The inlet gas temperature is lower than the upper wall temperature, such that the coolest gas lies in a region near to, but below the top wall. This cooler gas region is reflected in the trichlorosilane mole fraction contours shown in [Figure 4-16](#). Depletion as a result of chemical reaction causes the low SiCl_3H mole fractions near the lower wall, but thermal diffusion causes the heavier gas to move away from the upper wall. A simulation run without thermal diffusion gives uniform SiCl_3H mole fractions in the upper part of the reactor. [Figure 4-17](#) shows how the deposition rate of solid silicon varies as a function of axial distance. Initially, the deposition rate is quite high, but it drops rapidly as the SiCl_3H near the surface is depleted, indicating that the deposition process is transport limited in this system. [Figure 4-18](#) shows gas-phase mole fractions near the lower surface as a function of axial distance. The extent of SiCl_3H depletion and HCl formation is notably larger than the formation of the other silicon-chlorine species (SiCl_2 , SiCl_2H_2 and SiCl_4), which indicates that deposition of solid silicon is the dominant reaction pathway.

Figure 4-15 Trichlorosilane CVD—Gas Temperatures vs. Axial and Radial Distance

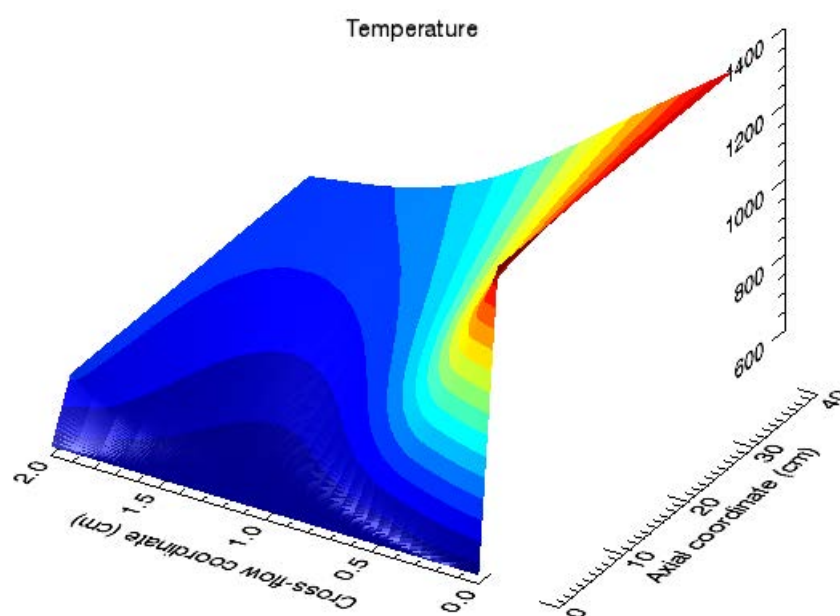


Figure 4-16 Trichlorosilane CVD—Trichlorosilane Mole Fraction

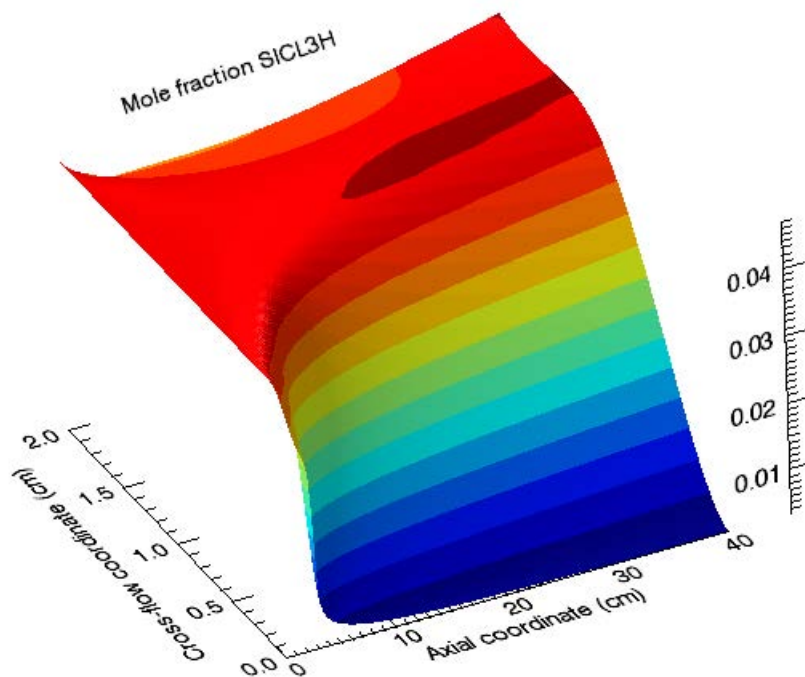


Figure 4-17 Trichlorosilane CVD—Silicon Deposition Rate

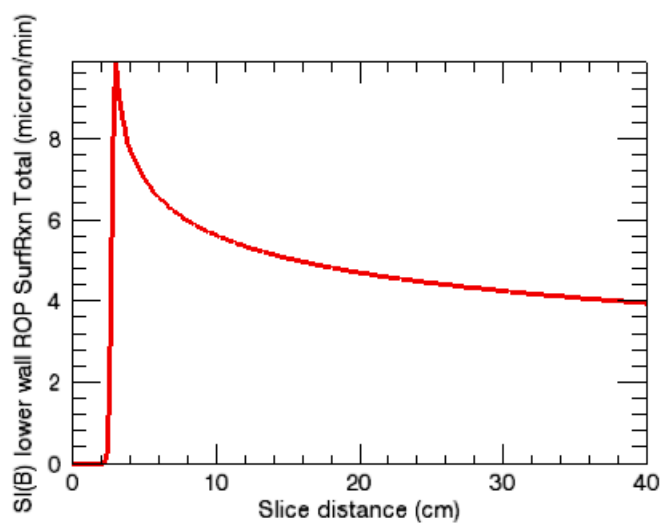
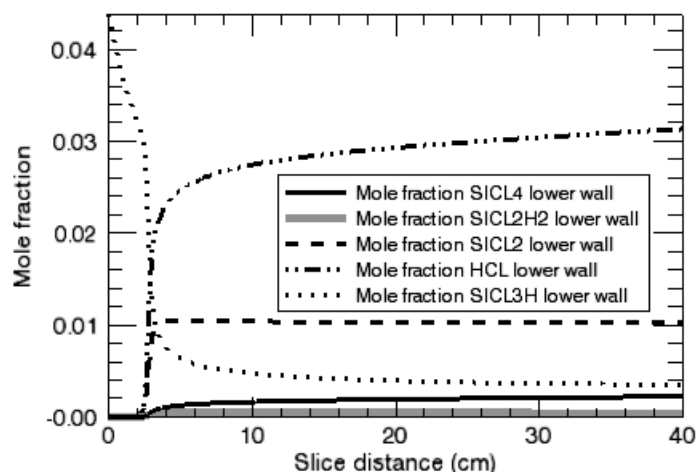


Figure 4-18 Trichlorosilane CVD—Mole Fractions



4.2 Atomic Layer Deposition (ALD)

The CHEMKIN software includes several reactor models that can be used for simulating ALD processes. ALD is a technique used to deposit thin films of solid materials in a very controlled manner, and differs from CVD primarily in that it is a transient process with the deposition surface being exposed to pulses of alternating gases. Ideally, the deposition chemistry in ALD is self-limiting, with growth occurring in a layer-by-layer manner and the deposition thickness being controlled only by the number of cycles. ALD is also called: ALE, Atomic Layer Epitaxy, NLD, Nano Layer Deposition, ALCVD, Atomic Layer Chemical Vapor Deposition, and AVD, Atomic Vapor Deposition. There are also plasma enhanced variations such as PENLD, Plasma Enhanced Nano Layer Deposition. It is a relatively new technology, having made the transition from the research lab to production in the last decade.

The transient models within the CHEMKIN software are useful for optimizing pulse sequences and thus minimizing cycle times in ALD. The major advantage of ALD over CVD is the improved control over the deposition process and more conformal deposition. The inherently lower deposition rates, however, lead to longer process times and higher costs. During a pulse, it is important that enough molecules react with all parts of the substrate to be coated. But many of the precursor materials are expensive. Thus one of the process optimization goals is to reduce the amount of precursor that flows through the reactor but does not react at the surface. Considering the effects of finite-rate kinetics for surface reactions can be an important part of such an optimization, as reactions do not always behave in an ideal manner.

4.2.1 Time-dependent Simulations of ALD Process

4.2.1.1 Project Description

This user tutorial demonstrates two ways of simulating a time-dependent ALD process. The transient Perfectly Stirred Reactor Model runs relatively quickly and is useful for developing and initial testing of the chemical reaction mechanism. The transient stagnation flow model more realistically simulates a production-scale shower-head ALD reactor by including mass-transport effects. The alumina ALD chemistry described in [Section 4.4.4](#) is used. The process operates at a pressure of 1 Torr, and a relatively low surface temperature (compared to CVD) of 450° C (723 K). This sample demonstrates four cycles of the flow sequence including: metalorganic precursor in argon; argon purge; ozone in oxygen and argon; and argon purge. The four cycles are sufficient, in this case, to characterize the process.

4.2.1.2 Project Setup

This project file is an example that contains multiple reactor models or sub-projects. It is called ***multiple_models_atomic_layer_deposition.ckprj***. The data files used for this sample are located in the ***samples2010\multiple_models\atomic_layer_deposition*** directory. The two reactor diagrams in this project each contain three gas inlets and either a Perfectly Stirred Reactor or a Stagnation-flow CVD Reactor Model.

In this project, the names of the gas inlets, and their corresponding input panels, have been changed away from the default names of R1_IN1, etc., to **METORG**, **OXIDIZER** and **PURGE**, which reflect the function of the gas flowing through the inlets. The listings of flow rate as a function of time for each gas-flow inlet are saved as time-dependent profile files:

- ✓ *SCCMPRO_METORG.ckprf*
- ✓ *SCCMPRO_OXIDIZER.ckprf*
- ✓ *SCCMPRO_PURGE.ckprf*

In this case, the profiles of total flow rates for each gas inlet are in volumetric flow units of sccm, but flow profiles can also be specified in mass flow units. The PSR and stagnation-flow models use the same flow-profile files.

Although both simulations run for the same length of process time, the stagnation flow simulation takes significantly more compute time to run, due to the inclusion of mass-transport effects.

4.2.1.2.1**Transient PSR**

The names of the flow-profile files are designated on the Stream Property Data tab of each Gas Inlet panel. If a profile file already exists, it can be selected by browsing or by the pull-down menu, if it has already been accessed. The Edit button opens a panel that allows profile files to be edited or created. In this case, inlet temperatures are not specified on the Gas Inlet panel, as this is a fixed-gas temperature simulation. The composition of each reactant gas inlet is specified on the Species-specific Property panel of the corresponding Gas Inlet panel.

The choice of fixed gas temperature for this simulation is made with the Problem-type drop-down list on the Reactor Physical Property tab of the C1_ PSR panel. The gas temperature, pressure, volume and surface area (which are generally representative of ALD reactors) are also input here. In this case, the gas temperature for the PSR simulation was chosen to reproduce the degree of ozone decomposition to O atoms and match the deposition rate observed in the higher dimensional simulation. The surface temperature is different from the gas temperature, and it is also specified on the Reactor Physical Properties tab. On the Species-specific Data tab, the starting gas composition of pure argon is specified on the Initial Gas Fraction sub-tab, the starting surface composition of complete O(S) coverage is specified on the Surface Fraction sub-tab, and an activity of 1.0 specified for AL₂O₃(B) on the Bulk Activity sub-tab. These correspond to a reasonable starting condition where the substrate might have an initial oxide coating, and the system was purged with argon after loading. No entries are made on the other parts of this panel.

The end time of the transient simulation is specified on the Reactor Physical Properties panel. The solver maximum and minimum step time is on the Advanced tab of the Solver panel. Intervals for saving and for printing solution data are given on the Output Control panel. No entries are required on the Solver, Output Control or Continuations panels for this problem.

4.2.1.2.2**Transient Stagnation Flow Reactor**

The names of the flow-profile files are designated on the Stream-property panel of each Gas Inlet panel. In this case, the gas energy equation is being solved, so an inlet temperature of 150° C (423 K) is a required input for each gas inlet. The composition of each reactant gas inlet is specified on the Species-specific Property tab of the corresponding Gas Inlet panel.

Choices to solve a transient problem, include the gas energy equation, use multicomponent diffusion but not the Soret effect, etc., are input in the Reactor Physical Property tab, Basic sub-tab of the C1_ Stagnation Flow panel. The process pressure and surface temperature are input on this sub-tab, along with the name of

file containing the initial guess for the gas temperatures as a function of height above the disk, and a cross sectional flow area used for translating volumetric flow rates to linear flow velocities. The end time of the transient simulation is also specified on the Basic sub-tab. There are no entries on the other sub-tabs of the Reactor Physical Property tab.

The Initial Grid Property tab of the C1_ Stagnation Flow panel allows the input of the number of points in the grid of distance above the substrate, along with the ending axial distance. In transient simulations, the grid currently does not adapt as it does in steady-state stagnation flow simulations. Thus, a reasonably dense initial grid should be specified, and the adaptive gridding parameters are ignored. Note that the surface is defined as being at a coordinate value of $x = 0$, and the maximum distance of 1.2 cm is the location of the gas inlets (showerhead). In other words, the solution is given as a function of distance from the surface.

On the Species-specific Data tab of the C1_ Stagnation Flow panel, the starting gas composition of pure argon is specified on the Initial Gas Fraction sub-tab, the starting surface composition of complete O(S) coverage is specified on the Surface Fraction sub-tab and an activity of 1.0 specified for AL₂O₃(B) on the Bulk Activity sub-tab. These are the same as were used in the PSR simulation, and correspond to a reasonable starting condition where the substrate might have an initial oxide coating, and the system was purged with argon after loading. No entries are made on the other parts of this panel.

The interval for printing data to the output file (on the Output Control panel) and some tolerance parameters that have been relaxed from the default values (on the Basic tab of the Solver panel). The Advanced tab of the Solver panel contains a time-step specification and a solver parameter that have been altered from the default values. No entries are made on the Continuations panel for this problem.

4.2.1.3 Project Results

Figure 4-19 shows the gas pulses used in this example for the metal-organic and oxidizer gas inlets. The pure-argon purge gas pulses are not shown. The metal-organic gas (trimethyl aluminum; TMA) pulses are considerably shorter than the oxidizer gas pulses, but appear to be sufficient. The contour plot of one TMA pulse from the stagnation-flow simulation in *Figure 4-20* clearly shows that the TMA is consumed at the surface only at the beginning of the pulse. By the end of the pulse, all the TMA flowing into the reactor is also flowing out again.

Figure 4-19 Time-dependent ALD Simulations—PSR, Total Flow Rates vs. Time

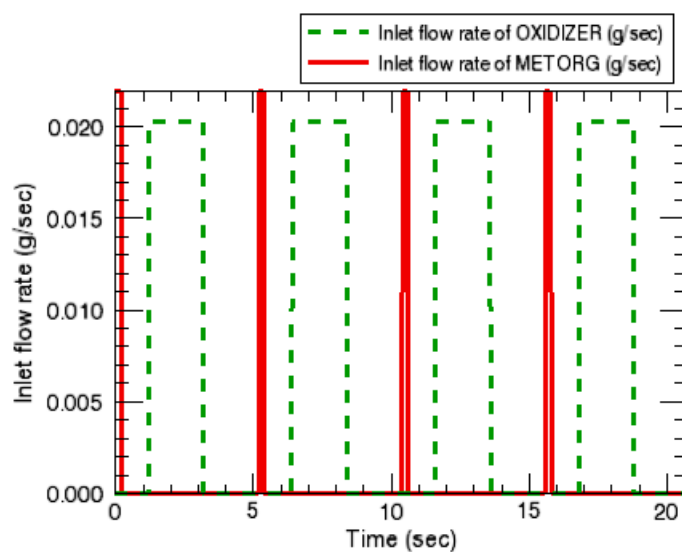
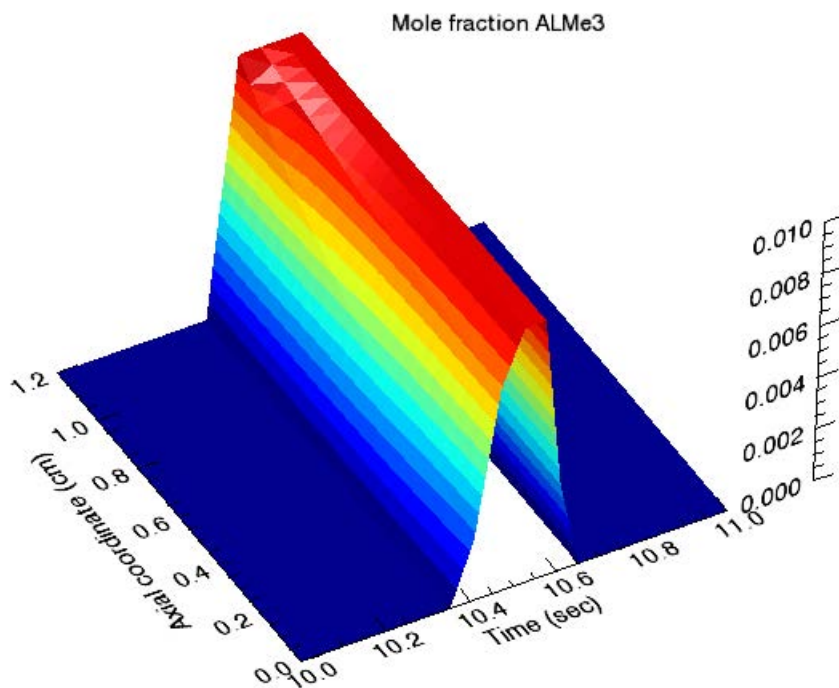


Figure 4-20 Time-dependent ALD Simulations—TMA Contour Plot



The chemistry that occurs during the oxidizer pulses is more complex. The contour plot of O atom mole fractions in [Figure 4-21](#) show how the O atoms are formed by gas-phase decomposition of ozone in the hotter regions of the gas, and then react away at the surface. The site fractions in [Figure 4-22](#) show that the methylated surface species, ALME2(S) and ALMEOALME(S), are not completely converted to O(S) during the oxidizer pulse. This probably results from the fact that the oxidation

occurs as two sequential steps and the kinetics are limiting the process. The O atom mole fractions in [Figure 4-23](#) shows that the O atoms are not being depleted at the surface in the stagnation flow simulations, which suggests a kinetic limitation, possibly resulting from the default reaction orders in this simple mechanism. The incomplete oxidation of the methylated surface species in turn leads to less than unity O(S) coverage at the beginning of the TMA pulse, which in turn leads to less efficient use of TMA and some notable differences between the first and subsequent pulses.

Figure 4-21 Time-dependent ALD Simulations—O Mole Fraction

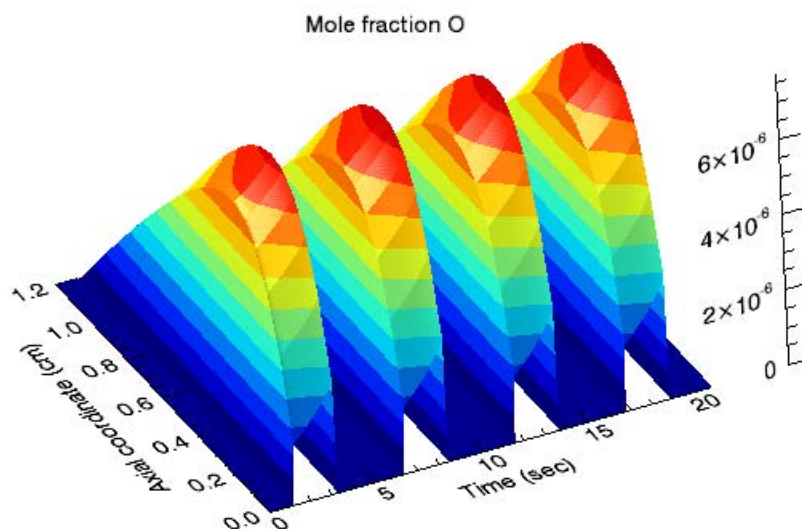


Figure 4-22 Time-dependent ALD Simulations—Stagnation-flow Site Fractions

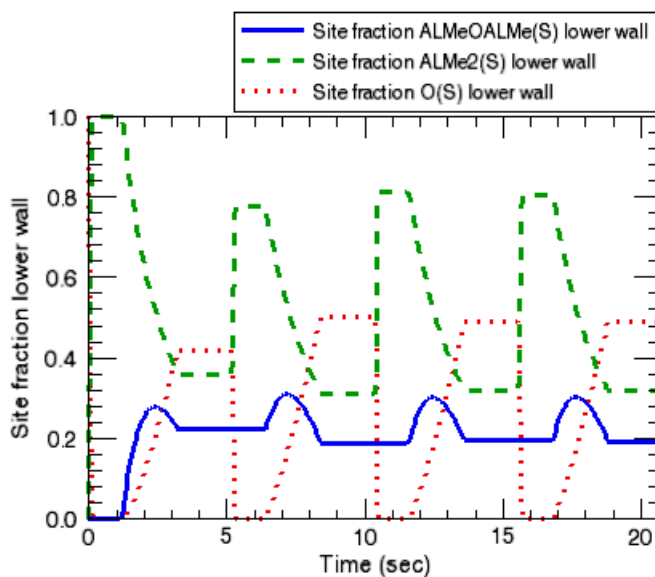
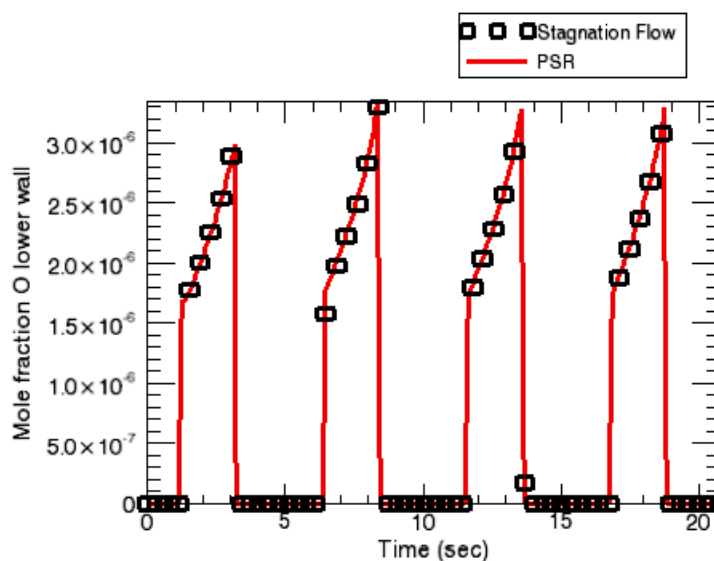
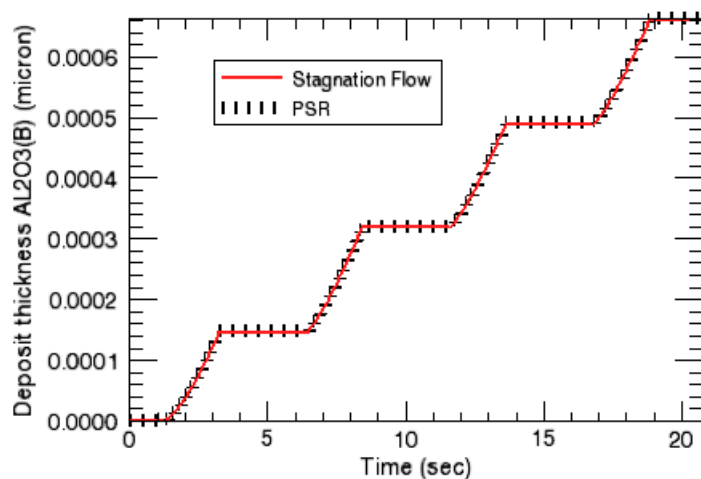


Figure 4-23 Time-dependent ALD Simulations—O Mole Fractions Comparison



The O atom mole fractions in [Figure 4-23](#) from the stagnation flow simulations agree well with those from the PSR simulations. Within the limits of this simple deposition chemistry, this directly leads to the good agreement for deposition thickness shown in [Figure 4-24](#). The agreement between the two models, in this case, results from the fitting of the gas-phase temperature in the PSR simulation to reproduce the O atom mole fractions in the higher-dimensional simulation. This kind of a calibration allows the faster-running PSR simulation to be used to quickly explore a wide range of pulse sequences and other experimental conditions of interest, before returning to higher-dimensional simulations for more careful study.

Figure 4-24 Time-dependent ALD Simulations—Deposition Thickness Comparison



4.3 Plasma Etching

The CHEMKIN software includes a number of special features for modeling plasmas, most of which are demonstrated in these examples. For treating non-equilibrium plasmas, the plasma models allow you to specify different temperatures for the neutral gas, electrons, ions, and surfaces. A gas-phase reaction rate can be designated to depend on the electron temperature rather than the default neutral gas temperature. An electron-impact reaction can also be designated to involve a specified energy loss per collision. This option is used to describe excitation energy losses for electrons in solving the electron energy equation, without explicitly defining each vibrationally or electronically excited-state as a separate species within the corresponding thermodynamic data. For surface reactions, ion-assisted reactions can have yields that depend on the ion energy. Such reactions can also be designated as Bohm reactions, which means that the ion flux is limited by the Bohm velocity of the ions, rather than by the ion's thermal speed. The implementation of the Bohm criterion is described in detail in [Section 8.5.3](#) of the *CHEMKIN Theory Manual*. This factor has been introduced to account for the fact that the ion interaction with the surface will be subject to transport limitations, such that a gradient near the walls in the ion density will occur. A zero-dimensional model cannot capture this effect, such that a Bohm-flux correction model is used.

4.3.1 Steady-state Chlorine Plasma

4.3.1.1 Project Description

This user tutorial provides an example of modeling a low-pressure plasma reactor as a steady-state Perfectly Stirred Reactor, using the chlorine plasma chemistry set described in [Figure 4.4.5](#). The plasma pressure is 5 mtorr and pure chlorine gas flows into the reactor at 35 sccm. The energy equation and the electron energy equation are solved, and a heat-transfer correlation is used to account for heat loss through the wall of the reactor.

4.3.1.2 Project Setup

The project file is called *plasma_psr__chlorine.ckprj*. The data files used for this sample are located in the *samples2010\plasma_psr__chlorine* directory. This reactor diagram contains one gas inlet, one plasma PSR, and one outlet.

The reactant gas mixture, which is pure Cl_2 in this case, is input on the Species-specific Property tab of the C1_Inlet1 panel. The initial guess for the steady-state gas composition, which is input on the Initial Gas Fraction subtab of the Species-specific Data tab of the C1_Plasma PSR panel, is quite important. A good initial guess (one that is close to the steady-state solution) will result in fast convergence, while a poor initial guess can at worst lead to failure of the simulation.

The Reactor Physical Property tab of the C1_Plasma PSR panel is where problem type and reactor parameters such as pressure, temperatures, volume, area, heat loss, and plasma power are entered. Solving the electron energy equation requires that an initial guess for the electron temperature be input on this tab, as well as an inlet electron temperature on the Stream Property tab of the C1_Inlet1 panel. The latter has no impact on the solution unless there are electrons in the inlet gas mixture. The Sheath Loss parameter describes the ion energy gained crossing the sheath and may be specified differently for each material in the system. On the Solver panel, skipping the intermediate fixed-temperature solution is usually more robust for plasma simulations than trying to solve it first.

4.3.1.3 Project Results

[Figure 4-25](#) shows the electron temperature as a function of power for this chlorine plasma. The electron temperature shows only small changes over the large variation in plasma power, since most of the power is transferred into ionization and dissociation rather than electron heating. However, as the plasma power drops, the electron temperature rises as the plasma nears extinction, since there are fewer electrons and electron-driven events. The mole fractions of the electrons and positive ions, increase steadily with increasing plasma power, as shown in [Figure 4-26](#), but the chlorine negative ions show a maximum at intermediate powers. [Figure 4-27](#) shows that the net dissociation of molecular chlorine to atomic chlorine steadily increases with increasing plasma power, as expected.

Figure 4-25 Steady-state Chlorine Plasma—Electron Temperatures vs. Power

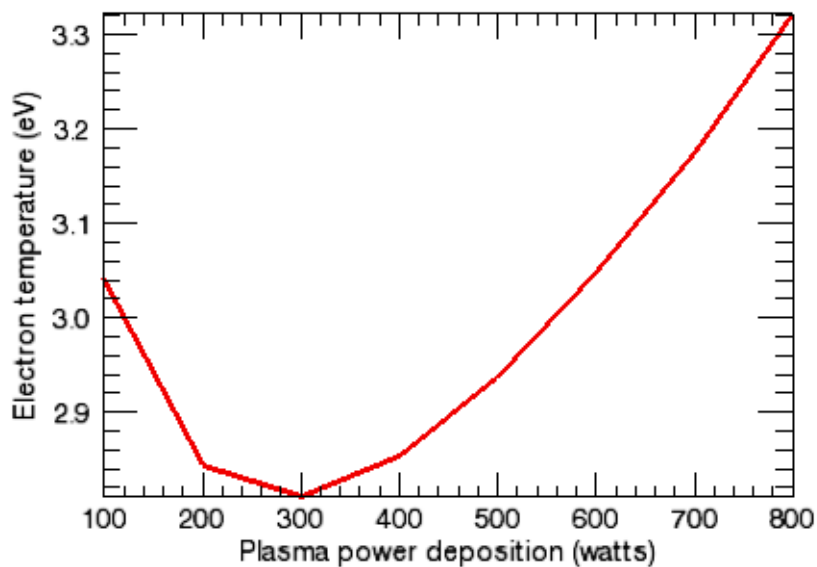


Figure 4-26 Steady-state Chlorine Plasma—Mole Fractions

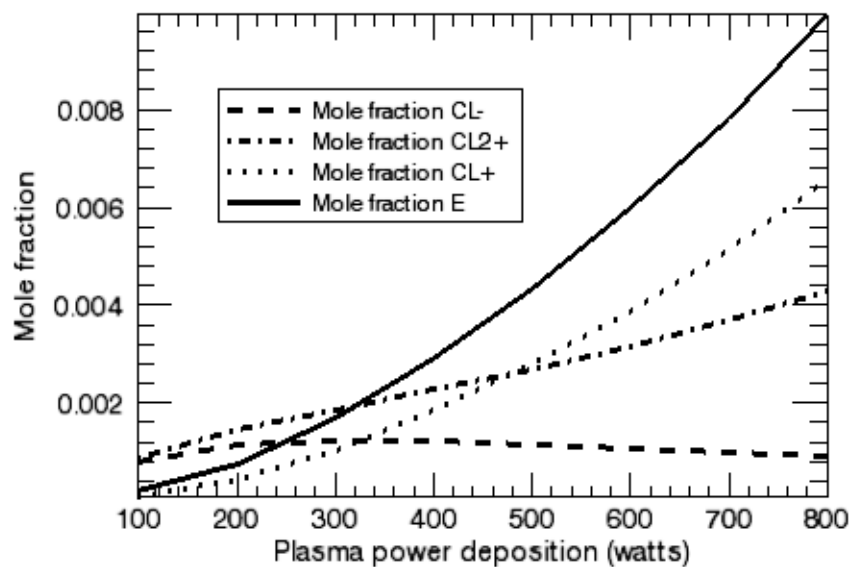


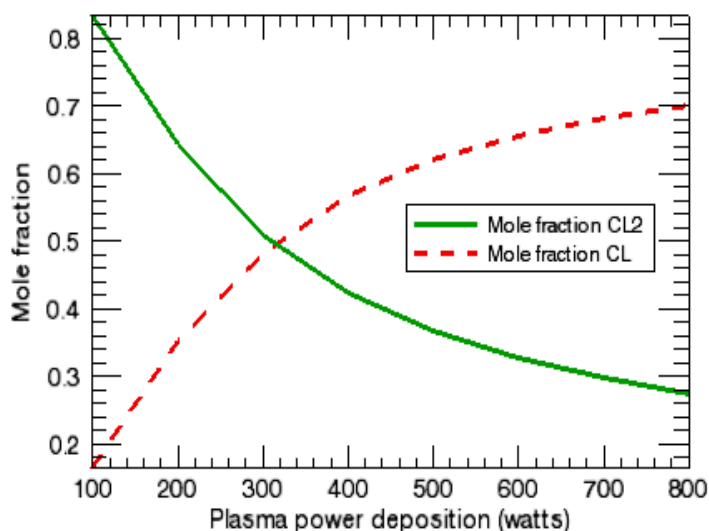
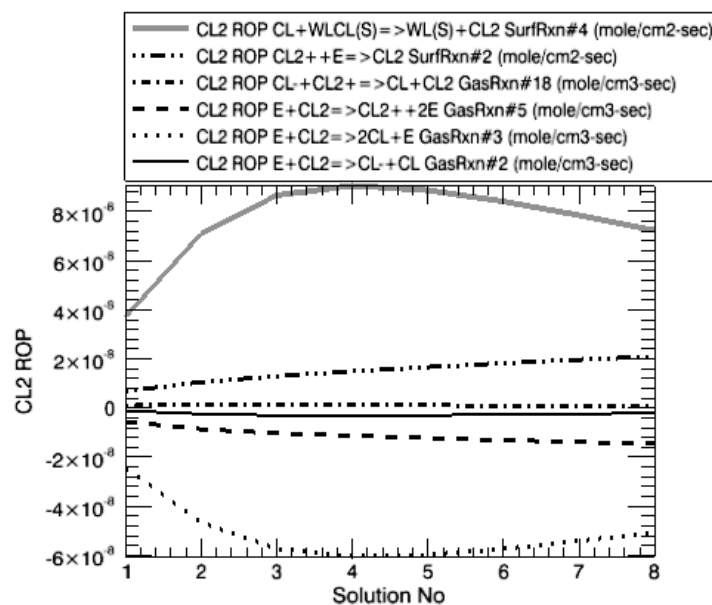
Figure 4-27 Steady-state Chlorine Plasma—Cl and Cl₂ Mole Fractions

Figure 4-28 shows a rate-of-production analysis for the input gas Cl₂. (To create this plot with plasma power deposition as the x-axis, select **Include variables from other plot sets** in the CHEMKIN Visualizer. For details, see the *Control Tabs* section in *Chapter 3* of the *CHEMKIN Visualization Manual*.) In this case, there are clear major and minor pathways. The primary reaction consuming molecular chlorine is gas-phase reaction #3, which is the electron-impact dissociation to two Cl atoms. Gas reactions #5 and 2, the electron-impact ionization and dissociative attachment reactions of Cl₂, respectively, are minor channels for Cl₂ consumption. The primary reaction producing Cl₂ is surface reaction #4, the reaction between gas-phase and adsorbed Cl atoms producing molecular chlorine in the gas phase. Gas reaction #18, the neutralization reaction between Cl⁻ and Cl₂⁺, and surface reaction #2, the neutralization of Cl₂⁺ on the wall, are minor channels for Cl₂ production.

Figure 4-28 Steady-state Chlorine Plasma—ROP Analysis



4.3.2 Spatial Chlorine Plasma PFR with Power Profile

4.3.2.1 Project Description

This user tutorial presents an example of a Plasma Plug Flow Reactor with a specified power versus distance profile. This feature might be used to model an experimental apparatus where the inductive coils providing the power are spaced unevenly. Alternatively, this could be used to model a system where there is a lower-power region where a probe is used that cannot operate in a high-plasma density region, or where a measurement window is located.

This example is for a plasma at a total pressure of one torr with pure chlorine gas flowing into the reactor at 35 cm³/s, using the chlorine plasma chemistry set described in [Section 4.4.5](#). The electron energy equation is solved, and there is consideration of heat loss through the wall of the reactor. The area used for surface chemistry and heat loss corresponds to the physical walls of the tubular reactor.

4.3.2.2 Project Setup

The project file is called **plasma_pfr_cl_power_profile.ckprj**. The data files used for this sample are located in the `samples2010\plasma_pfr\cl_power_profile` directory. This reactor diagram contains a gas inlet, a Plasma Plug Flow Reactor, and an outlet.

The reactant gas mixture is input on the Species-specific Property tab of the C1_Inlet1 panel. Although the input gas is actually pure Cl_2 , in order to have the plasma “light” in the simulation, we have modified the inlet gas to include a small amount of electrons and ions in the inlet gas.

The Reactor Physical Property tab of the C1_Plasma PFR panel is where problem type and reactor parameters such as pressure, temperatures, geometry, heat loss, and plasma power are entered. The value for the electron temperature input on the Reactor Physical Property tab of the C1_Plasma PFR panel is used as the inlet electron temperature. The plasma power profile can be entered by using the Profile tool or by selecting an existing profile file on the Reactor Physical Property tab of the C1_ panel. This is an alternative to entering a constant value for the Plasma Power Deposition parameter. The profile is entered as a list of pairs of numbers giving the power as a function of position. Values at intermediate points are straight-line interpolations of the two nearest specified values. Unphysically abrupt changes in the power profile can cause convergence problems in the simulation unless solver time steps are set accordingly. Note that the power deposition for a plug-flow reactor profile must be specified in per-distance units, as it will be integrated over the channel distance.

As a simulation that marches forward from the inlet state, this sample problem has no “initial guess” for the gas composition, but Surface Fractions are provided on the Species-specific Data tab of the C1_Plasma PFR panel. These site fractions provide initial estimates for the surface state of the channel inlet. An initial pseudo-steady calculation will be performed to determine consistent surface state based on these estimates and the inlet gas composition, prior to the channel integration. The Sheath Loss parameter on the Material-specific Data tab of the C1_Plasma PFR panel describes the ion energy gained crossing the sheath.

4.3.2.3 Project Results

Figure 4-29 shows the profile of electrical power deposited into the plasma as a function of distance down the Plug Flow Reactor. As expected, the mole fractions of the electrons and atomic chlorine, shown in *Figure 4-30* and *Figure 4-31*, respectively, generally follow the plasma power profile, with differing degrees of non-linearity. This is consistent with the fact that the Cl is created in the plasma by electron-impact dissociation of molecular chlorine. The mole fractions for the Cl^+ and Cl_2^+ ions, shown in *Figure 4-32* also follow the plasma power profile.

Figure 4-29 Spatial Chlorine Plasma—Plasma Power vs. Distance

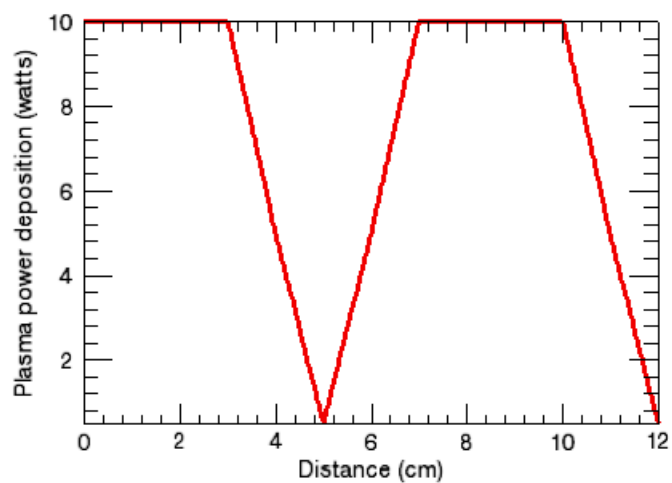


Figure 4-30 Spatial Chlorine Plasma—Electron Mole Fraction

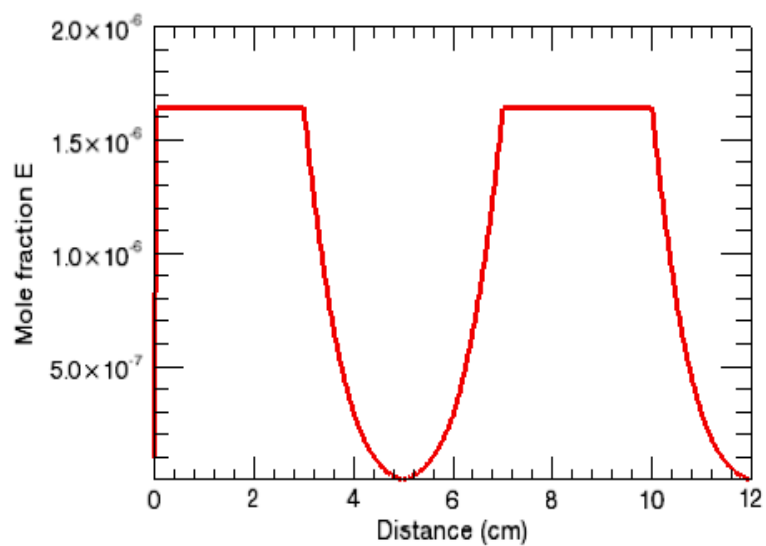
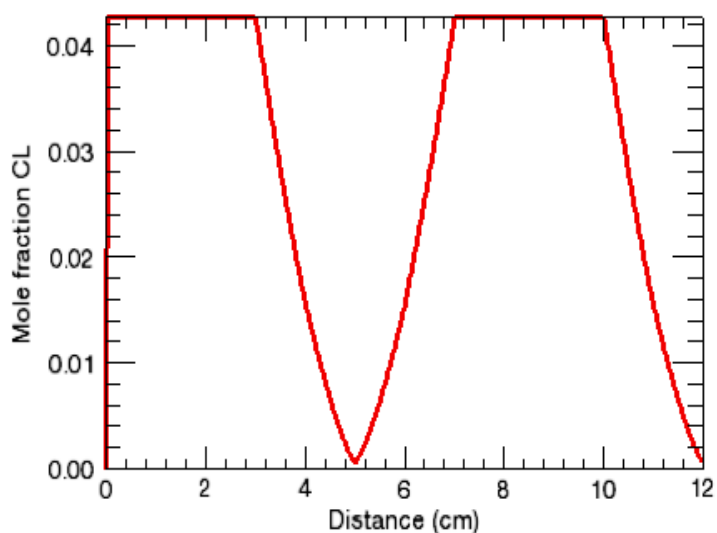
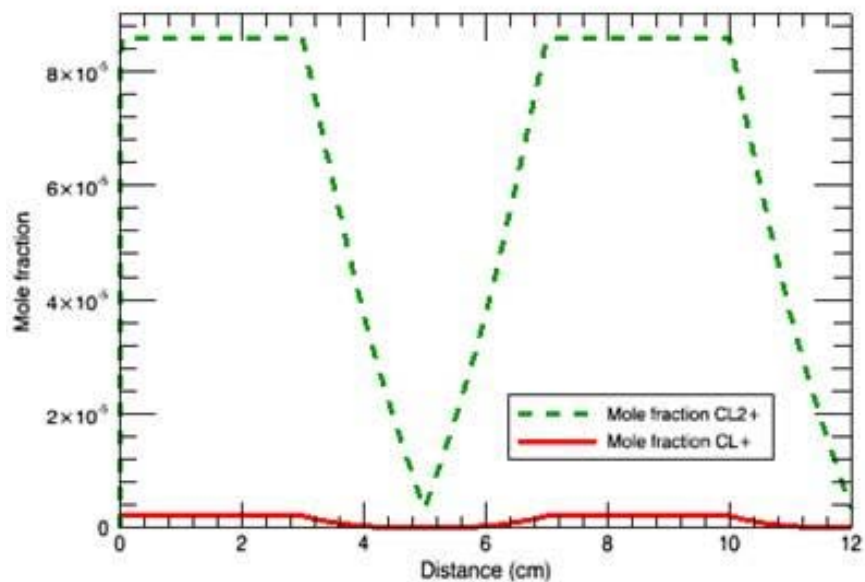
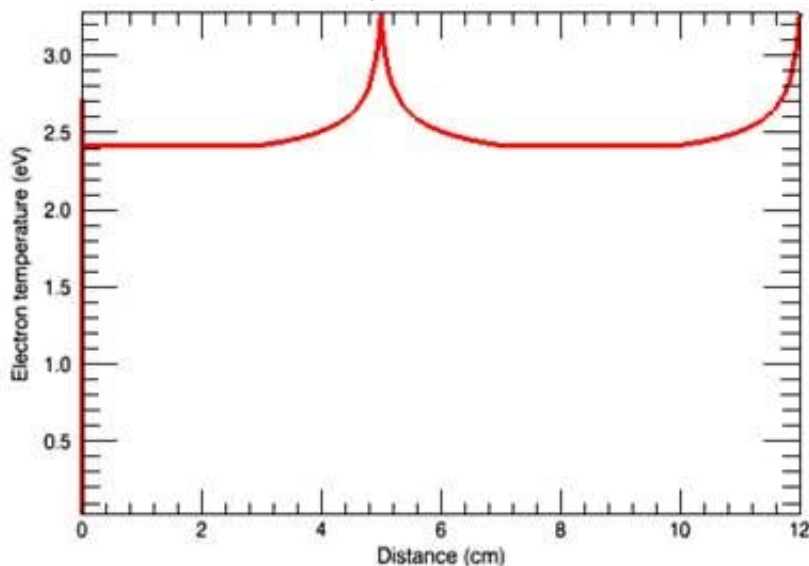


Figure 4-31 Spatial Chlorine Plasma—Cl Mole Fraction

Figure 4-32 Spatial Chlorine Plasma—Cl⁺ and Cl₂⁺ Mole Fractions

The electron temperature rises somewhat in the lower-power regions of the reactor tube. This is consistent with the inverse trend between electron densities and electron temperatures seen at low power densities in [Section 4.3.1](#).

Figure 4-33 Spatial Chlorine Plasma—Electron Temperature



4.3.3 Fluorocarbon Plasma Etching of Silicon Dioxide

4.3.3.1 Project Description

This user tutorial is an example of modeling a low-pressure plasma reactor as a steady-state Perfectly Stirred Reactor, using the fluorocarbon plasma chemistry set described in [Section 4.4.6](#). This example is representative of a high-density plasma, with a plasma power of 3000 Watts and a pressure of 10 mtorr. Pure hexafluoroethane is the inlet gas. The energy equation and the electron energy equation are solved, and a heat-transfer correlation is used to account for heat loss through the wall of the reactor. This example illustrates the use of multiple materials, each with a different set of surface reactions, as well as the use of continuations with varying flow rate and ion impact energy.

4.3.3.2 Project Setup

The project file is called ***plasma_psr_c2f6_et.ch.ckprj***. The data files used for this sample are located in the *samples2010\plasma_psr_c2f6_et.ch* directory. This reactor diagram contains a gas inlet and a plasma PSR.

The reactant gas mixture, which is pure C_2F_6 in this case, is input on the Species-specific Property tab of the C1_Inlet1 panel. The gas flow rate (30 sccm), inlet gas temperature and inlet electron temperature are input on the Stream Property tab of the R1_IN1 panel. The latter is required, but has little impact on the solution unless there are electrons in the input gas mixture.

The C1_ Plasma PSR panel is where most of the parameters are input. The Reactor Physical Property tab allows selection of problem type, as well as places to enter parameters such as the plasma power, pressure (10 mTorr), volume, internal area, heat loss parameters, cross-section for electron momentum loss, and initial guesses for the electron, neutral, and ion temperatures. The Species-specific Data tab allows input of initial guesses for the steady-state gas composition, surface site fractions, and bulk activities, on the corresponding sub-tabs, as well as species-specific values for electron-momentum loss cross-sections. A good initial guess for the gas and surface compositions (one that is close to the steady-state solution) will result in fast convergence, while a poor initial guess can lead to failure of the simulation. The Bulk-phase -specific Data tab is used to indicate that all the bulk materials are being etched, which affects some of the equations. The Material-specific Properties tab is for specifying properties like surface temperature (if different from the neutral gas temperature), ion energy or bias power, Bohm factor, sheath energy loss factor, area fraction, or heat loss, either for all materials, or on a per-material basis. For this non-parameter-study problem, the bottom part of the panel is used to set up values that are dependent on the material. Material-independent properties can be set on the Reactor Physical Properties panel. In this example, the WAFER is held at a temperature near room temperature (consistent with active cooling), while the TOPWALL is held at an elevated temperature (consistent with active heating), while the SIDEWALL temperature is allowed to float with the gas temperature (the default). A relatively high ion energy (in electron Volts) is specified for the WAFER, reflecting that this material substrate has an applied electrical bias, separate from the main power, for this system. The low ion energy for the SIDEWALL is consistent with the plasma self-bias, rather than active biasing of this surface. The TOPWALL has no ion energy specified, as no ion-energy dependent reactions occur on this material.

On the Solver panel, a number of parameters on both the Basic and Advanced tabs have been altered from the defaults in order to help get a good solution. Skipping the intermediate fixed-temperature solution is the default for plasma simulations and is recommended. The Output Control panel allows specification of whether sensitivities should be calculated and printed in the output and solution files, and whether ROPs should be printed and saved. In this case, sensitivities for temperature, growth (etch) rate, F atoms and SiF₄ will be calculated. ROPs for 6 species will be included. The Continuations panel specifies two continuations. First, the ion energy for the wafer is changed from 200 to 300 V, and the flow rate is increased from 30 to 50 sccm. Second, the flow rate is returned to the initial lower value, while leaving the ion energy at the higher value. In this example, the plasma power is entered on both continuation panels, although it is not changed. This is not necessary, but will not cause any problems and may serve as a useful reminder.

4.3.3.3 Project Results

In [Figure 4-34](#), the SiO_2 etch rates for variations of C_2F_6 flow rate and Wafer ion energy are: 1) 30 sccm, 200 V. 2) 50 sccm, 300 V. 3) 30 sccm, 300 V. This shows that oxide etch rates (negative growth rates) on the Wafer are much larger than those on the Sidewall, in accord with the higher ion energy for that material. Comparing solutions 1 and 3 shows that increasing the Wafer ion energy increases the etch rate, as expected. But comparing solutions 2 and 3 shows that increasing the reactant flow rate also increases the etch rate, indicating that the etching system may be reagent-supply limited. This is consistent with the results shown in [Figure 4-35](#), which shows the 10 neutral species with the highest mole fractions. C_2F_6 , the reactant species, does not appear, as it is mostly decomposed to smaller fragments in the plasma. The species with the highest mole fraction, F atoms, is a reactant fragment that can contribute to etching, as are CF and CF_3 , which are also present in relatively high concentrations. These species have higher mole fractions in solution 2, which has the highest flow rate, whereas etch-product species, such as CO and SiF_3 , have lower mole fractions at the shorter residence time. [Figure 4-36](#) shows that CF^+ is the most prevalent positive ion, with F^+ , CF_2^+ and CF_3^+ about a factor of 2 lower. There is less F^+ than CF^+ , even though there is more F than CF, and the major pathways producing F^+ and CF^+ are ionization of F and CF, respectively. This reflects a higher rate for the CF ionization reaction than the F ionization reaction. Although not shown, the electron is the most prevalent negatively charged species, with CF_3^- roughly a factor of 6 lower. Negative ions stay in the body of the plasma and do not participate in reactions at the surface due to the presence of an electronegative sheath.

Figure 4-34 Fluorocarbon Plasma Etching of Silicon Dioxide— SiO_2 Etch Rates Variations

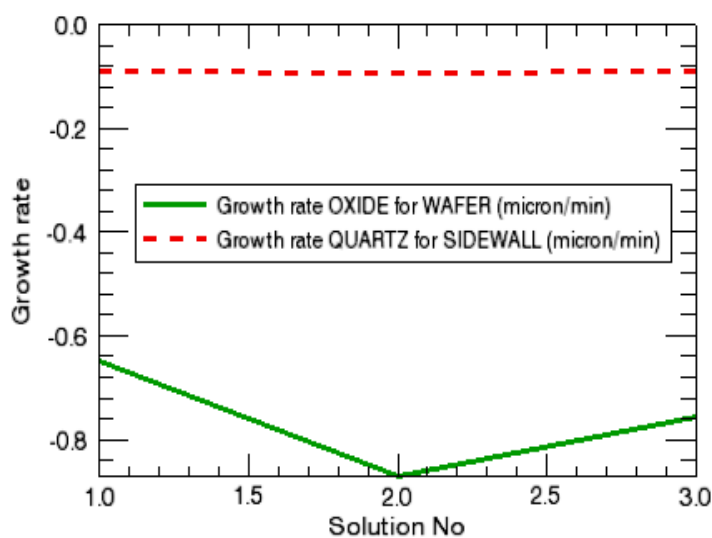


Figure 4-35 Fluorocarbon Plasma Etching of Silicon Dioxide—10 Highest Mole Fractions

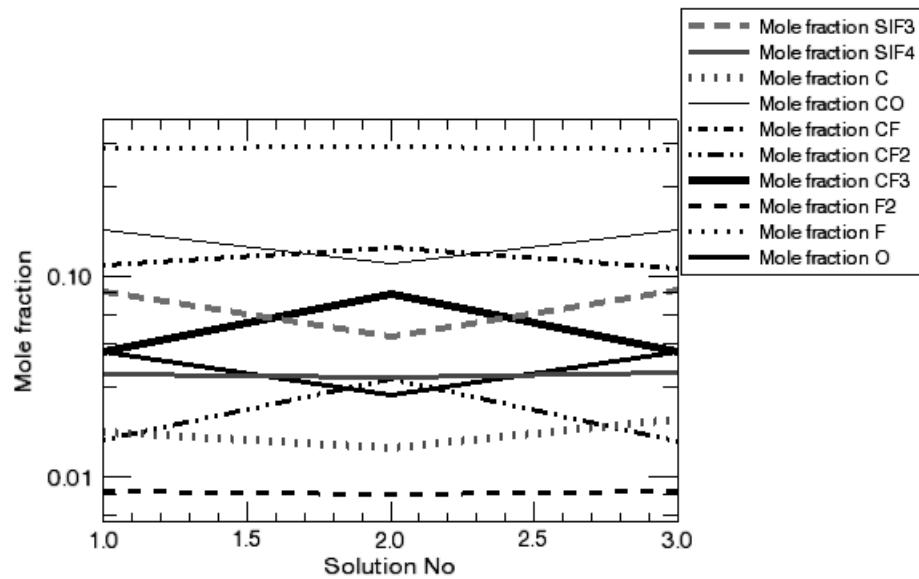
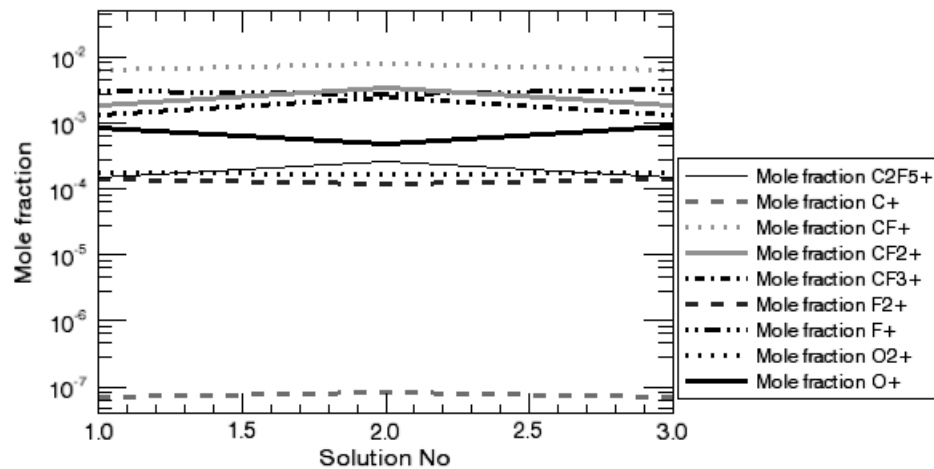


Figure 4-36 Fluorocarbon Plasma Etching of Silicon Dioxide—Positive Ion Mole Fractions



The surface site fractions shown in [Figure 4-37](#) show minor changes with conditions. Comparing solutions 1 and 3 shows that increasing the Wafer ion energy increases the fraction of open sites and decreases the fraction of fluorocarbon-covered sites. This is consistent with the increased ion energy causing an increase in yield for the ion-enhanced etching reactions. Comparing solutions 3 and 2 shows that increasing the C₂F₆ flow rate decreases the fraction of open sites and increases the fraction of fluorocarbon-covered sites. This is consistent with an increased supply of fluorocarbon radicals that can react with the open sites. [Figure 4-38](#) shows the 5 reactions with the largest contribution to the loss of silicon dioxide from the wafer. In order of decreasing importance, surface reactions 13, 14, 11, and 12 are etching of

WSIO₂_CF₂(S) sites assisted by CF⁺, F⁺, CF₂⁺, and CF₃⁺, respectively. Reaction 5 is the F⁺ ion-assisted etching reaction of the WSIO₂_F₂(S) site. These five reactions are responsible for most of the etching, but a number of other reactions contribute to the total etch rate.

Figure 4-37 Fluorocarbon Plasma Etching of Silicon Dioxide—Surface Site Fractions

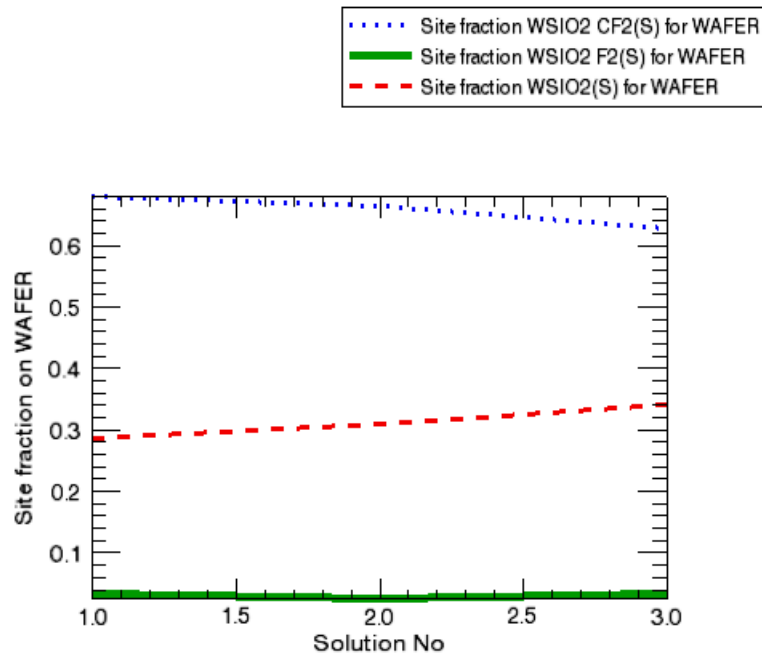
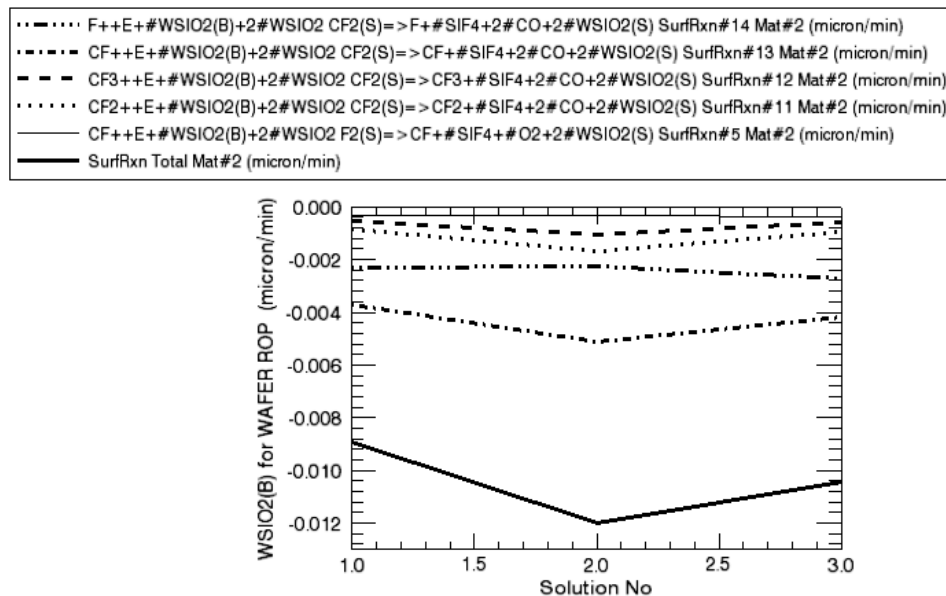


Figure 4-38 Fluorocarbon Plasma Etching of Silicon Dioxide—Highest ROP



4.4 Chemistry Sets

In this section, we describe in more detail the chemistry sets employed in the tutorials described in [Chapter 4](#).

4.4.1 Silicon Nitride CVD from Silicon Tetrafluoride and Ammonia

This chemistry set describes the deposition of silicon nitride (Si_3N_4) from a mixture of SiF_4 and NH_3 .⁴⁵ This mechanism demonstrates one way of describing the deposition of a compound solid, but it should generally be considered as illustrative only and not as a source of kinetic data for Si_3N_4 deposition.

The *chem.inp* file includes 4 elements, 17 gas-phase species and 33 reactions. The first 27 of these reactions describe the pyrolysis of ammonia, and are taken from published models for ammonia oxidation and De-NOx.⁴⁶ The other 6 reactions describe SiF_4 decomposition and likely cross reactions between Si and N-containing species. Rate parameters were not available in the literature for these reactions, so the mechanism uses estimates based on bond strengths and analogies with related gas-phase reactions.

The *surf.inp* file defines six surface species in the Si_3N_4 surface phase and the Si_3N_4 solid, which is defined in terms of two bulk phases, Si(D) and N(D). The surface species all occupy more than one site, and have placeholder thermodynamic data. Six irreversible surface reactions are also defined in this file. The surface reactions are “lumped” reactions, meaning that they each represent several elementary steps that have been combined into one reaction. Rate parameters for these surface reactions were determined by fitting the model results to experimental deposition-rate data. The activation energies for the surface reactions are all zero, which reflects the limitations of the experimental data set used to derive the rate parameters. Although it is not immediately obvious, the surface species and reactions were designed to produce a bulk-phase stoichiometry of 3 Si to 4 N. The densities of bulk species has been defined to force the linear deposition rates of either Si(D) or N(D) match the experimentally observed deposition rate for Si_3N_4 . These reactions have zero for activation energies because they were fit to an experimental data set taken at one temperature. These rates would therefore not be likely to be valid at other temperatures.

45. M. E. Coltrin, P. Ho, Sandia National Laboratories, private communication.

46. J. A. Miller, M. D. Smooke, R. M. Green, and R. J. Kee, *Comb. Sci. Technol.* **34**:149 (1983).

4.4.2 Silicon Deposition from Silane

This chemistry set described the CVD of silicon from silane. This CVD system has been the subject of numerous studies, facilitated by the simplicity of the precursor molecule. This reaction mechanism was published by Coltrin and coworkers at Sandia National Laboratories in the last⁴⁷ of a series of papers. This mechanism has been validated with a variety of optical diagnostic measurements and deposition rate data in a variety of experimental reactor geometries.

The *chem.inp* file includes 3 elements (helium is used as a carrier gas), 9 gas-phase species, and 10 reversible gas-phase reactions. Many of the reactions are unimolecular decomposition reactions with explicit treatment of pressure dependent rate parameters. The most important reaction is the decomposition of SiH_4 to SiH_2 and H_2 . The other reactions include the reaction of SiH_2 with SiH_4 to form Si_2H_6 , which can then react again to form Si_3H_8 , or decompose to H_3SiSiH and H_2 . Other reactions involve interconversion between various silicon-hydride species, plus the formation of atomic silicon, which was one of the experimentally measured species. This mechanism was originally much larger, but over time, it was substantially reduced by the elimination of species and reactions deemed to be unimportant.

The *surf.inp* file includes two surface species, open Si sites and hydrogen covered silicon sites, plus solid silicon as a bulk species. There are 8 surface reactions, all written as irreversible reactions with placeholders for the thermodynamic data of the surface species. These reactions include the two-site dissociative adsorption of silane, disilane and trisilane, which form hydrogenated silicon sites, deposited bulk silicon, and H_2 . Collisions of Si atoms, SiH_2 , H_3SiSiH and H_2SiSiH_2 species with the surface result in deposition of bulk silicon and formation of gas-phase H_2 with unit probability. Adsorbed hydrogen is removed from the surface by the associative desorption of H_2 , where a coverage dependence parameter has been used to alter the default second-order dependence to the experimentally observed first order.

4.4.3 Silicon Deposition from Trichlorosilane

This chemistry set describes the deposition of silicon from trichlorosilane in a hydrogen carrier gas. This mechanism is built on a significant number of independently published chemical kinetic parameters, and is described in more detail in a publication by Ho, *et al.*⁴⁸

47. "Laser-Induced Fluorescence Measurements and Kinetic Analysis of Si Atom Formation in a Rotating Disk Chemical Deposition Reactor", P. Ho, M. E. Coltrin, W. G. Breiland, *J. Phys. Chem.* **98**: 10138 (1994), and references therein.

The *chem.inp* file includes 3 elements, 11 gas-phase species, and 9 reversible gas-phase reactions. The gas-phase reactions are reversible decomposition reactions of various chlorosilanes and chlorinated disilanes. These reactions cause the conversion of some of the initial chlorosilane starting material to these other gas-phase species, which can be significant because the less-chlorinated molecules have higher surface reactivities. These reactions are written as unimolecular decomposition reactions at their high-pressure limit, so this reaction mechanism would tend to overstate the importance of gas-phase chemistry if it were used at lower total pressures.

The *surf.inp* file has 3 surface species: open silicon surface sites, hydrogen-covered sites, and chlorine-covered sites, plus solid silicon as a bulk phase. There are 10 surface reactions, all written as irreversible reactions with placeholders for the thermodynamic data of the surface species. These reactions include the dissociative adsorption of SiCl_3H , SiCl_2H_2 and SiCl_4 , which result in the formation of deposited silicon and hydrogenated/chlorinated silicon surface species. These are “lumped reactions” to the extent that the initial adsorption event, plus the successive transfer of H and Cl atoms from the initially adsorbed Si to other surface Si atoms, are all described as one step. The physical interpretation of this “lumping” is that adsorption of the gas-phase species is assumed to be slow compared to subsequent transfer of H and Cl atoms on the surface. For a chemically balanced reaction, this is written as involving 4 open sites, which by default would make the reaction fourth order in open sites, so the coverage dependence option has been used to set the kinetics to a more reasonable first-order dependence. Other reactions include the dissociative adsorption and associative desorption of H_2 , HCl and SiCl_2 , plus the dissociative adsorption of HSiCl. In many cases, the rate parameters are based on experimental surface-science studies, in other cases they are the result of fitting a model to experimental silicon deposition rate data from a specific CVD reactor.

4.4.4 Alumina ALD

This chemistry set describes the atomic layer deposition (ALD) of alumina from trimethylaluminum (TMA) and ozone. This mechanism is deliberately simplistic for illustration purposes only. It demonstrates one way of describing the ALD of alumina, but it should generally be considered as illustrative only and not used as a source of kinetic data for this process. This mechanism is designed to deposit stoichiometric

48. “Chemical Kinetics for Modeling Silicon Epitaxy from Chlorosilane”, P. Ho, A. Balakrishna, J. M. Chacin, A. Thilderkvist, B. Haas, and P. B. Comita, in “Fundamental Gas-Phase and Surface Chemistry of Vapor-Phase Materials Synthesis”, T. J. Mountziaris, M. D. Allendorf, K. F. Jensen, R. K. Ulrich, M. R. Zachariah, and M. Meyyappan, Editors, PV 98-23, p. 117-122, Proceedings of the 194th Meeting of the Electrochemical Society, 11/1-6/98, The Electrochemical Society Proceedings Series, Pennington, NJ (1999).

alumina, with three oxygen atoms being deposited for each two aluminum atoms. If the goal of a simulation was to track the elemental make-up of a material with a wide range of possible compositions, the choice of surface species and reactions would have to be quite different.

The fact that the different chemicals are separately pulsed into the system, rather than being mixed in the gas, prevents many possible gas-phase reactions from occurring in this process. The gas-phase chemistry described in the *chem.inp* file has 5 elements: Al, C, H, O, and Ar; and 6 gas-phase species: AlMe_3 , O, O_2 , O_3 , C_2H_6 and Ar. There are only two gas phase reactions; the collisionally-induced decomposition of ozone and the reaction of O atoms with ozone to form molecular oxygen. The rate parameters are from Benson and Axworthy.⁴⁹ This mechanism does not include reactions for TMA decomposition because it was determined to be too slow at the temperatures of interest. But if such reactions were included, they would be listed in the same chemistry input file. The temporal separation of the gas mixtures is accounted for by omitting reactions between gas-phase species that would not be present in the reactor at the same time, such as reactions between TMA and O atoms. A reaction mechanism for alumina CVD, in contrast, would need to include all such reactions.

The surface chemistry described in the *surf.inp* file defines three surface species: O(S), ALME2(S) and ALMEOALME(S); where the last species occupies two surface sites, plus the bulk alumina AL2O3(B). There are only three surface reactions, each of which represents several elementary surface processes. The first surface reaction represents the dissociative adsorption of TMA on the oxygenated surface species O(S) to form the ALME2(S), combined with the recombination of two methyl groups and desorption of an ethane molecule. This reaction has been given a moderately high sticking coefficient of 0.1, and is written in terms of a half ethane molecule in order to have a balanced reaction that is first order in TMA. This reaction only occurs in the presence of TMA, and will terminate when all of the O(S) surface species have reacted. The second surface reaction describes gas-phase oxygen atoms reacting with the two ALME2(S) to form the ALMEOALME(S) species and a gas-phase ethane molecule. The third surface reaction describes an O atom reacting with the ALMEOALME(S) species to deposit AL2O3(B), regenerate O(S), and form gas-phase ethane, where fractional molecules are used to write balanced reactions. Oxygen atoms are expected to be very reactive, so these reactions have been given high sticking coefficients of 1.0. These reactions only occur in the presence of O atoms generated from ozone decomposition, and will terminate when all the methylated

49. S. W. Benson and A. E. Axworthy, Jr., *J. Chem. Phys.*, **26**:1718 (1957).

surface species have reacted. All the surface reactions are irreversible. As a result, the thermodynamic properties for surface species provide the elemental composition of the surface species, but the polynomial fitting parameters are merely placeholder values.

4.4.5 Chlorine Plasma

This chemistry set is for a pure chlorine plasma without surface etching reactions that is based on work published by Meeks and coworkers.^{50, 51}

The gas-phase chemistry in the chlorine plasma is relatively simple. The element list contains 3 elements: E (the electron), Cl and Si. Si does not actively participate in any chemical reactions, as it only appears in *surf.inp* in the composition of surface species on the wall material, but it still needs to be included in the element list in the GAS-PHASE KINETICS input file. The gas-phase species list contains seven species: Cl₂, Cl, Cl* (chlorine atoms in a metastable electronically excited state), Cl₂⁺, Cl⁺, Cl⁻ and E. The gas-phase reactions include electron collisions with Cl₂ leading to vibrational and electronic excitation, dissociation, ionization, and dissociative attachment. Electron reactions with Cl include electronic excitation into a number of excited states, including Cl* formation, and ionization. The gas-phase reaction mechanism also includes electron collisions with Cl⁻ leading to electron detachment, electron collisions with Cl* leading to ionization, and gas-phase neutralization of Cl⁻ with Cl⁺ and Cl₂⁺ ions. All the reactions are irreversible as is typical of non-thermal plasmas. In low-pressure plasmas, ionization and dissociation are balanced primarily by surface recombination reactions. The rates for the electron-impact reactions depend on the electron energy, rather than the neutral gas temperature.

The surface mechanism for reactions occurring on the reactor wall is also fairly simple. It only involves neutralization of Cl⁺ and Cl₂⁺ with electrons (subject to the Bohm criterion), de-excitation of Cl* and radical recombination reactions for Cl to Cl₂. The neutralization and de-excitation reactions are non-site specific, but the recombination reactions are described in terms of open and Cl covered sites. Although this example problem does not include surface etching reactions, surface recombination and neutralization reactions can be quite important in determining the

50. "Modeling of Plasma-Etch Processes Using Well Stirred Reactor Approximations and Including Complex Gas-Phase and Surface-Reactions", E. Meeks and J. W. Shon, *IEEE Transactions On Plasma Science*, **23**(#4):539-549 (1995).

51. "Effects of Atomic Chlorine Wall Recombination: Comparison of a Plasma Chemistry Model With Experiment," E. Meeks, J. W. Shon, Y. Ra, P. Jones, *JVSTA* **13**(#6):2884-2889 (1995).

overall composition of these kinds of low-pressure plasmas. All the surface reactions are irreversible. The thermodynamic properties for surface species, therefore, provide the elemental composition of the surface species, but the polynomial fitting parameters are considered placeholder values and are not used in the simulation.

4.4.6 Fluorocarbon Plasma with SiO₂ Etch Products

This chemistry set is for a fluorocarbon plasma (C₂F₆) used for etching silicon dioxide films, a process that is used in the fabrication of microelectronic and MEMS devices. The chemistry set includes detailed surface reactions, including multiple materials with different reaction sets. Although it is quite complex, this mechanism is actually a small, early version of a more complete mechanism developed by Meeks and coworkers for etching several fluorocarbon precursors. Detailed descriptions of the full mechanisms, including information on the sources of rate parameters, can be found in their publications.^{52, 53, 54}

The gas-phase chemistry described in the *chem.inp* file involves 6 elements, 36 species, of which there are 9 positive ions, 3 negative ions, the electron, and 23 neutral species. There are 149 gas-phase reactions. Of these, 75 are electron-impact reactions leading to dissociation, dissociative ionization, attachment, vibrational and electronic excitation. Such reactions are included for the starting reactant C₂F₆, dissociation fragments such as CF₃ and CF₂, as well as etching products such as O₂ and SiF₄. The electron-impact reactions are all irreversible, and the rates depend on the electron energy, rather than the neutral gas temperature. There are 22 irreversible reactions describing the neutralization between positive and negative ions in the gas phase. Such reactions have high A-factors and are not energy dependent. The remaining 46 reactions are reactions of neutral gas-phase species, mostly reversible, some with explicitly specified reverse reaction rates. Many of the reactions include the participation of new specific collision partners (M), and a number of the unimolecular decomposition/bimolecular recombination reactions have detailed descriptions of the pressure dependence of the rate parameters.

52. "Modeling the Plasma Chemistry of C₂F₆ and CHF₃ Etching of Silicon Dioxide, with Comparisons to Etch Rate and Diagnostic Data", P. Ho, J. E. Johannes, R. J. Buss, and E. Meeks, *J. Vac. Sci. Technol. A* **19**:2344 (2001).

53. "Plasma Modeling", E. Meeks and P. Ho, Chapter 3 in "Advanced Plasma Processing Technologies", edited by R. J. Shul and S. J. Pearton, Springer-Verlag, Heidelberg, (2000).

54. "Chemical Reaction Mechanisms for Modeling the Fluorocarbon Plasma Etch of Silicon Oxide and Related Materials", P. Ho, J. E. Johannes, R. J. Buss and E. Meeks, Sandia National Laboratories Technical Report No. SAND2001-1292.

The surface chemistry described in the surf.inp file involves three materials with different reaction sets. The different materials in the model correspond to different physical parts of a plasma reactor that are all exposed to the plasma, but are affected by the plasma in different ways. The material called `SIDEWALL` and the material called `WAFER` are both silicon dioxide. The wafer is expected to have an applied electrical bias, resulting in higher ion energies. It thus has a more extensive set of reactions, especially ion-enhanced chemical reactions that result in etching. Although both sets of reactions describe the chemical species in the plasma interacting with silicon dioxide, the mechanism description needs to have unique names for the two sets of materials, surface sites, surface species, and bulk species to allow for different reaction sets. The material `SIDEWALL` has a surface site called `GLASS` with species `SIO2(S)` and `SIO2_F2(S)`, and a bulk phase `QUARTZ` with a bulk species `SIO2(B)`. The material `WAFER` has a surface site called `AMOXIDE` (for amorphous oxide) with species `WSIO2(S)`, `WSIO2_F2(S)`, and `WSIO2_CF2(S)`, and a bulk phase `OXIDE` with a bulk species `WSIO2(B)`. In the species names, the (S) is a convention often used to indicate a surface species, the `_F2` and the `_CF2` indicate a surface silicon oxide site with two F atoms or a C atom and two F atoms bonded to it, respectively, and the (B) indicates a bulk species. All the surface reactions are irreversible. All ion-surface reactions are subject to the Bohm flux criterion.

There are 31 surface reactions for the material `WAFER`. First there is a reaction describing the spontaneous etching of silicon dioxide by F atoms, and a reaction describing the adsorption reaction of F atoms with an open-site surface species to form a fluorinated surface species. There are 5 reactions describing the ion-enhanced etching of SiO_2 from the fluorinated surface species, producing SiF_4 and O_2 as etch products, and regenerating the open `SIO2(S)` species. These reactions have yields (number of surface sites converted per ion) that depend on the ion energy, as well as overrides of the default order of the reaction. More details about these features are provided in the input manual. Next are reactions describing the adsorption of CF_x radicals to form the `WSIO2_CF2(S)` species, and 5 reactions describing the ion-enhanced etching of SiO_2 from the fluorocarbon-covered surface species, producing SiF_4 and CO as etch products, and regenerating the open `SIO2(S)` species. These reactions also have ion energy dependent yields and overrides of the default order of the reaction. There are 9 reactions describing ion-neutralization with electrons on the surface, plus 7 reactions describing the direct sputtering of SiO_2 by ions.

The reaction set for the material `SIDEWALL` is a 16 reaction subset of that for the material `WAFER`, but with the appropriate species names. The material called `TOPWALL` is defined as silicon with two surface species. However, the reactions consist only of non-site specific neutralization reactions of positive ions with electrons.

5 Chemical Mechanism Analysis

5.1 Mechanism Analyzer

In the CHEMKIN software, the specification of the chemical reaction rates and thermochemical data is necessarily very compact and efficient. As a result, however, the information that might be most useful to a user in developing or analyzing a reaction mechanism is often not readily available because it is “hidden” in the terse Pre-processor input files. One example is rate information about the reverse rate of a reversible reaction, which is not easily determined by examining the chemistry input or output files. Other examples would be the free energy or enthalpy change associated with a particular reaction, or the relative rates of two reactions for a specific set of conditions. Another category of information that could be useful to extract from a CHEMKIN mechanism are simple measures of transport rates, expressed in terms of dimensionless numbers, or quantities such as the pure species viscosity, pure species thermal conductivity, or binary diffusion coefficient for various gas-phase species in the mechanism.

The Mechanism Analyzer provides a means to obtain this type of information, without requiring the user to do any programming. It presents, in tabular and graphical form, detailed information about the temperature and pressure dependence of chemical reaction rate constants and their reverse rate constants, reaction equilibrium constants, reaction thermochemistry, chemical species thermochemistry and transport properties. In general, the user will want to select only a few of the many types of information to be calculated and output, but there is a great deal of flexibility in specifying the desired output. The current version does not, however, handle all of the special rate options available in GAS-PHASE KINETICS and SURFACE KINETICS. Specifically, it does not consider: (1) user-provided rate routines, (2) rate-order

changes, (3) options associated with modeling plasma reactions, (4) the Chebyshev polynomial option for describing pressure-dependent gas-phase reactions, the (5) Landau-Teller rate formulation used for energy transfer processes, or (6) multiple materials. If such options are included in a reaction mechanism, they will be ignored.

5.1.1 Background Information

5.1.1.1 Bath Gas and Carrier Gas

The concept of a “bath gas” is used throughout the Mechanism Analyzer. The specification of a bath gas consists of a characteristic temperature, pressure, and composition at which quantities are to be evaluated by default. Composition, here, refers to the default composition for all phases defined in the mechanism. Reaction rate information is evaluated at the bath gas conditions, unless it is tabulated as a function of a system parameter, such as temperature. In this case, all other parameters are fixed at the bath gas conditions in the table. The default temperature for the bath gas is 298.15 K. The default pressure is 1 atmosphere, and the default composition is an equimolar composition in each phase. All defaults can be overridden by selections in the CHEMKIN Interface input panels.

The concept of a “carrier gas” is also used in the Mechanism Analyzer. Unless overridden, the carrier gas is assumed to be the gas component having the largest mole fraction. CHEMKIN calculates a single number for the characteristic time scale of diffusion (to be compared with the characteristic time scale of reaction). To make this comparison, the diffusion coefficient is calculated for a specified “major” species in the carrier gas. For example, the diffusion of the major species CH₄ in the carrier gas H₂ is used to calculate the characteristic diffusion time scale. Unless overridden, the major species in the gas phase is assumed to be the gas component having the second largest mole fraction.

5.1.1.2 Uniform-dimensional and Non-dimensional Reaction Rate Information

It is often useful to know, in some sense, which reactions in a mechanism are “fast” and which are “slow.” It is difficult or misleading to simply compare rate constants, which can have different units depending on the molecularity of the reaction. In order to compare the rates of reactions in the mechanism, we define a quantity

Equation 5-1

$$k_f^* = k_f [G]^g \prod_n [S_n]^{s_n}$$

which we call the “uniform-dimensional” rate constant. Regardless of the order of reaction, it will have units of mole • cm⁻³ • sec⁻¹ for a gas-phase reaction or mole • cm⁻² • sec⁻¹ for a surface reaction. In this expression, k_f is the rate constant for the forward reaction, $[G]$ is the total concentration of gas-phase species determined at the bath gas conditions (in mole • cm⁻³), g is the sum of the stoichiometric coefficients of all gas-phase species appearing as reactants in the reaction, $[S_n]$ is the total site density of surface phase n determined at the bath gas conditions, S_n is the sum of the stoichiometric coefficients of all surface species in phase n participating as reactants in this reaction.

Using the usual rate constant, one calculates the forward reaction rate as k_f times the product of the concentrations of the reactant species (in mole • cm⁻³ for gas species, or mole • cm⁻² for surface species) raised to the power of their stoichiometric coefficients. With the uniform-dimensional rate constant, one calculates the same reaction rate as k_f^* multiplied by the (dimensionless) species mole fractions (gas-phase reactants) or site fractions (surface species) raised to the power of their stoichiometric coefficients. Thus, independent of the molecularity of the reaction, the reaction rate is k_f^* times quantities that have maximum values on the order of unity (the mole and site fractions), and it is easier to compare one reaction to another.

The quantity k_f^* just discussed can point out which reactions are fast relative to one another. It can also be of interest to know if a reaction is “fast” relative to a competing process like molecular transport. The Damköhler number for gas-phase reactions, Da , allows for such a comparison.

Equation 5-2

$$Da = \frac{k_f^*}{D[G]/L^2}$$

In [Equation 5-2](#), D is a diffusion coefficient and L is a characteristic length scale for diffusion; for example, a boundary-layer thickness or a characteristic reactor dimension. The Damköhler number is a dimensionless number that is a measure of the relative importance of gas-phase kinetics versus molecular mass transport. If Da is much greater than 1, then a reaction is fast relative to transport; if it is much less than 1, then transport processes occur on a shorter time scale than kinetic processes.

One must supply a diffusion coefficient in [Equation 5-2](#) to evaluate Da . To do this, the Mechanism Analyzer requires the user to name a “major species” and a “carrier gas species.” Through internal calls to the TRANSPORT Subroutine Library, CHEMKIN evaluates the binary diffusion coefficient between these two species at the specified bath temperature and pressure. The user may also specify the length scale L . The default value for L is 1 cm.

For each gas-phase reaction, a report is generated of k^* and Da for the forward and reverse directions. In some cases, the input reaction mechanism specifies the reaction to be irreversible. In these cases, the quantities k^* and Da are still calculated for the reverse direction, but the numbers are enclosed in square brackets [] to flag these reactions as not being part of the mechanism.

A uniform-dimensional rate constant of [Equation 5-1](#) is also calculated for surface reactions. In this case, k_f^* has units of $\text{mole} \cdot \text{cm}^{-2} \cdot \text{sec}^{-1}$. Thus, one can make a comparison between reaction rates for surface reactions. The surface Damköhler number is defined to be

Equation 5-3

$$Da = \frac{k_f^*}{D[G]/L}$$

The equation for the surface Damköhler number differs from the equation for the gas-phase Damköhler number by a factor of the length scale L . As before, it provides a measure of the relative speed of the surface reaction rate versus the molecular mass transport rate.

5.1.2 Reaction Mechanism for Diamond CVD

5.1.2.1 Project Description

This user tutorial demonstrates the use of the Mechanism Analyzer model to extract a wider variety of detailed thermodynamic, chemical kinetic, and transport data from a reaction mechanism. The chemistry set nominally describes a diamond CVD process and is a subset of a published mechanism,⁵⁵ but one that has now been superseded by the authors.⁵⁶ The reactions in this example, especially the surface reactions, have been contrived to demonstrate the capabilities of the Mechanism Analyzer and should not be used as a source of kinetic data for diamond deposition.

55. “Analysis of diamond growth in subatmospheric dc plasma-gun reactors.” Michael E. Coltrin and David S. Dandy, *Journal of Applied Physics*, **74**(#9):5803 (1993).

5.1.2.2 Project Setup

The project file is called *mechanism_analyzer__diamond_cvd.ckprj*. The data files used for this sample are located in the *samples2010\mechanism_analyzer\diamond_cvd* directory. This reactor diagram contains only the Mechanism Analyzer. [Section 5.1.2.3](#) illustrates which sections of the output result from which choices on the input panels, so only brief usage instructions are provided here.

The Output Control tab of the Output Control panel contains a number of selections that determine the kinds of information that will be put into the output file and XML Solution File (*XMLdata.zip*). At the top of the Output Control tab, there is a choice to turn All Tables On or Off. Turning All Tables On will result in a very large output file, so this is generally **not** recommended, except for the smallest reaction mechanisms. The usage of these controls is as follows. To obtain All output of a certain type, turn it On at the highest level. To limit the output of a certain type to specific species or reactions, turn it Off at the higher level(s), then On for the class (gas, surface or bulk) of species/reactions or by listing the specific species/reactions of interest.

As an illustration of how to use the levels of choices to specify data types, consider the case of thermodynamic data tables. There are two types of data tables available: summary tables which are given at the bath gas conditions, and detailed tables which cover a range of temperatures. In this example, the Summary Thermo Tables are turned Off in general, but then back On for Species, but not for Reactions. Turning All Summary Thermo Tables On is equivalent to checking all three boxes, but is simpler. In the case of the more detailed Species Thermo Tables, they are turned Off in general, and On for the Bulk species only. In addition, on the Species-specific Data panel, Species Thermo Tables are specified for two gas phase species, CH₃ and CH₄, plus two surface species, CH₂(S) and CH(S). The results of these selections are shown in [Section 5.1.2.3](#). For reaction information, most of the output types are turned On at the general level, so there are no entries on the Reaction-specific Data tab of the Output Control panel.

56. The authors now prefer the mechanism in: "A simplified analytical model of diamond growth in direct current arcjet reactors." David S. Dandy and Michael E. Coltrin, *Journal of Materials Research*, **10**(#8):1993 (1995). Private communication, M. E. Coltrin, Feb. 1998.

The C1_ Mechanism Analyzer panel allows specification of the physically based parameters that affect the output file. The Reactor Physical Property tab allows the user to override the default values for pressure and temperature of the bath gas, as well as the ranges used for the thermodynamics and kinetics tables. The Species-specific Data tab allows specification of the composition of the bath gas, as well as overriding the default definitions for the carrier gas and major species. No entries are made on the Cluster Properties, Solver, or Continuations panels for this problem.

5.1.2.3 Project Results

Although an XML Solution File is created and the graphical CHEMKIN Post-Processor can be used for viewing the results, the output file is generally the more useful form of output for this application, as the user is generally looking for values of specific chemical or transport parameters. This section reproduces the Mechanism Analyzer diagnostic output file, which has been augmented in a number of places by comments in larger font. The information in the tables is generally self-explanatory, so these comments general deal with the input controls that produce that section of output.



The output file first echoes the input file created by the CHEMKIN Interface.

```
*****
*                   CHEMKIN-PRO Release 15101                   *
*                   SURFTHERM Application                       *
*                   REACTION MECHANISM ANALYSIS                 *
* Copyright(c) 1997-2009 Reaction Design. All Rights Reserved. *
*****
```

WORKING SPACE REQUIREMENTS		
	PROVIDED	REQUIRED
LOGICAL	54	54
INTEGER	1009	1009
REAL	2443	2443
CHARACTER*16	43	43
CHARACTER*64	10	10

```
Initializing CHEMKIN Gas-phase Library a component of CHEMKIN-PRO Release 15101, Build date: Aug 17, 2010
This and All Other CHEMKIN(R) Libraries are Copyright (c) 1997-2009 Reaction Design. All rights reserved.
```

LICENSE INFORMATION:

```
LicNum: 9555
Licensed to Reaction Design
Contact: A. User
Expiring: 03-feb-2011
Platform: win64
```

```
Initializing SURFACE CHEMKIN Library a component of CHEMKIN-PRO Release 15101, Build date: Aug 17, 2010
This and All Other CHEMKIN(R) Libraries are Copyright (c) 1997-2009 Reaction Design. All rights reserved.
```

Surface material name: MATERIAL1

```
Initializing TRANSPORT Library a component of CHEMKIN-PRO Release 15101, Build date: Aug 17, 2010
This and All Other CHEMKIN(R) Libraries are Copyright (c) 1997-2009 Reaction Design. All rights reserved.
```

```

KEYWORD INPUT
NONE
GEN ALL
GRXN ALL
GTHB ALL
NDIM ALL
PFAL ALL
SCOV ALL
SRXN ALL
STCK ALL
TFAL ALL
THRM NONE
TRAN ALL
TSUM NONE
CARR H2
LSCL 1.3
MAJ CH4
PBTH 20.0
PHIG 700.0
PLOW 100.0
PNUM 3
TBTH 1100.0
TDEL 400.0
THIG 1200.0
TLOW 300.0
THRM BULK
THRM CH(S)
THRM CH2(S)
THRM CH3
THRM CH4
TSUM SPECIES
XBTH CH3 0.03
XBTH CH4 0.05
XBTH H 0.02
XBTH H2 0.9
END

```



The **Turn On General Tables** button in the Output Control tab gives the following general information about the elements, species, phases, and reactions in the mechanism.

```

=====
GENERAL INFORMATION CONCERNING THE CHEMKIN MECHANISM
=====
Total number of elements declared      = 2 ( H C )
Total number of species                = 12
Total number of phases                 = 3
Total number of gas-phase reactions    = 5
Total number of surface-phase reactions = 4
Universal gas constant                 = 8.31447E+07 erg/(mol-K)
Universal gas constant used for activation energies = 1.99 cal/(mol-K)
Pressure of one standard atmosphere     = 1.01325E+06 dyne/cm^2

GAS PHASE (Always phase # 1, with the name, "GAS")
-----
Number of species                      = 5
Number of surface reactions where the # of gas
products is different than the # of gas reactants = 2
Number of elements in the phase        = 2 ( H C )
-----

SURFACE PHASES
-----
Phase  Phase      SS Site Density  Species  Element  Site_changing Elements:
Number Name        mole/cm^2     Count    Count    Surf_rxns
-----
  2    DIAMOND      5.2200E-09    6        2        0        ( H C )
      Tot SS Site Dens 5.2200E-09
      (used in sticking coefficient express)
-----

BULK PHASES
-----
Phase  Phase      Species  Element  Mole_changing Elements:
Number Name        Count    Count    Surf_rxns
-----
  3    BULK1        1        1        1        ( C )
-----

```



The **Turn On General Tables** button in the Output Control tab gives the following table of conditions. The bath gas conditions are set in the Reactor Physical Property tab. The bath gas composition, carrier gas and major species are set in the Species-specific Data tab.

```

=====
SUMMARY OF SPECIES IN THE MECHANISM, with a DESCRIPTION OF BATH GAS COMPOSITION
=====
Total pressure           = 20.00   torr
Temperature (where needed) = 1100.00 K
Carrier Gas (used in diff. calcs) = H2
Major Gas Species (used in nondim calcs) = CH4
=====
Number  Name           Mole_fraction  Concentration
-----
 1    CH3             3.0000E-02     8.7471E-09 mol/cm^3
 2    C2H6            0.000          0.000 mol/cm^3
 3    CH4             5.0000E-02     1.4579E-08 mol/cm^3
 4    H              2.0000E-02     5.8314E-09 mol/cm^3
 5    H2             0.9000        2.6241E-07 mol/cm^3
 6    CH(S)          0.1667        8.7000E-10 mol/cm^2
 7    C(S,R)         0.1667        8.7000E-10 mol/cm^2
 8    CH3(S)        0.1667        8.7000E-10 mol/cm^2
 9    CH2(S)        0.1667        8.7000E-10 mol/cm^2
10    CH2(S,R)      0.1667        8.7000E-10 mol/cm^2
11    CH(S,R)       0.1667        8.7000E-10 mol/cm^2
12    D              1.000         (activity) unitless
=====

```



The **Turn On Summary Tables for Species** checkbox gives the following table of thermochemical data.

```

=====
SUMMARY OF STANDARD STATE THERMODYNAMIC FUNCTIONS FOR SPECIES AT BATH GAS CONDITIONS
=====
Bath Gas Temperature = 1100.00K
=====
Number  Name           H(298 K)  H(T_bath)  Cp(T_bath)  S(T_bath)  G(T_bath)
-----
          kcal/mol    kcal/mol    cal/(mol-K) cal/(mol-K) kcal/mol
-----
 1    CH3             34.82     44.55     14.64     61.47     -23.06
 2    C2H6            -20.67    -2.14     30.89     82.90     -93.33
 3    CH4            -17.90    -7.00     18.07     60.84     -73.92
 4    H              52.10     56.08     4.97     33.88     18.82
 5    H2              0.00      5.67      7.32     40.39     -38.77
 6    CH(S)           0.00      4.84      8.80      7.16     -3.04
 7    C(S,R)         43.36    46.63     5.24     5.15     40.96
 8    CH3(S)        17.30    26.17    16.04    16.57     7.95
 9    CH2(S)        -11.49   -4.63    12.69    10.13    -15.77
10    CH2(S,R)      50.66    57.52    12.69    10.13    46.38
11    CH(S,R)       31.88    36.71     8.80     7.16     28.84
12    D              0.45     3.72     5.24     5.15     -1.95
=====

```



The **Turn On General Tables** button in the Output Control tab gives the following general information about reactions in the mechanism.

SURFTHERM Mechanism Analyzer: Initializing gas reactions...

```

=====
SHORT DESCRIPTION OF GAS-PHASE REACTIONS
=====
-----
Number  Description                                     Gas_Mole  Gas_Mole
          Change                                     Reactants
-----

```

```

-----
1  2CH3 (+M) <=>C2H6 (+M)          -1.00   2.00
2  CH4+H<=>CH3+H2                  0.00   2.00
3  CH3+H (+M) <=>CH4 (+M)          -1.00   2.00
4  2H+M<=>H2+M                     -1.00   2.00
5  2H+H2<=>2H2                     -1.00   3.00
-----

```

SURFTHERM Mechanism Analyzer: Initializing surface reactions...

=====
SHORT DESCRIPTION OF SURFACE-PHASE REACTIONS
=====

Number	Description	Gas Mole Change	Surf Mole Change	Bulk Mole Change	Surf_Site Change
1	CH (S) +H<=>C (S,R) +H2	0.00	0.00	0.00	0.00
2	C (S,R) +H=>CH (S)	-1.00	0.00	0.00	0.00
3	C (S,R) +CH3<=>D+CH3 (S)	-1.00	0.00	1.00	0.00
4	CH2 (S,R) +CH (S,R) <=>CH2 (S) +CH (S)	0.00	0.00	0.00	0.00



The **Turn On Uni-dimensional Rate Tables** button in the Output Control panel gives the following tables of “uniform-dimensional” rates that allow comparisons between reactions of different orders. The length scale used for evaluating the relative importance of kinetics to transport is set on the Reactor Physical Property tab.

=====
NON-DIMENSIONAL GAS REACTION RATE CONSTANTS AT THE BATH GAS CONDITIONS
=====

Total Pressure = 20.00 torr
Temperature = 1100.00 K

Number	Description	k_star mol/(cm ³ -s)	k_star_rev	Gas_Da_For	Gas_Da_Rev
1	2CH3 (+M) <=>C2H6 (+M)	0.2703	4.2798E-09	6113.	9.6773E-05
2	CH4+H<=>CH3+H2	4.5456E-02	2.0959E-03	1028.	47.39
3	CH3+H (+M) <=>CH4 (+M)	2.8128E-02	1.5344E-14	636.0	3.4694E-10
4	2H+M<=>H2+M	2.2528E-06	5.6662E-20	5.0939E-02	1.2812E-15
5	2H+H2<=>2H2	3.4125E-05	8.5829E-19	0.7716	1.9407E-14

NOTE ON THE ABSOLUTE NUMBERS IN THIS TABLE:

The rate constants (mol/(cm³-s)) should be compared to rate of mass transport in order to characterize their values as being fast or slow. The nondimensionalization of the mass transport involves the following multiplicative factor, which also has the units of mol/(cm³-s):

Total_Concentration * Diffusivity / Length_scale²
Using the binary diffusion coefficient between H2 and CH4, the following factors are calculated at bath gas conditions:
Total Concentration = 2.9155E-07 mol/cm³
Binary Diffusion Coefficient = 256.4 cm²/s
Length scale = 1.300 cm

Therefore, the non-dimensionalization factor for gas reactions becomes:
Conc * Diff / Length² = 4.4226E-05 mol/(cm³-s)

Note that this number is independent of pressure

=====
NON-DIMENSIONAL SURFACE REACTION RATE CONSTANTS AT THE BATH GAS CONDITIONS
=====

Total Pressure = 20.00 torr
Temperature = 1100.00 K

Number	Description	k_star mol/(cm ² -s)	k_star_rev	Surf_Da_For	Surf_Da_Rev
1	CH (S) +H<=>C (S,R) +H2	2.8714E-03	5.7498E-06	49.94	0.1000
2	C (S,R) +H=>CH (S)	1.2367E-02 [1.5531E-13]		215.1	[2.7014E-09]
3	C (S,R) +CH3<=>D+CH3 (S)	3.5161E-03	54.64	61.16	9.5040E+05
4	CH2 (S,R) +CH (S,R) <=>CH2 (S) +CH (S)	654.8	1.3621E-16	1.1390E+07	2.3691E-12

[] indicates that this reaction is not in mechanism

NOTE ON THE ABSOLUTE NUMBERS IN THIS TABLE:

The rate constants (mol/(cm²-s)) should be compared to rate of mass transport to the surface in order to characterize their values as being fast or slow. The nondimensionalization of the mass transport involves the following multiplicative factor, which also has the units of mol/(cm²-s):

Total_Concentration * Diffusivity / Length_scale
Using the binary diffusion coefficient between H2

and CH₄, the following factors are calculated at bath gas conditions:

```

Total Concentration      = 2.9155E-07 mol/cm^3
Binary Diffusion Coefficient = 256.4 cm^2/s
Length scale            = 1.300 cm

```

Therefore, the non-dimensionalization factor for surface reactions becomes:

```

Conc * Diff / Length    = 5.7493E-05 mol/(cm^2-s)

```

Note that this number is independent of pressure



Listing these species on the Species-specific Data tab, combined with the **Turn On Bulk Species Thermo Tables** checkbox in the Output Control panel gives the following tables of thermodynamic data for two gas-phase species, two surface species and the one bulk species. The **Turn On Transport Tables** button adds the table of Viscosity, Thermal Conductivity and Binary Diffusion Coefficients to the tables for the gas-phase species. The temperature intervals are set on the Reactor Physical Property tab.

```

=====
THERMO TABLE FOR MOLECULE "CH3" IN PHASE "GAS"
=====
Overall, this is the 1th species in the mechanism
It is the 1th species in phase GAS
Elemental Composition:
  H: 3
  C: 1
L-J Potential well depth      = 144.0 K
L-J collision diameter        = 3.800 Angstroms
Dipole Moment                 = 0.000 Debye
Polarizability                = 0.000 Angstroms^3
Rotational Collision number at 298K = 0.000
This molecule is linear
Heat of Formation at 298      = 34.823 kcal/mol
Molecular Weight             = 15.04 gm/mol
=====
Temp      H-H298      G-H298      Cp      S      Viscosity      Therm_Cond      Dif_Co_with_H2
K          kcal/mol      kcal/mol      cal/(mol-K)      erg/(cm-s-K)      cm^2/s
-----
298.15    0.000      -13.828      9.21      46.38      1.0685E-04      3556.      28.00
300.00    0.017      -13.914      9.23      46.44      1.0739E-04      3581.      28.30
700.00    4.336      -34.452      12.20     55.41      2.0316E-04      9207.      119.0
1100.00   9.732      -57.882      14.64     61.47      2.7667E-04      1.4856E+04      252.8
=====
[Pressure for binary diffusion coeff. calc. = 20.00 torr]

```

```

=====
THERMO TABLE FOR MOLECULE "CH4" IN PHASE "GAS"
=====
Overall, this is the 3th species in the mechanism
It is the 3th species in phase GAS
Elemental Composition:
  H: 4
  C: 1
L-J Potential well depth      = 141.4 K
L-J collision diameter        = 3.746 Angstroms
Dipole Moment                 = 0.000 Debye
Polarizability                = 2.600 Angstroms^3
Rotational Collision number at 298K = 13.00
This molecule is non-linear
Heat of Formation at 298      = -17.900 kcal/mol
Molecular Weight             = 16.04 gm/mol
=====
Temp      H-H298      G-H298      Cp      S      Viscosity      Therm_Cond      Dif_Co_with_H2
K          kcal/mol      kcal/mol      cal/(mol-K)      erg/(cm-s-K)      cm^2/s
-----
298.15    0.000      -13.259      8.40      44.47      1.1427E-04      3406.      28.41
300.00    0.016      -13.341      8.43      44.52      1.1484E-04      3436.      28.71
700.00    4.464      -33.081      13.70     53.64      2.1673E-04      1.0920E+04      120.7
1100.00   10.904     -56.016      18.07     60.84      2.9497E-04      1.8790E+04      256.4
=====
[Pressure for binary diffusion coeff. calc. = 20.00 torr]

```

```

=====
THERMO TABLE FOR MOLECULE "CH(S)" IN PHASE "DIAMOND"
=====
Overall, this is the 6th species in the mechanism
It is the 1th species in phase DIAMOND
Elemental Composition:

```

```

H: 1
C: 1
Number of surface sites occupied by the species = 1
Heat of Formation at 298      = 0.000 kcal/mol
Molecular Weight             = 13.02 gm/mol
-----
Temp      H-H298      G-H298      Cp      S
K          kcal/mol          cal/(mol-K)
-----
298.15    0.00      -0.106     1.45    0.357
300.00    2.701E-03 -0.107     1.47    0.366
700.00    1.70      -0.858     6.52    3.65
1100.00   4.84      -3.04      8.80    7.16
-----

```

```

=====
THERMO TABLE FOR MOLECULE "CH2(S)" IN PHASE "DIAMOND"
=====
Overall, this is the 9th species in the mechanism
It is the 4th species in phase DIAMOND
Elemental Composition:
H: 2
C: 1
Number of surface sites occupied by the species = 1
Heat of Formation at 298      = -11.490 kcal/mol
Molecular Weight             = 14.03 gm/mol
-----
Temp      H-H298      G-H298      Cp      S
K          kcal/mol          cal/(mol-K)
-----
298.15    0.00      -0.152     2.04    0.511
300.00    3.809E-03 -0.153     2.08    0.524
700.00    2.38      -1.21      9.20    5.12
1100.00   6.86      -4.28     12.7    10.1
-----

```

```

=====
THERMO TABLE FOR MOLECULE "D" IN PHASE "BULK1"
=====
Overall, this is the 12th species in the mechanism
It is the 1th species in phase BULK1
Elemental Composition:
C: 1
Bulk Density                  = 3.515 gm/cm^3
Activity (bath gas dependent) = 1.000
Heat of Formation at 298      = 0.454 kcal/mol
Molecular Weight             = 12.01 gm/mol
-----
Temp      H-H298      G-H298      Cp      S
K          kcal/mol          cal/(mol-K)
-----
298.15    0.00      -0.113     1.44    0.378
300.00    2.684E-03 -0.113     1.46    0.387
700.00    1.29      -0.762     4.48    2.93
1100.00   3.27      -2.40      5.24    5.15
-----

```



The **Turn On Gas Reaction Tables** button in the Output Control tab gives the following tables of high-pressure rates constants as a function of temperature for the gas-phase reactions. Reactions 1 and 3 have (+M), so for these reactions, the **Turn On Pressure Tables** button adds a table of rate constants as a function of pressure at the bath-gas temperature, and the **Turn On Temperature Tables** buttons add a table of rate constants as a function of temperature at the bath-gas pressure. Reaction 4 has +M, so for this reaction, the **Turn On 3rd Body Reaction Tables** button adds a table where the effect of the third body is lumped into the rate constants. The bath gas conditions and temperature/pressure intervals are set on the Reactor Physical Property tab.

```

=====
Gas Reaction # 1 2CH3 (+M) <=> C2H6 (+M)
=====
Change in moles in the reaction = -1.00
This reaction does have third body effects.
1 enhanced third body efficiencies were input

```

Species "H2" enhanced third body efficiency for the reaction = 2.000
 This is a reversible reaction, having 2.00 reactant species and 1.00 product species
 $k \text{ cm}^3/(\text{mol}\cdot\text{s}) = 9.0300\text{E}+16 T^{(-1.180)} \exp(-0.65 \text{ kcal/mol} / \text{RT})$
 Reaction has a pressure-dependent behavior with a 6 parameter Troe function form:
 $k_{\text{low}} \text{ cm}^6/(\text{mol}^2\cdot\text{s}) = 3.1800\text{E}+41 T^{(-7.030)} \exp(-2.76 \text{ kcal/mol} / \text{RT})$
 $a = 0.6041$
 $T^{***} = 6927. \text{ K}$
 $T^* = 132.0 \text{ K}$

HIGH PRESSURE GAS REACTION RATE CONSTANTS AS A FUNCTION OF TEMPERATURE

Temp K	k $\text{cm}^3/(\text{mol}\cdot\text{s})$	Afact $\text{cm}^3/(\text{mol}\cdot\text{s})$	Ea kcal/mol	DeltaG kcal/mol	DeltaH kcal/mol	DeltaS cal/(mol-K)	k_rev sec-1	Afact_rev mol/($\text{cm}^3\cdot\text{s}$)	Ea_rev kcal/mol	UnifDimensnl k_star mol/($\text{cm}^3\cdot\text{s}$)	Rate_Const k_star_rev mol/($\text{cm}^3\cdot\text{s}$)
298.15	3.601E+13	3.337E+13	-0.05	-79.16	-90.32	-37.42	1.384E-49	7.552E+16	89.68	38.8	1.384E-55
300.00	3.600E+13	3.313E+13	-0.05	-79.09	-90.33	-37.45	3.519E-49	7.590E+16	89.68	38.2	3.496E-55
700.00	2.479E+13	1.219E+13	-0.99	-63.31	-91.52	-40.30	7.410E-12	5.018E+16	89.14	2.83	1.846E-18
1100.00	1.725E+13	7.151E+12	-1.93	-47.21	-91.25	-40.03	7.964E-02	1.633E+16	87.14	0.270	4.280E-09

PRESSURE-DEPENDENT BEHAVIOR AS A FUNCTION OF TEMPERATURE

Reaction # 1

Bath Gas Pressure = 20.00 torr

Temp K	k $\text{cm}^3/(\text{mol}\cdot\text{s})$	Afact $\text{cm}^3/(\text{mol}\cdot\text{s})$	Ea kcal/mol	k/kinf $\text{cm}^6/(\text{mol}^2\cdot\text{s})$	klow $\text{cm}^6/(\text{mol}^2\cdot\text{s})$	Reduc_Pres FC	EffConc mol/ cm^3	k_rev sec-1	Afact_rev mol/($\text{cm}^3\cdot\text{s}$)	Ea_rev kcal/mol	
298.15	3.350E+13	2.644E+13	-0.14	0.930	1.209E+22	686.	0.931	2.044E-06	1.287E-49	5.983E+16	89.59
300.00	3.345E+13	2.615E+13	-0.15	0.929	1.192E+22	672.	0.931	2.031E-06	3.270E-49	5.991E+16	89.59
700.00	1.348E+13	1.279E+12	-3.28	0.544	4.356E+20	15.3	0.579	8.705E-07	4.030E-12	5.264E+15	86.85
1100.00	3.181E+12	7.839E+10	-8.09	0.184	3.738E+19	1.20	0.338	5.539E-07	1.468E-02	1.790E+14	80.97

PRESSURE-DEPENDENT BEHAVIOR AS A FUNCTION OF PRESSURE

Reaction # 1

Bath Gas Temperature = 1100.00K

Low Pressure Limiting Reaction Rate = klow = 3.7385E+19 $\text{cm}^6/(\text{mol}^2\cdot\text{s})$

Pres torr	k $\text{cm}^3/(\text{mol}\cdot\text{s})$	Afact $\text{cm}^3/(\text{mol}\cdot\text{s})$	Ea kcal/mol	k/kinf $\text{cm}^3/(\text{mol}\cdot\text{s})$	klow*EffConc $\text{cm}^6/(\text{mol}^2\cdot\text{s})$	Reduc_Pres FC	EffConc mole/ cm^3	k_rev sec-1	Afact_rev mol/($\text{cm}^3\cdot\text{s}$)	Ea_rev kcal/mol	
700.00	1.151E+13	1.447E+12	-4.53	0.667	7.248E+14	42.0	0.683	1.939E-05	5.312E-02	3.306E+15	84.53
264.58	9.107E+12	5.942E+11	-5.97	0.528	2.739E+14	15.9	0.561	7.328E-06	4.203E-02	1.357E+15	83.09
100.00	6.451E+12	2.165E+11	-7.42	0.374	1.035E+14	6.00	0.436	2.770E-06	2.977E-02	4.944E+14	81.64

Gas Reaction # 2 CH4+H<=>CH3+H2

Change in moles in the reaction = 0.00

This reaction does not have any third body effects

This is a reversible reaction, having 2.00 reactant species and 2.00 product species

 $k \text{ cm}^3/(\text{mol}\cdot\text{s}) = 2.2000\text{E}+04 T^{(3.000)} \exp(-8.75 \text{ kcal/mol} / \text{RT})$

HIGH PRESSURE GAS REACTION RATE CONSTANTS AS A FUNCTION OF TEMPERATURE

Temp K	k $\text{cm}^3/(\text{mol}\cdot\text{s})$	Afact $\text{cm}^3/(\text{mol}\cdot\text{s})$	Ea kcal/mol	DeltaG kcal/mol	DeltaH kcal/mol	DeltaS cal/(mol-K)	k_rev $\text{cm}^3/(\text{mol}\cdot\text{s})$	Afact_rev $\text{cm}^3/(\text{mol}\cdot\text{s})$	Ea_rev kcal/mol	UnifDimensnl k_star mol/($\text{cm}^3\cdot\text{s}$)	Rate_Const k_star_rev mol/($\text{cm}^3\cdot\text{s}$)
298.15	2.249E+05	1.171E+13	10.53	-1.08	0.63	5.73	3.612E+04	6.546E+11	9.90	2.602E-07	4.179E-08
300.00	2.509E+05	1.193E+13	10.54	-1.09	0.63	5.75	4.004E+04	6.612E+11	9.91	2.868E-07	4.575E-08
700.00	1.399E+10	1.516E+14	12.92	-3.81	1.31	7.31	9.043E+08	3.820E+12	11.61	2.937E-03	1.898E-04
1100.00	5.348E+11	5.881E+14	15.31	-6.73	1.14	7.15	2.466E+10	1.613E+13	14.17	4.546E-02	2.096E-03

Gas Reaction # 3 CH3+H(+M)<=>CH4(+M)

Change in moles in the reaction = -1.00

This reaction does have third body effects.

1 enhanced third body efficiencies were input

Species "H2" enhanced third body efficiency for the reaction = 2.000

This is a reversible reaction, having 2.00 reactant species and 1.00 product species

 $k \text{ cm}^3/(\text{mol}\cdot\text{s}) = 6.0000\text{E}+16 T^{(-1.000)} \exp(-0.00 \text{ kcal/mol} / \text{RT})$

Reaction has a pressure-dependent behavior with a Lindeman function form:

 $k_{\text{low}} \text{ cm}^6/(\text{mol}^2\cdot\text{s}) = 8.0000\text{E}+26 T^{(-3.000)} \exp(-0.00 \text{ kcal/mol} / \text{RT})$

HIGH PRESSURE GAS REACTION RATE CONSTANTS AS A FUNCTION OF TEMPERATURE

Temp K	k $\text{cm}^3/(\text{mol}\cdot\text{s})$	Afact $\text{cm}^3/(\text{mol}\cdot\text{s})$	Ea kcal/mol	DeltaG kcal/mol	DeltaH kcal/mol	DeltaS cal/(mol-K)	k_rev sec-1	Afact_rev mol/($\text{cm}^3\cdot\text{s}$)	Ea_rev kcal/mol	UnifDimensnl k_star mol/($\text{cm}^3\cdot\text{s}$)	Rate_Const k_star_rev mol/($\text{cm}^3\cdot\text{s}$)
298.15	2.012E+14	7.403E+13	-0.59	-96.09	-104.82	-29.30	3.047E-61	2.820E+15	103.64	54.6	7.690E-68
300.00	2.000E+14	7.358E+13	-0.60	-96.03	-104.83	-29.34	8.961E-61	2.836E+15	103.64	52.9	2.216E-67
700.00	8.571E+13	3.153E+13	-1.39	-83.31	-106.69	-33.41	1.463E-17	4.041E+15	103.91	0.416	1.551E-25
1100.00	5.455E+13	2.007E+13	-2.19	-69.68	-107.63	-34.51	8.675E-06	2.845E+15	103.26	2.813E-02	1.534E-14

PRESSURE-DEPENDENT BEHAVIOR AS A FUNCTION OF TEMPERATURE

Reaction # 3

Bath Gas Pressure = 20.00 torr

Temp K	k cm ³ /(mol-s)	Afact cm ³ /(mol-s)	Ea kcal/mol	k/kinf cm ⁶ /(mol ² -s)	klow cm ⁶ /(mol ² -s)	Reduc_Pres FC	EffConc mol/cm ³	k_rev sec-1	Afact_rev sec-1	Ea_rev kcal/mol	
298.15	4.722E+13	1.748E+12	-1.95	0.235	3.018E+19	0.307	1.00	2.044E-06	7.149E-62	6.659E+13	102.28
300.00	4.626E+13	1.696E+12	-1.97	0.231	2.963E+19	0.301	1.00	2.031E-06	2.073E-61	6.536E+13	102.27
700.00	1.983E+12	3.894E+10	-5.47	2.314E-02	2.332E+18	2.369E-02	1.00	8.705E-07	3.386E-19	4.990E+12	99.83
1100.00	3.309E+11	6.172E+09	-8.70	6.067E-03	6.011E+17	6.104E-03	1.00	5.539E-07	5.263E-08	8.751E+11	96.74

PRESSURE-DEPENDENT BEHAVIOR AS A FUNCTION OF PRESSURE

Reaction # 3

Bath Gas Temperature = 1100.00K

Low Pressure Limiting Reaction Rate = klow = 6.0105E+17 cm⁶/(mol²-s)

Pres torr	k cm ³ /(mol-s)	Afact cm ³ /(mol-s)	Ea kcal/mol	k/kinf cm ³ /(mol-s)	klow*EffConc cm ⁶ /(mol-s)	Reduc_Pres FC	EffConc mole/cm ³	k_rev sec-1	Afact_rev sec-1	Ea_rev kcal/mol	
700.00	9.602E+12	2.982E+11	-7.59	0.176	1.165E+13	0.214	1.00	1.939E-05	1.527E-06	4.228E+13	97.86
264.58	4.075E+12	9.340E+10	-8.25	7.471E-02	4.404E+12	8.075E-02	1.00	7.328E-06	6.481E-07	1.324E+13	97.19
100.00	1.615E+12	3.234E+10	-8.55	2.962E-02	1.665E+12	3.052E-02	1.00	2.770E-06	2.569E-07	4.584E+12	96.90

Gas Reaction # 4 2H+M<=>H2+M

Change in moles in the reaction = -1.00

This reaction does have third body effects.

1 enhanced third body efficiencies were input

Species "H2" enhanced third body efficiency for the reaction = 0.000

This is a reversible reaction, having 3.00 reactant species and 2.00 product species (including the third body)

k cm⁶/(mol²-s) = 1.0000E+18 T^(-1.000) exp(-0.00 kcal/mol / RT)

HIGH PRESSURE GAS REACTION RATE CONSTANTS AS A FUNCTION OF TEMPERATURE

Temp K	k cm ⁶ /(mol ² -s)	Afact cm ⁶ /(mol ² -s)	Ea kcal/mol	DeltaG kcal/mol	DeltaH kcal/mol	DeltaS cal/(mol-K)	k_rev cm ³ /(mol-s)	Afact_rev cm ⁶ /(mol-s)	Ea_rev kcal/mol	UnifDimensnl k_star mol/(cm ³ -s)	Rate_Const k_star_rev mol/(cm ³ -s)
298.15	3.354E+15	1.234E+15	-0.59	-97.17	-104.20	-23.57	8.156E-61	2.627E+15	103.01	4.174E-04	9.437E-74
300.00	3.333E+15	1.226E+15	-0.60	-97.13	-104.20	-23.59	2.383E-60	2.619E+15	103.01	4.072E-04	2.723E-73
700.00	1.429E+15	5.255E+14	-1.39	-87.12	-105.38	-26.09	1.576E-17	1.698E+15	102.60	1.374E-05	3.308E-31
1100.00	9.091E+14	3.344E+14	-2.19	-76.40	-106.50	-27.36	6.666E-06	1.301E+15	102.13	2.253E-06	5.666E-20

ANALYSIS OF THIRD BODY REACTIONS: LUMPING [M] WITH RATE CNST

Reaction # 4

Bath Gas Pressure = 20.00 torr

Temp K	k cm ³ /(mol-s)	Afact cm ³ /(mol-s)	Ea kcal/mol	Concentration mol/cm ³	C_eff mol/cm ³	k_rev sec-1	Afact_rev cm ³ /(mol-s)	Ea_rev kcal/mol
298.15	3.6077E+08	4.8825E+07	-1.18	1.0757E-06	1.0756E-07	8.7733E-68	1.0395E+08	102.42
300.00	3.5633E+08	4.8224E+07	-1.19	1.0691E-06	1.0690E-07	2.5474E-67	1.0301E+08	102.41
700.00	6.5449E+07	8.8575E+06	-2.78	4.5818E-07	4.5814E-08	7.2210E-25	2.8611E+07	101.21
1100.00	2.6504E+07	3.5869E+06	-4.37	2.9157E-07	2.9155E-08	1.9435E-13	1.3949E+07	99.94

Gas Reaction # 5 2H+H2<=>2H2

Change in moles in the reaction = -1.00

This reaction does not have any third body effects

This is a reversible reaction, having 3.00 reactant species and 2.00 product species

k cm⁶/(mol²-s) = 9.2000E+16 T^(-0.6000) exp(-0.00 kcal/mol / RT)

HIGH PRESSURE GAS REACTION RATE CONSTANTS AS A FUNCTION OF TEMPERATURE

Temp K	k cm ⁶ /(mol ² -s)	Afact cm ⁶ /(mol ² -s)	Ea kcal/mol	DeltaG kcal/mol	DeltaH kcal/mol	DeltaS cal/(mol-K)	k_rev cm ³ /(mol-s)	Afact_rev cm ⁶ /(mol-s)	Ea_rev kcal/mol	UnifDimensnl k_star mol/(cm ³ -s)	Rate_Const k_star_rev mol/(cm ³ -s)
298.15	3.014E+15	1.654E+15	-0.36	-97.17	-104.20	-23.57	7.329E-61	3.522E+15	103.25	3.751E-03	8.480E-73
300.00	3.003E+15	1.648E+15	-0.36	-97.13	-104.20	-23.59	2.147E-60	3.520E+15	103.25	3.668E-03	2.453E-72
700.00	1.806E+15	9.912E+14	-0.83	-87.12	-105.38	-26.09	1.993E-17	3.202E+15	103.16	1.737E-04	4.182E-30
1100.00	1.377E+15	7.557E+14	-1.31	-76.40	-106.50	-27.36	1.010E-05	2.939E+15	103.00	3.412E-05	8.583E-19



The **Turn On Surface Reaction Tables** button in the Output Control tab gives the following tables of information about surface reactions in the mechanism. The first two surface reactions were input as sticking coefficients, and the third reaction can be described that way, so for these reactions, the **Turn On Sticking Coefficient Tables** button adds tables of sticking coefficients as a function of temperature. The first reaction also has a surface coverage dependence, so the **Turn On Surface Coverage Dependence Tables** button adds a table of rate constants that include the effect of the surface coverage at bath-gas conditions for that reaction.

```

=====
Surface Reaction # 1 CH(S)+H<=>C(S,R)+H2
=====
Change in gas moles in the reaction = 0.00
Change in surface moles in the reaction = 0.00
Change in bulk moles in the reaction = 0.00

This reaction has 1 species whose surface coverage modify the rate constant
Each of these species has three parameters that multiplicatively modify the rate constant as follows:
k_prime = k * 10^(Z_k*nu_ki) * Z_k^mu_ki * exp[ - eps_ki*Z_k / RT ]
where
Z_k = Site Fraction of species k
Species = CH(S)
nu_ki = 0.1000
mu_ki = 0.000
eps_ki = 0.00 kcal/mol

This is a reversible surface reaction, having the following types of reactant species:
1.00 gas-phase species
1.00 surface-phase species
0.00 bulk-phase species

and the following types of product species:
1.00 gas-phase species
1.00 surface-phase species
0.00 bulk-phase species

The reaction rate constant was input via a sticking coefficient in the interpreter input file
Motz-Wise Correction factor is used
Sticking Coeff = MIN(1, 2.140 exp( - 7.30 kcal/mol / RT ) )
It can be fit to the following general rate constant form:
k cm^3/(mol-s) = 5.3961E+11 T^( 0.6423 ) exp( - 7.18 kcal/mol / RT )
The reverse rate constant can be fit to the following form:
k(rev) cm^3/(mol-s) = 1.4817E+11 T^( 0.5045 ) exp( - 15.83 kcal/mol / RT )
The reverse rate constant can also be expressed in a sticking coefficient form:
Sticking Coeff(rev) = 0.3030 T^( 4.0223E-03 ) exp( - 15.83 kcal/mol / RT )

FORWARD AND REVERSE SURFACE REACTION RATE CONSTANTS
=====
Temp k Afact Ea DeltaG DeltaH DeltaS k_rev Afact_rev Ea_rev Bath Gas Dependent
K cm^3/(mol-s) kcal/mol kcal/mol kcal/mol cal/(mol-K) cm^3/(mol-s) kcal/mol kcal/mol UnifDimensnl Rate_Const
298.15 1.143E+08 4.229E+13 7.60 -9.88 -8.73 3.84 6.56 6.115E+12 16.33 6.672E-07 3.827E-14
300.00 1.237E+08 4.242E+13 7.60 -9.89 -8.73 3.85 7.77 6.098E+12 16.33 7.176E-07 4.508E-14
700.00 2.078E+11 6.713E+13 8.04 -11.70 -8.33 4.82 4.619E+07 5.938E+12 16.36 5.166E-04 1.148E-07
1100.00 1.816E+12 9.631E+13 8.68 -13.58 -8.62 4.51 3.635E+09 9.939E+12 17.30 2.871E-03 5.750E-06
=====

ANALYSIS OF FORWARD AND REVERSE COVERAGE DEPENDENT SURFACE RATE CONSTANTS AT BATH GAS CONDITIONS
=====
Temp k_prime Afact Ea k Cov_fac(cgs) k_rev krev_prime Afact_rev Ea_rev
K cm^3/(mol-s) kcal/mol cm^3/(mol-s) cm^3/(mol-s) cm^3/(mol-s) kcal/mol
298.15 1.188E+08 4.394E+13 7.60 1.143E+08 1.04 6.56 6.82 6.355E+12 16.33
300.00 1.286E+08 4.408E+13 7.60 1.237E+08 1.04 7.77 8.08 6.336E+12 16.33
700.00 2.160E+11 6.975E+13 8.04 2.078E+11 1.04 4.619E+07 4.800E+07 6.170E+12 16.36
1100.00 1.887E+12 1.001E+14 8.68 1.816E+12 1.04 3.635E+09 3.778E+09 1.033E+13 17.30
=====

BREAKDOWN OF FORWARD REACTION'S STICKING COEFFICIENT
Surface site density divisor = 5.2200E-09 mol^1.00/cm^2.00
=====
Temp Stck_Coeff Afact Ea Eff_Vel Vel_Corr Sden_Ratio k* k
K unitless kcal/mol cm/s cm/s 1.000 1.000 cm/s cm^3/(mol-s)
298.15 9.5391E-06 2.140 7.30 6.2563E+04 1.000 1.000 0.5968 1.1433E+08
300.00 1.0292E-05 2.140 7.30 6.2757E+04 1.000 1.000 0.6459 1.2374E+08
=====

```

```

700.00 1.1254E-02 2.140      7.30  9.5863E+04 1.006      1.000      1085.      2.0785E+11
1100.00 7.5871E-02 2.140      7.30  1.2017E+05 1.039      1.000      9477.      1.8155E+12

```

BREAKDOWN OF REVERSE REACTION'S STICKING COEFFICIENT
Surface site density divisor = 5.2200E-09 mol^{1.00}/cm^{2.00}

Temp K	Stck_Coeff unitless	Afact	Ea kcal/mol	Eff_Vel cm/s	Vel_Corr	Sden_Ratio	k* cm/s	k cm ³ /(mol-s)
298.15	7.7387E-13	0.4377	16.03	4.4239E+04	1.000	1.000	3.4235E-08	6.558
300.00	9.1439E-13	0.4351	16.03	4.4376E+04	1.000	1.000	4.0577E-08	7.773
700.00	3.5571E-06	0.2773	15.67	6.7786E+04	1.000	1.000	0.2411	4.6192E+07
1100.00	2.2330E-04	0.3700	16.20	8.4974E+04	1.000	1.000	18.98	3.6355E+09

=====
Surface Reaction # 2 C(S,R)+H=>CH(S)
=====

Change in gas moles in the reaction = -1.00
Change in surface moles in the reaction = 0.00
Change in bulk moles in the reaction = 0.00

This is an irreversible surface reaction, having the following types of reactant species:
1.00 gas-phase species
1.00 surface-phase species
0.00 bulk-phase species

and the following types of product species:
0.00 gas-phase species
1.00 surface-phase species
0.00 bulk-phase species

The reaction rate constant was input via a sticking coefficient in the interpreter input file
Motz-Wise Correction factor is used

Sticking Coeff = MIN(1, 0.3000 exp(- 0.00 kcal/mol / RT))
It can be fit to the following general rate constant form:
k cm³/(mol-s) = 2.4498E+11 T^(0.5000) exp(- 0.00 kcal/mol / RT)
Even though this reaction is IRREVERSIBLE, the reverse rate constant will also be analysed:
The reverse rate constant can be fit to the following form:
k(rev) 1/s = 9.0322E+10 T^(1.096) exp(- 94.69 kcal/mol / RT)

FORWARD AND REVERSE SURFACE REACTION RATE CONSTANTS

(note: reverse rate constant is not in mechanism)

Temp K	k cm ³ /(mol-s)	Afact	Ea kcal/mol	DeltaG kcal/mol	DeltaH kcal/mol	DeltaS cal/(mol-K)	k_rev 1/s	Afact_rev	Ea_rev kcal/mol	Bath Gas Dependent UnifDimensnl Rate_Const	
										k_star mol/(cm ² -s)	k_star_rev
298.15	4.230E+12	6.974E+12	0.30	-87.29	-95.46	-27.41	1.793E-56	1.027E+14	95.17	2.375E-02	9.361E-65
300.00	4.243E+12	6.996E+12	0.30	-87.24	-95.47	-27.44	4.829E-56	1.040E+14	95.17	2.368E-02	2.521E-64
700.00	6.482E+12	1.069E+13	0.70	-75.41	-97.05	-30.91	3.218E-16	3.902E+14	96.36	1.550E-02	1.680E-24
1100.00	8.125E+12	1.340E+13	1.09	-62.82	-97.88	-31.87	2.975E-05	5.048E+14	96.79	1.237E-02	1.553E-13

BREAKDOWN OF FORWARD REACTION'S STICKING COEFFICIENT
Surface site density divisor = 5.2200E-09 mol^{1.00}/cm^{2.00}

Temp K	Stck_Coeff unitless	Afact	Ea kcal/mol	Eff_Vel cm/s	Vel_Corr	Sden_Ratio	k* cm/s	k cm ³ /(mol-s)
298.15	0.3000	0.3000	0.00	6.2563E+04	1.176	1.000	2.2081E+04	4.2301E+12
300.00	0.3000	0.3000	0.00	6.2757E+04	1.176	1.000	2.2150E+04	4.2432E+12
700.00	0.3000	0.3000	0.00	9.5863E+04	1.176	1.000	3.3834E+04	6.4816E+12
1100.00	0.3000	0.3000	0.00	1.2017E+05	1.176	1.000	4.2413E+04	8.1252E+12

=====
Surface Reaction # 3 C(S,R)+CH3<=>D+CH3(S)
=====

Change in gas moles in the reaction = -1.00
Change in surface moles in the reaction = 0.00
Change in bulk moles in the reaction = 1.00

This is a reversible surface reaction, having the following types of reactant species:
1.00 gas-phase species
1.00 surface-phase species
0.00 bulk-phase species

and the following types of product species:
0.00 gas-phase species
1.00 surface-phase species
1.00 bulk-phase species

A sticking coefficient was not used though the forward reaction could have used one

k cm³/(mol-s) = 4.0000E+12 exp(- 1.20 kcal/mol / RT)
The forward rate constant (with Motz-Wise correction) can be fit to the following sticking coefficient expression:
Sticking Coeff = 13.56 T^(-0.4622) exp(- 1.08 kcal/mol / RT)
The reverse rate constant can be fit to the following form:
k(rev) 1/s = 1.0000E+13 T^(-8.1728E-12) exp(- 15.00 kcal/mol / RT)
k(rev) 1/s = 1.0000E+13 exp(- 15.00 kcal/mol / RT)

FORWARD AND REVERSE SURFACE REACTION RATE CONSTANTS

Temp K	k cm ³ /(mol-s)	Afact	Ea kcal/mol	DeltaG kcal/mol	DeltaH kcal/mol	DeltaS cal/(mol-K)	k_rev 1/s	Afact_rev	Ea_rev kcal/mol	Bath Gas Dependent	
										UnifDimensnl k_star mol/(cm ² -s)	Rate_Const k_star_rev
298.15	5.278E+11	4.000E+12	1.20	-47.78	-60.43	-42.43	101.	1.000E+13	15.00	2.964E-03	5.280E-07
300.00	5.344E+11	4.000E+12	1.20	-47.70	-60.44	-42.46	118.	1.000E+13	15.00	2.982E-03	6.172E-07
700.00	1.688E+12	4.000E+12	1.20	-29.94	-61.58	-45.19	2.074E+08	1.000E+13	15.00	4.038E-03	1.08
1100.00	2.310E+12	4.000E+12	1.20	-11.90	-61.29	-44.90	1.047E+10	1.000E+13	15.00	3.516E-03	54.6

BREAKDOWN OF FORWARD REACTION'S STICKING COEFFICIENT

Surface site density divisor = 5.2200E-09 mol^{1.00}/cm^{2.00}

Temp K	Stck_Coeff unitless	Afact	Ea kcal/mol	Eff_Vel cm/s	Vel_Corr	Sden_Ratio	k* cm/s	k cm ³ /(mol-s)
298.15	0.1567	0.6393	0.83	1.6199E+04	1.085	1.000	2755.	5.2779E+11
300.00	0.1581	0.6368	0.83	1.6249E+04	1.086	1.000	2790.	5.3442E+11
700.00	0.3015	0.4103	0.43	2.4821E+04	1.178	1.000	8812.	1.6882E+12
1100.00	0.3247	0.3382	0.09	3.1115E+04	1.194	1.000	1.2059E+04	2.3102E+12

Surface Reaction # 4 CH2(S,R)+CH(S,R)<=>CH2(S)+CH(S)

Change in gas moles in the reaction = 0.00
 Change in surface moles in the reaction = 0.00
 Change in bulk moles in the reaction = 0.00

This is a reversible surface reaction, having the following types of reactant species:

0.00 gas-phase species
 2.00 surface-phase species
 0.00 bulk-phase species

and the following types of product species:

0.00 gas-phase species
 2.00 surface-phase species
 0.00 bulk-phase species

k cm²/(mol-s) = 6.0000E+19 exp(- 2.00 kcal/mol / RT)

The reverse rate constant can be fit to the following form:

k(rev) cm²/(mol-s) = 5.9991E+19 T^(2.0901E-05) exp(- 96.02 kcal/mol / RT)

FORWARD AND REVERSE SURFACE REACTION RATE CONSTANTS

Temp K	k cm ² /(mol-s)	Afact	Ea kcal/mol	DeltaG kcal/mol	DeltaH kcal/mol	DeltaS cal/(mol-K)	k_rev cm ² /(mol-s)	Afact_rev	Ea_rev kcal/mol	Bath Gas Dependent	
										UnifDimensnl k_star mol/(cm ² -s)	Rate_Const k_star_rev
298.15	2.052E+18	6.000E+19	2.00	-94.03	-94.03	0.00	2.436E-51	6.000E+19	96.03	55.9	6.637E-68
300.00	2.095E+18	6.000E+19	2.00	-94.03	-94.03	0.00	6.618E-51	6.000E+19	96.03	57.1	1.803E-67
700.00	1.425E+19	6.000E+19	2.00	-94.03	-94.03	0.00	6.257E-11	6.000E+19	96.03	388.	1.705E-27
1100.00	2.403E+19	6.000E+19	2.00	-94.03	-94.03	0.00	5.00	6.000E+19	96.03	655.	1.362E-16

Index

A

adiabatic flame temperature 23
 A-factors 201
 aftertreatment 181
 aftertreatment, engine exhaust 191
 aggregation 162
 simple model 159
 ALD 226
 ALD processes 226
 alumina 248
 alumina, ALD of 248
 ammonia 246
 approximations, cylindrical channel flow 214
 Arrhenius pre-exponential factors 201
 atomic layer deposition 226, 248
 autoignition for hydrogen/air 30
 autoignition, ignition times for propane 33
 axisymmetric results visualization 138

B

bath gas 254, 255
 burner-stabilized laminar premixed flame 38

C

C1_Inlet1 panel 40
 calculation, equilibrium 23, 208
 carrier gas 254, 256
 catalytic combustors 181
 catalytic converters 181
 catalytic oxidation 200
 Center for Energy Research 175
 Chapmen-Jouguet detonation 111
 chemical mechanism analysis 253
 chemical vapor deposition 207
 chemistry sets 173, 204, 246
 alumina ALD 248
 chlorine plasma 250

ethylene/air combustion 175
 fluorocarbon plasma 251
 GRMech 3.0 174
 hydrogen/air 173
 methane air 174
 methane oxidation on Pt 204
 methane/air 174
 methane/air reduced mechanism 174
 propane/air 175
 Pt/Rh three-way catalyst 205
 reduced mechanism 174
 silicon deposition from silane 247
 silicon deposition from trichlorosilane 247
 silicon nitride CVD 246

CHEMKIN

format 110

CHEMKIN-PRO

reactor models 19

chlorine plasma 250

spatial 237

steady-state 233

chlorosilane CVD 208

closed homogeneous panel 30, 34

coefficients, normalized sensitivity 83

colorbar property panel 139

combustion 142

combustion in complex flows 111

combustion, hydrogen 28

combustion, propane 33

combustion, steady-state gas-phase 28

combustor, gas turbine 111

combustor, homogeneous 186

combustor, two stage catalytic 181

continuations panel 24, 29, 208, 211, 216, 219, 242

CRUPROF subroutine 137

Curl's model, modified 129

CVD 207

chlorosilane 208

diamond 256

steady-state thermal 210
 trichlorosilane 223
 CVD reactor 210
 cylindrical channel flow 214
 cylindrical shear flow panel 215
 cylindrical shear flow reactor 207, 214

D

Damköhler number 255, 256
 DDASPK solver 129
 decomposition pathway
 Reaction Path Analyzer 66
 deposition in a rotating disk 219
 detonation, Chapmen-Jouguet 111
 diagnostic output file 258
 diamond CVD 256
 DVODE solver 129

E

EGR
 estimating initial gas composition
 EGR project
 results 125
 element filter
 Reaction Path Analyzer 66
 engine exhaust aftertreatment, transient flow 191
 engineout 193
 equilibrium analysis 26, 208
 equilibrium calculation 23, 208
 equilibrium panel 24, 208
 equivalence ratio 23, 71
 etching, fluorocarbon plasma 241
 etching, plasma 233
 exhaust gas recirculation. See EGR.
 extinction
 flames 85
 Extinction of Premixed or Opposed Flow Flame reactor
 85

F

files
 diagnostic output 258
 XML solution 31, 211, 257, 258
 flame speed 71
 flame speed panel 55
 flame speed, laminar 55
 flames 28
 burner-stabilized premixed laminar 38
 burner-stabilized with gas radiation 41
 extinction 85
 hydrogen/air 81

methane/air premixed 55
 methane-air 86
 non-premixed jet 114
 opposed-flow diffusion 81
 stagnation 94

Flame-speed Calculator
 Particle Tracking Feature 147
 flammability 28
 fluorocarbon plasma 251
 etching 241
 FORTRAN subroutine 192
 fusion 162

G

gas composition
 estimating initial with EGR
 gas inlet panel 228
 gas radiation for burner burner-stabilized flame 41
 Gas Research Institute 174
 gas turbine combustor 111
 gas turbine network 111
 gas, bath 254, 255
 gas, carrier 254, 256
 gas-phase combustion, steady-state 28
 GRI 3.0 methane oxidation mechanism 120
 GRI mech 3.0 174

H

HCCI 97
 HCCI engine
 estimating initial gas composition
 multi-zone 103
 with exhaust gas recirculation 119
 HCCI_EGR project 119
 heat-transfer correlation 99
 homogeneous charge compression ignition 97
 homogeneous combustor 186
 honeycomb monolith panel 185
 honeycomb monolith reactor 184
 hydrogen combustion 28
 hydrogen/air chemistry set 173
 hydrogen/air flame 81
 hydrogen/air system 23
 hydrogen/air, autoignition for 30

I

IC engine panel 98
 IC engine, single-zone 97
 ic_engine__EGR_network.ckprj 120
 ignition 28
 ignition time, defining 34

ignition times for propane autoignition 33
internal combustion engine 97

J

jet flame network 114
JSR/PFR system , soot formation 141

L

laminar flame speed 55
low-pressure plasma reactor 233

M

mass flow rate ratio 122
mechanism analysis, chemical 253
mechanism analyzer panel 258
mechanism analyzer tool 253
methane oxidation on Pt 204
methane/air chemistry set 174
methane/air, partially stirred reactor for 127
modified Curl's model 129
Monte Carlo mixing model 128
multiple reactor models 227
multi-zone HCCI engine 103
multi-zone model 104
 icon 104
 solution file, reduce size 105
multi-zone project
 number of reactors 104

N

networks
 gas turbine 111
 jet flame 114
 PSR 112, 115, 215
 PSR-PFR hybrid 112
non-dimensional reaction rate 254
non-premixed jet flame 114
normalized sensitivity coefficients 83
NO_x-mutual sensitization 119
number, Damköhler 255, 256

O

opposed-flow diffusion flame 81
opposed-flow flame
 soot and radiation 47
opposed-flow flame panel 82
Opposed-flow Flame Simulator
 Particle Tracking Feature 147
opposed-flow flames
 extinction 85

output control panel 29, 31, 82, 211, 215, 242, 257, 261,
 262

P

panel
 reactor properties 129
panels
 C1_Inlet1 40
 closed homogeneous 30, 34
 continuation 24, 29, 208, 211, 216, 219, 242
 cylindrical shear flow 215
 equilibrium 24, 208
 flame speed 55
 gas inlet 228
 honeycomb monolith 185
 IC engine 98
 mechanism analyzer 258
 opposed-flow flame 82
 output control 29, 31, 82, 211, 215, 242, 257, 261,
 262
 PFR 215
 planar shear flow 223
 plasma PFR 238
 plasma PSR 234, 242
 preferences 136
 pre-mixed burner 38, 39
 PSR 28, 193, 211, 215, 228
 R1_IN 55
 recycling 116
 rotating disk 219
 solver 29, 40, 82, 193, 215, 223, 229, 234, 242
 stagnation flow 228
panels (Post-Processor)
 colorbar property (Post-Processor) 139
Parameter Study Facility 71, 200
partially stirred reactor 127
particle aggregation 162
Particle Tracking Feature
 Flame-speed Calculator 147
 Opposed-flow Flame Simulator 147
Particle Tracking feature
 aggregation 162
particle-size distribution 153
PaSR 128
perfectly stirred reactor 183, 210, 214, 227, 233
PFR panel 215
planar channel flow 223
planar shear flow panel 223
planar shear flow reactor 207
plasma chlorine 233
plasma etching 233
 silicon dioxide 241
plasma PFR panel 238

- plasma plug flow reactor 237
- plasma PSR panel 234, 242
- plasma, fluorocarbon 251
- plug flow
 - side inlet 132
- plug flow reactor 183, 184, 207, 214
- Post 131
- power profile, with spatial chlorine plasma 237
- preferences panel 136
- Preferences tab
 - Reaction Path Analyzer 65
- pre-mixed burner panel 38, 39
- premixed flames
 - extinction 85
 - stagnation 94
- Pre-mixed Laminar Burner-Stabilized Stagnation Flame 153
- probability density functions 129
- Progress Monitor
 - EGR_network project 125
- propane
 - ignition times for autoignition 33
- propane-air mixtures 71
- PSR analysis 210
- PSR network 112, 115
- PSR panel 28, 193, 211, 215, 228
- PSR-PFR network 111
- Pt/Rh three-way catalyst 205

R

- R1_IN panel 55
- radiation
 - opposed-flow flame with soot 47
- rate constant, uniform-dimensional 255
- Rate of Production
 - Reaction Path Analyzer 67
- rate-of-production analysis 236
- rate-of-production options 210
- reaction mechanism for diamond CVD 256
- Reaction Path Analyzer 55, 59
 - colors 71
 - decomposition pathway 66
 - element filter 66
 - Rate of Production 67
 - Reaction Path Analyzer 65
 - reduce diagram complexity 69
 - relative rate analysis 68
 - Sensitivity 67
 - solution file point selection 62
 - species, isolated 70
 - species, number of 66
 - split paths 68
 - tree layout 68

- Y variable 62
- zoom 65
- reaction paths 59
- reaction rates 254
- reactor network
 - recirculation 119
 - tear stream 119
- reactor properties panel 129
- recycling panel 116
- reduced mechanism, methane/air 174
- relative rate analysis
 - Reaction Path Analyzer 68
- ROP 210
- rotating disk panel 219
- rotating disk reactor 207, 219
- RPA 59

S

- sample problems, models used 20
- sectional method
 - aggregation model 159
- sectional model 153
- segregated solution technique 147
- Sensitivity
 - Reaction Path Analyzer 67
- sensitivity
 - Reaction Path Analyzer 60
- shock-heated air 110
- shock-tube experiment 33, 110
- side inlet on plug flow reactor 132
- silane 247
- silicon deposition from silane 247
- silicon deposition from trichlorosilane 247
- silicon dioxide 251
- silicon nitride CVD 246
- silicon tetrafluoride 246
- single-zone IC engine 97
- solution file
 - Reaction Path Analyzer point selection 62
 - zone average option for multi-zone 105
- solver panel 29, 40, 82, 193, 215, 223, 229, 234, 242
- solvers
 - DDASPK 129
 - DVODE 129
 - transient 192
- soot
 - opposed-flow flame and radiation 47
- soot formation 141
- soot nucleation reaction 142
- spatial chlorine plasma 237
- species, number of
 - Reaction Path Analyzer 66
- splits paths

Reaction Path Analyzer 68
Splitter node, Project tree 122
stagnation
 flames 94
stagnation flow panel 228
stagnation flow reactor 207
steady-state gas-phase combustion 28
steady-state thermal CVD 210
stoichiometric hydrogen/air mixture 30
stoichiometric methane/air premixed flame 55
sub-projects 227
subroutine library
 TRANSPORT 256
surface chemistry analysis 200

T

tear stream 120
Tear Stream Controls node, Project tree 124
tear stream reactor network
temperature, adiabatic flame 23
time-dependent simulations of ALD process 227
titania 162
titanium tetrachloride 162
TMA 248
transient inlet flow 191
transient solver 192
TRANSPORT subroutine library 256
tree layout
 Reaction Path Analyzer 68
trichlorosilane CVD 223
trichlorosilane, silicon deposition from 247
trimethylaluminum 248
TRIT 181
turbine rotor inlet temperature 181
two stage catalytic combustor 181

U

unburnt gas temperature 71
uniform-dimensional rate constant 255
uniform-dimensional reaction rate 254
UPROF keyword 137
user-defined subroutine 191
USRINLET 192
USRINLET subroutine 194

V

vapor deposition, chemical 207

W

Woschni correction 99

X

XML solution file 31, 211, 257, 258
XMLdata.zip 129, 257

Y

Y variable
 Reaction Path Analyzer 62

Z

zone-average option for multi-zone solution file 105
zones, multiple 104
zoom
 Reaction Path Analyzer 65

